Molecular studies of the sources and significance of archaeal lipids in the oceans

by

Sara Ann Lincoln

B.S. Geosciences
B.S. Geological Oceanography
University of Rhode Island (2006)

SUBMITTED TO THE DEPARTMENT OF
EARTH, ATMOSPHERIC AND PLANETARY SCIENCES
IN PARTIAL FULFILLMENT OF THE REQUIREMENTS FOR THE DEGREE OF

DOCTOR OF PHILOSOPHY IN GEOCHEMISTRY

SEPTEMBER 2013

Author:.....
Department of Earth, Atmospheric and Planetary Sciences

Certified by:.....
Roger E. Summons
Professor of Geobiology
Department of Earth, Atmospheric and Planetary Sciences
Thesis supervisor

.....
Edward F. DeLong
Morton and Claire Goulder Family Professor in Environmental Systems
Department of Civil and Environmental Engineering
Thesis supervisor

Accepted by: .....
Robert van der Hilst
Schlumberger Professor of Earth Sciences
Head, Department of Earth, Atmospheric and Planetary Sciences

THIS PAGE INTENTIONALLY LEFT BLANK

Molecular studies of the sources and significance of archaeal lipids in the oceans

by

Sara Ann Lincoln

Submitted to the Department of Earth, Atmospheric and Planetary Sciences on July 29, 2013 in partial fulfillment of the requirements for the Degree of Doctor of Philosophy in Geochemistry

ABSTRACT

Marine archaea are ubiquitous and abundant in the modern oceans and have a geologic record extending >100 million years. However, factors influencing the populations of the major clades – chemolithoautotrophic Marine Group I Thaumarchaeota (MG-I) and heterotrophic Marine Group II Euryarchaeota (MG-II) – and their membrane lipid signatures are not well understood. Here, I paired techniques of organic geochemistry and molecular biology to explore the sources and significance of archaeal tetraether lipids in the marine water column. Using metagenomics, 16S rDNA pyrosequencing, QPCR and mass spectrometric analyses, I found that uncultivated MG-II Euryarchaeota synthesize glycerol dialkyl glycerol tetraether (GDGT) lipids - including crenarchaeol, previously thought limited to autotrophic Thaumarchaeota. This finding has important implications for paleoenvironmental proxies reliant upon GDGTs.

To investigate the effects of organic matter and bicarbonate + ammonia amendments on archaeal tetraether lipids and microbial community composition, I conducted large scale microcosm experiments. Experimental conditions did not promote the overall growth of archaea, but several changes in tetraether lipid abundance and relative ring distribution suggest that future incubation labeling studies using whole seawater may be valuable in probing the metabolism of individual archaeal clades in mixed populations. A rapid decrease in GDGT concentrations was observed within the first 44 h of the experiment, suggesting that the residence time of these compounds in the open ocean may be short. Changes in functional gene representation and microbial community composition over the course of the experiment provide potential insight into mechanisms of copiotrophy and the identity of bacteria that may degrade GDGTs.

Finally, I present the results of a study of the sources and patterns of bacterial and archaeal GDGTs detected in the Lost City Hydrothermal Vent Field. Branched GDGTs, generally considered markers of terrestrial input to marine sediments, were detected in carbonate chimneys of this alkaline site near the mid-Atlantic Ridge. A relatively

uncommon H-shaped GDGT was also present, and appears to be a marker of hydrothermal archaeal input rather than a mesophilic euryarchaeotal signal.

Taken together, the work presented in this thesis emphasizes the necessity of understanding the biological underpinnings of archaeal lipids in the environment, increasingly used as biomarkers in microbial ecology and paleoenvironmental reconstruction.

Thesis Supervisors:

Roger E. Summons
Professor of Geobiology
Department of Earth, Atmospheric and Planetary Sciences

Edward F. DeLong
Morton and Claire Goulder Family Professor in Environmental Systems
Department of Civil and Environmental Engineering

Acknowledgments

I have immense gratitude for the many people who have supported the work represented in this thesis. Most of all, I am indebted to my advisors, Roger Summons and Ed DeLong, for their generosity, patience and good humor throughout this journey. I also appreciate the enthusiastic support and insight that my committee members Mick Follows and Edward Boyle have shown for my thesis research.

When I first started talking to Roger about potential graduate studies he had the wonderful idea of introducing me to Ed. Though I had little background in organic geochemistry, they seemed inexplicably excited to take me on as a student and to let me work in a second area – marine microbiology – in which I had even less experience. Their leap of faith has proved very rewarding for me, and I'll be forever grateful that they took it. It would be an honor to work with one scientist of their caliber, but it has been my good fortune to work with two. I am deeply inspired by their passionate dedication to answering fundamental questions about how microbial life drives and shapes our planet.

Trying to bridge disciplines can be, at turns, exhilarating, frustrating, and terrifying – like most experiences that help people grow. Roger and Ed have patiently helped me through a few iterations of each of those stages while guiding my thesis research and fostering my development as a scientist.

I have also benefitted from time spent with the outstanding groups of researchers that both Ed and Roger have drawn together in their labs. Learning the once foreign languages of mass spectrometry and metagenomics would have been impossible - and far less fun - without them. In the DeLong lab I was especially lucky to work with John Eppley, Tracy Mincer, Jay McCarren, Frank Stewart, Jess Bryant, Julie Maresca and Chon Martinez, all of whom graciously answered the sometimes stupid questions of a newcomer to the field without disdain, and were always generous with their time. Similarly, Alex Bradley, Gordon Love, Amy Kelly, Lindsay Hays and Laura Sherman quickly and cheerfully eased the steepness of the organic geochemistry learning curve for me in my early days in the Summons lab. Florence Schubotz has been an invaluable source of LCMS wisdom in the last few years.

At MIT I have been given the opportunity and freedom to explore the exciting interface between geochemistry and environmental microbiology. When at a loss to explain what I do in just one word, as hyphens and prefixes (bio-geo-eco-oceano-meta-chem-microbio ... ologist?) run through my head, I recall what Maria Zuber told my entering class during orientation: "Nature doesn't care what you call yourself; just follow the interesting questions." That spirit infuses groundbreaking

interdisciplinary research across EAPS and, especially, in the E25 geobiology community. It was wonderful to witness it grow and flourish, especially with the arrival of Tanja Bosak and Shuhei Ono. I have appreciated both the discussions I have had with them and their lab members and the ready access they granted me to their labs. Many times their centrifuge/plate reader/flowhood/balance/lysozyme etc. saved the day! Rick Kayser in the Boyle lab has also been a great resource.

EAPS also has great administrative staff, without whom I would have been lost. Many thanks to Vicki McKenna, Carol Sprague, Jacqui Taylor and Allison Provaire in the Green Building. In E25 Alla Skorokhod, Mary Eliff and Lesly Adkins-Shellie guided me through paperwork and shipping emergencies, and offered me candy, sympathy and advice on many occasions.

I spent a lot of time in my first few years in Woods Hole and am grateful to have had the opportunity to work closely with Joan Bernhard, Dan McCorkle and Helena Filipsson there. Helen Fredricks, Melissa Soule and Sean Sylva were cheerful and invaluable fonts of technical wisdom in Fye. I miss the meals, beers and rants shared with WHOI friends, especially James Saenz, Laura Hmelo, Dave Griffith, Maya Bhatia, Eoghan Reeves, and Fern Gibbons. Thanks especially to Fern and Maya for letting me stay with you so often!

Oceanography is inherently collaborative. I participated in six research cruises during my Ph.D. and none of the work presented here would have been possible without the expertise, support and friendship of the many people with whom I have gone to sea. I was lucky to work with DeLong labmates Jess Bryant, Liz Ottesen, Frank Stewart, Jay McCarren, and Adrian Sharma in the field, but am also indebted to a large cast of collaborators, support scientists and crew, especially: Stefan Sievert, Osvaldo Ulloa, Gadiel Alarcon, Alejandra Prieto-Davo, Sam Wilson, Julie Robidart, Tara Clemente, Blake Watkins, and Cesar Hormazabal Fritz.

My time at C-MORE Hale in Manoa was productive, and I appreciate the access that David Karl and the other scientists gave me to their labs and resources. More generally, I have benefitted greatly from participation in the Center for Microbial Oceanography: Research and Education (C-MORE), and it has been great to see how science operates at that scale. I am thankful to both C-MORE and the Agouron Institute for funding my thesis research through grants to Ed and Roger. Other funding that made this work possible came from the Linden Earth System Fellowship, the Martin Family Society of Fellows for Sustainability, the Geological Society of America, the American Philosophical Society, and the American Association of Petroleum Geologists.

I am grateful to Jürgen Rullkötter for opening his lab in Oldenburg to me on several occasions. It was there that I learned most of what I know about polar lipids, and I enjoyed working with his students Jörn Logemann and Michael Seidel. Bernd

Kopke provided great technical support and advice. Contact with members of Kai Hinrichs's lab in Bremen has also been valuable; in particular, Julius Lipp and Xiaolei Liu have been very kind and helpful.

Both the Summons and DeLong labs have skilled technicians who enable us to see our research ideas become reality. Carolyn Colonero, Tsultrim Palden, and Rachel Barry all gave me invaluable personalized help, well beyond their general responsibilities keeping things running. I also extend thanks to all lab members past and present – far too many to list here – for making my time at MIT intellectually stimulating and fun.

The people I have met at MIT have made my experience here so much richer. I've especially valued my friendships with Alex Bradley, Jess Fitzsimmons, Jess Bryant, Julie Maresca, Amy Kelly, Anthony Carrasquillo, Dave Griffith, Flo Schubotz, Aimee Gillespie, Marie Giron, Sharon Newman, Ross Williams, Christian Illing, and Changqun Cao. Neighbors Kris Ellis, Ilan Levy, Martin Duennwald, Gilbert Morian, and Judith Staerk became dear friends and made Cambridge home. The teachers who inspired and encouraged me also deserve thanks, from my undergraduate mentor David Fastovsky back to Gary Haffeman, the grade school teacher who humored me in my very first incubation experiments investigating the effect of acid rain on algae (strangely similar to what I do today). Kate Freeman, Laurence Bird, Heather Graham and Eliot Codner have helped smooth my transition from MIT to Penn State, where I will do postdoctoral research. Thanks, everyone.

My deepest gratitude is for my family. My brother Bradley Lincoln and brother-in-law Peter Duckler have provided a great deal of emotional support throughout graduate school. Without the love and early encouragement our entire family gave me to pursue my wide and ever-changing interests, I would be living a much less interesting life – and certainly would not have had the imagination to pursue this research. I regret that I cannot share this thesis with my father, John Lincoln, who used to tell me fantastical stories of things like the shallow seas that once covered our land and rocks that were made of animals.

Contents

Chapter 1

Introduction

Microbes have driven fundamental cycles of matter and energy on Earth for billions of years. They sometimes leave a record of their activity in the form of fossil organic molecules –biomarkers–that can be valuable tools for understanding the environments that they have helped to shape. Interrogation of the biomarker record has provided information about pivotal events and processes in Earth history, such as mass extinction mechanisms (Grice et al., 2005), the rise of atmospheric oxygen (Summons, Jahnke, Hope, & Logan, 1999), and the evolution of eukaryotes (Brocks, 1999). The sedimentary record is, however, imperfect; only a small fraction of organic matter is preserved, and it is preserved and transformed with bias. In addition to such geological caveats, an incomplete understanding of the biosynthesis, phylogeny, and environmental distributions of many biomarkers can also hinder our ability to interpret and employ them with confidence. Continued investigation of these factors is important for validating the assumptions that underlie specific biomarker applications, refining their utility, and, ultimately, leading to a more robust toolkit for paleoenvironmental and ecological studies.

In this thesis I have sought to improve our understanding of a ubiquitous yet enigmatic class of microbial biomarkers: tetraether membrane lipids of marine archaea, collectively termed glycerol dialkyl glycerol tetraether (GDGT) lipids (Fig. 1). Since the discovery that members of the domain Archaea are widespread in the

oceans (Delong, 1992; Fuhrman, 1992), numerous studies have confirmed their abundance. Once thought to be obligate extremophiles requiring high temperatures, acidic environments, or hypersaline conditions, archaea are now known to be cosmopolitan. Cultivation-independent surveys revealed that archaea inhabit all marine environments, spanning the euphotic zone (Frigaard, Martínez, Mincer, & Delong, 2006), the mesopelagic (Karner, Delong, & Karl, 2001; Massana, Murray, Preston, & DeLong, 1997), and the benthos (Biddle et al., 2006). Their range includes tropical to polar and coastal to oligotrophic waters.

Archaea synthesize ether-linked isoprenoidal lipids that contain 2,3-*sn*-*g*lycerol stereochemistry rather than bacterial 1,2-*sn*-glycerol (Fig. 2). Tetraether forms of these lipids (GDGTs) have been detected as frequently in the modern oceans as archaeal nucleic acids (Schouten, Hopmans, & Damsté, 2012), and their presence in black shales (Kuypers et al., 2001) provides evidence that archaea have been active in the oceans since at least the mid-Cretaceous. Generally, marine GDGTs are assumed to be derived from chemolithoautotrophic Marine Group I Thaumarchaeota (MG-I; (Schouten et al., 2012), but the possibility that Marine Group II Euryarchaeota (MG-II) also contribute to the GDGT pool has been raised (Turich et al., 2008; Turich, Freeman, Bruns, & Conte, 2007) and debated (Schouten, van der Meer, Hopmans, & Damsté, 2008).

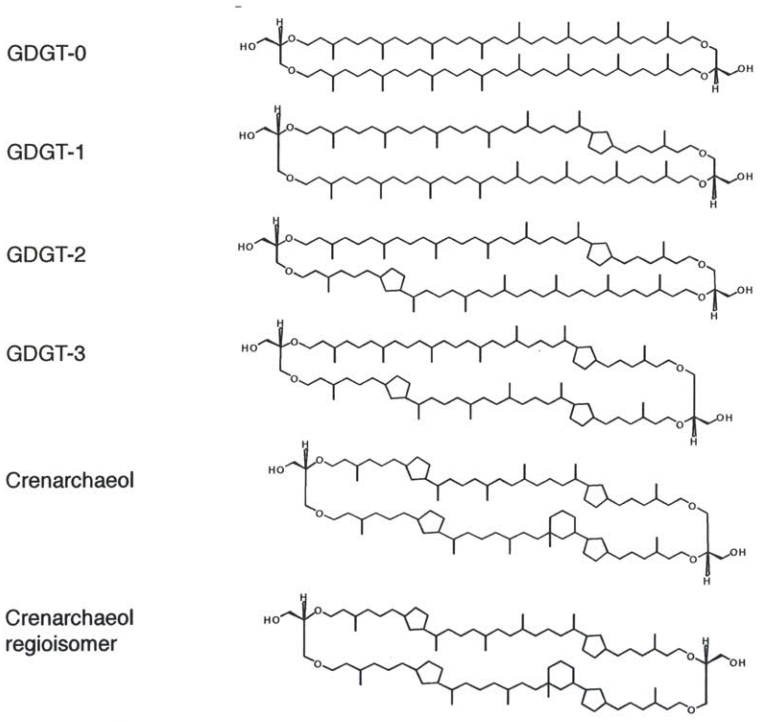

Fig. 1. Structures of core glycerol dialkyl glycerol tetraether (GDGT) molecules discussed in text.

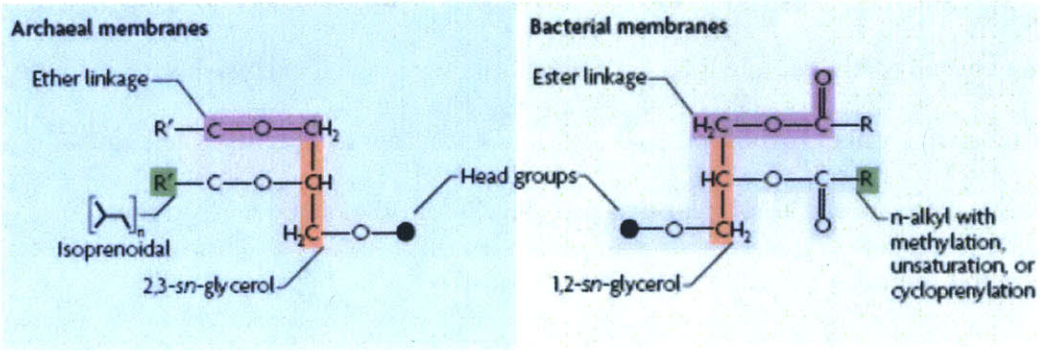

Fig. 2. Features distinguishing archaeal and bacterial membrane lipids.

(Valentine, 2007).

In the time since GDGTs were first identified in the oceans (DeLong et al., 1998), these compounds have been analyzed with increasing frequency in the water column and sediments. Such exploration and expansion was fueled in large part by the popularity of the TEX_{86} (tetraether index of 86 C atoms) paleotemperature proxy that is based on sedimentary distributions of individual GDGTs with different numbers of cyclohexane moieties (Schouten, Hopmans, Schefuß, & Sinninghe Damsté, 2002). Core-top calibration studies show a strong correlation between TEX_{86} and sea surface temperature (Kim, Schouten, Hopmans, Donner, & Sinninghe Damsté, 2008), but the mechanisms underlying the proxy are poorly understood (Pearson & Ingalls, 2013).

A second major motivation for measuring GDGTs is to understand the *in situ* ecology and metabolism of uncultivated marine archaeal clades. Carbon isotopic studies have been especially useful in that regard, yielding an estimate that marine archaea are 83% autotrophic at depth (Ingalls et al., 2006).

To date, both ecological and paleoenvironmental studies employing GDGTs have generally assumed that MG-I are their primary or even exclusive source in the marine environment (Schouten et al., 2012). Tetraether lipid biosynthesis is, however, widespread among the archaea (Fig. 3) and the trait occurs in the *Thermoplasmatales*, the closest relatives of MG-II.

The question of whether MG-I, MG-II or both groups synthesize GDGTs is critical because these groups are very different: MG-I are chemolithoautotrophs, fixing carbon via energy obtained from the oxidation of ammonia (Könneke et al.,

2005), while MG-II appear to be strictly heterotrophic (Iverson et al., 2012). Understanding what factors drive each population should thus provide insight into global carbon cycles in which marine archaea must be significant agents, if only by virtue of their abundance and ubiquity.

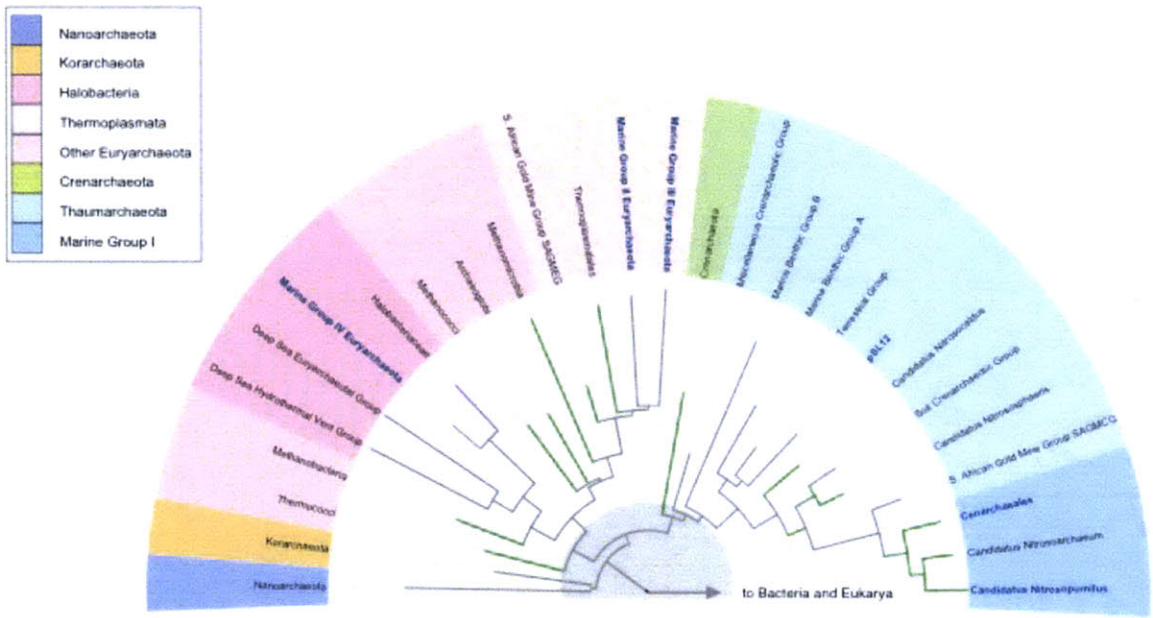

Fig. 3

Maximum likelihood phylogenetic tree of Archaea, constructed in ARB (Ludwig et al., 2004)using PhyML (Guindon et al., 2010) with the Jukes-Cantor 69 substitution model and a customized base frequency filter ignoring positions in which special characters and ambiguity codes appear most often. Green lines indicate clades within which at least one member is known to synthesize GDGTs.

The gray region at the base of clades indicates a region with unstable / unsupported branching.

Thesis foci

In this thesis I have used an interdisciplinary approach to investigate the sources and significance of marine archaeal lipids in the water column. Specifically, I have tried to address the following questions using tools of molecular biology, metagenomics and organic geochemistry.

(1) What factors influence the distribution of MG-I and MG-II, the two most abundant groups of marine archaea?

(2) Can the lipids of Marine Group I Thaumarchaeota and Marine Group II Euryarchaeota be deconvolved? Are there any lipid motifs unique to either group?

(3) What are the responses of MG-I and MG-II to organic matter and bicarbonate amendments, and are they reflected in the lipid composition? Is it possible to induce a community shift toward either group in bulk seawater? Can changes in the composition and metagenome of the broader microbial community be informative about the fate of GDGTs?

(4) What are the sources of tetraether lipids in alkaline hydrothermal vent system, how should they be interpreted, and what are the implications for vent ecology and paleoproxies?

In Chapter 2 I address **1-2** in a study of a depth profile of size-fractionated suspended particulate organic matter collected in the North Pacific Subtropical Gyre using 16S rDNA amplicon sequencing, QPCR, metagenomics and lipid analysis. MG-II was most abundant at shallow to intermediate depths, more diverse than MG-I, and may show a slightly greater tendency toward particle association. Most significantly, I present evidence that MG-II synthesizes GDGTs, including crenarchaeol – until this work, a biomarker thought to be exclusive to MG-I.

In Chapter 3 I address **1-3**, finding that an organic matter amendment appeared to induce both an archaeal community shift and a change in the GDGT composition of a microcosm experiment. These changes were somewhat difficult to interpret. However, by demonstrating the power of an approach pairing metagenomics and lipid analysis to address this problem, I have laid the groundwork for future studies. Tracing functional genes along with community composition and lipids, I found potential insight into the sinks for GDGTs, as well as surprisingly high degradation rates (a 43% loss in 44 h). This finding has important implications for the interpretation of GDGTs in the water column, suggesting that "fossil" GDGT forms (lacking a polar head group) may be more closely linked to living archaeal populations than previously thought.

In Chapter 4 I address **4 and 1**. Branched (bacterial) and archaeal GDGTs including crenarchaeol were detected in carbonate chimneys of the Lost City Hydrothermal Vent Field, the most alkaline system in which branched GDGTs have been reported. These compounds, thus, are not strictly associated with acidic

environments and not likely to be derived from terrestrial soil bacteria in all cases. These results have implications for paleoproxies that use branched GDGTs to determine the amount of terrestrial input to marine sediments. When possible, GDGTs in this study were tentatively assigned to source microbes.

Taken as a whole, the work presented here emphasizes the necessity of understanding the biological bases and sources of biomarkers used in geochemical applications. Experimental research in environmental microbiology, linked with geochemical measurements, holds promise for efforts to understand drivers of marine archaeal populations and the biomarker legacy they leave in the geologic record.

References

Biddle, J. F., Lipp, J. S., Lever, M. A., Lloyd, K. G., Sorensen, K. B., Anderson, R., et al. (2006). Heterotrophic Archaea dominate sedimentary subsurface ecosystems off Peru. *PNAS, 103*(10), 3846–3851. doi:10.1073/pnas.0600035103

Brocks, J. J. (1999). Archean Molecular Fossils and the Early Rise of Eukaryotes. *Science, 285*(5430), 1033–1036. doi:10.1126/science.285.5430.1033

Delong, E. F. (1992). Archaea in coastal marine environments. *Proceedings of the National Academy of Sciences, 89*(12), 5685–5689. Retrieved from http://www.pnas.org/content/89/12/5685.full.pdf

DeLong, E. F., King, L. L., Massana, R., Cittone, H., Murray, A., Schleper, C., & Wakeham, S. G. (1998). Dibiphytanyl ether lipids in nonthermophilic crenarchaeotes. *Applied and Environmental Microbiology, 64*(3), 1133–1138.

Frigaard, N.-U., Martínez, A., Mincer, T. J., & Delong, E. F. (2006). Proteorhodopsin lateral gene transfer between marine planktonic Bacteria and Archaea. *Nature,*

439(7078), 847–850. doi:10.1038/nature04435
Fuhrman, J. A. (1992). Novel major archaebacterial group from marine plankton. *Nature, 356*(6365), 148–149.
Grice, K., Cao, C., Love, G. D., Böttcher, M. E., Twitchett, R. J., Grosjean, E., et al. (2005). Photic zone euxinia during the Permian-Triassic superanoxic event. *Science, 307*(5710), 706–709. doi:10.1126/science.1104323
Guindon, S., Dufayard, J.-F., Lefort, V., Anisimova, M., Hordijk, W., & Gascuel, O. (2010). New algorithms and methods to estimate maximum-likelihood phylogenies: assessing the performance of PhyML 3.0. *Systematic biology, 59*(3), 307–321. doi:10.1093/sysbio/syq010
Ingalls, A. E., Shah, S. R., Hansman, R. L., Aluwihare, L. I., Santos, G. M., Druffel, E. R., & Pearson, A. (2006). Quantifying archaeal community autotrophy in the mesopelagic ocean using natural radiocarbon. *Proceedings of the National Academy of Sciences, 103*(17), 6442–6447.
Iverson, V., Morris, R. M., Frazar, C. D., Berthiaume, C. T., Morales, R. L., & Armbrust, E. V. (2012). Untangling Genomes from Metagenomes: Revealing an Uncultured Class of Marine Euryarchaeota. *Science, 335*(6068), 587–590. doi:10.1126/science.1212665
Karner, M. B., Delong, E. F., & Karl, D. M. (2001). Archaeal dominance in the mesopelagic zone of the Pacific Ocean. *Nature, 409*(6819), 507–510. doi:10.1038/35054051
Kim, J.-H., Schouten, S., Hopmans, E. C., Donner, B., & Sinninghe Damsté, J. S. (2008). Global sediment core-top calibration of the TEX86 paleothermometer in the ocean. *GEOCHIMICA ET COSMOCHIMICA ACTA, 72*(4), 1154–1173. doi:10.1016/j.gca.2007.12.010
Könneke, M., Bernhard, A. E., la Torre, de, J. R., Walker, C. B., Waterbury, J. B., & Stahl, D. A. (2005). Isolation of an autotrophic ammonia-oxidizing marine archaeon. *Nature, 437*(7058), 543–546. doi:10.1038/nature03911
Kuypers, M. M., Blokker, P., Erbacher, J., Kinkel, H., Pancost, R. D., Schouten, S., & Damsté, J. S. S. (2001). Massive expansion of marine archaea during a mid-Cretaceous oceanic anoxic event. *Science, 293*(5527), 92–95.
Ludwig, W., Strunk, O., Westram, R., Richter, L., Meier, H., Buchner, A., et al. (2004). ARB: a software environment for sequence data. *Nucleic acids research, 32*(4), 1363–1371. doi:10.1093/nar/gkh293
Massana, R., Murray, A., Preston, C., & DeLong, E. (1997). Vertical distribution and phylogenetic characterization of marine planktonic Archaea in the Santa Barbara Channel. *Applied and Environmental Microbiology, 63*(1), 50–56.
Pearson, A., & Ingalls, A. E. (2013). Assessing the Use of Archaeal Lipids as Marine Environmental Proxies. *Annual Review of Earth and Planetary Sciences, 41*(1), 359–384. doi:10.1146/annurev-earth-050212-123947
Schouten, S., Hopmans, E. C., & Damsté, J. S. S. (2012). The organic geochemistry of glycerol dialkyl glycerol tetraether lipids: a review. *Organic Geochemistry*, 1–183. doi:10.1016/j.orggeochem.2012.09.006
Schouten, S., Hopmans, E. C., Schefuß, E., & Sinninghe Damsté, J. S. (2002).

Distributional variations in marine crenarchaeotal membrane lipids: a new tool for reconstructing ancient sea water temperatures? *Earth and Planetary Science Letters, 204*(1), 265–274.

Schouten, S., van der Meer, M. T. J., Hopmans, E. C., & Damsté, J. S. S. (2008). Comment on "Lipids of marine Archaea: Patterns and provenance in the water column and sediments" by Turich et al. (2007). *GEOCHIMICA ET COSMOCHIMICA ACTA, 72*(21), 5342–5346. doi:10.1016/j.gca.2008.03.028

Summons, R., Jahnke, L., Hope, J., & Logan, G. (1999). 2-Methylhopanoids as biomarkers for cyanobacterial oxygenic photosynthesis. *Nature.*

Turich, C., Freeman, K. H., Jones, A. D., Bruns, M. A., Conte, M., & Wakeham, S. G. (2008). Reply to the Comment by S. Schouten, M. van der Meer, E. Hopmans, and J.S. Sinninghe Damsté on "Lipids of marine Archaea: Patterns and provenance in the water column." *GEOCHIMICA ET COSMOCHIMICA ACTA, 72*(21), 5347–5349. doi:10.1016/j.gca.2008.04.042

Turich, C., Freeman, K., Bruns, M., & Conte, M. (2007). Lipids of marine Archaea: Patterns and provenance in the water-column and .... *et Cosmochimica Acta.*

Valentine, D. L. (2007). Adaptations to energy stress dictate the ecology and evolution of the Archaea. *Nature Publishing Group, 5*(4), 316–323.

Chapter 2

Planktonic Euryarchaeota are a major source of archaeal tetraether lipids in the ocean

Abstract

Archaea are ubiquitous marine plankton, and the presence of fossil forms of their tetraether membrane lipids in sedimentary rocks indicates their active participation in marine biogeochemical cycles for more than 100 million years. Cultivation-independent surveys have identified four major clades of planktonic archaea, but to date tetraether lipids have been characterized in only one, the ammonia-oxidizing Marine Group I Thaumarchaeota (MG-I). The membrane lipid composition of the other planktonic archaeal groups – all uncultured Euryarchaeota – is unknown. Using 16S rDNA pyrotag sequencing, metagenomics, qPCR, and mass spectrometric analyses, we found that Marine Group II Euryarchaeota (MG-II) contributed significantly to the tetraether lipid pool in the North Pacific Subtropical Gyre at shallow to intermediate depths. Both MG-I and MG-II DNA were most abundant in the small size fraction of suspended particulate matter (SPM), while tetraether lipids were concentrated in the large fraction, suggesting both groups are predominantly free-living and that aggregation of detrital cell material into larger SPM is a likely pathway for tetraether lipid export. Our data also suggest that MG-II synthesize crenarchaeol, a tetraether lipid previously considered to be diagnostic for Thaumarchaeota. Metagenomic datasets spanning five years indicated that the stratification of planktonic archaeal groups is a stable feature in the NPSG. The consistent predominance of MG-II at depths at which the bulk of exported organic matter originates, together with their broad distribution across diverse oceanographic provinces, suggests they are a significant source of tetraether lipids to marine sediments. These findings have important implications for the use of archaeal lipids in microbial ecology and their interpretation in the geologic record.

---

* For submission to Proceedings of the National Academy of Sciences of the United States of America, August 2013.

Lincoln, S.A., Wai, B., Church, M.J., Summons, R.E., and DeLong, E.F., 2013. Planktonic Euryarchaeota are a major source of archaeal tetraether lipids in the ocean.

Since their discovery in the oceans (1, 2), ubiquitous planktonic archaea have been recognized as important agents in global biogeochemical cycles. Although few representatives of marine archaea have been isolated, cultivation-independent methods have provided considerable insight into their abundance and ecological distributions. In addition to phylogenetic and metagenomic surveys, organic geochemical studies have detected distinctive archaeal tetraether membrane lipids (Fig. S1) throughout the oceans. These compounds, collectively referred to as glycerol dialkyl glycerol tetraethers (GDGTs), have been useful as tracers of archaeal biomass (3) and, via their isotopic composition, have provided new information about archaeal community carbon metabolism (4-6). GDGTs are relatively recalcitrant; they can be exported with little alteration to marine sediments, where their distributions have been exploited to develop proxies for reconstructing sea surface temperature (7) and terrigenous organic matter input (7, 8). On the basis of GDGT abundances in a black shale dated at 112 million years (9), it was suggested that archaea have been significant members of marine ecosystems since at least the Mesozoic Era.

Although tetraether lipids are employed with increasing frequency in paleoceanography and microbial ecology, their specific sources in the water column have not been well constrained. Of the four groups of planktonic archaea identified in the oceans, representatives of only one – the Marine Group I (MG-I) Thaumarchaeota (1, 10, 11), previously classified as Crenarchaeota – have been isolated. All MG-I strains isolated to date are chemolithoautotrophic, fixing

inorganic carbon using energy obtained from the oxidation of ammonia to nitrite (12). Recent evidence suggests that MG-I contribute to the flux of potent greenhouse gases nitrous oxide (13) and methane (14) from the water column to the atmosphere. The membrane lipid assemblage of MG-I Thaumarchaeota includes GDGTs with 0-4 cyclopentyl moieties and crenarchaeol, a GDGT containing one cyclohexyl and 4 cyclopentyl moieties (15). Crenarchaeol has been considered uniquely diagnostic for Thaumarchaeota (16) and, by extension, has been postulated as a biomarker for archaeal nitrification (17).

In addition to MG-I Thaumarchaeota, three other groups of archaea – all Euryarchaeota - have been reported in the marine water column: Groups II (1), III (2), and IV (18). Of these, Marine Group II Euryarchaeota (MG-II) are the most abundant and frequently detected, spanning a wide range of depths in diverse oceanographic provinces including the oligotrophic North Pacific Subtropical Gyre (19, 20); coastal California (21-23); the North Sea (24); Arctic (25, 26) and Antarctic (27-29) waters; the coastal Mediterranean Sea (30); the eastern tropical South Pacific oxygen minimum zone (31); waters surrounding a tropical atoll (32); the deep North Atlantic (33); and the East China Sea (34). The potential contribution of this cosmopolitan group to the marine tetraether lipid pool has been debated (35-38), but the lack of cultivated representatives of MG-II precludes direct analysis of their membrane lipids, and incomplete knowledge of the genetic basis of archaeal tetraether lipid biosynthesis limits the ability of metagenomic studies to address this question. High genetic diversity within MG-II (25) can also complicate efforts to

target them using group-specific probes. Despite these challenges, accurate characterization of the full archaeal community is vital for understanding the biological sources of GDGTs and interpreting their occurrence in the water column and sedimentary record.

We approached this problem using 16S rDNA pyrosequencing, qPCR and metagenomics to characterize archaeal community composition and link it to tetraether lipid distributions measured in size-fractionated suspended particulate matter in the North Pacific Subtropical Gyre (NPSG).

Results and discussion

Suspended particulate matter (SPM) for this study was collected in the NPSG in September 2011 using in situ pumps deployed at depths ranging from 11 to 559 m (Fig. S2-S3). SPM was fractionated into two size classes (0.3-3 μm and 3-57 μm) in an effort to separate the archaeal community into free-living and particle-associated/detrital components. Lipids and DNA (Fig. S4) were extracted from the same filters to facilitate comparison of GDGT and genetic datasets.

Stratification of archaeal phyla

To determine archaeal community composition we pyrosequenced amplicons of the V1-V3 region of the 16S rRNA gene in filter DNA. Data analyses focused on samples from 8 depths that yielded >1000 amplicons in each size fraction (Fig. S5-S6, Table S1), along with the 0.22-1.6 μm size fraction from 800 and 1000 m. In total this sample set contained 323,924 archaeal amplicon sequences

after curation for quality control (removal of duplicate sequences and 454 artifacts). These sequences were clustered into 4900 operational taxonomic units (OTUs) at the 97% identity level using QIIME (39). Taxonomic assignments were made by comparison to the ARB-SILVA SSU reference database using BLASTn.

The 10 most prevalent OTUs across the entire dataset, each representing >2000 amplicon sequences, were all assigned to either the Thaumarchaeota (primarily MG-I) or MG-II Euryarchaeota (Fig. 1). Among the Thaumarchaeota, OTU 4 was predominant in both size fractions of SPM and represented a higher percent of total archaeal OTUs with increasing depth. At 1000 m, however, OTU 1 had a higher relative abundance than OTU 4, and OTU 3 rose in abundance. This shift in prominent phylotypes is consistent with previous reports of genetic diversity of Thaumarchaeota in depth profiles (22).

In sharp contrast to Thaumarchaeota, MG-II represented a higher proportion of total archaeal OTUs at shallower depths, and the MG-II population was not dominated by a single phylotype (Fig.1). Rather, 4 OTUs - numbers 5,6,8, and 9 - were abundant in the 131 and 157 m samples, and OTU 9 became more prominent with depth. This intra-group stratification may reflect niche partitioning, with ecotypes bearing the light-driven proton pump proteorhodopsin (40, 41) inhabiting the photic zone, and eurybathyl ecotypes lacking proteorhodopsin dominating the MG-II community in the mesopelagic zone. Patterns of MG-II OTU abundance also vary between size classes; at 131 m, for instance, OTU 6 is more highly represented in the 3-57 μm fraction than in the 0.3-3 μm fraction. Potential explanations include

variations in ecotype cell sizes and possible free-living vs. particle-associated modes of existence.

Representative sequences of the 20 most prevalent OTUs and their three nearest neighbors from the ARB/SILVA rRNA database were aligned and a phylogenetic tree (Fig. 1) inferred. With the exception of a single sequence most closely related to Marine Benthic Group A Thaumarchaeota, all of the top 20 OTUs clustered with either MG-I or MG-II. Within MG-I, most OTUs were grouped with sequences from previous water column studies rather than sequences of isolated MG-I strains; only one OTU appeared to be closely related to *Nitrosopumilus maritimus*.

The near-binary nature of the archaeal community in the sample set enabled quantitative estimation of the MG-II population. We used community composition data derived from amplicon sequences and MG-I cell densities inferred from qPCR experiments to infer MG-II cell densities (Fig. 2A-B). MG-II vastly outnumbered MG-I throughout the photic and upper mesopelagic zones, becoming less abundant than MG-I below 268 m and 440 m in the small and large size fractions, respectively. Overall, MG-I and MG-II distributions were very similar to those reported in a previous NPSG study (42) in which MG-II rRNA-containing clones constituted a higher percent of the fosmid library than MG-I clones at 10-500 m, and peaked at 130 m. Inferred MG-II cell densities peaked at 4.2×10^6 cells/L at 157 m; this was 4 times the maximum MG-I density measured (at 440 m). We estimated that MG-II were approximately 2% of total heterotrophic microbes at 157 m.

MG-I and MG-II were both more abundant in the 0.3-3 μm than the 3-57 μm size fraction, consistent with a predominantly free-living existence. The two MG-I profiles (Fig. 2A-B) each showed a gradual increase in cell density with depth, possibly indicating that a small percent (10-15%) of a predominantly free-living Thaumarchaeotal population is consistently captured on the large filters during sampling or incorporated into aggregates in the water column. Some fraction of DNA in the large size class may be derived from dormant or dead but intact cells that have been incorporated into larger particles, but nucleic acid degradation is expected to be rapid in the oligotrophic ocean.

MG-II profiles, unlike those of MG-I, differ between size fractions, with the cells captured on the large filter ranging from 2-90% of the total MG-II detected at a given depth. This high variability may be related to differences in cell size and the extent of particle association between ecotypes, as MG-II have been reported to be pleomorphic and larger than MG-I cells. We cannot, however, exclude a role for differences in the concentration, size and coherence of particles over the depth profile.

Tetraether lipid distributions and partitioning

Core GDGT molecules (Fig. S1) are composed of two isoprenoidal C_{40} hydrocarbon cores linked to glycerol by ether bonds at each end. Many GDGTs contain internal cyclopentyl moieties, and crenarchaeol has an additional 6-membered ring (Fig. S1). In intact polar lipid (IPL) GDGTs glycerol is linked to polar head groups, which are often hexose moieties (Fig. 2E). Because polar head groups

have been found to degrade rapidly after cell death (43, 44), IPLs are generally considered indicators of live biomass; only a small proportion of GDGTs in live cells are thought to exist as free core GDGTs. Sample processing, storage and analysis may also convert some IPL GDGTs to cores.

We measured core GDGT concentrations in lipid extracts using high performance liquid chromatography - atmospheric pressure chemical ionization (APCI) mass spectrometry (45, 46). Free core GDGTs (Fig. 2 C-D) were most abundant in the large size fraction, where their concentrations ranged from 16-490 pg/L. They reached an upper water column maximum at 331 m but the highest concentration was measured at 559 m. Similar partitioning, with a higher proportion of core GDGTs detected in the larger size fraction, was reported in a study of size-fractionated SPM collected in Puget Sound (47). In the small size fraction NPSG samples free GDGT concentrations were 1-20 pg/L and peaked at 157 m. Notably, 157 m is the depth at which MG-II were inferred to be most abundant.

Marine euryarchaeota contain crenarchaeol and other tetraether lipids

To investigate the influence of archaeal community composition on the composition of GDGT pools, we focused on two small size class samples that were dominated by either MG-I or MG-II: 131 m, in which 98% of amplicon sequences were identified as MG-II; and 559 m, in which 83% of the amplicon sequences were identified as MG-I.

Several series of very late eluting peaks were prominent in extracted ion chromatograms of masses corresponding to GDGTs 0-3 and crenarchaeol in both of these samples (Fig. 3, Fig. S7), but were absent from most other small size class and all large size class samples. Within each series, the order of retention times was identical to that of commonly detected free GDGTs. Because they eluted at the stage of analysis at which HPLC eluents are most polar, we postulated that these peaks represented IPL GDGTs that lost their head groups during in-source fragmentation in the mass spectrometer. A hydrolysis experiment supported the IPL GDGT hypothesis: after the extracts were treated with hydrochloric acid (48), the late-eluting peaks disappeared and the peak areas of core GDGTs increased (Fig. 3, Fig. S7). This difference was most pronounced in the 131 m sample, in which concentrations of IPL-bound GDGTs including crenarchaeol (Fig. 2C) exceeded those of free core GDGTs by more than an order of magnitude.

Variations in head group structure and composition are likely to cause the observed chromatographic separation of putative IPLs with identical core GDGTs, resulting in the multiple series of late eluting peaks observed in these two samples. To investigate head group composition, we used the core GDGT method (using atmospheric pressure chemical ionization (APCI)) to analyze several environmental extracts in which IPL GDGTs with either glycosyl or phosphatidyl head groups were previously detected using established electrospray ionization (ESI) methods for IPL analysis (49, 50). Only monoglycosyl GDGTs appeared in the analytical window, creating late-eluting peaks with retention times similar to those seen in our two

NPSG samples. Thus, these samples likely contain IPL GDGTs with several different hexose isomers as head groups. We cannot, however, exclude the possibility that they also contain more polar IPL GDGTs that are outside the window of detection of the core method.

The identification of monoglycosyl crenarchaeol in the 131 m and 559 m samples was confirmed by measurements using an established IPL method (50) on an accurate-mass quadrupole time of flight mass spectrometer (Fig. S8). This IPL method could not resolve the putative diversity of GDGT head groups detected using the extended core GDGT method, so the latter may prove useful in further exploration of the identity of these polar moieties.

Several lines of convergent evidence indicate that MG-II Euryarchaeota are a major source of tetraether lipids in the NPSG. First, IPL-bound GDGTs, established biomarkers for living archaea (49, 51-53), were detected in the sample collected at 131 m depth, where the archaeal community was comprised nearly exclusively of MG-II. Second, free core GDGTs were detected in both SPM size fractions at multiple depths at which MG-II predominated (Fig. 2). Although the majority of free core GDGTs are likely derived from membranes of dead cells, the shared maxima of GDGTs and MG-II cell densities at 157 m suggests a close connection between these core GDGTs and live cells. The free core GDGT pool in this sample may be dominated by GDGTs from MG-II cells that have recently died, perhaps even as a result of physical and chemical stress induced by filtration and exposure to enzymes in organic matter concentrated on filters during pump deployments. Minor

contributions from core GDGTs associated with viable cells or dissociated from detrital cell matter in the larger size fraction are also possible. In any case, free core GDGTs detected in a given sample must be derived from archaea that lived at or above the depth at which it was collected.

NPSG distributions of MG-I and MG-II similar to those determined from amplicon data were reported in a previous study using samples collected in 2002-2004 (42); this continuity suggests that the pattern of MG-II dominance in the upper open ocean is not ephemeral. To improve the temporal resolution of the historical record, we queried datasets from four metagenomic profiles and one metatranscriptomic profile generated from SPM collected in the NPSG between March 2006 and September 2009. This approach was greatly facilitated by the addition of the first fully assembled MG-II metagenome (41) to the reference database. Subsequent analysis of the relative contributions of Euryarchaeota and Thaumarchaeota to total protein-coding reads (Fig. S9) revealed a pattern similar to that seen in the amplicon dataset. Thus, consistent depth distributions determined from fosmid, amplicon and metagenomic datasets generated from samples spanning nearly a decade all indicate that Euryarchaeotal dominance in the upper ocean is a permanent feature in the NPSG.

Our finding that Euryarchaeota are a major source of GDGTs in the marine water column is in retrospect not so surprising, considering that tetraether lipid biosynthesis – a broadly but not universally distributed trait among Euryarchaeota

– is ubiquitous among the Thermoplasmatales (54), the cultivars most closely related to MG-II.

Biosynthesis of crenarchaeol by MG-II was previously proposed on the basis of water column GDGT distributions (38, 55). Although it has been postulated as a biomarker for archaeal nitrification, to date there is no evidence of molecular interactions between crenarchaeol and the membrane-bound enzyme ammonia monooxygenase that catalyzes ammonia oxidation. A role for the cyclohexyl moiety in maintaining tetraether membrane fluidity at low temperatures, possibly enabling the expansion of thermophilic MG-I from hydrothermal environments to the open ocean, was proposed (9, 56) but countered by the subsequent detection of crenarchaeol in hot springs (57, 58) and thermophilic MG-I isolates (17, 59). The richest and most robust biomarkers are those that can be linked to physiological processes in known taxa; in the case of crenarchaeol no such connection has been established, and the molecule now appears to be less taxonomically specific than previously thought.

Although crenarchaeol biosynthesis has been confirmed in MG-I isolates (e.g. 15), determining its sources - and sources of other tetraether lipids - in the environment has been challenging. Previous studies examining correlations between crenarchaeol and MG-I 16S or amoA gene transcript copy numbers were likely compromised by an early focus on core rather than IPL GDGTs and the use of filters with different pore sizes for collection of lipids and nucleic acids or cells for fluorescence in situ hybridization. More importantly, few studies have attempted to

quantify MG-II or characterize the broader archaeal community in conjunction with lipid studies, missing information vital to efforts to evaluate potential contributions of diverse members of heterogeneous marine archaeal populations to the GDGT pool. The absence of an apparent correlation between community composition and the relative proportions of individual GDGTs detected in this study (Table 1) suggests that it may not be possible to structurally deconvolve marine planktonic GDGT pools in the case of mixed archaeal populations.

Geological and ecological implications

Together with the widespread predominance of MG-II in the epipelagic zone, where exported GDGT signals have been reported to originate (60, 61), our finding that MG-II are a source of tetraether lipids suggests that a significant percent of GDGTs delivered to sediments may be synthesized by Euryarchaeota rather than Thaumarchaeota. This paradigm shift has important implications for the interpretation of archaeal tetraether lipids in the geologic record.

A recently developed paleotemperature proxy, TEX_{86} (tetraether index of 86 carbon atoms), relies on an empirical relationship between sea surface temperature (SST) and relative abundances of GDGTs in sediments that are presumed to be derived from planktonic Thaumarchaeota (7, 62). Although TEX_{86} is now widely used in paleoceanography and core top calibration studies have found correlations between temperatures inferred with it and SSTs to be strong (62), mechanisms underlying the proxy remain poorly understood (63). One critical but as yet unresolved issue is how SST signals can be closely reflected in the membrane lipid

composition of planktonic Thaumarchaeota, which are typically less abundant in epipelagic than mesopelagic waters, where less exported organic matter originates. Tetraether lipid biosynthesis by MG-II provides a possible solution: if temperature affects the membrane lipid composition of MG-II, MG-II GDGTs are more likely than those of deeper-dwelling MG-I to reflect sea surface temperatures. Significant physiological differences between the groups, however, may complicate this scenario. Heterotrophic MG-II populations are likely influenced by very different ecological factors than those that impact chemolithoautotrophic MG-I populations. For instance, the extremely high specific affinity of the MG-I representative *N. maritimus* for reduced nitrogen enables it to grow exponentially under nutrient-limited conditions similar to those of the oligotrophic ocean (64); it appears unlikely that MG-I are ever truly ammonia or carbon limited in the marine water column. Seasonal changes in MG-I abundances have been reported, but no clear evidence of what drives them has emerged (e.g. 60). Heterotrophic MG-II populations, by contrast, likely respond to changes in organic matter availability, and their abundances have been observed to vary seasonally (e.g. 27). Reinterpreting a previously reported correlation between fluxes of GDGTs and phytol (61), a constituent of the chlorophyll molecule and phytoplankton biomarker, we suggest that phytoplankton blooms may both promote MG-II growth by providing a carbon substrate and increase GDGT export via formation of sinking particles that may entrain MG-II cells or cell detritus in the upper ocean.

Because TEX_{86} relies on relative rather than absolute abundances of GDGTs to estimate SST it may in theory be immune to changes in GDGT flux or changes in community composition, provided that temperature is the only factor influencing archaeal membrane lipid composition in the ocean. This assumption is probably simplistic, since the tetraether lipid composition of cultured archaea has been observed to change with factors such as pH (65). Moreover, the high degree of genetic diversity within MG-II raises uncertainty over whether lipids of members of this group are likely to show a uniform response to changes in environmental variables.

Analyses of one sample in this study (440 m, small size fraction) underscored the point that our understanding of factors influencing the relative proportions of GDGTs in the ocean water column is incomplete. GDGTs in this sample showed an atypical marine pattern (Fig. S10), with GDGT-2 more abundant than GDGT-0 or crenarchaeol – yet the archaeal community was dominated by the same MG-I OTU as at other depths with similar in situ temperatures. Neither temperature nor community composition seem likely explanations for this unusual GDGT signal, although the full genetic diversity of MG-I ecotypes is unlikely to be reflected in 16S rDNA data.

On a broader level, a mixed biological origin for GDGTs detected in marine sediments may confound attempts to develop new paleoceanographic tools that employ them. A recent attempt to detect marine carbon isotope excursions by measuring the C isotopic composition ($\delta^{13}C$) of GDGTs (66)made the assumption

that these compounds were synthesized by autotrophic Thaumarchaeota, and argued that the $\delta^{13}C$ of GDGTs should closely reflect the $\delta^{13}C$ of the dissolved inorganic carbon (DIC) substrate. If, however, heterotrophic Euryarchaeota also contributed to the GDGT pool (as appears likely from our results) the isotopic signal would be mixed, reflecting the $\delta^{13}C$ of their organic carbon substrates as well as that of DIC.

Prospectus

Enrichment and isolation of representatives of MG-II would greatly aid attempts to understand the ecology, physiology and membrane lipid composition of this group, as would the full elucidation of the genetic basis of GDGT biosynthesis. However, paired nucleic acid and lipid studies of mixed communities in bulk seawater also hold promise for illuminating which conditions favor certain MG-II phylotypes over other MG-II or MG-I phylotypes, and what concurrent impacts on the GDGT pool may be. Carbon isotope analyses of natural communities may be less informative. Radiocarbon studies are unable to distinguish between autotrophic and heterotrophic archaea in the epipelagic ocean (4). The stable carbon isotopic composition of GDGTs could be difficult to interpret if MG-II are heterotrophic specialists consuming proteins (41), which are typically enriched in ^{13}C relative to other compound classes and bulk biomass in the Pacific (67); in that case, MG-II GDGTs could be isotopically indistinguishable from those of autotrophic MG-I utilizing dissolved inorganic carbon (DIC). Further complicating the outlook for the

study of natural isotopes of GDGTs, the MG-II genome also encodes genes for degrading lipids (41), which are depleted in ^{13}C relative to bulk biomass (67).

Isotopically labeled tracer experiments hold more promise. Early microcosm studies using ^{13}C labeled bicarbonate amendments were valuable in predicting the physiology of MG-I communities (6, 68) before any representatives were isolated. Similar experiments using labeled organic substrates may prove equally informative about the physiology and membrane lipid composition of MG-II, a diverse and cosmopolitan component of marine microbial plankton.

Materials and methods

Sample Collection

Suspended particulate matter samples were collected on the BioLINCS cruise (9/6/2011- 9/21/2011, R/V Kilo Moana, Fig. S2-S3) near Hawaii Ocean Time-series Station ALOHA using in situ pumps (WTS-LV08, McLane Laboratories) equipped with three-tiered filter housings for size fractionation. Seawater was sequentially filtered through 57 μm nylon mesh (Nitex, U.S.A) and two 142 mm diameter glass fiber filters: a 3 μm glass fiber filter (Pall) and a 0.3 μm glass fiber filters (Sterlitech). Between 648 and 2096 L were filtered during deployments (2-4 h). Actual deployment depths were measured using a submersible data logger (Vemco, Canada) attached to the pumps and ranged from 11 to 559 m. Upon retrieval of

pumps, filter segments designated for DNA analysis were excised and frozen in lysis buffer (40 mM EDTA, 50 mM Tris, 0.73 M sucrose) at -80 ºC until DNA extraction. These subsamples corresponded to 20-70 L of seawater (average 50 L). Remaining filter material was wrapped in combusted aluminum foil and stored at -20 ºC until lipid extraction.

In one instance suspended particulate matter was sampled on ship for metagenomic analysis. Seawater was collected from a depth of 130 m at Station ALOHA using a conductivity-temperature-depth rosette water sampler equipped with 24 12-L sampling bottles. 20 L were filtered in series through a combusted 3μm glass fiber filter (47 mm diameter, Pall) and a 0.22 μm Sterivex filter unit (Millipore) using a peristaltic pump and platinum-fired silicone tubing (Masterflex, Cole Parmer). After filtering, excess water was removed from the Sterivex filter unit, 1.8 ml lysis buffer were added, and the sample was frozen at -80 ºC until DNA extraction.

DNA extraction

DNA was extracted from glass fiber filter sections using a Quick-Gene 610 l system (Fujifilm, Japan) and DNA tissue kit L using a modified lysis protocol. Cryovials containing filter sections stored in lysis buffer were thawed on ice and additional lysis buffer was added to bring the volume to 1.6 ml. Cryovials were vortexed for 2 minutes. Lysozyme (Fisher) dissolved in lysis buffer was added to a final concentration of 5 mg/ml, and vials were incubated with rotation at 37 ºC for

45 min. 90 µl proteinase K EDT-01 and 90 µl tissue lysis buffer MDT-01 (Fujifilm, Japan) were added and vials were incubated with rotation at 55 ºC for 2 hours. Lysate was decanted from filter material and transferred to a falcon tube. 1.8 ml Lysis Buffer LDT-01 were added, and samples were incubated with rotation at 55 ºC for 15 min. Finally, 2.4 ml >99% ethanol were added, and samples were vortexed and loaded on the Quick-Gene instrument. DNA was eluted in 400 µl and quantified using the PicoGreen dsDNA assay (Invitrogen). Yields of DNA/L across the depth profile are shown in Fig. S4.

DNA was extracted from Sterivex filter units using the same protocol, except that lysis buffer and reagents were added directly to the filter cartridge.

Quantitative PCR

QPCR assays consisted of duplicate 25 µl reactions containing: 12.5 µl 2X SYBRGreen Master Mix (Applied Biosystems), 8 µl of nuclease-free water, 2 µl of environmental DNA, and 0.5 µM final concentration of both forward (MGI_751F; 5'-GTCTACCAGAACAYGTTC) and reverse (MGI_956R; 5′-HGGCGTTGACTCCAATTG) primers. QPCR reactions were analyzed using an Applied Biosystems Real-Time PCR system 7300, following the thermal cycling reaction conditions described in Mincer et al. (22). QPCR standards consisted of serial 10-fold dilutions of a plasmid containing a 16S rRNA gene amplified from Station ALOHA environmental DNA using the primers Ar20F (21) and 1390R (22). The resulting gene copies in the standard dilution series ranged from 3x10-1 to 3x105 copies per reaction.

16S rDNA amplification and sequencing

The V1-V3 variable region of the archaeal16S rRNA gene in environmental DNA samples was amplified using the forward primer 20F 5'-TCCGGTTGATCCYGCCRG-3' (21) and the reverse primer 519R, 5'-GGTDTTACCGCGGCKGCT-3' (69). 20F was linked to a 454 adaptor, and 519R was linked to both a 454 adaptor and a barcode tag consisting of 5-7 nucleotides. Each sample was assigned a unique barcode designed by the Human Microbiome Project Working Group (http://www. hmpdacc.org/doc/HMP_MDG_454_16S_Protocol.pdf).

PCR reactions were carried out in triplicate 20 µl reactions, with each containing 2 µl environmental DNA template, 1 µl forward primer (10 µM), 1 µl B-adapter (10 µM), 13.8 µl DNAse-free water, 0.2 µl Taq DNA polymerase (Accuprime Taq Hifi, Invitrogen), and 2 µl AccuPrime Buffer II (Invitrogen) The thermal cycling program was as follows: initial hold at 95 ºC; 20 repetitions of a cycle of 95 ºC for 20 s, 60 ºC for 30 s, and 72 ºC for 5 minutes. PCR products were run on 1% agarose gel to verify amplification and confirm amplicons were of appropriate size. Plasmid DNA containing a cloned 16s MG-I sequence and DNAse-free water were used as positive and negative controls, respectively. PCR products were pooled, purified using a QIAquick PCR purification kit (Qiagen) and quantified using the PicoGreen dsDNA assay (Invitrogen). Additional PCR reactions were performed for samples that initially yielded <400 ng amplicons. Finally, 400 ng of each barcoded amplicon set were pooled in two batches, each containing 16 unique barcodes.

All samples were sequenced using the 454 Genome Sequencer (Roche). Amplicon library preparation followed the Titanium Rapid Library Preparation protocol (Roche), except that adaptor-ligated libraries were not diluted with AMPure XP beads before size selection, and 1/4 of the recommended volume of amplification primers was used for emulsion PCR. Libraries were quantified using the Titanium Slingshot kit (Fluidigm), added to emulsion PCR reactions at a concentration of 0.1 molecules per bead, and sequenced in a half plate run on a GS FLX system (Roche).

DNA from the 130 m sample collected by CTD rosette was prepared and sequenced in a quarter plate run following the GS FLX Titanium protocol.

Amplicon data analysis

The AmpliconNoise algorithm (70) was used to remove 454 sequencing errors and PCR single base errors from the amplicon dataset. QIIME scripts (39) were used to sort multiplexed reads into sets containing a single barcode. In the process, reads were filtered again, and any low quality or ambiguous reads were removed using default parameters (minimum quality score = 25, minimum/maximum length = 200/1000, no ambiguous bases allowed, and no mismatches allowed in the primer sequence). Primer and adapter sequences were removed in this step. The number of amplicon reads per sample ranged from 4 to 22,364 (Table S2). Low amplicon counts likely reflect low archaeal cell numbers at shallow depths, but may have also have stemmed from inaccuracies in template

DNA quantification or differences in amplification efficiency at any depth. To reduce noise caused by comparison of samples containing significantly different numbers of amplicon sequences, we chose to focus the study on samples from which ≥1000 archaeal sequences were amplified.

To examine the effect of this cutoff on community composition, we used BLASTn to assign the reads in each demultiplexed set to their closest relatives in the ARB-SILVA SSU reference database (top hit, e values <0.001, bit score >50, ARB-SILVA release 111). All archaeal reads identified below the domain level could be binned into one of three categories: thaumarchaeota (primarily MG-I), MG-II euryarchaeota, and "other euryarchaeota" (Fig. S5-S6). The last category, including reads identified as belonging to MG-III and Unidentified Hydrothermal Vent Euryarchaeon PVA, was generally detected at low abundance at depths <130 m, but reached a maximum of 26% of the archaeal population in the 23 m, 3-57 μm size fraction sample. When a threshold of ≥100 archaeal amplicons in both size fractions was adopted, however, this category was eliminated. We adopted a still more stringent criterion requiring ≥1000 amplicons in both size fractions at a given depth because it reduced sample size disparity while preserving the general patterns of MG-I and MG-II as seen in the ≥100 amplicon plots (Fig S5-S6).

Demultiplexed sequences were clustered into operational taxonomic units (OTUs) at the 97% identity level using QIIME OTU-picking scripts based on the uclust clustering method (71). Continuing with the QIIME workflow, representative sequences for each of the 4900 OTUs were selected for downstream analysis and

taxonomy was assigned to each using the Ribosomal Database Project classifier. A matrix of OTUs in samples from focus depths (131, 157, 231, 268, 331, 440, 450, and 559 m), 800 and 1000 m (0.22-1.6 μm size fraction only) was generated and displayed as an interactive heat map. Representative sequences for the 20 most abundant OTUs (each representing >500 amplicon sequences across the focus depths) were extracted for further phylogenetic analysis. The heatmap of the 10 most abundant OTUs (representing >2000 amplicon sequences) detected at the focus depths was modified using the statistical software R (www.R-project.org) so that OTU abundance was ranked within each depth and size class, rather than across the entire matrix. Darkest shades of gray indicate the most abundant OTU in a single sample (Fig. 1).

Phylogenetic analysis

Representative sequences of the 20 most abundant OTUs were aligned with the SILVA Incremental Aligner (SINA, http://www.arb-silva.de/aligner/) using the archaea variability profile. The three nearest neighbors and selected archaeal 16S sequences (e.g. pSL12, Marine Group III) were added to the dataset for phylogenetic context. Aligned sequences were imported to a pared SSU database (SILVA release 106, non-redundant) in ARB (72). A maximum likelihood tree of these sequences was constructed in ARB using PhyML with the Jukes-Cantor 69 substitution model and a customized base frequency filter ignoring positions in which special characters and ambiguity codes appear most often. Bootstrap values >80 (percent of

100 replicates) are displayed. The tree was visualized and annotated using the Interactive Tree of Life (73).

Archaeal community representation in metagenomic and metatranscriptomic datasets

In order to determine relative contributions of MG-I and MG-II to total protein-coding reads at Station ALOHA over time, we queried four metagenomic datasets generated from SPM profiles collected on Hawaii Ocean Time-series research cruises HOT 179 (March 2006; (74)), HOT 186 (October 2006; (75)), HOT 194 (August 2007) and HOT 215 (September 2009) and a metatranscriptomic dataset from HOT 186. To understand the extent to which archaeal community composition as determined from 16S rDNA amplicon data and pyrosequencing data correspond, we also analyzed metagenomic data generated from the 130 m Station Aloha sample collected on the BioLINCs cruise.

Analysis of DNA and cDNA datasets began with the removal of duplicate (100% identity level) sequences. Duplicate-free fasta files were divided into rRNA and non rRNA reads by using BLASTn (top hit, e-values <0.0001, bit scores >50) to compare them to a rRNA database comprised of combined SILVA release 106 SSU and LSU databases and a 5S database (76). Using BLASTx, non-rRNA reads were compared with a reference database comprised of NCBI RefSeq release 54, protein sequences from the Moore Marine Microbial Genomes project, and several recently published marine microbial genomes. Matches with bit scores >50 were retained.

Top BLASTn hits (e value <0.001, bit score >50) against the rRNA database described above were used to divide the input files into rRNA and non-rRNA reads. Hits with a score within 10% of the best hit were exported to MEGAN (77) and their putative taxonomic affiliations determined.

For HOT 194 and 215 metagenomic datasets, we used LAST http://last.cbrc.jp/ instead of BLASTn.

For each sample, the proportion of thaumarchaeal and euryarchaeal reads was calculated as a percent of total reads assigned at or below the phylum level. In metagenomic and metatranscriptomic analyses we did not attempt to compensate for differences in genome size. The assembled MG-II genome is 25% longer than the *N. maritimus* genome (41), and we acknowledge that this difference could lead to slight bias in favor of MG-II. However, given the diversity of both MG-I and MG-II and uncertainty over how closely the sequenced genomes correspond to the genomes of NPSG archaea, we chose not to weight MG-I reads more heavily in the comparison.

Lipid extraction, hydrolysis and sample preparation

Lipids were extracted from glass fiber filters containing SPM following a modified Bligh-Dyer protocol after Sturt et al. (49). Sections of filters were placed in 250 ml Teflon bottles (Nalgene Nunc), submerged in a monophasic solution of 2:1:0.8 methanol:dichloromethane:phosphate-buffered saline (PBS, Sigma-Aldrich) and sonicated for 20 minutes. Solvent was decanted and this step repeated twice.

The decanted solvents were combined in a separatory funnel and phase separation was achieved with the addition of 1:1 dichloromethane:water. The organic phase was removed and the aqueous phase extracted with dichloromethane three times. Combined extracts were rinsed with dichloromethane-extracted Nanopure water three times.

Filters were then submerged in a monophasic solution of 10:5:4 methanol:dichloromethane:trichloroacetic acid (Sigma-Aldrich, 2.5% in Nanopure water) and sonicated for 20 minutes. Solvent was decanted and this step repeated twice. Phase separation was achieved as above, and the resultant organic phase was washed with Nanopure water three times. Total lipid extracts (TLEs) were combined with those from the previous step, evaporated under a gentle stream of N_2, and stored at -20°C until analysis.

TLE aliquots designated for core GDGT analysis were dissolved in 99:1 hexane:isopropanol, filtered (0.45 μm syringe filters, Millipore), evaporated, and redissolved in 99:1 hexane:isopropanol containing 1 ng/μl of a synthetic C_{46} tetraether lipid internal standard (78, 79).

Separate aliquots of TLE were subjected to acid hydrolysis to cleave head groups of intact polar GDGTs, converting them to core GDGTs (48). 1 ml of a mixture of 6 M HCl:methanol:dichloromethane (1:9:1, v/v) was added to dried TLE and vials were sealed and incubated at 70°C for 12 h. The hydrolysate was evaporated under N2 and prepared as core GDGT aliquots, above.

TLE aliquots designated for IPL analysis were dissolved in 9:1 dichloromethane:methanol, filtered, dried and redissolved in the same solvent mixture.

Lipid analysis

Core GDGTs were analyzed by high performance liquid chromatography - atmospheric pressure chemical ionization (APCI) mass spectrometry in positive mode using an Agilent 1260 Infinity series LC coupled to an Agilent 6130 mass spectrometer. 10 µl of extract were injected, typically corresponding to ~150 L of seawater. Separation was achieved on a Prevail Cyano column (150mm x 2.1mm, 3µm, Grace) maintained at 30°C, using a method modified from Liu et al. (80) and Hopmans et al. (81). Compounds were eluted isocratically with 100% eluent A (hexane:isopropanol 99:1) for 5 minutes, followed sequentially by: 1) a linear gradient to 15% eluent B (hexane:isopropanol 9:1) over 15 minutes; 2) a linear gradient to 100% eluent B over 15 minutes; and 3) a 5 min isocratic hold at 100% eluent B, at a constant flow rate of 0.4 ml/min. The column was re-equilibrated with 100% eluent A for 10 min between analyses. APCI-MS conditions were: gas temperature 350°C, vaporizer temperature 380°C, drying gas flow 6 l/min., nebulizer pressure 30psi, capillary 2000V, corona 5µA. GDGTs were detected by selected monitoring of [M+H]+ ions m/z 1302.3, 1300.3, 1298.3, 1296.3, 1294.3, 1292.2 and 743.7; full scans were run periodically to monitor background (m/z 400-2000) and to confirm compound identification (m/z 1200-1750).

Intact polar lipids in TLEs of the 0.3- 3 μm size fraction of SPM from 131 and 559 m were analyzed by ultra high performance liquid chromatography-electrospray ionization mass spectrometry using an Agilent 1200 series HPLC system coupled to an Agilent 6520 Accurate-Mass Quadrupole Time-of-Flight (Q-TOF; Agilent Technologies) mass spectrometer operated in positive mode. Chromatographic separation was achieved using a UPLC BEH HILIC column (Waters; 2.1 x 150 mm, 1.7 μm particle size) following the method of Wörmer et al. (82). Mass spectrometer source parameters were as follows: gas temperature 200°C, drying gas flow 6 L/min, nebulizer pressure 40 psi, capillary voltage 3000, and fragmentor voltage 175. The Q-TOF was set to a range of m/z 400-2000 in MS^1 and 100-2000 in MS^2. In MS^2 the scan rate was set to 2.99 and a maximum of 3 precursors were selected per cycle, with active exclusion after 5 spectra. Collision energy was set to 70 over the m/z range of IPL GDGTs (1400-2000).

Cell density inference

Two assumptions enable inference of MG-II cell densities: 1) The number of MG-I thaumarchaea/L ($n_{MG\text{-}I}$) is equal to MG-I 16S copy numbers/L, and 2) The number of archaeal cells in a sample equals the sum of MG-I + MG-II, which is true because the population is binary across our focus depths. By extension, the sum of the population fractions of MG-I ($f_{MG\text{-}I}$) and MG-II ($f_{MG\text{-}I}$) equals 1. Given these assumptions, we infer MG-II cell densities using the equation:

$$n_{MG-II} = f_{MG-II} \frac{n_{MG-I}}{f_{MG-I}}$$

MG-II % of cells

We estimated the percent of the archaeal community MG-II constitutes using data from the Hawaii Ocean Time-Series website, http://hahana.soest.hawaii.edu/hot/hot-dogs/index.html. Average heterotrophic cell counts (determined by flow cytometry) were 2.2 x 10^8 heterotrophic cells/L at 150-200 m in 2011. Because flow cytometry counts come from whole seawater and our MG-II counts are derived from size-fractionated SPM fraction, we consider our estimates for MG-II to be conservative.

Acknowledgements
We thank the Captain and crew of the R/V Kilo Moana, BioLINCs chief scientists Julie Robidart and Sam Wilson; John Waterbury for help with sampling; Jessica Bryant, Florence Schubotz and Asuncion Martinez for advice on analytical methods, data processing and helpful discussions; John Eppley for bioinformatics support; Tsultrim Palden and Rachel Barry for sequencing; and Carolyn Colonero for laboratory assistance.

References

1. Delong EF (1992) Archaea in coastal marine environments. *Proceedings of the National Academy of Sciences* 89:5685–5689.

2. Fuhrman JA, Davis AA (1997) Widespread Archaea and novel Bacteria from the deep sea as shown by 16S rRNA gene sequences. *Marine Ecology Progress Series* 150:275–285.

3. Damste J, Rijpstra W (2002) Distribution of Membrane Lipids of Planktonic Crenarchaeota in the Arabian Sea. *Applied and ....*

4. Ingalls AE et al. (2006) Quantifying archaeal community autotrophy in the mesopelagic ocean using natural radiocarbon. *Proceedings of the National Academy of Sciences* 103:6442–6447.

5. Pearson A, McNichol AP, Benitez-Nelson BC, Hayes JM, Eglinton TI (2001) Origins of lipid biomarkers in Santa Monica Basin surface sediment: a case study using compound-specific Δ 14 C analysis. *GEOCHIMICA ET COSMOCHIMICA ACTA* 65:3123–3137.

6. Wuchter C, Schouten S, Boschker HTS, Sinninghe DamstÃ JS Bicarbonate uptake by marine Crenarchaeota. *FEMS Microbiology Letters* 219:203–207.

7. Schouten S, Hopmans EC, Schefuß E, Sinninghe Damsté JS (2002) Distributional variations in marine crenarchaeotal membrane lipids: a new tool for reconstructing ancient sea water temperatures? *Earth and Planetary Science Letters* 204:265–274.

8. Hopmans EC et al. (2004) A novel proxy for terrestrial organic matter in sediments based on branched and isoprenoid tetraether lipids. *Earth and Planetary Science Letters* 224:107–116.

9. Kuypers MM et al. (2001) Massive expansion of marine archaea during a mid-Cretaceous oceanic anoxic event. *Science* 293:92–95.

10. Fuhrman JA (1992) Novel major archaebacterial group from marine plankton. *Nature* 356:148–149.

11. Brochier-Armanet C, Boussau B, Gribaldo S, Forterre P (2008) Mesophilic crenarchaeota: proposal for a third archaeal phylum, the Thaumarchaeota. *Nat Rev Micro* 6:245–252.

12. Könneke M et al. (2005) Isolation of an autotrophic ammonia-oxidizing marine archaeon. *Nature* 437:543–546.

13. Santoro AE, Buchwald C, McIlvin MR, Casciotti KL (2011) Isotopic Signature of N2O Produced by Marine Ammonia-Oxidizing Archaea. *Science* 333:1282–1285.

14. Metcalf WW et al. (2012) Synthesis of Methylphosphonic Acid by Marine Microbes: A Source for Methane in the Aerobic Ocean. *Science* 337:1104–1107.

15. Schouten S et al. (2008) Intact Membrane Lipids of "Candidatus Nitrosopumilus maritimus," a Cultivated Representative of the Cosmopolitan Mesophilic Group I Crenarchaeota. *Applied and Environmental Microbiology* 74:2433–2440.

16. Damsté JSS (2002) Crenarchaeol: the characteristic core glycerol dibiphytanyl glycerol tetraether membrane lipid of cosmopolitan pelagic crenarchaeota. *The Journal of Lipid Research* 43:1641–1651.

17. la Torre de JR, Walker CB, Ingalls AE, Könneke M, Stahl DA (2008) Cultivation of a thermophilic ammonia oxidizing archaeon synthesizing crenarchaeol. *Environ Microbiol* 10:810–818.

18. López-García P, Moreira D, López López A, Rodriguez-Valera F (2001) A novel haloarchaeal-related lineage is widely distributed in deep oceanic regions. *Environ Microbiol* 3:72–78.

19. Karner MB, Delong EF, Karl DM (2001) Archaeal dominance in the mesopelagic zone of the Pacific Ocean. *Nature* 409:507–510.

20. DeLong EF (2006) Community Genomics Among Stratified Microbial Assemblages in the Ocean's Interior. *Science* 311:496–503.

21. Massana R, Murray A, Preston C, DeLong E (1997) Vertical distribution and phylogenetic characterization of marine planktonic Archaea in the Santa Barbara Channel. *Applied and Environmental Microbiology* 63:50–56.

22. Mincer TJ et al. (2007) Quantitative distribution of presumptive archaeal and bacterial nitrifiers in Monterey Bay and the North Pacific Subtropical Gyre. *Environ Microbiol* 9:1162–1175. Available at: http://onlinelibrary.wiley.com/doi/10.1111/j.1462-2920.2007.01239.x/full.

23. Ottesen EA et al. (2013) Pattern and synchrony of gene expression among sympatric marine microbial populations. *Proceedings of the National Academy of Sciences* 110:E488–E497.

24. Herfort L et al. Variations in spatial and temporal distribution of Archaea in the North Sea in relation to environmental variables. *FEMS Microbiology Ecology* 62:242–257.

25. Bano N, Ruffin S, Ransom B, Hollibaugh JT (2004) Phylogenetic Composition of Arctic Ocean Archaeal Assemblages and Comparison with Antarctic Assemblages. *Applied and Environmental Microbiology* 70:781–789.

26. Galand PE, Casamayor EO, Kirchman DL, Potvin M, Lovejoy C (2009) Unique archaeal assemblages in the Arctic Ocean unveiled by massively parallel tag sequencing. 3:860–869.

27. Murray AE et al. (1998) Seasonal and spatial variability of bacterial and archaeal assemblages in the coastal waters near Anvers Island, Antarctica. *Applied and Environmental Microbiology* 64:2585–2595.

28. López García P, López López A, Moreira D, Rodríguez Valera F (2001) Diversity of free-living prokaryotes from a deep-sea site at the Antarctic Polar Front. *FEMS Microbiology Ecology* 36:193–202.

29. Alonso-Sáez L, Andersson A, Heinrich F, Bertilsson S (2011) High archaeal diversity in Antarctic circumpolar deep waters. *Environmental Microbiology Reports* 3:689–697.

30. Hugoni M et al. (2013) Structure of the rare archaeal biosphere and seasonal dynamics of active ecotypes in surface coastal waters. *Proceedings of the National Academy of Sciences* 110:6004–6009.

31. Belmar L, Molina V, Ulloa O (2011) Abundance and phylogenetic identity of archaeoplankton in the permanent oxygen minimum zone of the eastern tropical South Pacific. *FEMS Microbiology Ecology* 78:314–326.

32. Michotey V et al. (2012) Spatio-temporal diversity of free-living and particle-attached prokaryotes in the tropical lagoon of Ahe atoll (Tuamotu Archipelago) and its surrounding oceanic waters. *Marine Pollution Bulletin* 65:525–537.

33. Herndl GJ et al. (2005) Contribution of Archaea to total prokaryotic production in the deep Atlantic Ocean. *Applied and Environmental Microbiology* 71:2303–2309.

34. Liu M, Xiao T, Wu Y, Zhou F, Zhang W (2011) Temporal distribution of the archaeal community in the Changjiang Estuary hypoxia area and the adjacent East China Sea as determined by denaturing gradient gel electrophoresis and multivariate analysis. *Can J Microbiol* 57:504–513.

35. DeLong E (2006) Archaeal mysteries of the deep revealed. *Proceedings of the National Academy of Sciences.*

36. Turich C et al. (2007) Lipids of marine Archaea: Patterns and provenance in the water-column and sediments. *GEOCHIMICA ET COSMOCHIMICA ACTA* 71:3272–3291.

37. Schouten S, van der Meer MTJ, Hopmans EC, Damsté JSS (2008) Comment on "Lipids of marine Archaea: Patterns and provenance in the water column and sediments" by Turich et al. (2007). *GEOCHIMICA ET COSMOCHIMICA ACTA* 72:5342–5346.

38. Turich C et al. (2008) Reply to the Comment by S. Schouten, M. van der Meer, E. Hopmans, and J.S. Sinninghe Damsté on "Lipids of marine Archaea: Patterns and provenance in the water column." *GEOCHIMICA ET COSMOCHIMICA ACTA* 72:5347–5349.

39. Caporaso JG et al. (2010) qiime. *Nature Publishing Group* 7:335–336.

40. Frigaard N-U, Martínez A, Mincer TJ, Delong EF (2006) Proteorhodopsin lateral gene transfer between marine planktonic Bacteria and Archaea. *Nature* 439:847–850.

41. Iverson V et al. (2012) Untangling Genomes from Metagenomes: Revealing an Uncultured Class of Marine Euryarchaeota. *Science* 335:587–590.

42. DeLong EF (2006) Community Genomics Among Stratified Microbial Assemblages in the Ocean's Interior. *Science* 311:496–503.

43. White DC, Davis WM, Nickels JS, King JD, Bobbie RJ (1979) Determination of the sedimentary microbial biomass by extractible lipid phosphate. *Oecologia* 40:51–62.

44. Harvey HR, Fallon RD, Patton JS (1986) The effect of organic matter and oxygen on the degradation of bacterial membrane lipids in marine sediments. *GEOCHIMICA ET COSMOCHIMICA ACTA* 50:795–804.

45. Liu X-L, Summons RE, Hinrichs K-U (2012) Extending the known range of glycerol ether lipids in the environment: structural assignments based on tandem mass spectral fragmentation patterns. *Rapid Commun Mass Spectrom* 26:2295–2302.

46. Hopmans EC, Schouten S, Pancost RD, van der Meer MT, Sinninghe Damsté JS (2000) Analysis of intact tetraether lipids in archaeal cell material and sediments by high performance liquid chromatography/atmospheric pressure chemical ionization mass spectrometry. *Rapid Commun Mass Spectrom* 14:585–589.

47. Ingalls A, Huguet C (2012) Distribution of intact and core membrane lipids of Archaea (GDGTs) among size fractionated particulate organic matter in the Hood Canal. *Applied and Environmental ....*

48. Lipp JS, Hinrichs K-U (2009) Structural diversity and fate of intact polar lipids in marine sediments. *GEOCHIMICA ET COSMOCHIMICA ACTA* 73:6816–6833.

49. Sturt HF, Summons RE, Smith K, Elvert M, Hinrichs K-U (2004) Intact polar membrane lipids in prokaryotes and sediments deciphered by high-performance liquid chromatography/electrospray ionization multistage mass spectrometry—new biomarkers for biogeochemistry and microbial ecology. *Rapid Commun Mass Spectrom* 18:617–628.

50. Wörmer L, Lipp JS, Schröder JM, Hinrichs K-U (2013) Application of two new LC-ESI-MS methods for improved detection of intact polar lipids (IPLs) in

environmental samples. *Organic Geochemistry*:1–43.

51. Biddle JF et al. (2006) Heterotrophic Archaea dominate sedimentary subsurface ecosystems off Peru. *PNAS* 103:3846–3851.

52. Lipp JS, Morono Y, Inagaki F, Hinrichs K-U (2008) Significant contribution of Archaea to extant biomass in marine subsurface sediments. *Nature* 454:991–994.

53. Schubotz F, Wakeham SG, Lipp JS, Fredricks HF, Hinrichs K-U (2009) Detection of microbial biomass by intact polar membrane lipid analysis in the water column and surface sediments of the Black Sea. *Environ Microbiol* 11:2720–2734.

54. Langworthy TA (1972) Lipids of Thermoplasma acidophilum. 1–9.

55. Turich C, Freeman K, Bruns M, Conte M (2007) Lipids of marine Archaea: Patterns and provenance in the water-column and .... *et Cosmochimica Acta.*

56. Damsté JSS (2002) Crenarchaeol: the characteristic core glycerol dibiphytanyl glycerol tetraether membrane lipid of cosmopolitan pelagic crenarchaeota. *The Journal of Lipid Research* 43:1641–1651.

57. Pearson A et al. (2004) Nonmarine Crenarchaeol in Nevada Hot Springs. *Applied and Environmental Microbiology* 70:5229–5237.

58. Pitcher A, Schouten S, Sinninghe Damste JS (2009) In Situ Production of Crenarchaeol in Two California Hot Springs. *Applied and Environmental Microbiology* 75:4443–4451.

59. Pitcher A et al. (2009) Crenarchaeol dominates the membrane lipids of Candidatus Nitrososphaera gargensis, a thermophilic Group I.1b Archaeon. *ISME J* 4:542–552.

60. Wuchter C, Schouten S, Wakeham SG, Sinninghe Damsté JS (2005) Temporal and spatial variation in tetraether membrane lipids of marine Crenarchaeota in particulate organic matter: Implications for TEX 86paleothermometry. *Paleoceanography* 20:n/a–n/a.

61. Wuchter C, Schouten S, Wakeham SG, Sinninghe Damsté JS (2006) Archaeal tetraether membrane lipid fluxes in the northeastern Pacific and the Arabian Sea: Implications for TEX 86paleothermometry. *Paleoceanography* 21.

62. Kim J-H, Schouten S, Hopmans EC, Donner B, Sinninghe Damsté JS (2008) Global sediment core-top calibration of the TEX86 paleothermometer in the ocean. *GEOCHIMICA ET COSMOCHIMICA ACTA* 72:1154–1173.

63. Pearson A, Ingalls AE (2013) Assessing the Use of Archaeal Lipids as Marine Environmental Proxies. *Annu Rev Earth Planet Sci* 41:359–384.

64. Martens-Habbena W, Berube PM, Urakawa H, Torre JR de L, Stahl DA (2009) Ammonia oxidation kinetics determine niche separation of nitrifying Archaea and Bacteria. *Nature* 461:976–979.

65. Macalady JL et al. (2004) Tetraether-linked membrane monolayers in Ferroplasma spp: a key to survival in acid. *Extremophiles* 8:411–419.

66. Schoon PL et al. (2013) Recognition of Early Eocene global carbon isotope excursions using lipids of marine Thaumarchaeota. *Earth and Planetary Science Letters* 373:160–168.

67. Wang X-C, Druffel ER, Griffin S, Lee C, Kashgarian M (1998) Radiocarbon studies of organic compound classes in plankton and sediment of the northeastern Pacific Ocean. *GEOCHIMICA ET COSMOCHIMICA ACTA* 62:1365–1378.

68. Wuchter C et al. (2006) Archaeal nitrification in the ocean. *Proceedings of the National Academy of Sciences* 103:12317–12322.

69. Teske A, Sorensen KB (2007) Uncultured archaea in deep marine subsurface sediments: have we caught them all? *ISME J* 2:3–18.

70. Quince C, Lanzen A, Davenport RJ, Turnbaugh PJ (2011) 1471-2105-12-38. *BMC Bioinformatics* 12:38.

71. Edgar RC (2010) Search and clustering orders of magnitude faster than BLAST. *Bioinformatics* 26:2460–2461.

72. Ludwig W et al. (2004) ARB: a software environment for sequence data. *Nucleic Acids Research* 32:1363–1371.

73. Letunic I, Bork P (2006) Interactive Tree Of Life (iTOL): an online tool for phylogenetic tree display and annotation. *Bioinformatics* 23:127–128.

74. Frias-Lopez J et al. (2008) Microbial community gene expression in ocean surface waters. *Proceedings of the National Academy of Sciences* 105:3805–3810.

75. Martínez A, Tyson GW, Delong EF (2010) Widespread known and novel phosphonate utilization pathways in marine bacteria revealed by functional screening and metagenomic analyses. *Environ Microbiol* 12:222–238. Available at: http://onlinelibrary.wiley.com/doi/10.1111/j.1462-2920.2009.02062.x/full.

76. Nucl. Acids Res.-2002-Szymanski-176-8 (2001) Nucl. Acids Res.-2002-Szymanski-176-8. 1–3.

77. Huson DH, Mitra S, Ruscheweyh HJ, Weber N, Schuster SC (2011) Integrative analysis of environmental sequences using MEGAN4. *Genome Research* 21:1552–1560.

78. Patwardhan AP, Thompson DH (1999) Efficient Synthesis of 40- and 48-Membered Tetraether Macrocyclic Bisphosphocholines. *Org Lett* 1:241–244.

79. Huguet C et al. (2006) An improved method to determine the absolute abundance of glycerol dibiphytanyl glycerol tetraether lipids. *Organic Geochemistry* 37:1036–1041.

80. Liu X-L, Summons RE, Hinrichs K-U (2012) Extending the known range of glycerol ether lipids in the environment: structural assignments based on tandem mass spectral fragmentation patterns. *Rapid Commun Mass Spectrom* 26:2295–2302.

81. Hopmans EC, Schouten S, Pancost RD, van der Meer MT, Sinninghe Damsté JS (2000) Analysis of intact tetraether lipids in archaeal cell material and sediments by high performance liquid chromatography/atmospheric pressure chemical ionization mass spectrometry. *Rapid Commun Mass Spectrom* 14:585–589.

82. Wörmer L, Lipp JS, Schröder JM, Hinrichs K-U (2013) Application of two new LC-ESI-MS methods for improved detection of intact polar lipids (IPLs) in environmental samples. *Organic Geochemistry*:1–43.

83. Guindon S et al. (2010) New algorithms and methods to estimate maximum-likelihood phylogenies: assessing the performance of PhyML 3.0. *Systematic Biology* 59:307–321.

Figure Legends

Fig. 1.

Phylogenetic analysis of the 20 OTUs (97% similarity level) that represent the most sequences across the dataset (A) and matrices showing the depth and size class distribution of the 10 most frequently detected representative archaeal OTUs (B,C) . Representative sequences were aligned using the SILVA Incremental Aligner (SINA, http://www.arb-silva.de/aligner/) using the archaea variability profile. Nearest neighbors of each OTU and selected archaeal 16S sequences (e.g. pSL12, Marine Group III) were added to the dataset for phylogenetic context; environment of origin and accession numbers are listed for each. Aligned sequences were imported to a pared SSU database (SILVA release 106, non-redundant) in ARB (72). A maximum likelihood tree was inferred in ARB with PhyML (83) using the Jukes-Cantor 69 substitution model, and Bacteria as an outgroup. Bootstrap values > 80 (% of 100 replicates) are displayed. The scale bar represents 0.1 substitutions per nucleotide.

Matrices show the relative abundances of the 10 OTUs representing the most sequences (each OTU representing >2000 sequences) in the small (A) and large (B) size fractions of suspended particulate matter are shown with data normalized by row; darkest grey represents the most abundant OTU in a sample.

*800 and 1000 m data (A) are from 0.22-1.6 μm SPM.

Fig. 2.

Inferred cell densities of MG-I Thaumarchaeota and MG-II Euryarchaeota and glycerol dialkyl glycerol tetraether (GDGT) lipid concentrations in small (A,C) and large (B,D) size fractions of suspended particulate matter in the NPSG. MG-I cell densities were determined by QPCR. MG-II cell densities were inferred from archaeal community composition as determined from 16S rRNA amplicon data and MG-I cell densities (equation S1). Lipid plots show free core GDGTs lacking polar head groups and, at 131 and 559 m, the sum of free core GDGTs and cores released from intact polar GDGTs by acid hydrolysis. Mean values of replicate GDGT analyses are shown; error bars indicating the range of measurements are smaller than the data points. Note variable scales on x axes. Monoglycosyl crenarchaeol (E) is an intact polar GDGT detected by HPLC-ESI-MS in the small size fraction of SPM at 131 and 559 m (Fig. S8).

Fig. 3. HPLC-APCI-MS composite extracted ion chromatograms (EIC) of total lipid extract from 131 m, 0.3-3 μm size fraction sample before (A) and after (B) acid hydrolysis. Colored traces are EICs of m/z values of individual core GDGTs and the internal standard. Late eluting peaks in A represent three putative series of core GDGTs released from IPL GDGTs by fragmentation in the APCI source. After acid hydrolysis, late-eluting peaks disappeared and the peak area of core GDGTs increased, supporting this interpretation.

Table 1. 16S rDNA amplicon-derived archaeal community composition and relative abundances of individual GDGTs (Fig S1). "S" marks the small (0.3-3 μm) size fraction and "L" the large (3-57 μm). Relative abundances of GDGTs in hydrolysates of the 131 and 559 m lipid extracts are shown at bottom.

Figures

Fig. 1

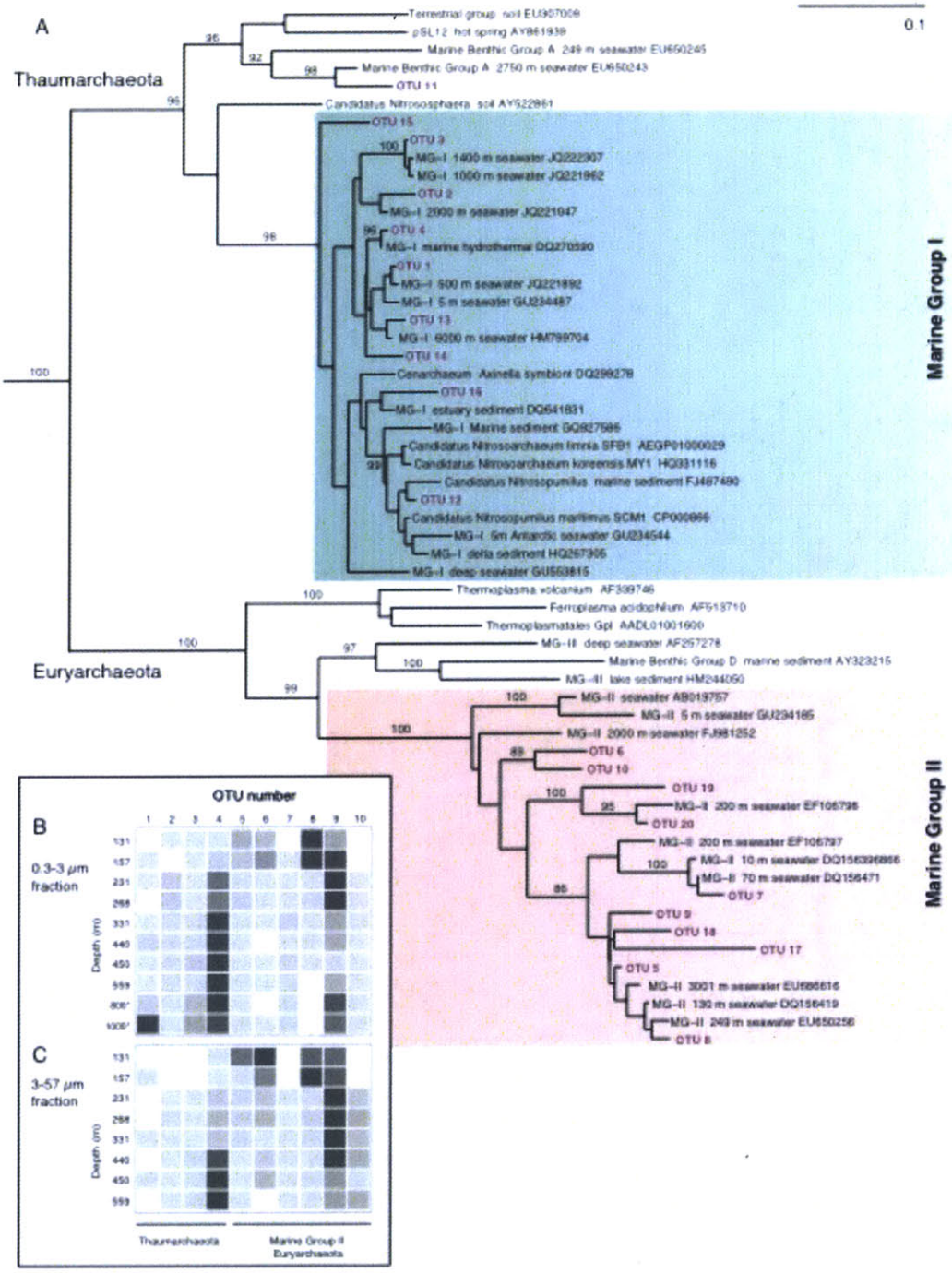

Fig. 2.

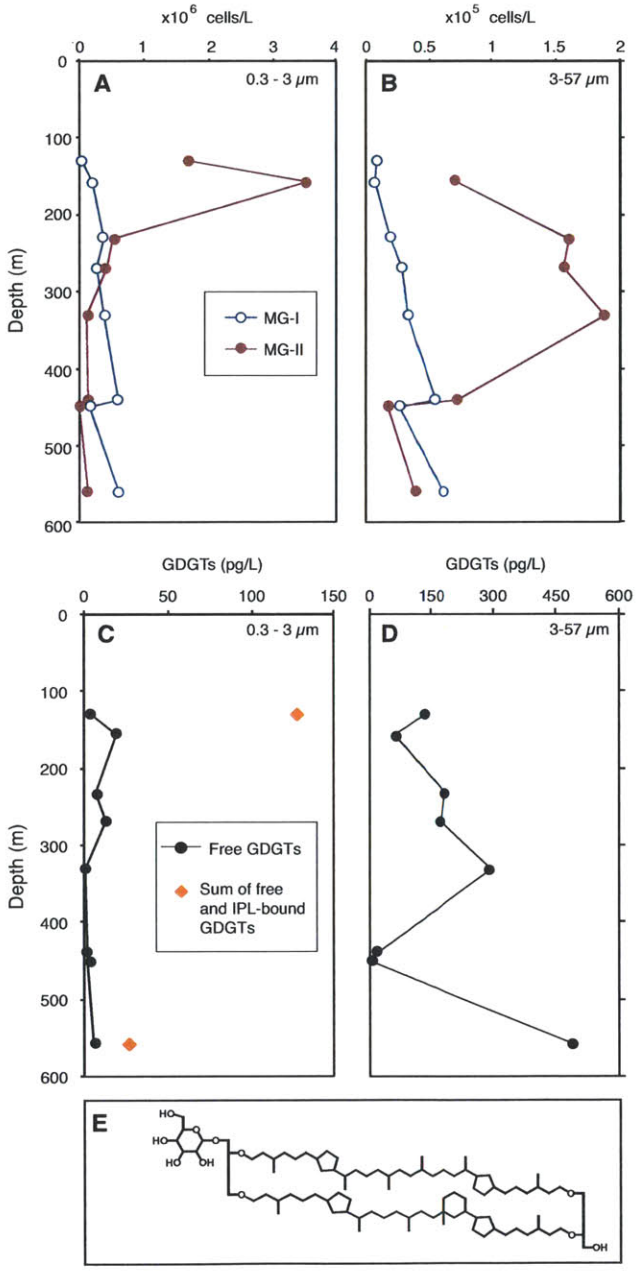
x10^6 cells/L
0 1 2 3 4
A
0.3 - 3 μm
x10^5 cells/L
0 0.5 1 1.5 2
B
3-57 μm
Depth (m)
0 100 200 300 400 500 600
MG-I
MG-II
GDGTs (pg/L)
0 50 100 150
C
0.3 - 3 μm
GDGTs (pg/L)
0 150 300 450 600
D
3-57 μm
Free GDGTs
Sum of free and IPL-bound GDGTs
E
HO
HO
HO
OH
OH

Fig. 3.

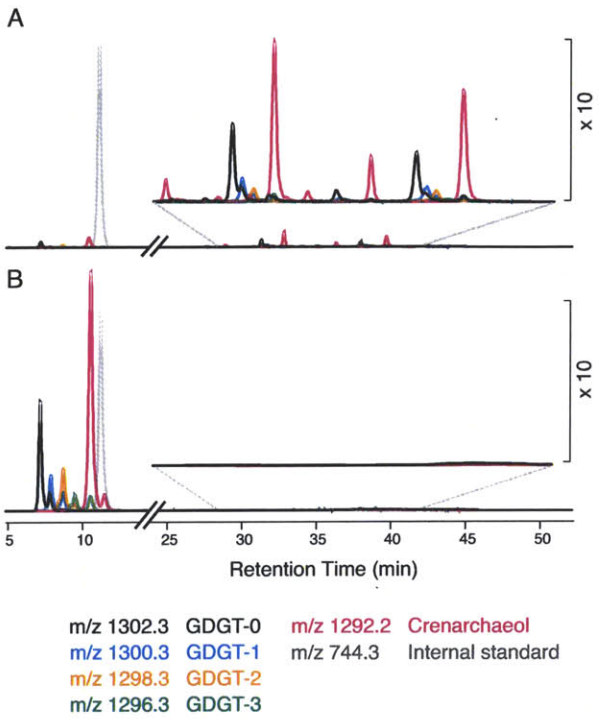
A
x 10
B
x 10
5
10
25
30
35
40
45
50
Retention Time (min)
m/z 1302.3 GDGT-0
m/z 1300.3 GDGT-1
m/z 1298.3 GDGT-2
m/z 1296.3 GDGT-3
m/z 1292.2 Crenarchaeol
m/z 744.3 Internal standard

Supplementary Information

Fig. S1. Structures of glycerol dialkyl glycerol tetraether (GDGT) lipids discussed in text.

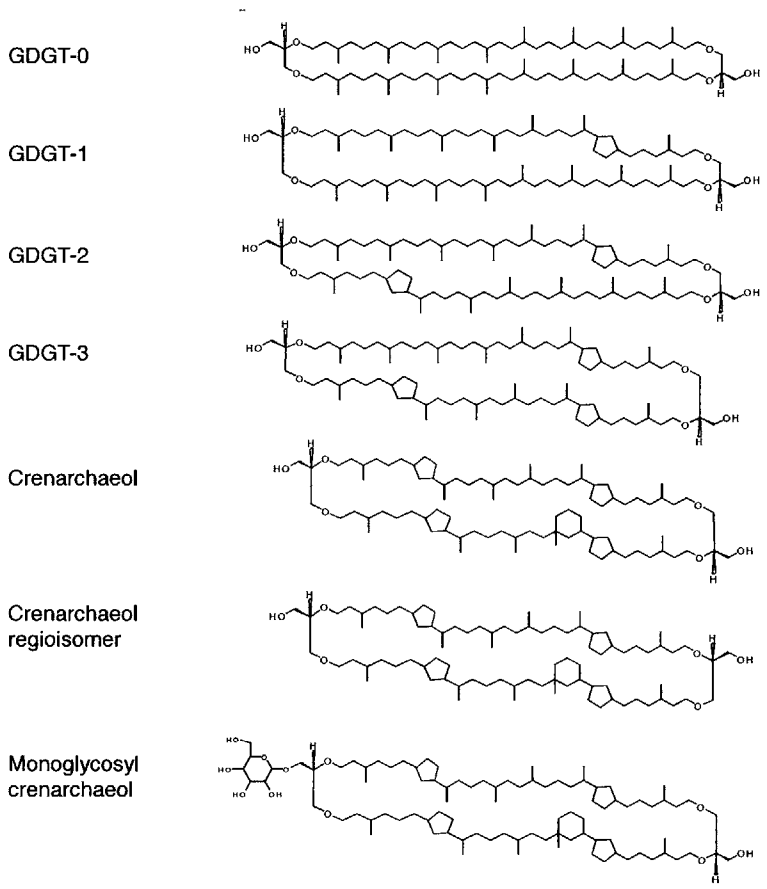

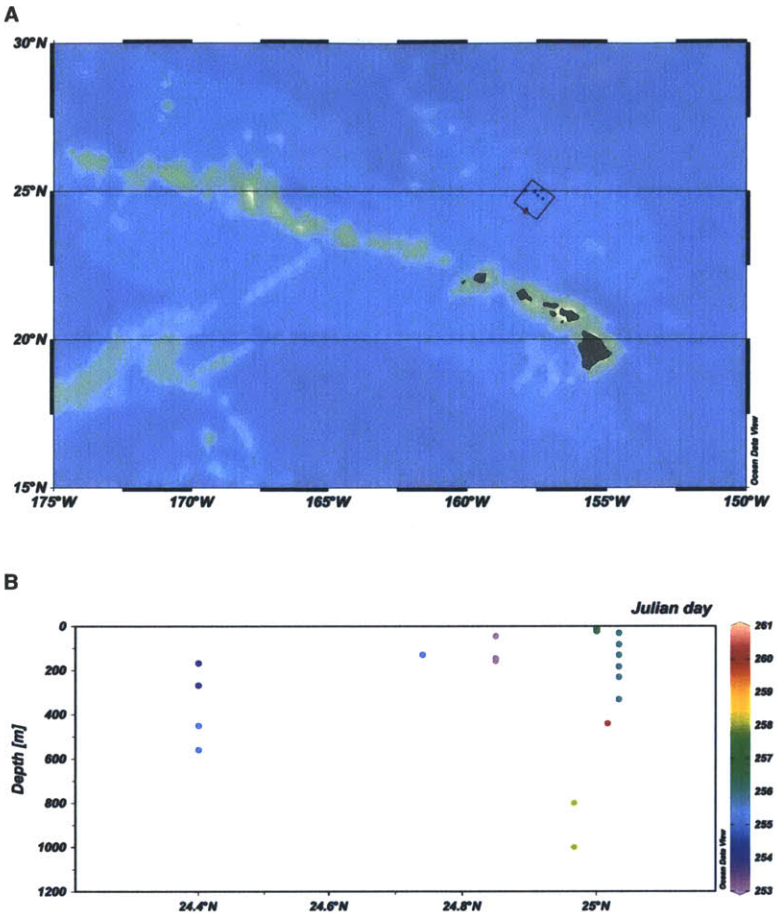

Fig. S2. Spatial and temporal distribution of BioLINCS in situ pump sampling locations: (A) map view, (B) section view. Colored points in (B) indicate Julian days during which samples were collected at the depth and latitude shown; color key at right. The Julian day span of 253-261 corresponds to 9/10/2011-9/17/2011.

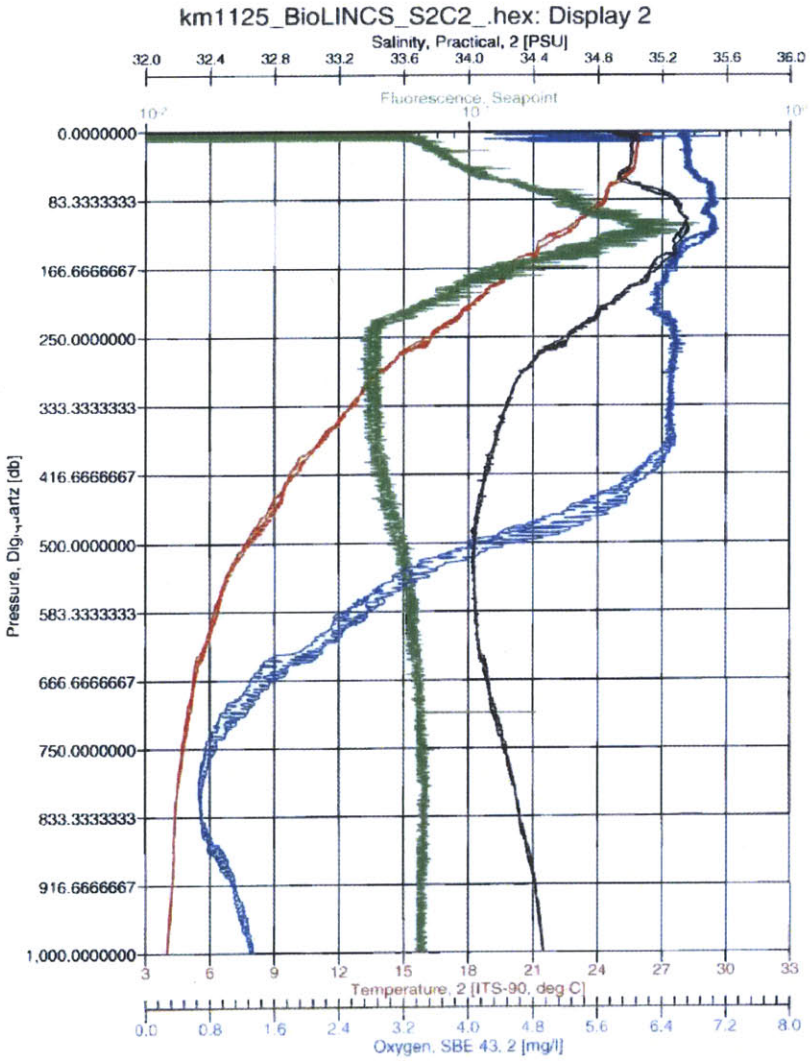

Fig. S3. CTD profile from the BioLINCS cruise, showing temperature (red), salinity (black), fluorescence (green) and oxygen concentration (blue) vs. pressure.

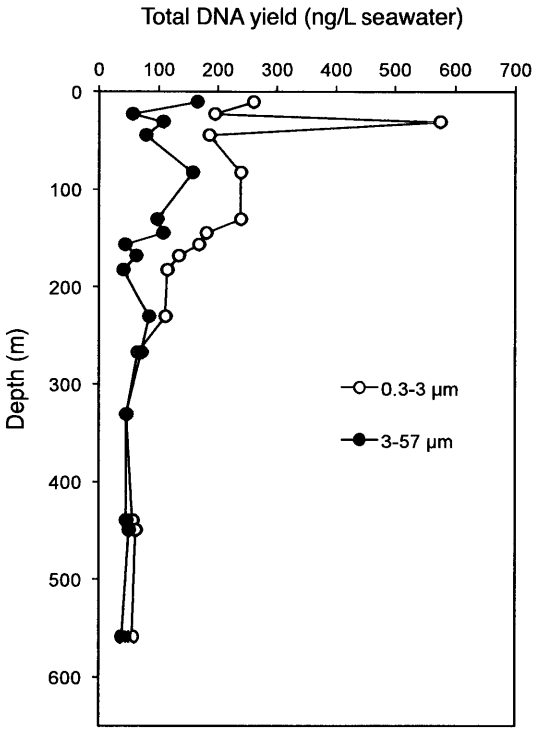

Fig. S4. Total DNA yield from glass fiber filters.

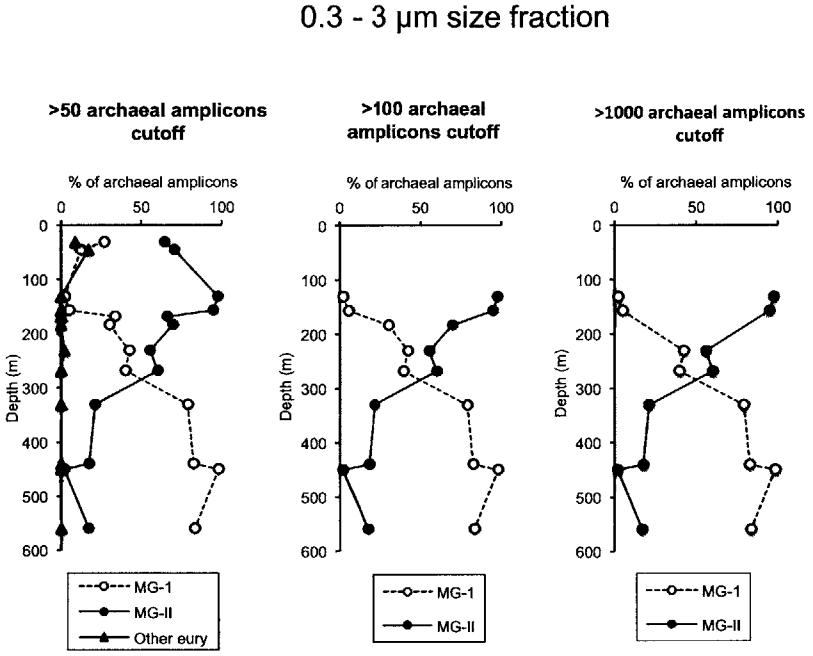

Fig. S5. Effect of different amplicon cutoff criteria on archaeal community composition profiles, 0.3-3 µm size fraction. The category "other euryarchaeota" includes sequences with top BLAST hits to MG-III Euryarchaeota and Unidentified Hydrothermal Vent Archaeon PVA.

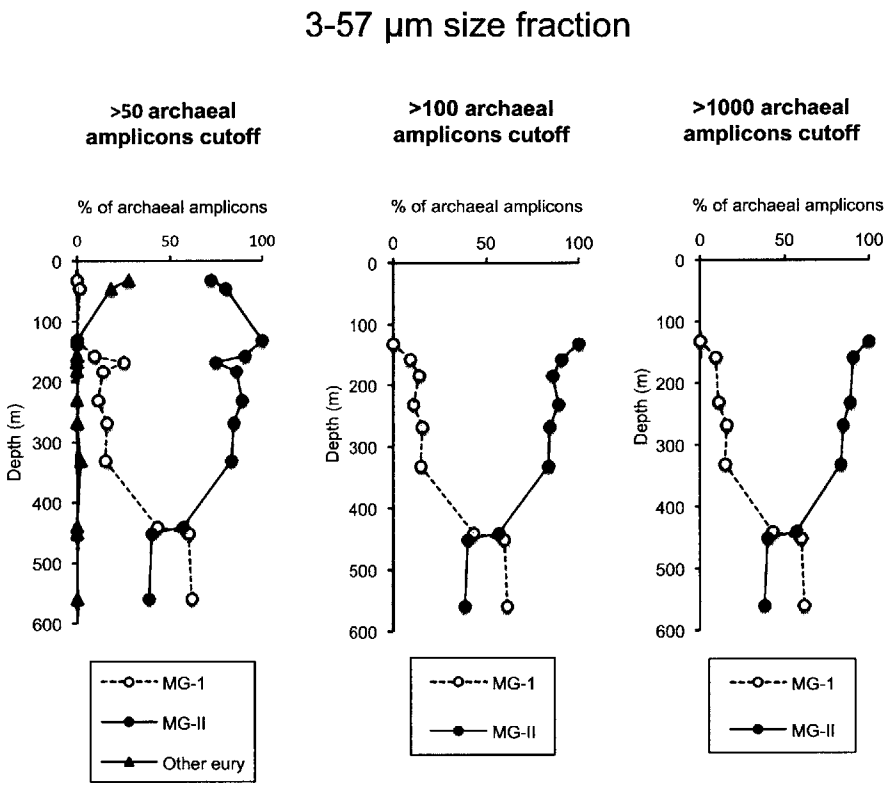

Fig. S6. Effect of different amplicon cutoff criteria on archaeal community composition profiles, 3-57 µm size fraction. As in the small size fraction, the category "other euryarchaea" includes sequences with top BLAST hits to MG-III euryarchaea and the Unidentified Hydrothermal Vent Archaeon PVA.

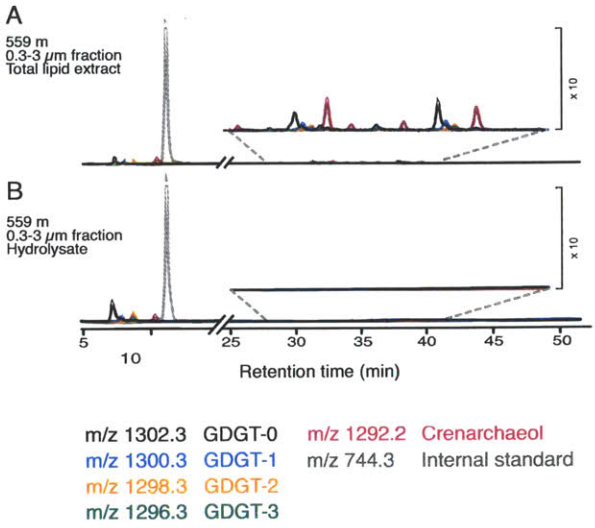

Fig. S7. HPLC-APCI-MS composite extracted ion chromatograms (EIC) of TLE from 559 m, 0.3-3 μm size fraction before (A) and after (B) acid hydrolysis. Colored traces are EICs of m/z values of individual core GDGTs and the internal standard (key at right). Late eluting peaks in A represent three putative series of core GDGTs released from IPL GDGTs by fragmentation in the APCI source. After acid hydrolysis, late-eluting peaks disappeared and the peak area of core GDGTs increased, supporting this interpretation. We analyzed environmental samples known to contain GDGTs with either predominantly mono- and diglycosyl GDTS or predominantly phosphatidyl GDGTs (not shown), and only monoglycosyl GDGTs eluted using this method. Thus, the three late-eluting series (A) may be core GDGTs released from monoglycosyl GDGTs containing different sugar moieties, or unknown IPL GDGTs of similar polarity. A contribution of IPL GDGTs outside of this method's window of detection to the core GDGTs released by acid hydrolysis is possible. The relative response factor of IPL and core GDGTs detected using this method has not been determined.

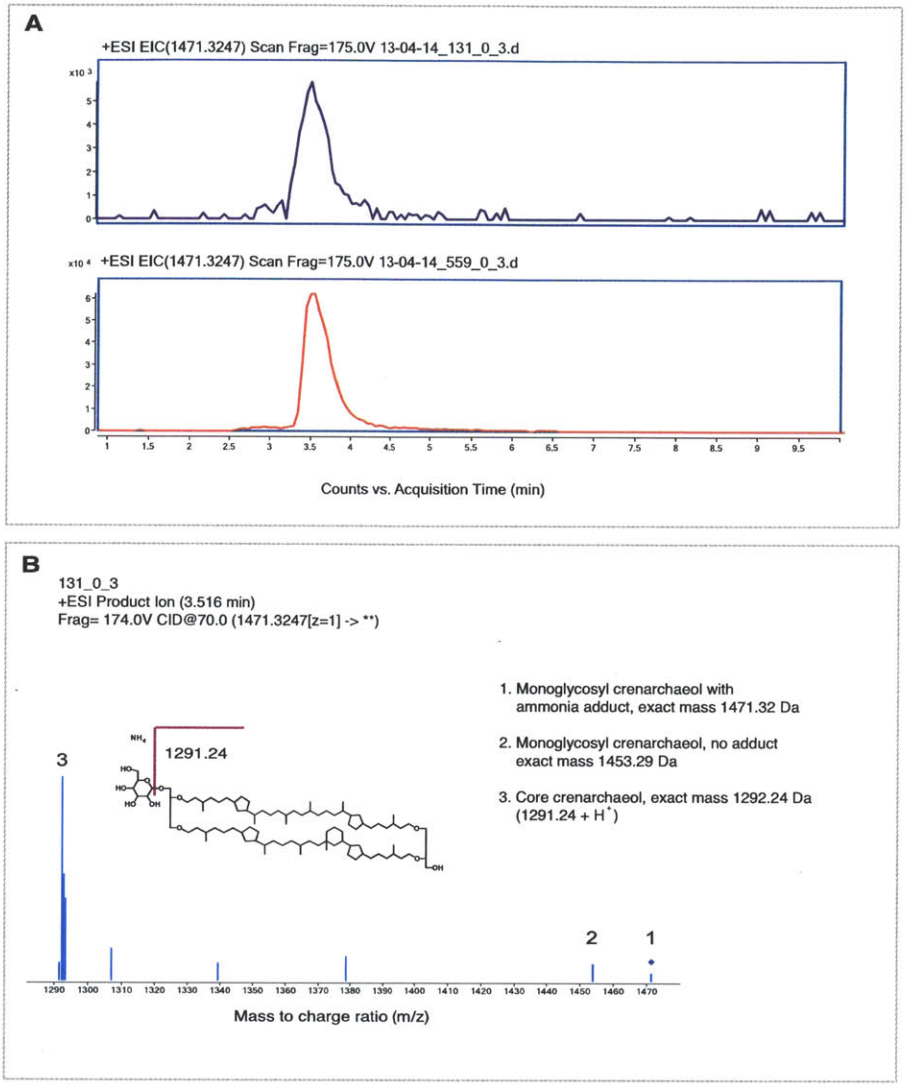

Fig. S8. HPLC-ESI-MS analyses of 131 m and 559 m samples, small size fraction. Extracted ion chromatograms (A) of m/z 1471.3247 corresponding to monoglycosyl crenarchaeol + ammonia adduct (formula mass 1471.3244), indicate that this compound is present in both samples; characteristic fragments are visible in the MS^2 spectrum of the 131 m sample (B).

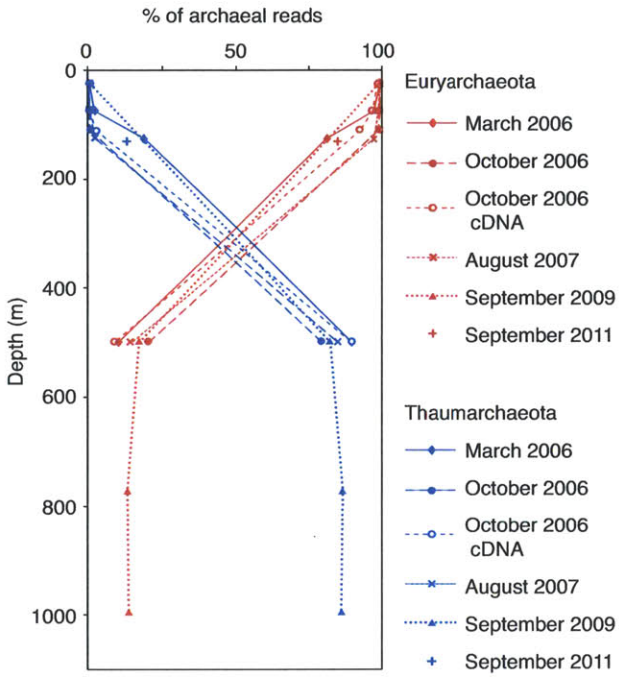

Fig. S9. Euryarchaeal and thaumarchaeal representation in metagenomic and metatranscriptomic datasets generated from SPM (0.22-2.6 μm) collected at Station ALOHA from March 2006 to September 2011. Putative protein-coding reads assigned at or below each phylum level are shown as a percent of total archaeal reads assigned.

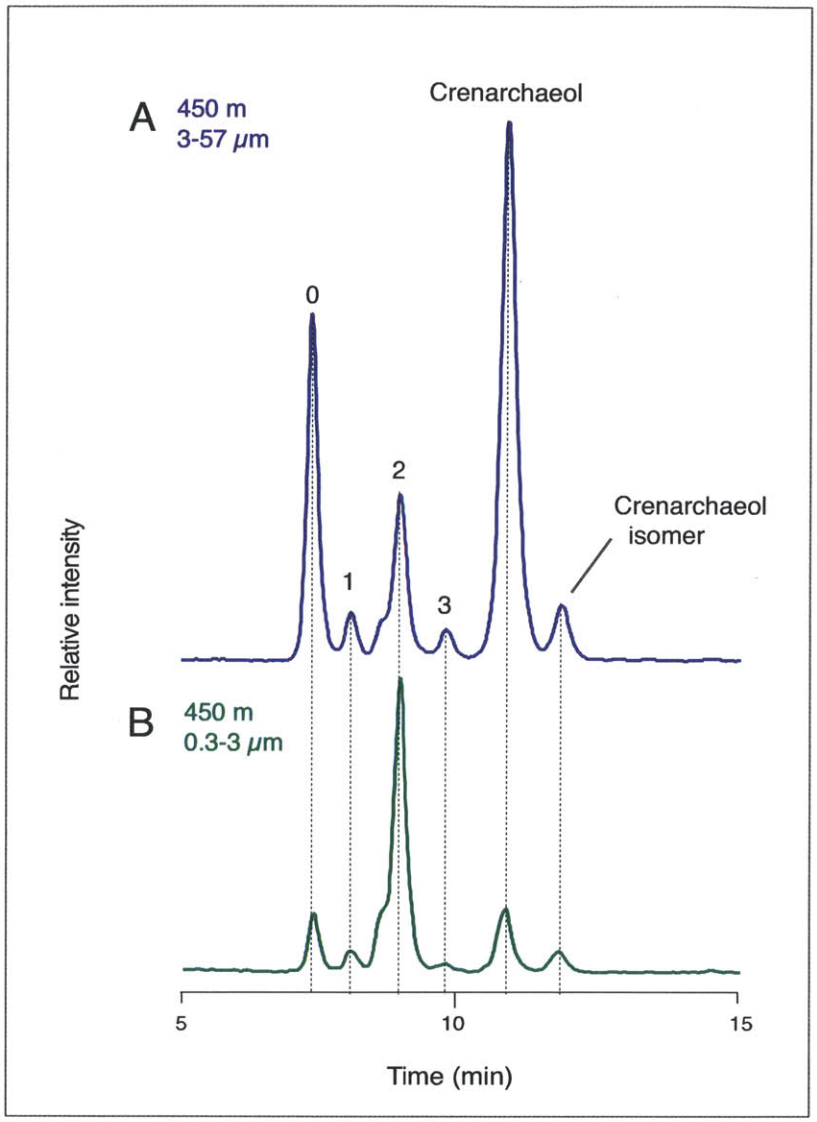

Fig. S10. Composite extracted ion chromatograms of core GDGTs in the small (bottom, green trace) and large size fractions (top, violet trace) of SPM collected during the same in situ pump deployment at 450 m. Numbered peaks correspond to structures in Fig. S1 (e.g. "0" denotes GDGT-0). MG-I Thaumarchaeota comprised 98% of the archaeal community in the small size fraction and 60% of the community in the large size fraction.

Table S1. Comparison of archaeal community composition as determined through analysis of 16S rDNA amplicons from SPM collected on Sterivex filters (0.22-2.6 μm size fraction) and glass fiber filters (0.3-3 μm) and metagenomic data. Two amplicon samples (131 and 450 m, 0.3–3 μm) were processed and sequenced in duplicate using different tags.

Depth (m)	Size fraction	Replicate	Analysis type	% Thaumarchaeota	% MG-II Euryarchaeota	% Other Euryarchaeota	% Other archaea
130	0.22-2.6		16S amplicon	5.1	94.8	0.0	0.0
130	0.22-2.6		metagenome	12.9	79.7	4.9	0.2
131	0.3-3	a	16S amplicon	2.3	97.7	0.0	0.0
131	0.3-3	b	16S amplicon	0.0	100.0	0.0	0.0
450	0.3-3	a	16S amplicon	98.1	1.9	0.0	0.0
450	0.3-3	b	16S amplicon	97.3	2.7	0.0	0.0

Table S2. Amplicon statistics. Boxes indicate samples that meet the threshold criterion of >1000 amplicons in both size fractions and were used for comparison with lipid data. Bold blue type denotes replicate samples amplified using different tags.

Depth (m)	Size fraction (μm)	Total reads (archaeal + eukaryotic)	Archaeal reads	Mean length of archaeal reads
11	0.3 - 3	82	51	392.55
11	3 - 57	33	26	393.76
23	0.3 - 3	5	4	400.00
23	3 - 57	1132	209	393.05
31	0.3 - 3	98	82	390.85
31	3 - 57	1172	613	395.91
45	0.3 - 3	132	82	394.55
45	3 - 57	2421	1768	398.41
83	0.3 - 3	426	408	397.38
83	3 - 57	33	32	389.61
130	0.22 – 1.6	22364	21805	399.69
131	0.3 - 3	7261	5514	396.77
131	**0.3 – 3**	**21642**	**15187**	**398.62**
131	3 - 57	16166	2477	381.57
145	0.3 - 3	25229	16662	394.97
145	3 - 57	57	41	395.28
157	0.3 - 3	4013	2226	392.58
157	3 - 57	3023	1605	379.85
168	0.3 - 3	760	83	389.52
168	3 - 57	1524	1381	396.01
183	0.3 - 3	615	106	397.51
183	3 - 57	324	172	396.02
231	0.3 - 3	16136	14075	399.03
231	3 - 57	11066	6449	396.08
268	0.3 - 3	3073	2990	398.02
268	3 - 57	7891	3260	391.15
331	0.3 - 3	16004	14080	397.15
331	3 - 57	1437	1115	397.87
440	0.3 - 3	18690	16839	392.33
440	3 - 57	7183	4050	395.80
450	0.3 - 3	19480	18818	399.56
450	**0.3 – 3**	**9598**	**9385**	**396.20**
450	3 - 57	17562	9038	391.50
559	0.3 - 3	19794	18379	393.04
559	3 - 57	15739	8437	393.77
800	0.22 - 1.6	5199	4194	399.07
1000	0.22 – 1.6	3712	2716	399.62

Chapter 3

Ammonia, bicarbonate and amino acid amendments elicit changes in archaeal tetraether lipids, microbial community composition and functional genes in experimental microcosms

Abstract

Planktonic marine archaea are phylogenetically and physiologically diverse, and evidence of autotrophic, heterotrophic and mixotrophic growth has been found among different taxa. We conducted microcosm experiments to probe the effects of ammonia, bicarbonate and amino acid amendments on archaeal community and their tetraether lipid biomarker composition in whole seawater microcosms. Although experimental conditions did not promote the overall growth of archaea, we observed shifts in the relative representation of different archaeal taxa in metagenomic datasets and changes in the concentrations and structures of archaeal glycerol dialkyl glycerol tetraether (GDGT) lipids. Notably, the amino acid amendment was associated with a different pattern of GDGT relative abundances than initial field samples, control, or bicarbonate-amended microcosm; this suggests that carbon substrate and nutrient conditions may influence the membrane lipid composition of, and perhaps enrich for, a subset of some marine archaeal clades. To our knowledge, this is the first direct evidence that factors other than temperature can influence the degree of internal cyclization in marine archaeal tetraether membrane lipids. Further, rapid loss of core GDGT lipids was observed, with concentrations of GDGTs dropping by 43% within 44 h of collection. This suggests that free core GDGTs have a very short residence time in the aerobic water column. In addition to measuring archaeal community composition and GDGTs, we tracked the relative representation of bacteria, eukaryotes and viruses in metagenomic datasets generated from samples collected at three time points (field, T_0 and T_F for 3 treatments). Moving beyond taxonomy, we analyzed changes in the relative abundance of genes for specific pathways over time and between experimental treatments. Predictable changes included decreases in photosynthesis proteins after the microcosms were established in the dark, as well as a correlation between steroid biosynthesis pathways and eukaryotic abundance. An increased importance for motility appeared in the initial decomposition stage and amino acid amendment. Shifts in pathways for biosynthesis and metabolism of particular lipid classes provide insight into potential mechanisms behind community succession and lipid degradation; for instance, increased representation of glycosphingolipid biosynthesis pathways in the amino acid amendment may be related to the success of copiotrophic Alteromonads in that microcosm.

Lincoln, S.A., DeLong, E.F., Summons, R.E. Manuscript in preparation.

Introduction and rationale

Planktonic marine archaea are cosmopolitan and abundant, representing ~20% of total picoplankton at depths below 100 m (Karner, Delong, & Karl, 2001), but their roles in marine and global carbon cycling are not fully understood. The physiological and phylogenetic diversity of marine archaeal groups – one Thaumarchaeotal (Marine Group I) and three Euryarchaeota (Marine groups II-IV) – means that they are unlikely to react to environmental factors in a monospecific manner.

Marine Group I Thaumarchaeota (MG-I) cultivars are chemolithoautotrophs that fix inorganic carbon via energy obtained from the oxidation of reduced nitrogen species (Könneke et al., 2005). However, several lines of evidence suggest that marine Thaumarchaeota may also be mixotrophs able to utilize organic carbon. A catalyzed reporter deposition-fluorescence in situ hybridization study showed that some MG-I incorporated leucine in field incubations (Herndl et al., 2005). Other evidence of potential mixotrophy comes from the presence of genes predicted to encode a tricarboxylic acid (TCA) cycle for the oxidation of organic compounds in the genomes of the sponge symbiont *Cenarchaeum symbiosum* (Hallam et al., 2006) and *Nitrosopumilus maritimus,* which also contains predicted transporters of amino acids and other organic compounds (Walker et al., 2010). Natural radiocarbon measurements of archaeal tetraether lipids enabled an isotopic mass balance model showing that mesopelagic marine archaea – generally presumed to be dominated by MG-I – were 83% autotrophic at 670 m in the North Pacific Subtropical Gyre (Ingalls

et al., 2006). Recently, pyruvate and α-ketoglutarate were reported to promote growth of *N. maritimus* cultures (Stahl & de la Torre, 2012).

The genome of Marine Group II Euryarchaeota (MG-II), another abundant marine archaeal group, contains no evidence of known autotrophic pathways. Instead, MG-II genes encoding glycolysis, a complete TCA cycle, peptidases and fatty acid degradation indicate that this group is probably strictly heterotrophic (Iverson et al., 2012).

Probing the *in situ* carbon metabolism of uncultivated marine archaeal communities can be challenging. Experiments tracing the incorporation of ^{13}C labeled bicarbonate into archaeal glycerol dialkyl glycerol tetraether (GDGT) lipids provided early evidence of autotrophy in MG-I (Wuchter et al., 2003); similar approaches may prove useful in testing hypotheses about mixotrophy and investigating what factors promote the growth of specific groups or ecotypes over others. The use of isotopically labeled substrates could also enable deconvolution of marine archaeal lipid pools and establish links between taxa and carbon metabolisms.

Here, we conducted microcosm experiments with whole seawater from the oligotrophic North Pacific Subtropical Gyre (NPSG), seeking to measure the incorporation of ^{13}C labeled bicarbonate and amino acids into GDGTs. We monitored concurrent changes in concentrations of nutrients, the isotopic evolution of dissolved and inorganic carbon, microbial community composition, and functional gene categories in the metagenome over the course of the experiments.

Low initial concentrations of GDGTs and poor response of the archaeal population to experimental conditions precluded isotope analysis, but it was possible to quantify individual GDGTs, relative concentrations and proportions of which differed between treatment endpoints. More generally, we were able to study succession of microbial communities and functional gene representation patterns under different treatment conditions and draw preliminary connections between microbes and their potential substrates and metabolites..

Methods

Sampling and incubation setup

Seawater for incubation experiments was collected from 130 m (the persistent shallow nitrite maximum) at the Hawaii Ocean Time-series Station ALOHA on the BioLINCs cruise on 9/20/2011 in 3 deployments of a CTD-rosette. Field samples for lipid, DNA, nutrient and C isotopes were filtered or collected immediately; remaining was stored in carboys at 2~1-22 °C during transit to shore and transported to an environmental chamber in C-MORE Hale, University of Hawaii. Seawater was homogenized, transferred to three 115 L tanks, and maintained in the dark at 21 °C (the in situ field temperature). Amendments were added at 44 h after collection. $H_2{}^{13}CO_2$ was added to Tank A at a target concentration of low μM, and NH_4Cl was added for a final concentration of 650 nM. Tank B treatment received an amendment of a $^{13}C^{15}N$ algal amino acid mixture (Sigma Aldrich) at a target concentration of 10 μM amino acids. Tank C was

unamended and treated as a control. All setup and sampling of all treatments was conducted with minimal exposure to light, with the goal of fostering the growth of ammonia oxidizing MG-I that were thought to be abundant at the nitrite maximum. Tanks were mixed by manual agitation at every sampling point, at minimum every 24 h.

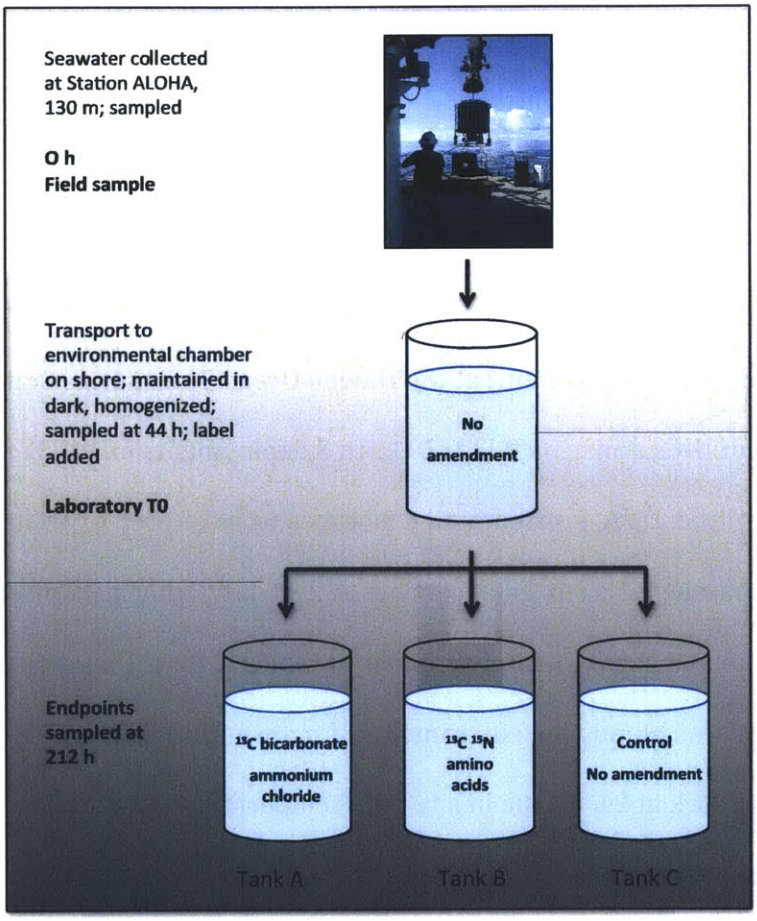

Fig. 1. Incubation setup. Seawater collected by CTD-rosette was transported in carboys to an environmental chamber maintained at 20°C, homogenized and transferred to 115 L tanks. At 44 h Laboratory T_0 samples were collected and amendments were added to tanks. Endpoints were sampled at 212 h.

Lipid and DNA sampling

Suspended particulate matter designated for lipid and nucleic acid analysis was filtered from carboys of seawater (on ship) or from tanks (shore) using a peristaltic pump and platinum-fired silicone tubing (Masterflex, USA). Water was pumped sequentially through 57 μm mesh (Nitex, USA) and a 0.3 μm glass fiber filter (Sterlitech, USA). Filters designated for nucleic acid analysis were stored in lysis buffer and frozen at -80°C until extraction.

DNA extraction and analysis

DNA was extracted from glass fiber filter sections using a Quick-Gene 610 l system (Fujifilm, Japan) and DNA tissue kit L using a modified lysis protocol. Cryovials containing filter sections stored in lysis buffer were thawed on ice and additional lysis buffer was added to bring the volume to 1.6 ml. Cryovials were vortexed for 2 minutes. Lysozyme (Fisher) dissolved in lysis buffer was added to a final concentration of 5 mg/ml, and vials were incubated with rotation at 37 ºC for 45 min. 90 μl proteinase K EDT-01 and 90 μl tissue lysis buffer MDT-01 (Fujifilm, Japan) were added and vials were incubated with rotation at 55 ºC for 2 hours. Lysate was decanted from filter material and transferred to a falcon tube. 1.8 ml Lysis Buffer LDT-01 were added, and samples were incubated with rotation at 55 ºC for 15 min. Finally, 2.4 ml >99% ethanol were added, and samples were vortexed and loaded on the Quick-Gene instrument. DNA was eluted in 400 μl.

DNA from each of the 5 samples (ALOHA 130 field, Laboratory T_0, and Tanks A-C) was prepared and sequenced in quarter plate runs following the GS FLX Titanium protocol. Sequence statistics are shown in Table 1.

Sample	Reads	Unique reads	Mean read length (bp)	rRNA reads	Reads matching RefSeq
ALOHA 130 field sample	246788	244953	319	1203	146690
Laboratory T_0	221248	218934	338	1071	166784
Tank A: Bicarbonate + ammonia	217237	210446	315	699	103911
Tank B: Amino acid amendment	224235	217759	310	1367	87145
Tank C: Control	230393	224089	298	1284	97999

Table 1. DNA sequence statistics.

Lipid extraction and hydrolysis

Lipids were extracted from glass fiber filters containing SPM following a modified Bligh-Dyer protocol after Sturt et al. (Sturt, Summons, Smith, Elvert, & Hinrichs, 2004). Sections of filters were placed in 250 ml Teflon bottles (Nalgene Nunc), submerged in a monophasic solution of 2:1:0.8 methanol:dichloromethane:phosphate-buffered saline (PBS, Sigma-Aldrich) and sonicated for 20 minutes. Solvent was decanted and this step repeated twice. The decanted solvents were combined in a separatory funnel and phase separation was achieved with the addition of 1:1 dichloromethane:water. The organic phase was removed and the aqueous phase extracted with dichloromethane three times. Combined extracts were rinsed with dichloromethane-extracted Nanopure water three times.

Filters were then submerged in a monophasic solution of 10:5:4 methanol:dichloromethane:trichloroacetic acid (Sigma-Aldrich, 2.5% in Nanopure water) and sonicated for 20 minutes. Solvent was decanted and this step repeated twice. Phase separation was achieved as above, and the resultant organic phase was washed with Nanopure water three times. Total lipid extracts (TLEs) were combined with those from the previous step, evaporated under a gentle stream of N_2.

Because of low GDGT concentrations upon initial analysis, TLE were subjected to acid hydrolysis to cleave head groups of intact polar GDGTs, converting them to core GDGTs and improving detection. 1 ml of a mixture of 6 M HCl:methanol: (1:9:1, v/v) was added to dried TLE and vials were sealed and incubated at 70°C for 12 h. The hydrolysate was evaporated under N_2.

Lipid analysis

Samples were analyzed by high performance liquid chromatography – atmospheric pressure chemical ionization mass spectrometry (HPLC-APCI-MS) in positive mode using an Agilent 1260 Infinity series LC coupled to a 6130 quadrupole mass spectrometer using a method modified from Hopmans et al. (2000). Separation was achieved on a Prevail Cyano column (150mm x 2.1mm, 3µm, Alltech, USA) maintained at 25°C. The injection volume was 10µl and compounds were eluted isocratically with 100% eluent A (hexane:isopropanol 99:1) for 5 minutes, followed by a linear gradient to 15% eluent B (hexane:isopropanol 9:1) over 15 minutes and a return to 100% eluent A over 5 minutes, all at a flow rate of

0.4ml/min. Between analyses the column was equilibrated with 100% eluent A at 0.6ml/min. for 10 minutes. APCI-MS conditions were as follows: gas temperature 350°C, vaporizer temperature 380°C, drying gas flow 6l/min., nebulizer pressure 30psi, capillary 2000V, corona 5μA. GDGTs and were detected by selected ion monitoring; full scans were run periodically to monitor background and to confirm compound identification.

Nutrients

NH_4^+ concentrations were measured in the laboratory during the course of the experiment using the OPA fluorometric method (Holmes, Aminot, Kérouel, Hooker, & Peterson, 1999).

Water for NH_4^+, PO_4, NO_2+NO_3 and silicate measurements was collected in acid washed 40 ml vials and frozen at -20°C until analysis at the Nutrient Analytical Center at the Woods Hole Oceanographic Institute.

DIC and DOC concentrations and $\delta^{13}C$

Water samples for organic and inorganic carbon isotope analysis and quantification were collected in combusted glass beakers and filtered through 0.3 μm combusted glass filters (47 mm, Sterlitech, USA) held in Buchner funnels. Filtrate was transferred to precombusted 40 ml glass vials with airtight septa and kept refrigerated until analysis at the G.G. Hatch Stable Isotope Laboratory, University of Ottawa, Canada.

Microbial community representation in metagenomic datasets

Analysis of DNA datasets began with the removal of duplicate (100% identity level of equivalent length) sequences. Duplicate-free fasta files were divided into rRNA and non rRNA reads by using BLASTn (top hit, e-values <0.0001, bit scores >50) to compare them to a rRNA database comprised of combined SILVA release 106 SSU and LSU databases and a 5S database ("Nucl. Acids Res.-2002-Szymanski-176-8," 2001). Using BLAST, non-rRNA reads were compared with a reference database comprised of NCBI RefSeq release 54, protein sequences from the Moore Marine Microbial Genomes project, and several recently published marine microbial genomes. Matches with bit scores >50 were retained.

Top BLASTn hits (e value <0.001, bit score >50) against the rRNA database described above were used to divide the input files into rRNA and non-rRNA reads. Matches with a score within 10% of the best match were exported to MEGAN (Huson, Mitra, Ruscheweyh, Weber, & Schuster, 2011) and their putative taxonomic affiliations determined.

Functional gene analysis

Non rRNA reads were compared to Kyoto Encyclopedia of Genes and Genomes (KEGG) (Kanehisa & Goto, 2000) databases using BLASTx for functional analysis, with a BIT score >50 cutoff. Matches to KEGG (level 3 hierarchy) categories of interest (primarily relating to carbon metabolism and lipid biosynthesis and metabolism) that recruited >10 reads were selected for

visualization in a heat map. The heat map was constructed using the R software environment and normalized row-wise rather than across the entire dataset.

Results and Discussion

Nutrient concentrations across the course of the experiment are shown in Fig. 2. The most pronounced shifts are in ammonium concentrations measured at the time of the experiments with the OPA method; Tank A (ammonium + bicarbonate amendment) shows significant drawdown of ammonium from 650 to 240 nM between 75 and 200 h. Tank B (amino acid amendment) experienced a rapid spike in ammonium concentrations within 6 h of the amendment addition. Phosphate, nitrate + nitrite concentrations were very low throughout the course of the experiment.

Figs. 3-4 shows the concentration and isotopic evolution of dissolved inorganic carbon (DIC) and dissolved organic carbon (DOC) in microcosms over the course of the experiment. Progressive enrichment in ^{13}C DOC in the control treatment likely reflects slight contamination from neighboring tanks or alternatively during analysis.

Total lipid extracts (TLE) from different treatments showed different pigmentation patterns (Fig. 5). Degradation of chlorophylls was rapid, with transition from typical bright green to near clear TLEs within 44 h. Tank A and the control TLEs were straw-colored, likely due to pigments from *Rhodobacterales,* the relative abundance of which increased Tanks A and C. Some Rhodobacter are

known to synthesize a yellow pigment in the dark (Yue, Huang, Zhao, Yang, & Qu, 2009).

GDGTs

Relative proportions of individual archaeal tetraether lipids changed over the course of the incubations (Fig. 6) although the tanks were kept at the same relatively constant temperature (21-22 °C; in situ temperature in the field was 21°C). From the field sample to the 44 h incubation T_0 sample, the relative proportion of crenarchaeol increased. The relative proportion of GDGT-0 (containing 0 cyclopentyl moieties) decreased from the laboratory T_0 sample to the final Tank A and C samples, but increased in Tank B. Tank B GDGTs show a pattern distinct from A and C, with an increase in GDGT-0, decrease in crenarchaeol, and increases in GDGTs-2 and -3. To our knowledge, this is the first direct evidence that factors other than temperature can influence the relative proportion of GDGTs present in seawater; however, the mechanism underlying this shift, and whether it relates to changes in physiology, taxon composition, or both, cannot be determined from the available data.

Our data also indicate that GDGT turnover in ocean surface waters can be relatively rapid. Concentrations of GDGTs decreased by 43% in the 44 h between field sampling and Laboratory T_0 (Table 2). Total GDGT concentrations after 212 h were highest (131% of T_0 value) in the amino acid amendment endpoint. Such rapid GDGT degradation rates suggest that free core GDGTs detected in the oceans are

likely derived from archaea that have recently died and are not relicts of a long-dead historical population. It is possible, however, that incubation conditions promoted GDGT degradation to an extent not likely to exist in the natural environment. Future incubation studies that include more replicates could help resolve whether the rapid degradation rate we observed was caused by "bottle effects." In the current study, replicate incubations were impractical because of the large volumes that had to be filtered and incubated to analyze GDGTs in oligotrophic seawater, as well as the need to transport water to an environmental chamber large enough to hold multiple 115 L tanks.

Sample	Total GDGTs (pg/L)
ALOHA 130 field sample	134
Laboratory T_0	77
Tank A Bicarbonate + ammonia	92
Tank B Amino acid amendment	101
Tank C Control	86

Table 2. Concentrations of total GDGTs (acid-hydrolyzed cores) at different experimental time points.

Microbial community succession in experimental treatments

Archaea

The relative proportion of archaeal reads to total protein coding reads assigned on the domain and virus level declined from 7% to <1 % between field

sampling and laboratory T_0 (Fig. 7). Because this is a decline in relative rather than absolute percent, it alone does not indicate a drop in archaeal cells; archaea could simply be offset by the rapid growth of another domain. When combined with the rapid drop in GDGT concentrations, however, the decline seems to indicate that the total archaeal population was reduced significantly in the first 44 h. Perturbations including changes in temperature and light during transit to shore and transport to the laboratory likely contributed to this reduction. The decision to conduct the experiments in the dark may have been a greater issue. In sampling, we targeted the nitrite maximum in an effort to obtain a sample that contained significant numbers of nitrifying MG-I Thaumarchaeota, yet was shallow enough to also capture active MG-II Euryarchaeota. Contrary to expectation, the field sample was dominated by MG-II (Fig. 8). Many photic zone MG-II are photoheterotrophs containing the light-driven proton pump proteorhodopsin (Frigaard, Martínez, Mincer, & DeLong, 2006) (Iverson et al., 2012), and incubation in the dark may have been detrimental to those ecotypes.

The decline in the relative abundance of archaeal reads was offset by increases in reads assigned to bacteria (Fig. 7). This suggests that heterotrophic bacteria, rather than eukaryotes, may have been responsible for the decrease in GDGTs. No sediment was observed to accumulate at the bottom of tanks, and agitation was thorough, so it appears unlikely that GDGTs disappeared in sinking particles. Similarly, only rare particles accumulated on the 57 μm mesh prefilter, suggesting that consumption by comparatively large zooplankton or adhesion onto

particles was not a probable mechanism for reduction of GDGT concentrations in the first 44 h.

A dramatic increase in the relative percent of thaumarchaeotal reads between the field sample and laboratory T_0 suggests that Thaumarchaeota may be more resilient to perturbation than MG-II Euryarchaeota. Within the Euryarchaeota (Fig. 9), the relative abundance of reads identified as belonging to MG-II declined sharply from 88% in the field sample to 6% in Laboratory T_0, and never rebounded significantly. From 44 to 212 h in Tanks A and C (ammonia + bicarbonate and control) the percent of euryarchaeal reads assigned to MG-II increased slightly, from 6% in to 16 and 20%, respectively. In Tank B (amino acids) the percent of euryarchaeal reads assigned to MG-II only reached 8% in the same time period. The diversity of MG-II and the fact that only a single MG-II genome is available may distort this picture; it seems likely that reads identified as being from other Euryarchaeota may simply be derived from ecotypes of MG-II that are dissimilar to the assembled MG-II genome (Iverson et al., 2012). In any case, the euryarchaeal community response to the amino acid amendment (Tank B) appears different from that of the other treatments. This taxonomic shift may potentially be related to the distinct GDGT pattern (Fig. 6).

Bacteria

At the phylum level, bacterial reads in all samples were dominated by Proteobacteria (Fig. 10). As expected in the transition from light to dark incubation conditions, cyanobacterial reads declined sharply in relative percent from 24% to

<5% in the first 44 h, and then to < 3% in each of the three tanks by the end of the 212 h experiment. Bacteroidetes increased significantly between Incubation T_0 and the endpoint in Tank B, which received the amino acid amendment.

At the bacterial class level, reads affiliated with *Alteromonodales* became dominant in the first 44 h (Fig. 11). This is consistent with an understanding of Alteromonads as motile copiotrophs able to respond quickly to increases in dissolved organic carbon (McCarren et al., 2010; Shi, Tyson, Eppley, & Delong, 2010) that likely occurred during the demise of phytoplankton and cyanobacteria during the initial "rotting" phase of the experiment. Some Alteromonads are known to degrade lipids (e.g. (Duflos, Goutx, & Wambeke, 2009)) so this class may have contributed to the decline in GDGT concentrations between the field and Laboratory T_0.

A second wave of bacterial community succession involved the increase in the relative percent of reads affiliated with *Rhodobacterales*, which occurred between 44 and 212 h. Rhodobacter species are metabolically diverse, with some capable of photosynthesis, lithotrophy, and aerobic and anaerobic respiration. Such diversity makes it difficult to create hypotheses for the role of these bacteria in the incubations based solely on DNA. However, Rhodobacter species have shown chemotaxis toward ammonia under nitrogen limitation (Poole & Armitage, 1989), so they may have contributed to the ammonia drawdown observed in Tanks A and C. Thus, in these experiments in which MG-I are a minor component of the microbial

community, nitrification may have been a smaller sink for ammonia than use of ammonia as a nitrogen source by the abundant Rhodobacter.

Reads affiliated with Rhodobacter have the lowest relative abundance at an endpoint in Tank B (amino acids amendment), where they were offset by an increase in *Flavobacteriales*, sustained presence of *Alteromomodales* and an increase in *Ricketsialles*.

Eukarya

Eukaryotic community composition inferred from the taxonomic affiliation of protein coding reads assigned at the Kingdom level showed only minor variation across the sample set (Fig. 11). The greatest change was an increase in the relative percent of Stramenopiles and a 20% decrease in Viridiplantae reads from field to T_0, expected during the transition from light to dark incubation conditions.

Viruses

Viral community composition inferred in the same manner was also relatively consistent across time and between treatments. At the "species" level, reads most closely related to *Cafeteria roenbergensis* increased between Laboratory T_0 and all three treatment endpoints, with the greatest representation in Tank B.

Functional gene representation

We studied differential representation of genes encoding KEGG categories of interest to the investigation of C metabolism, lipid biosynthesis and lipid

metabolism in the five metagenomic datasets generated for this study (Fig. 14). An increased importance for motility in the "rotting experiment" stage of the first 44 h of the incubation was evidenced by increased relative representation of the KEGG categories for secretion systems, flagellar assembly and bacterial motility proteins between the field and Incubation T_0. These changes are consistent with those observed in an experimental metatranscriptomic study of dissolved organic matter degradation (McCarren et al., 2010).

Representation of lipid, fatty acid and terpenoid backbone biosynthesis KEGG pathways declined in the metagenome during the rotting stage, at the same time as glycosphingolipid biosynthesis pathways became more highly represented. Glycosphingolipids are present in some gram negative proteobacteria lacking lipopolysaccharide, and have been proposed to facilitate uptake of hydrophobic aromatic compounds (Kawahara, Kuraishi, & Zähringer, 1999); potentially, they contribute to the copiotrophic capacity of *Alteromonadales* that bloomed during the first 44 h.

Not surprisingly, the pattern of relative abundance of KEGG orthologs for steroid biosynthesis is closely related to the relative abundance of protein coding reads affiliated with eukaryotes (Fig. 7). The sharp decline seen in the abundance of KEGG orthologs for photosynthesis proteins, carotenoid biosynthesis and photosynthetic carbon fixation was also predictable given the incubation conditions.

Conclusions and prospectus

Although the poor response of archaeal groups to experimental conditions made it impossible to measure incorporation of ^{13}C into archaeal lipids, this study has provided novel information about factors that may influence the relative abundance of GDGTs in the water column. Specifically, the distinct GDGT pattern seen in the amino acid amendment warrants further investigation. Future incubation studies including replicates and additional carbon substrates such as lipids, with parallel community characterization, should be conducted to gain insight into how factors such as nutrients or carbon substrate might impact archaeal membrane lipid composition. The use of seawater from coastal or other less oligotrophic provinces likely to contain higher archaeal cell counts could improve the odds of successful measurement of isotopic label incorporation.

The addition of a MG-II genome (Iverson et al., 2012) to databases greatly increases the potential for experimental metatranscriptomic analyses to shed light on processes influencing and underpinning archaeal carbon metabolism and factors promoting growth of particular groups or ecotypes in mixed communities.

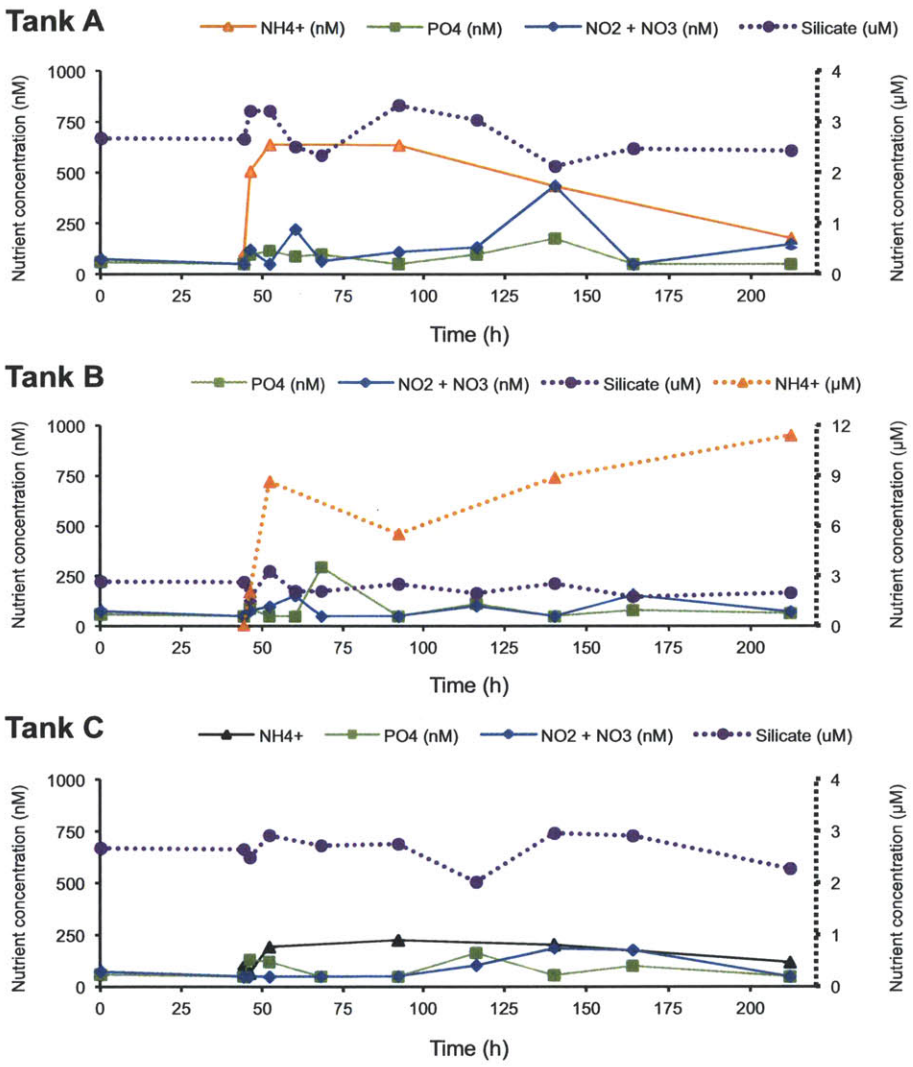

Fig. 2. Ammonium, phosphate, nitrate + nitrite, and silicate concentrations meas ured in incubation experiments. Solid lines indicate nutrient data in the nM range, plotted at the scale on the left y axis; dashed lines mark data in the µM range plotted at the scale on the right y axis. The vertical grey line marks the addition of label at 44h.

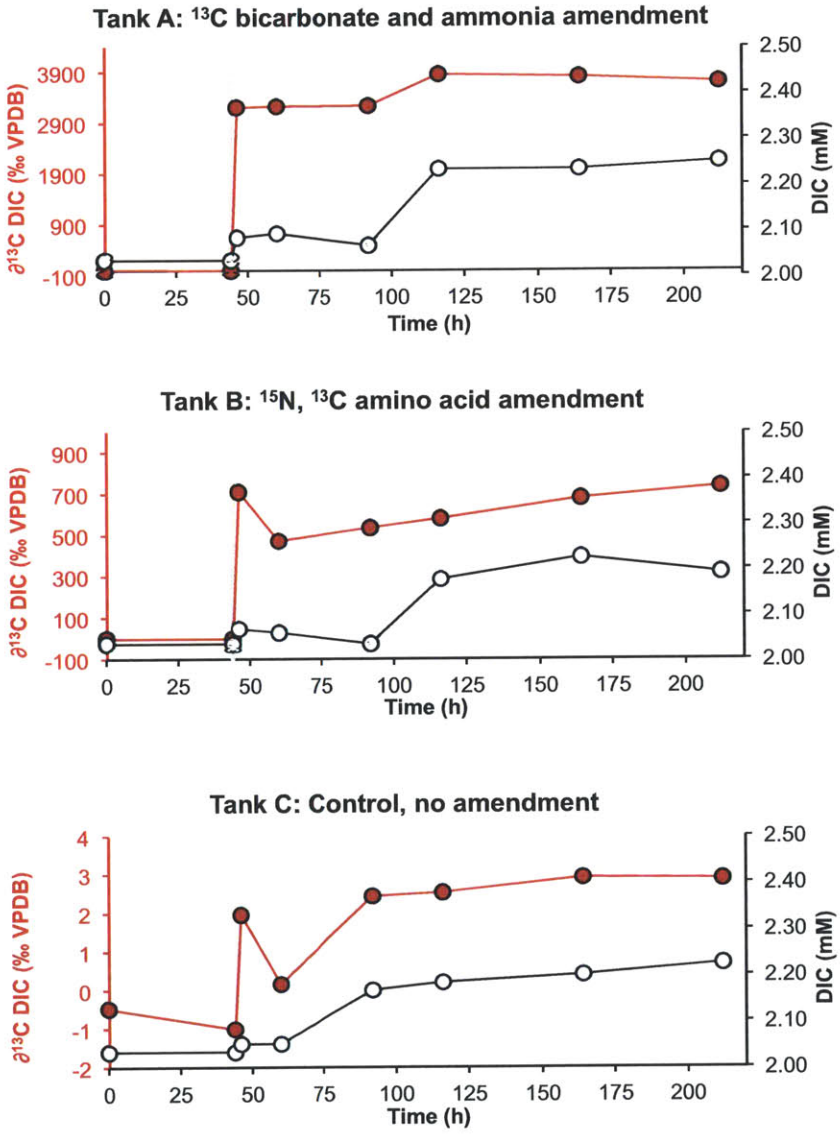

Fig. 3. Dissolved inorganic carbon data from incubation experiments. Filled red circles indicate $\partial^{13}C$ values plotted on the scale shown in the left y axis. Open circles indicate DIC concentrations (right y axis). The vertical grey line marks the addition of label at 44h.

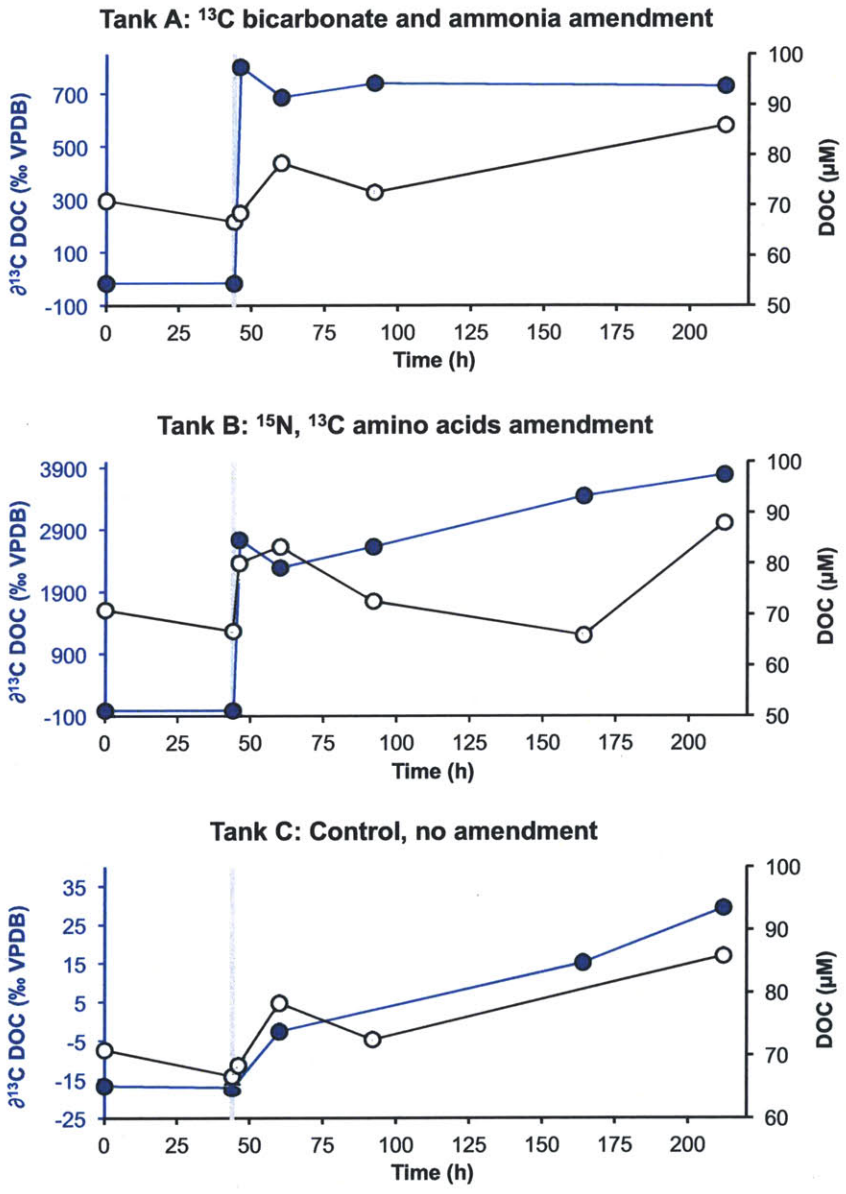

Fig. 4. Dissolved organic carbon data from incubation experiments. Filled blue circles indicate $\partial^{13}C$ values values plotted on the scale shown in the left y axis. Open circles indicate DIC concentrations (right y axis). The vertical grey line marks the addition of label at 44h.

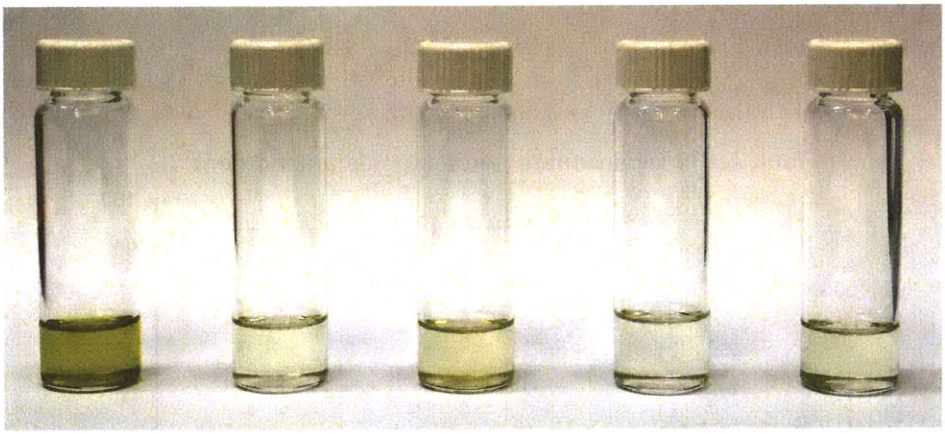

Fig. 5. Total lipid extracts from, left to right, ALOHA 130 m field sample; Laboratory T_0; Tank A ammonia + bicarbonate amendment T_F, Tank B amino acids amendment; Tank C control. Pigmentation increases in Tank A and C may be attributed to large increases in the relative proportion of Rhodobacter, which synthesizes yellow pigments in dark aerobic conditions (Yue et al., 2009).

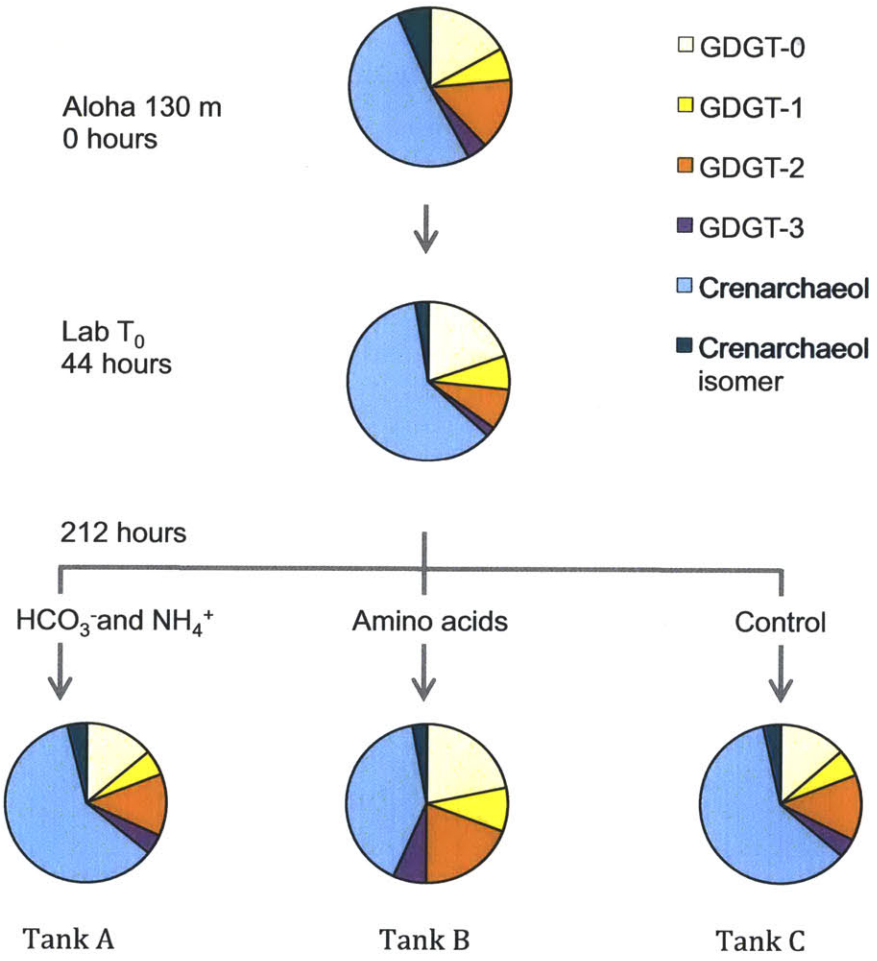

Fig. 6. Relative distributions of core GDGTs (sum of free + acid-hydrolyzed) detected in incubation experiments.

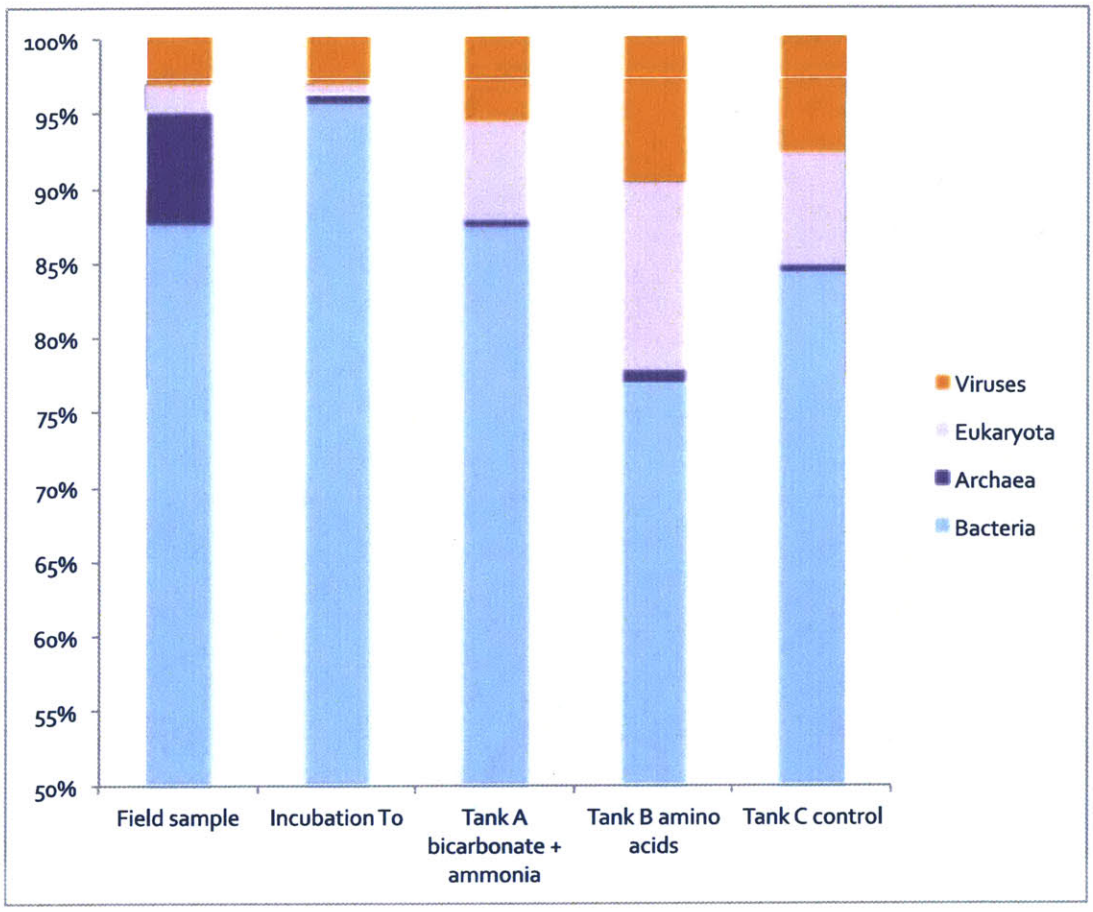

Fig. 7. Taxonomic affiliation of protein coding reads in incubation metagenomic datasets at the Domain level, with viruses, normalized to 100%, BIT score >50. Archaeal representation declined sharply from the field sample to Incubation T_0 sampled 44 h after collection of seawater at HOT Station ALOHA.

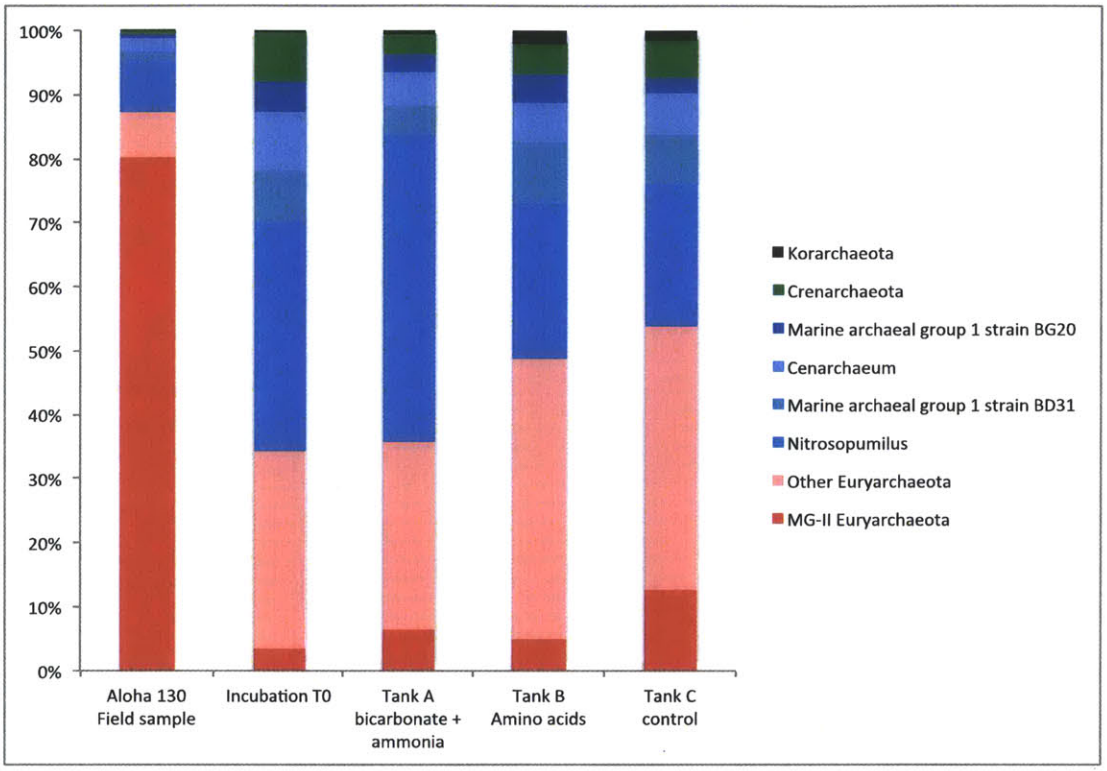

Fig. 8. Normalized taxonomic affiliation of archaeal protein coding reads in metagenomic datasets from incubation timepoints and treatments, BIT score >50.

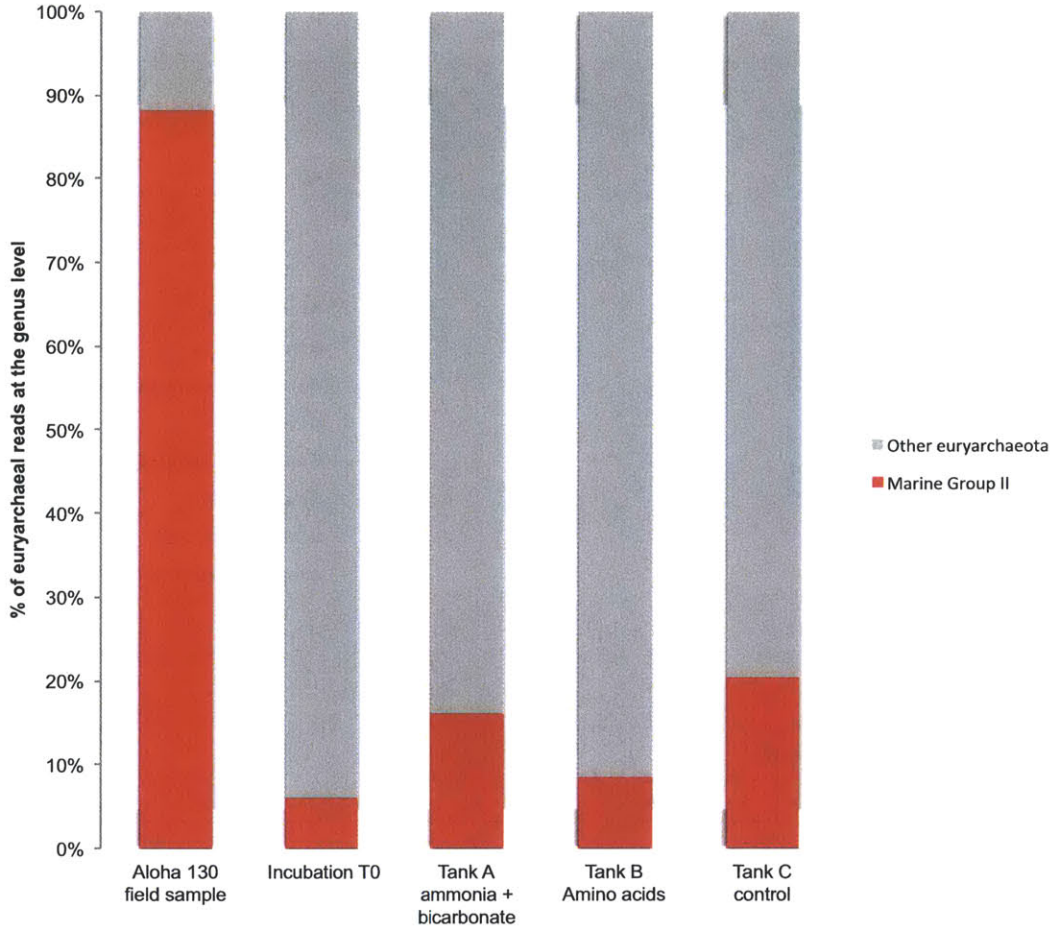

Fig. 9. Normalized taxonomic affiliation of euryarchaeal protein-coding reads assigned at the genus level, BIT score >50. The category "other Euryarchaeota" includes methanogens and halophiles, but its existence may be an artifact caused by the high diversity of MG-II and the presence of only one MG-II genome in the reference database.

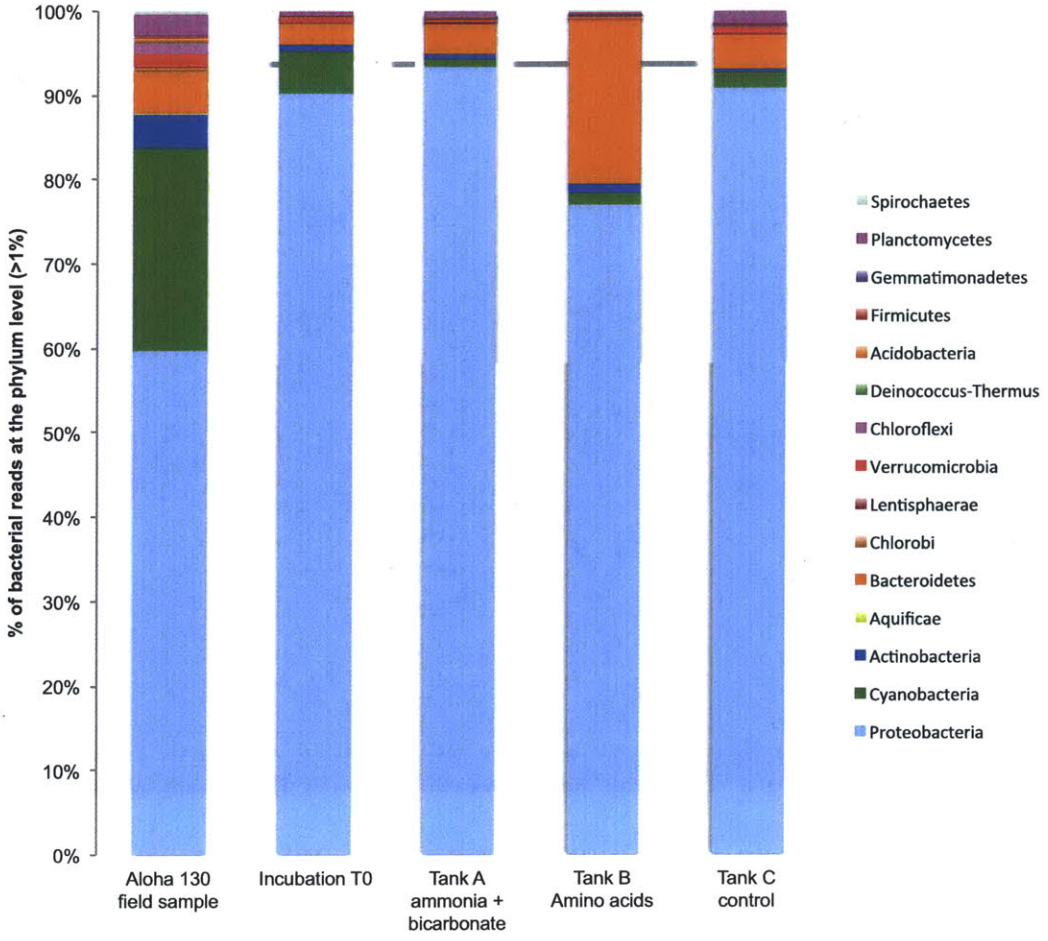

Fig. 10. Normalized taxonomic affiliation of bacterial protein-coding reads assigned at the Phylum level, bit score >50. Only taxa representing >1% of total matches were included in this plot.

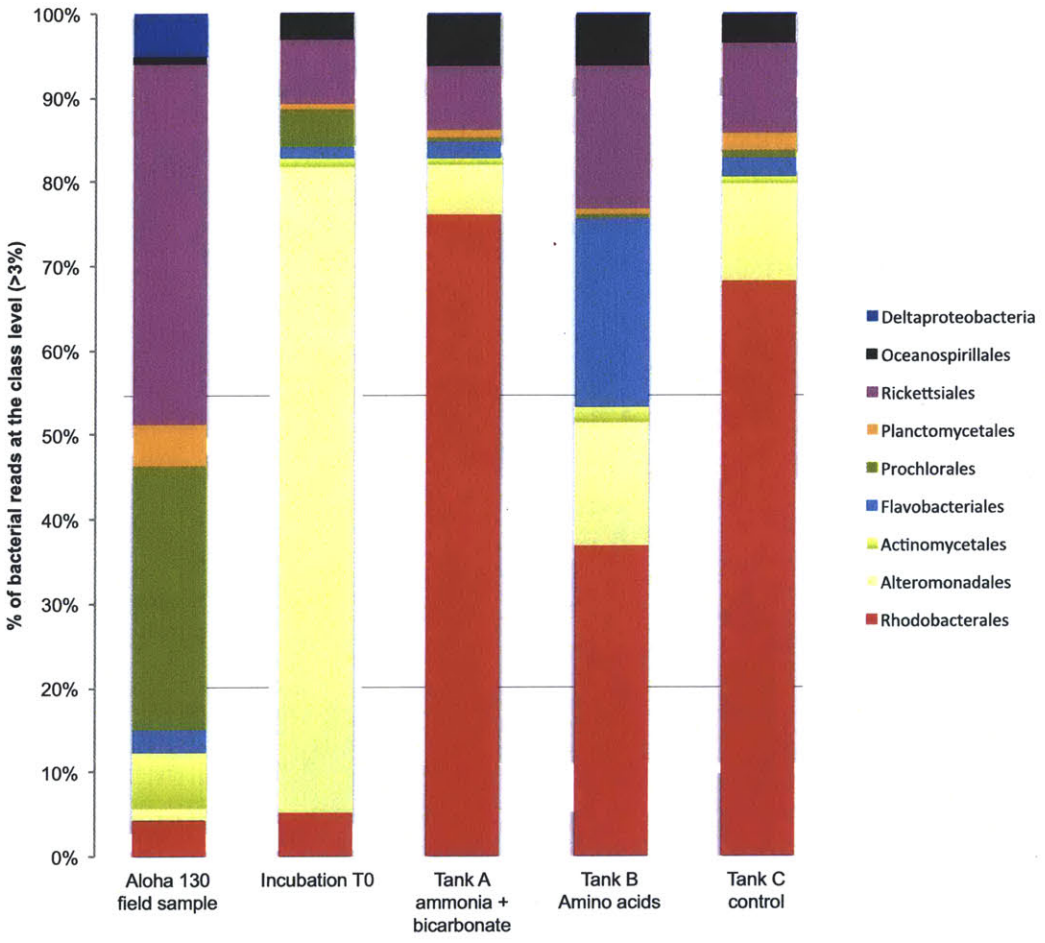

Fig. 11. Normalized taxonomic affiliation of bacterial protein-coding reads assigned at the Class level, bit score >50. Only taxa representing >3% of matches were included in this plot.

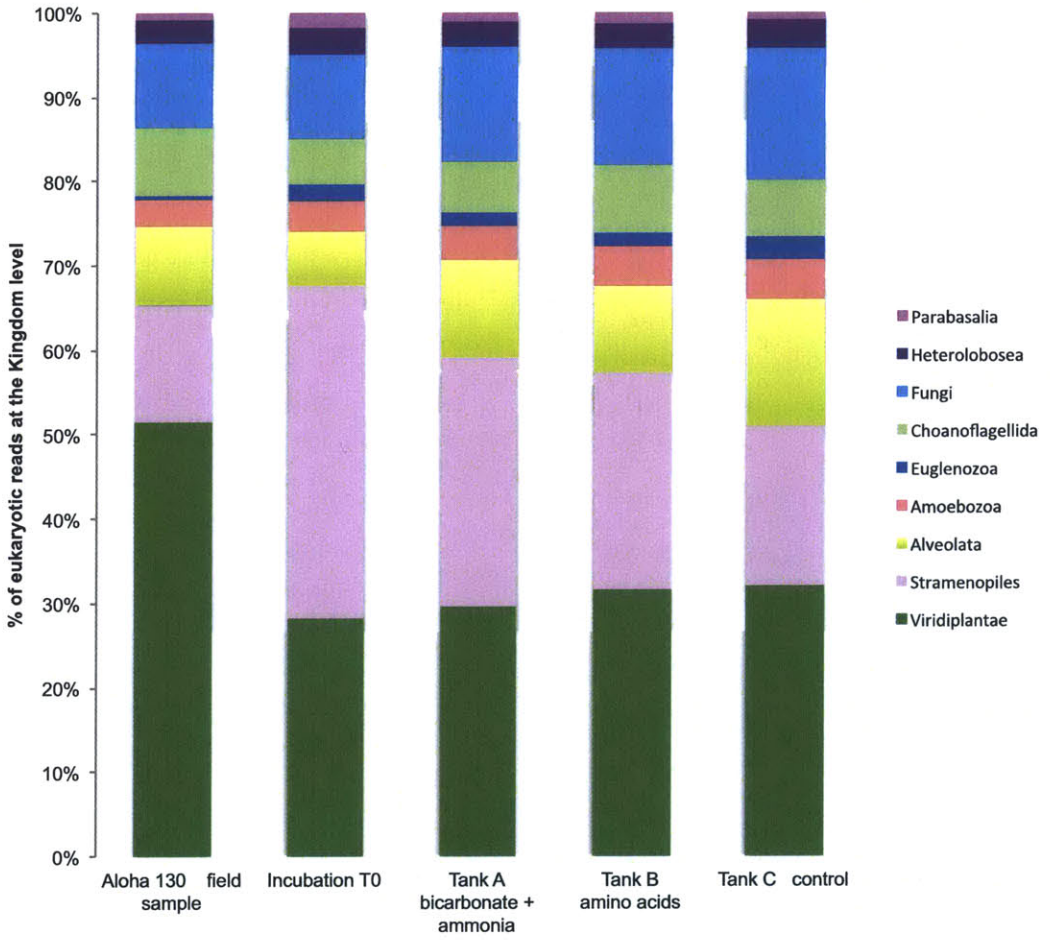

Fig. 12. Normalized taxonomic affiliation of eukaryotic protein-coding reads assigned at the Kingdom level, bit score >50.

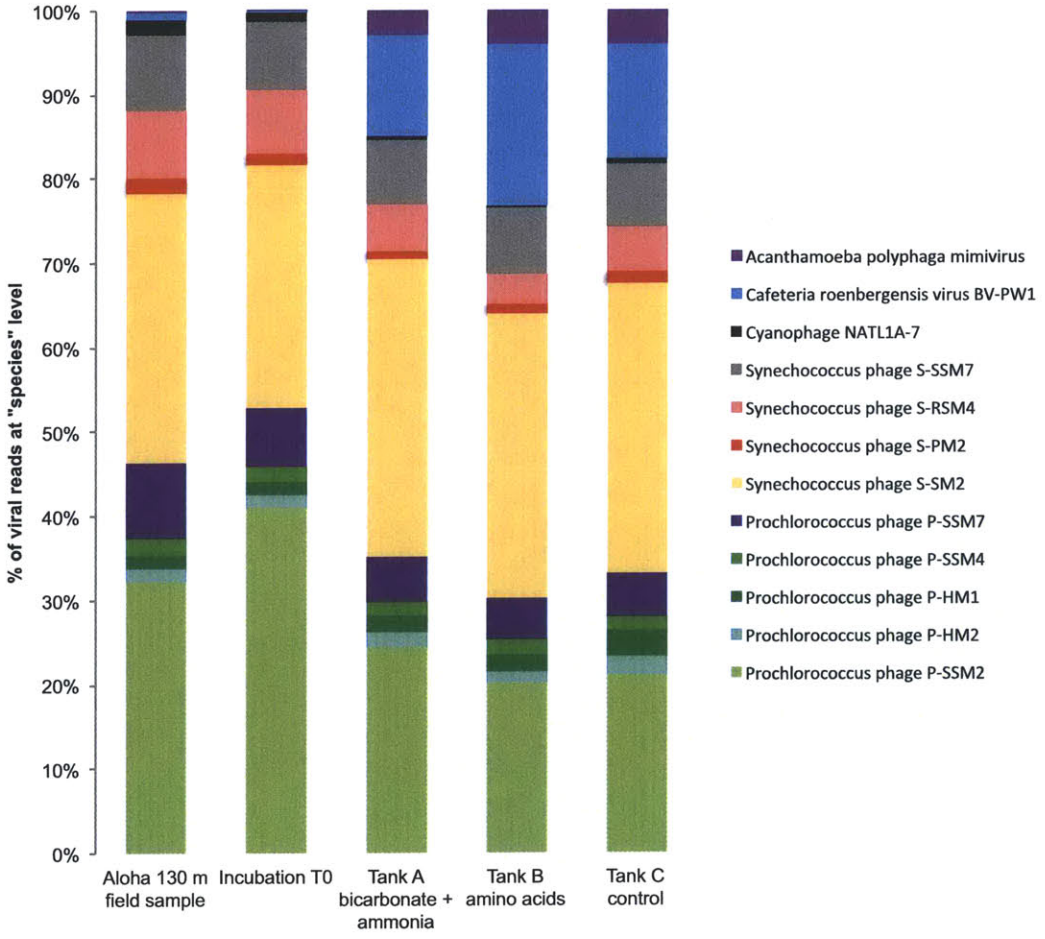

Fig. 13. Normalized taxonomic affiliation of viral protein-coding reads assigned at the Species level, bit score >50.

Fig. 14. Relative representation of KEGG pathways, level 3 hierarchy. Data in the heatmap are normalized row-wise; the least represented pathway is red, most represented green, and intermediate represented are gray.

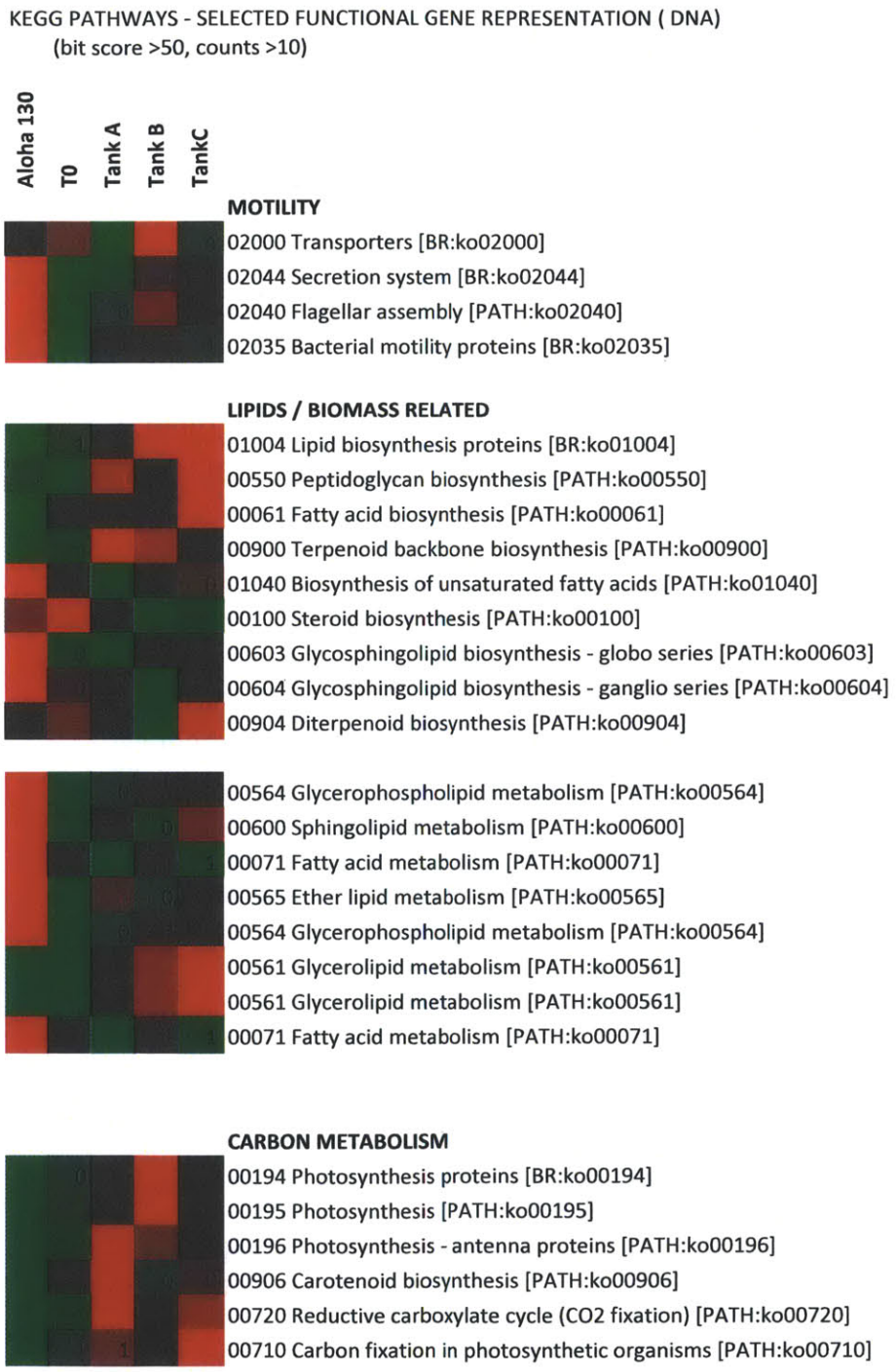

References

Duflos, M., Goutx, M., & Wambeke, F. (2009). Determination of Lipid Degradation by Marine Lipase-Producing Bacteria: Critical Evaluation of Lipase Activity Assays. *Lipids, 44*(12), 1113–1124. doi:10.1007/s11745-009-3358-7

Frigaard, N.-U., Martínez, A., Mincer, T. J., & DeLong, E. F. (2006). Proteorhodopsin lateral gene transfer between marine planktonic Bacteria and Archaea. *Nature, 439*(7078), 847–850. doi:10.1038/nature04435

Hallam, S. J., Mincer, T. J., Schleper, C., Preston, C. M., Roberts, K., Richardson, P. M., & Delong, E. F. (2006). Pathways of Carbon Assimilation and Ammonia Oxidation Suggested by Environmental Genomic Analyses of Marine Crenarchaeota. *PLoS Biology, 4*(4), e95. doi:10.1371/journal.pbio.0040095.st003

Herndl, G. J., Reinthaler, T., Teira, E., van Aken, H., Veth, C., Pernthaler, A., & Pernthaler, J. (2005). Contribution of Archaea to total prokaryotic production in the deep Atlantic Ocean. *Applied and Environmental Microbiology, 71*(5), 2303–2309. doi:10.1128/AEM.71.5.2303–2309.2005

Holmes, R. M., Aminot, A., Kérouel, R., Hooker, B. A., & Peterson, B. J. (1999). A simple and precise method for measuring ammonium in marine and freshwater ecosystems. *Canadian Journal of Fisheries and Aquatic Sciences, 56*(10), 1801–1808. doi:10.1139/f99-128

Huson, D. H., Mitra, S., Ruscheweyh, H. J., Weber, N., & Schuster, S. C. (2011). Integrative analysis of environmental sequences using MEGAN4. *Genome Research, 21*(9), 1552–1560. doi:10.1101/gr.120618.111

Ingalls, A. E., Shah, S. R., Hansman, R. L., Aluwihare, L. I., Santos, G. M., Druffel, E. R., & Pearson, A. (2006). Quantifying archaeal community autotrophy in the mesopelagic ocean using natural radiocarbon. *Proceedings of the National Academy of Sciences, 103*(17), 6442–6447.

Iverson, V., Morris, R. M., Frazar, C. D., Berthiaume, C. T., Morales, R. L., & Armbrust, E. V. (2012). Untangling Genomes from Metagenomes: Revealing an Uncultured Class of Marine Euryarchaeota. *Science, 335*(6068), 587–590. doi:10.1126/science.1212665

Kanehisa, M., & Goto, S. (2000). KEGG: kyoto encyclopedia of genes and genomes. *Nucleic acids research, 28*(1), 27–30.

Karner, M. B., Delong, E. F., & Karl, D. M. (2001). Archaeal dominance in the mesopelagic zone of the Pacific Ocean. *Nature, 409*(6819), 507–510. doi:10.1038/35054051

Kawahara, K., Kuraishi, H., & Zähringer, U. (1999). Chemical structure and function of glycosphingolipids of Sphingomonas spp and their distribution among members of the α-4 subclass of Proteobacteria. *Journal of industrial microbiology & biotechnology, 23*(4-5), 408–413.

Könneke, M., Bernhard, A. E., la Torre, de, J. R., Walker, C. B., Waterbury, J. B., & Stahl, D. A. (2005). Isolation of an autotrophic ammonia-oxidizing marine archaeon. *Nature, 437*(7058), 543–546. doi:10.1038/nature03911

McCarren, J., Becker, J. W., Repeta, D. J., Shi, Y., Young, C. R., Malmstrom, R. R., et al.

(2010). Microbial community transcriptomes reveal microbes and metabolic pathways associated with dissolved organic matter turnover in the sea. *Proceedings of the National Academy of Sciences, 107*(38), 16420–16427.

Nucl. Acids Res.-2002-Szymanski-176-8. (2001). Nucl. Acids Res.-2002-Szymanski-176-8, 1–3.

Pester, M., & Schleper, C. (2011). The Thaumarchaeota: an emerging view of their phylogeny and ecophysiology 10.1016/j.mib.2011.04.007 : Current Opinion in Microbiology | ScienceDirect.com. *Current opinion in microbiology*.

Poole, P. S., & Armitage, J. P. (1989). Role of metabolism in the chemotactic response of Rhodobacter sphaeroides to ammonia. *Journal of bacteriology, 171*(5), 2900–2902.

Shi, Y., Tyson, G. W., Eppley, J. M., & Delong, E. F. (2010). Integrated metatranscriptomic and metagenomic analyses of stratified microbial assemblages in the open ocean. *The ISME Journal, 5*(6), 999–1013. doi:10.1038/ismej.2010.189

Stahl, D. A., & la Torre, de, J. R. (2012). Physiology and Diversity of Ammonia-Oxidizing Archaea. *Annu. Rev. Microbiol., 66*(1), 83–101. doi:10.1146/annurev-micro-092611-150128

Sturt, H. F., Summons, R. E., Smith, K., Elvert, M., & Hinrichs, K.-U. (2004). Intact polar membrane lipids in prokaryotes and sediments deciphered by high-performance liquid chromatography/electrospray ionization multistage mass spectrometry—new biomarkers for biogeochemistry and microbial ecology. *Rapid Communications in Mass Spectrometry, 18*(6), 617–628. doi:10.1002/rcm.1378

Walker, C., La Torre, de, J., Klotz, M., Urakawa, H., Pinel, N., Arp, D., et al. (2010). Nitrosopumilus maritimus genome reveals unique mechanisms for nitrification and autotrophy in globally distributed marine crenarchaea. *Proceedings of the National Academy of Sciences, 107*(19), 8818.

Yue, H., Huang, X., Zhao, C., Yang, S., & Qu, Y. (2009). Regulation mechanism of photopigments biosynthesis via light and oxygen in Rhodobacter azotoformans 134K20]. *Wei sheng wu xue bao= Acta microbiologica Sinica, 49*(3), 331.

Chapter 4

Archaeal and bacterial glycerol dialkyl glycerol tetraether lipids in chimneys of the Lost City Hydrothermal Field *

Abstract

We detected archaeal and bacterial glycerol dialkyl glycerol tetraether (GDGT) lipids in carbonate chimneys of the Lost City Hydrothermal Field, an alkaline system near the mid-Atlantic Ridge. Isoprenoidal, archaeal tetraethers from this site include "H-shaped" GDGTs, crenarchaeol and GDGTs with 0-3 cyclopentane moieties (here referred to as GDGTs 0-3). Concentrations of GDGT-3 do not track those of GDGTs 0-2 across the sample set, suggesting that its biosynthesis may be subject to different controls. Two branched, bacterial GDGTs (brGDGTs) common in terrestrial environments were also detected. Consulting previously published surveys of microbial diversity at Lost City and literature on known precursor-product relationships, we investigated the provenance of these GDGTs. The principal source of GDGTs 0-3 is likely ANME-1 archaea, abundant at Lost City. H-shaped GDGTs are likely derived from thermophilic Methanobacteria and Thermoprotei. Marine Group I Thaumarchaea detected in Lost City chimneys are a potential source of crenarchaeol, but it is unclear whether they are autotrophic nitrifiers or representatives of a hydrothermal ecotype with different physiology. The detection of branched GDGTs, possibly synthesized by Acidobacteria at Lost City, adds to a growing body of evidence that the capacity for their biosynthesis is not restricted to acidophilic soil bacteria and that they cannot strictly be considered indicators of terrestrial contributions to marine sediments. Input of hydrothermally derived lipids has the potential to complicate paleoproxy applications based on GDGTs. We propose that H-GDGTs be viewed as indicators of hydrothermal input and that their detection in sediments warrants caution in proxy application when a hydrothermal origin for co-occurring isoprenoidal and brGDGTs cannot be excluded.

---

* In press, Organic Geochemistry. Included with permission of Elsevier.

Lincoln, S.A., Bradley, A.S., Newman, S.A., and Summons, R.E., 2013. Archaeal and bacterial glycerol dialkyl glycerol tetraether lipids in chimneys of the Lost City Hydrothermal Field.

1. Introduction

Membrane-spanning glycerol dialkyl glycerol tetraether (GDGT) lipids (Fig. 1) are widespread in the environment and the sedimentary record. Isoprenoidal GDGTs have *sn*-1 glycerol stereochemistry characteristic of the domain Archaea; *sn*-3 glycerol stereochemistry distinguishes branched GDGTs (brGDGTs) as bacterial in origin. The cores of brGDGTs are composed of hydrocarbon chains with varying numbers of methyl substituents and cyclopentane moieties. GDGT cores, composed of isoprenoid chains, can contain both cyclopentane and cyclohexane moieties.

The analysis of GDGTs in the environment has expanded significantly in recent years, driven largely by their utility in paleoproxies and microbial ecology. Despite advances in understanding the phylogenetic distribution of brGDGT and isoprenoidal GDGT biosynthesis (e.g. Knappy et al., 2011, Sinninghe Damsté et al., 2011) and reports of these molecules in many modern ecosystems and sedimentary records, controls on the occurrence of GDGTs and the ecology of the microbes that synthesize them remain poorly understood. Moreover, expanded analytical methods have revealed a previously unknown breadth of structural diversity in GDGTs (e.g. Liu et al., 2012a), highlighting gaps in our understanding of the provenance and significance of the full inventory of tetraether lipids in the environment.

Microbes that synthesize GDGTs have been isolated and enriched from the environment but it is unclear how their activity in culture compares to the activity of related organisms in complex natural communities. Parallel, cultivation-independent studies of GDGTs and nucleic acids in diverse environments have the

potential to provide new insight into the biogeochemical significance of these lipids and the microbes that synthesize them, as well as the foundations of paleoproxies that employ them.

Here, we document the occurrence of GDGTs in the Lost City Hydrothermal Field, an alkaline hydrothermal system near the mid-Atlantic Ridge (Kelley et al., 2005; Fig. 2). Relatively low temperature (<150°C) interactions between seawater and peridotite at Lost City give rise to serpentinization, a process involving a series of exothermic reactions that control hydrothermal fluid chemistry and sustain a rich microbial ecosystem. Lost City vent fluids are alkaline (pH 9-11), with calcium concentrations up to 30 mmol/kg. Calcium carbonate precipitates when these fluids mix with seawater, building chimneys as tall as 60 m. The vent field is estimated to have been active for at least 30,000 years **(Früh-Green et al., 2003)**, and contains both active and "extinct" chimneys. Unlike structures common to black smoker hydrothermal systems, Lost City chimneys lack a central orifice; rather, fluids emerge from networks of channels and fissures. Actively venting structures are more porous and friable than the inactive chimneys, which tend to be well lithified (Kelley et al., 2005).

Methane (1-2 mmol/kg) and hydrogen (1-15 mmol/kg) in hydrothermal fluids sustain the microbes that inhabit the carbonate structures (Kelley et al., 2005). Members of the most abundant bacterial phyla detected –Gammaproteobacteria, Alphaproteobacteria, Firmicutes and Chloroflexi – are thought to be capable of oxidizing reduced sulfur species and hydrogen in vent fluids (Brazelton et al., 2006).

Archaeal diversity was found to be low at the site, with biofilms in active chimneys composed primarily of the phylotype Lost City Methanosarcinales (Schrenk et al., 2004). Brazelton et al. (2010) further investigated archaeal diversity, obtaining sequences of >200,000 ribosomal RNA amplicons ("tag sequences" of the V6 region of the16S gene), and again found Methanosarcinales to be the dominant archaeon. Other major groups detected include ANME-1, common in inactive chimneys, and Marine Group I (MGI) archaea, present in the youngest, hottest chimneys and vent fluids.

Organic geochemistry provides complementary insights into the microbiology and biogeochemistry of Lost City and integrates a longer time-window than nucleic acid-based studies. Previous work focusing on diether membrane lipids common to Methanosarcinales found evidence for methanogenesis and carbon limitation at Lost City (Bradley et al., 2009). Here we survey the less abundant but ubiquitous GDGTs in order to expand the geochemical record of microbial activity at Lost City and, through comparison with tag sequence data, explore the provenance of these compounds in the environment.

2. Samples and methods

2.1 Sample sites and collection

Samples were collected from carbonate chimneys across the Lost City Hydrothermal Field during Atlantis cruise AT-7-41 using the submersible Alvin and numbered with eight digit identifiers standardized across cruise reports (Kelley et al., 2005). Those designated as "active" are from chimneys that were observed to be

venting fluids during collection; "inactive" samples are from chimneys with no detectable venting, but the duration of inactivity is unknown. Vent fluid temperatures at active chimneys ranged from 34-70°C; "inactive" samples were at ambient seawater temperature (~7°C) when collected. Chimneys sampled were 730-850 m below sea surface. After collection samples were stored in Teflon containers at -20°C until processing.

2.2 Sample preparation

Subsamples (15-25 g each) of chimney carbonates were freeze dried, crushed to a fine powder, and extracted by sonication in dichloromethane:methanol 3:1 (3x). Total lipid extracts were separated into polar and neutral lipid fractions by cold acetone precipitation (Kates, 1986). Both polar and neutral lipid fractions were analyzed, but only the neutral fraction contained core GDGTs. Polar lipid analyses are reported elsewhere (Bradley et al., 2009b).

Neutral fractions were dissolved in hexane:isopropanol 99:1 and filtered through a 0.45μm PTFE syringe filter, evaporated to dryness and brought to a concentration of 2μg/μl (pre-filtration mass) in hexane:isopropanol 99:1.

2.3 LC-MS

Samples were analyzed by high performance liquid chromatography – atmospheric pressure chemical ionization mass spectrometry (HPLC-APCI-MS) in positive mode using an Agilent 1260 Infinity series LC coupled to a 6130 quadrupole mass spectrometer using a method modified from Hopmans et al. (2000). Separation was achieved on a Prevail Cyano column (150mm x 2.1mm, 3μm, Alltech,

USA) maintained at 25°C. The injection volume was 10µl and compounds were eluted isocratically with 100% eluent A (hexane:isopropanol 99:1) for 5 minutes, followed by a linear gradient to 15% eluent B (hexane:isopropanol 9:1) over 15 minutes and a return to 100% eluent A over 5 minutes, all at a flow rate of 0.4ml/min. Between analyses the column was equilibrated with 100% eluent A at 0.6ml/min. for 10 minutes. APCI-MS conditions were as follows: gas temperature 350°C, vaporizer temperature 380°C, drying gas flow 6l/min., nebulizer pressure 30psi, capillary 2000V, corona 5µA. GDGTs and archaeol were detected by selected ion monitoring; full scans were run periodically to monitor background and to confirm compound identification.

Compounds were quantified through comparison of ion trace peak areas to an external standard curve of archaeol (Avanti Polar Lipids, USA) and a synthetic C_{46} tetraether (Huguet et al., 2006). The C_{46} tetraether was not used as an internal standard because of coelution with the crenarchaeol isomer. Quantification cannot be considered absolute because a 1:1 response factor between GDGTs and the C_{46} tetraether was assumed. Reproducibility for duplicate analysis of random samples was within 20% and the response factor of standards was within 10% over the course of analysis.

3. Results

3.1 GDGTs and archaeol

GDGTs and the isoprenoidal diether lipid archaeol were detected in all samples at concentrations ranging from pg to ng/µg extract (Fig. 3). All samples,

both active and inactive, contained archaeol. The highest concentration detected (614 pg/μg extract) was in an active sample, but average concentrations were higher in inactive samples. Branched GDGTs with 4 or 6 methyl substituents (**9** and **11**, Fig.1 and here termed brGDGT-4 and brGDGT-6) were detected in 9 of the 12 samples and were more common and abundant in inactive chimneys.

Selected chromatograms showing branched and isoprenoidal GDGTs in an active and inactive vent sample are shown in Fig. 4. Crenarchaeol was detected in 4 active and 4 inactive vent samples, with higher average concentrations in inactive vents. It was the dominant GDGT in sample 3877-1501, at a concentration of 1.6 ng/μg extract, the highest value for any GDGT in this study. The crenarchaeol isomer, when detected, was at 1-12% the concentration of crenarchaeol, with no significant difference between active and inactive sites. GDGT-0 was detected in all samples (2-916 pg/μg extract), with higher average concentrations in inactive sites; GDGTs 1-3 were present at lower concentrations but followed a similar pattern between active and inactive sites. Among GDGTs 0-3, concentrations decreased with increasing ring number.

Generally, concentrations of GDGTs 0-2 tracked each other across sites (Fig. 3). For instance, sample 3877-1501, with the highest concentration of GDGT-0, also contained the most GDGT-1 and GDGT-2 of any sample. GDGT-3, however, was most abundant in sample 3864-1647 and its concentration does not appear correlated with concentrations of GDGTs 0-2 across the sample set.

H-GDGT-0 was identified based on retention time and the lack of fragments

with masses corresponding to the loss of an alkyl side chain; only losses of water and glycerol were observed, as reported by Schouten et al. (2008a) and Liu et al. (2012a). This compound was detected in 3 active and 3 inactive vent samples and concentrations were highest (413 pg/μg extract) in sample 3867-1113, for which no information about activity is available. There was no significant difference between the average concentration of H-GDGT-0 in active and inactive sites. When present in active vent samples, however, it represented a slightly higher percent of total GDGTs and exceeded the concentration of GDGT-0. Peaks corresponding to putative H-GDGTs 1 and 2 (isoprenoidal GDGTs with covalently linked biphytane chains and 1-2 cyclopentane moieties) appear in the SIM traces of m/z 1298-1299 and 1296-1297 (Fig. 4). Clear spectra could not be obtained in scan mode because of low abundances. The ~5 minute offset in retention time between early and late peaks within these SIM traces is consistent with that seen between GDGT-1 and H-GDGT-0 in the m/z 1302-1303 trace.

3.2 Proxy calculations

GDGTs are the basis for the sea surface temperature proxy TEX_{86} (Schouten et al., 2002) and the branched and isoprenoidal tetraether (BIT) index (Hopmans et al., 2004), which has been considered a measure of terrestrial input to marine sediments. We have calculated TEX_{86} temperatures and BIT values following the equations of Kim et al. (2008) and Hopmans et al. (2004) at Lost City (Fig. 1, Table 1) in order to assess the potential impact input of hydrothermal sediments may have on these proxies. TEX_{86} temperatures ranged from 11 to 31°C, with averages of

25 and 20°C for active and inactive vents, respectively. BIT index values ranged from 0 to 1.

4. Discussion

4.1 Origins of tetraether lipids at Lost City

In considering the potential sources of isoprenoidal GDGTs at Lost City we rely on precedent literature concerning known product-precursor relationships and on 16S rRNA amplicon ("tag") sequence data of Brazelton et al. (2010). Near-asymptotic rarefaction curves showed the archaeal community to be thoroughly sampled; sampling of bacterial communities was less complete. Samples for lipid analysis and V6 sequencing were collected at different times and sites within Lost City. As a result, we view the microbial assemblages described by Brazelton et al. (2010; VAMPS database, http://vamps.mbl.edu) simply as catalogs of microbes known to be present in the ecosystem and make no attempt to correlate the abundance of specific GDGTs with tag counts in a quantitative manner.

4.1a GDGTs 0-3

Among the archaea detected at Lost City, ANME-1 and Methanosarcinales were dominant, accounting for 9 and 90% of the 160,475 tags in the database (Brazelton et al., 2010). The remaining 1% of the tags were split between 15 classes of Archaea. No members of the euryarchaeal order Methanosarcinales, which includes the dominant phylotype and major constituent of chimney biofilms at Lost City, are known to synthesize GDGTs. Multiple other archaeal clades at Lost City, however, have the potential to contribute to the pool of isoprenoidal GDGTs

detected in our samples.

The euryarchaeal class Methanomicrobia (containing ANME-1, the second most abundant archaeal phylotype detected by Brazelton et al. (2010)) includes archaea known to synthesize GDGT-0 (Koga et al., 1998). ANME-1 has not been cultivated, but Black Sea carbonate reef samples in which the phylotype predominates yielded biphytanes representative of GDGTs 0-3 upon ether cleavage (Blumenberg et al., 2004). Rossel et al. (2008) detected GDGTs with intact polar headgroups in a Black Sea microbial reef sample in which the archaeal community was comprised exclusively of ANME-1, providing strong evidence for GDGT synthesis within this clade. Because of its high representation in the V6 tag dataset (Brazelton et al., 2010) ANME-1 organisms are likely to be the primary source of GDGTs 0-3 at Lost City.

The less abundant members of the archaeal population may also contribute to the isoprenoidal GDGT pool at Lost City. Brazelton et al. (2010) detected Marine Group I (MGI) Thaumarchaea (previously classified as Crenarchaeota) in chimneys and fluids at the youngest, hottest chimneys surveyed. *N. maritimus*, a cultivated representative of MGI, is closely related to common marine phylotypes and synthesizes GDGTs 0-4 and crenarchaeol (Schouten et al., 2008a), suggesting MGI at Lost City may synthesize a similar suite of compounds.

The tag sequence dataset includes three representatives of the euryarchaeal class Thermoplasmata: Marine Groups II and III, and the South African Goldmine Group. Some Thermoplasmata synthesize GDGT-0 (Langworthy et al., 1972) as well

as GDGTs 1-3 (Uda et al., 2001), so these organisms cannot be excluded as a possible source of isoprenoidal GDGTs at Lost City. The class Methanobacteria, with members that synthesize GDGT-0 (Koga et al., 1998), has been detected at Lost City (Brazelton et al., 2010). Isoprenoidal GDGTs 0-3 are also synthesized by members of the crenarchaeal group Thermoprotei, which includes thermophiles such as the well-studied Sulfolobus (Langworthy et al., 1974). Thermoprotei were detected at Lost City at low abundance (Brazelton et al., 2010); other potential but likely minor sources of GDGTs 0-3 include uncultivated crenarchaea such as Marine Benthic Group A.

4.1b GDGTs: Crenarchaeol

Crenarchaeol has been detected in a wide range of marine, lacustrine, and terrestrial settings. To date, the capacity for its biosynthesis is thought to be limited to ammonia-oxidizing archaea (Spang et al., 2010). Initially identified in the marine water column, it was named for its association with pelagic Crenarchaeota (Sinninghe Damsté et al., 2002), since reclassified as Thaumarchaeota.

Mesophilic planktonic marine thaumarchaea potentially contribute to the pool of GDGTs 0-3 and crenarchaeol at Lost City via deposition from the water column. True hydrothermal sources of crenarchaeol, however, may be more significant in the vent field. There are several reports of crenarchaeol in terrestrial hydrothermal systems (e.g., Pearson et al., 2004, Schouten et al., 2007, and Pitcher et al., 2011) and the cultured thermophilic, ammonia-oxidizing Candidatus *Nitrosocaldus yellowstonii* synthesizes crenarchaeol (de la Torre et al., 2008).

Reports of crenarchaeol in submarine hydrothermal systems are limited. Hu et al. (2012) detected GDGTs in sediments of the Eastern Lau Spreading Center in a pattern typical of marine environments, with crenarchaeol and GDGT-0 predominant; concentrations were highest at sites proximal to vents, suggesting a hydrothermal origin.

Several metagenomic surveys have provided information about distributions of MGI ribosomal RNA (rRNA) genes in submarine hydrothermal sites and, by extension, may help explain the occurrence of crenarchaeol at Lost City. Huber et al. (2002) found MGI archaea to be well represented in clone libraries from diffuse flow vents at Axial Seamount (Juan de Fuca Ridge) but hypothesized that they were from ambient deep seawater entrained by hydrothermal circulation. A similar origin for crenarchaeol in Lost City chimneys cannot currently be excluded.

Takai et al. (2004) found a stronger association between MGI rRNA and hydrothermal activity at the Central Indian Ridge and the Okinawa Trough. Quantitative PCR at those sites showed that MGI constituted a higher proportion of the archaeal community in ambient seawater adjacent to chimneys and hydrothermal emissions than in deep, distal seawater or in hydrothermal plumes.

The occurrence of crenarchaeol, postulated to be a biomarker for thaumarchaeal nitrification (de la Torre et al., 2008), raises the question of whether this process is feasible at Lost City. The potential for abiotic ammonia production at this site exists (Russell et al., 2010), and ammonia concentrations as high as 6 μM have been reported (Lang et al., 2013). At pH 9-11 and temperatures of 40-90°C

chemical equilibrium favors ammonia over ammonium (Olofsson, G., 1975) but the fugacity of ammonia under these conditions is high and substantial loss from hydrothermal fluids is likely (Li et al., 2012). Thaumarchaea may be positioned at oxic-anoxic interfaces between vent fluids and ambient seawater, where some oxygen is available for the oxidation of this effluxed ammonia. The high specific affinity of *N. maritimus* strain SC1 for ammonia and its ability to function under low levels of ammonia (Martens-Habbema et al., 2009) suggests that thaumarchaea may be able to carry out nitrification at Lost City even if ammonia levels are low or the flux is not constant.

This scenario could explain the higher concentrations of MGI that Takai et al. (2004) detected in deep seawater proximal to chimneys and hydrothermal fluids. It is also consistent with the view of some MGI as interface organisms; hydrothermal fields may contain oxic-anoxic transition zones analogous to those of marine oxygen minimum zones (OMZs) such as the Eastern Tropical South Pacific OMZ, where MGI and close relatives have been found to be abundant, show high transcriptional activity, and are the predominant nitrifiers (Stewart et al., 2011).

Our detection of higher concentrations of crenarchaeol in inactive than in active vents may appear at odds with the findings of Brazelton et al. (2010), who reported MGI to be more abundant in the hottest chimney sample and absent from inactive sites. It is possible, however, that the inactive chimneys we sampled simply record a long history of MGI activity at those vents, and that the longevity of nucleic acids in this environment is significantly shorter than that of crenarchaeol.

4.1c GDGTs: H-GDGT

H-GDGTs were first identified in *Methanothermus fervidus* (Morii et al., 1998), a thermophilic methanogen with an optimal growth temperature of 83°C (Stetter et al., 1981). *M. fervidus* was found to be endemic to Icelandic hot springs (Lauerer et al., 1986). H-GDGTs were also detected in *Pyrococcus horikoshii* (Sugai et al., 2000), isolated from a hydrothermal vent in the Okinawa Trough; in three strains of *Thermococcus* grown at 85°C (Sugai et al., 2004); in *Methanobacter thermautotrophicus* (Knappy et al., 2009); and in *Aciduliprofundum boonei* (Schouten et al., 2008b). These archaea are all members of the Euryarchaeota, and H-GDGTs were initially considered restricted to that phylum. More recently Knappy et al. (2011) detected H-GDGTs with 0-4 cyclopentane moieties in the crenarchaeon *Ignisphaera aggregans*, expanding the known phylogenetic distribution of the capacity for H-GDGT biosynthesis to both major archaeal phyla. To date, however, H-GDGT biosynthesis appears to be confined to thermophiles. Among the archaea detected at Lost City (Brazelton et al., 2010), Thermoprotei (crenarchaea) and Methanobacteria (euryarchaea) fall within groups that include members known to synthesize H-GDGT.

H-GDGTs have only rarely been reported in environmental samples. Jaeschke et al. (2010) detected H-GDGTs 0-4 in an active sulfide chimney in the Loki's Castle black smoker field. Liu et al. (2012b) reported H-GDGT-0 in sediment from an ODP leg 201 site in the Peru Margin, one of 20 globally distributed marine sediments analyzed. Schouten et al. (2008b) detected H-GDGT-0 in 10 marine and lacustrine

sediments described as having been deposited in slightly basic, non-hydrothermal waters (T <35°C). H-GDGT-0 represented less than 1.5% of the total isoprenoidal GDGTs in these samples, with the exception of sediment from ODP site 913b (Norwegian-Greenland Basin, 75°29'N, 6°56'W) where it comprised 6% of isoprenoidal GDGTs. The Norwegian-Greenland Basin has been the site of submarine alkaline volcanic activity from the late Paleocene to the present (Chernysheva and Kharin, 2007), so it is difficult to exclude a marine hydrothermal source for H-GDGTs detected there.

Several other sites described by Schouten et al. (2008b) may be subject to input of hydrothermally derived biomarkers; Lake Tanganyika, for instance, has sublacustrine hydrothermal vents (Tiercelin et al., 1989) likely to host thermophilic archaea, and the watershed of Lake Malawi contains hydrothermal systems (Branchu et al., 2005). Therefore, it is not clear that an allochthonous hydrothermal source for H-GDGTs can be excluded in many of these settings. Although it has been suggested that Marine Group II Euryarchaea (MGII) may be the source of these lipids (Schouten et al., 2008b) – and these archaea are present at Lost City – H-GDGTs have never been detected in close relatives of MGII, are rare in marine sediments, and have not been reported in the marine water column where MGII are frequently detected.

4.1d brGDGTs

We detected brGDGTS-4 and-6 (Fig. 1, **9** and **11**) at Lost City. Branched GDGTs are common in terrestrial environments, lacustrine sediments and nearshore

marine sediments (Schouten et al., 2000). Based on glycerol stereochemistry determined by NMR these lipids were assigned a bacterial origin (Weijers et al., 2006) and Acidobacteria were proposed as the source because of their abundance in soils and peats where brGDGTs are found (Weijers et al., 2009). In addition, Weijers et al. (2006) suggested that the occurrence of brGDGTs in peat bogs might be associated with the acidic conditions in such environments.

Recently, brGDGT-4 (**9**, Fig.1) was detected in 3 of 17 Acidobacteria strains analyzed, all in aerobes (Sinninghe Damsté et al., 2011). Other brGDGT are also typically detected in terrestrial environmental samples, and the possibility that bacteria other than Acidobacteria contribute to the pool of brGDGTs was not excluded (Sinninghe Damsté et al., 2011). Sequences belonging to the *Acidobacteria* comprise a small proportion (113 of > 200,000 amplicons) of the 16S V6 tags sequenced by Brazelton et al. (2010); it is possible that *Acidobacteria* contribute some proportion of the brGDGTs observed at Lost City.

Although brGDGTs are typically inferred to derive from soil or peat bogs, they have also been reported in other environments. Several studies have found evidence for *in situ* production in lacustrine water columns and sediments (e.g. Tierney and Russell, 2009, Sinninghe Damsté et al., 2009, Bechtel et al., 2010), marine sediments (Peterse et al., 2009), estuaries (Zhang et al., 2011) and in stalagmites (Yang et al., 2011). Hu et al. (2012) detected brGDGTs in sediments from the Eastern Lau Spreading Center. They found that brGDGT concentrations were typically higher near sites with hydrothermal activity, suggesting that they originate

in or near hydrothermal vents. The absence of long chained C_{27} to C_{33} waxy hydrocarbons derived from land plants in these sediments provided evidence that they have not been subject to terrestrial input and that the brGDGTs detected in them are autochthonous. Blumenberg et al. (2007) found branched hydrocarbon chains potentially derived in part from brGDGTs in the ether cleavage products of extracts from an extinct hydrothermal sulfide chimney in the Turtle Pits Hydrothermal Field, mid-Atlantic Ridge. The authors considered these compounds as likely derived from the macrocyclic archaeols that are abundant at the site, but allowed for some contribution from brGDGTs, which were not directly measured. Schouten et al. (2008b) detected brGDGTs "in abundance" at ODP site 913b, where they co-occurred with H-GDGT-0 (Norwegian-Greenland Basin, **3.1b**, above).

Together with the presence of brGDGTs at Lost City, these results point to a pattern of brGDGT occurrence in hydrothermal environments with no obvious terrestrial inputs. In addition, the detection of brGDGTs in the highly alkaline Lost City system extends the range of pH at which brGDGTs are known to occur.

4.2 Implications for GDGT-based proxies

The TEX_{86} proxy rests on the assumption that isoprenoidal GDGTs are primarily autochthonous, derived from archaea that lived in the water column above the sediment studied. The major utility of the BIT index is in identifying sediments where allochthonous, terrestrial-derived GDGTs potentially influence paleotemperature reconstruction.

TEX_{86} temperatures calculated at Lost City (11.3-31.3°C, Table 1) fall in a

broad range with no evident trend toward high or low temperatures. As a result, a hydrothermally derived input of isoprenoidal GDGTs from this or similar sites could confound paleotemperature reconstructions. Similarly, the presence of brGDGTs and crenarchaeol at Lost City and other submarine hydrothermal systems warrants concern that their input to sediments may complicate the application of the BIT index as a proxy for terrestrial matter. Reconstructions of mean air temperature and soil pH that are based on distributions of brGDGTs (MBT/CBT, Weijers et al., 2007) in marine and lacustrine sites could also be impacted by hydrothermal GDGTs.

We suggest that the presence of H-GDGTs in sediments serves as an indicator of likely hydrothermal input and may preclude the application of GDGT-based proxies. However, in our study H-GDGTs did not always co-occur with brGDGTs and they were not present in some samples with outlying TEX_{86} temperatures; consequently, the absence of H-GDGTs alone does not ensure that sediments have been free of hydrothermal GDGT input.

5. Conclusions

Several clades of archaea are likely to synthesize isoprenoidal GDGTs detected at Lost City. The abundance of ANME-1 archaea suggests that they are the predominant source of GDGT-0, but there are several candidates for GDGT 0-3 biosynthesis among the less abundant thermophilic and mesophilic euryarchaea and crenarchaea reported at Lost City. Marine Group I Thaumarchaea may contribute to the pool of GDGTs 0-3, and are a likely source of crenarchaeol. The

detection of brGDGTs at Lost City adds to growing evidence that they are not limited to terrestrial systems or acidic environments.

H-GDGTs may be synthesized by several thermophilic euryarchaea and crenarchaea detected at Lost City. The presence of H-GDGTs in sediments is a likely indicator of hydrothermal input, and warrants caution in application of paleoproxies when hydrothermal origins for co-occurring GDGTs cannot be excluded.

Acknowledgments

We are grateful to Dr. Deborah Kelley for the opportunity to participate in the 2003 Lost City cruise and thank the Captain and crew of the R/V Atlantis and Alvin and the shipboard science party of AT-7-34 for enabling sample collection. We also thank Martin Blumenberg and an anonymous reviewer for helpful comments that improved the quality of this manuscript. This work was supported by grants from the Agouron Institute (SAL), the NASA Astrobiology Institute (RES) and the National Science Foundation (NSF) Program on Emerging Trends in Biogeochemical Cycles (OCE-0849940) supported, in turn, by NSF programs in Chemical Oceanography and Geobiology-Low Temperature Geochemistry (RES).

References

Bechtel, A., Smittenberg, R.H., Bernasconi, S.M., Schubert, C.J., 2010. Distribution of branched and isoprenoid tetraether lipids in an oligotrophic and a eutrophic Swiss lake: insights into sources and GDGT-based proxies. Organic Geochemistry 41, 822–832.

Blumenberg, M., Seifert, R., Reitner, J., Pape, T., and Michaelis, W., 2004. Membrane lipid patterns typify distinct anaerobic methanotrophic consortia. Proceedings of the National Academy of Sciences of the United States of America 101, 11111-11116.

Blumenberg, M., Seifert, R., Petersen, S., and Michaelis, W., 2007. Biosignatures present in a hydrothermal massive sulfide from the Mid-Atlantic Ridge. Geobiology 5, 435-450.

Bradley, A.S., Hayes, J.M., and Summons, R.E., 2009. Extraordinary 13C enrichment of diether lipids at the Lost City Hydrothermal Field indicates a carbon-limited ecosystem. Geochimica et Cosmochimica Acta 73, 102-118.

Bradley, A.S., Fredricks, H., Hinrichs, K.-U., and Summons, R.E., 2009b. Structural diversity of diether lipids in carbonate chimneys at the Lost City Hydrothermal Field. Organic Geochemistry 40, 1169-1178.

Branchu, P., Bergonzini, L., Delvaux, D., De Batist, M., Golubev, V., Benedetti, M., and Klerkx, J., 2005. Tectonic, climatic and hydrothermal control on sedimentation and water chemistry of northern Lake Malawi (Nyasa), Tanzania. Journal of African Earth Sciences 43, 433-446.

Brazelton, W.J., Schrenk, M.O., Kelley, D.S., and Baross, J.A., 2006. Methane- and sulfur-metabolizing microbial communities dominate the Lost City Hydrothermal Field ecosystem. Applied and Environmental Microbiology 72, 6257-6270.

Brazelton, W.J., Ludwig, K.A., Sogin, M.L., Andreishcheva, E.N., Kelley, D.S., Shen, C., Edwards, R.L., Baross, J., 2010. Archaea and bacteria with surprising microdiversity show shifts in dominance over 1,000-year time scales in hydrothermal chimneys. Proceedings of the National Academy of Sciences of the United States of America 107, 1612-1617.

Chernysheva, E.A., and Kharin, G.S., 2007. Alkaline volcanism in the history of the Norwegian-Greenland Basin.Petrology 15, 296-301.

de la Torre, J.R., Walker, C.B., Ingalls, A.E., Könneke, M., and Stahl, D.A., 2008. Cultivation of a thermophilic ammonia oxidizing archaeon synthesizing crenarchaeol. Environmental Microbiology 10, 810-818.

Früh-Green, G.L., Kelley, D.S., Bernasconi, S.M., Karson, J.A., Ludwig, K.A., Butterfield, D.A., Boschi, C., and Proskurowski, G., 2003. 30,000 years of hydrothermal activity at the Lost City Vent Field. Science 301, 495-498.

Hoefs, M., Schouten, S., De Leeuw, J.W., King, L.I., Wakeham, S.G., and Sinninghe Damsté, J.S., 1997. Ether lipids of planktonic archaea in the marine water column. Applied and Environmental Microbiology 63, 3090-3095.

Hopmans, E.C., Schouten, S., Pancost, R.D., van der Meer, M.J.T., Sinninghe Damsté, J.S., 2000. Analysis of intact tetraether lipids in archaeal cell material and sediments by high performance liquid chromatography/atmospheric pressure chemical ionization mass spectrometry. Rapid Communications in Mass Spectrometry 14, 585-589.

Hopmans, E.C., Weijers, J.W.H., Schefuß, E., Herfort, L., Sinninghe Damsté, J.S., 2004. A novel proxy for terrestrial organic matter in sediments based on branched and isoprenoid tetraether lipids. Earth and Planetary Science Letters 225, 107-116.

Hu, J., Meyers, P.A., Chen, G., Peng, P., Qunhui, Y., 2012. Archaeal and

bacterial glycerol dialkyl glycerol tetraethers in sediments from the Eastern Lau Spreading Center, South Pacific Ocean. Organic Geochemistry 43, 162-167.

Huber, J.A., Butterfield, D.A., and Baross, J.A., 2002. Temporal changes in archaeal diversity and chemistry in a mid-ocean ridge subseafloor habitat. Applied and Environmental Microbiology 68, 1585-1594.

Huguet, C., Hopmans, E.C., Febo-Ayala, W., Thompson, D.H., Sinninghe Damsté, J.S., Schouten, S., 2006. An improved method to determine the absolute abundance of glycerol dibiphytanyl glycerol tetraether lipids. Organic Geochemistry 37, 1036-1041.

Jaeschke, A., Bernasconi, S.M., Thorseth, I.H., Pedersen, R., and Früh-Green, G.L., 2010. Diversity of microbial communities of Loki's Castle black smoker field at the ultra-slow spreading Arctic Mid-Ocean Ridge. Abstract. American Geophysical Union Fall Meeting, San Francisco, CA.

Kates, M., 1986. Techniques of Lipidology, 2nd revised edition. Elsevier, New York.

Kelley, D.S., Karson, J.A., Früh-Green, G.L., Yoerger, D.R., Shank, T.M., Butterfield, D.A., Hayes, J.M., Schrenk, M.O., Olson, E.J., Proskurowski, G., Jakuba, M., Bradley, A., Larson, B., Ludwig, K., Glickson, D., Buckman, K., Bradley, A.S., Brazelton, W.J., Roe, K., Elend, M.J., Delacour, A., Bernasconi, S.M., Lilley, M.D., Baross, J.A., Summons, R.E., and Sylva, S.P., 2005. A Serpentinite-hosted ecosystem: The Lost City Hydrothermal Field. Science 307, 1428-1433.

Kim, J., Schouten, S., Hopmans, E.C., Donner, B., and Sinninghe Damsté, J.S., 2008. Global sediment core-top calibration of the TEX_{86} paleothermometer in the ocean. Geochimica et Cosmochimica Acta 72, 1154-1173.

Knappy, C.S., Chong, J.P.J., and Keely, B.J., 2009. Rapid discrimination of archaeal tetraether lipid cores by liquid chromatography-tandem mass spectrometry. Journal of the American Society for Mass Spectrometry 20, 51-59.

Knappy, C.S., Nunn, C.E.M., Morgan, H.W., and Keely, B.J., 2011. The major lipid cores of the archaeon *Ignisphaera aggregans*: implications for the phylogeny and biosynthesis of glycerol monoalkyl glycerol tetraether isoprenoid lipids. Extremophiles 15, 517-528.

Koga, Y., Morii, H., Akagawa-Matsushita, M., and Ohga, M., 1998. Correlation of polar lipid composition with 16S rRNA phylogeny in methanogens. Further analysis of lipid component parts. Bioscience, Biotechnology, and Biochemistry 62, 230-236.

Könneke, M., Bernhard, A.E., de la Torre, J.R., Walker, C.B., Waterbury, J.B., and Stahl, D.A., 2005. Isolation of an autotrophic ammonia-oxidizing marine archaeon. Nature 437, 543–546.

Lang, S.Q., Früh-Green, G.L., Bernasconi, S.M., and Butterfield, D.A., 2013. Sources of organic nitrogen at the serpentinite-hosted Lost City hydrothermal field. Geobiology 11, 154-169.

Langworthy, T.A., Smith, P.F., and Mayberry, W.R., 1972. Lipids of *Thermoplasma acidophilum*. Journal of Bacteriology 112, 1193-1200.

Langworthy, T.A., Mayberry, W.R., and Smith, P.F., 1974. Long-chain glycerol diether and polyol dialkyl glycerol triether lipids of *Sulfolobus acidocalarius*. Journal of Bacteriology 119, 106-116.

Lauerer, G., Kristjansson, J.K., Langworthy, T.A., König H., Stetter K.O., 1986. *Methanothermus sociabilis* sp. nov., a second species within the *Methanothermaceae* growing at 97°C. Systematic and Applied Microbiology 8, 100-105.

Li, L., Lollar, B.S., Li, H., Wortmann, U.G., and Lacrampe-Couloume, G., 2012. Ammonium stability and nitrogen isotope fractionations for NH_4^+-$NH_{3(aq)}$-$NH_{3(gas)}$ systems at 20-70°C and pH of 2-13: Applications to habitability and nitrogen cycling in low-temperature hydrothermal systems. Geochimica et Cosmochimica Acta 84, 28-296.

Liu, X., Summons, R.E., and Hinrichs, K.-U., 2012a. Extending the known range of glycerol ether lipids in the environment: structural assignments based on MS/MS fragmentation patterns. Rapid Communications in Mass Spectrometry 26, 2295-2302.

Liu, X., Lipp, J.S., Simpson, J.H., Lin, Y., Summons, R.E., and Hinrichs, K.-U., 2012b. Mono and dihydroxyl glycerol dibiphytanyl glycerol tetraethers in marine sediments: Identification of both core and intact polar lipid forms. Geochimica et Cosmochimica Acta 89, 102-115.

Ludwig, K.A., Kelley, D.S., Butterfield, D.A., Nelson, B.K., and **Früh-Green, G.L., 2006. Formation and evolution of carbonate chimneys at the Lost City Hydrothermal Field. Geochimica et Cosmochimica Acta 70, 3625-3645.**

Martens-Habbema, W., Berube, P.M., Urakawa, H., de la Torre, J.R., and Stahl, D.A., 2009. Ammonia oxidation kinetics determine niche separation of nitrifying Archaea and Bacteria. Nature 46, 976-981.

Morii, H., Eguchi, T., Nishihara, M., Kakinuma, K., König, H., and Koga, Y., 1998. A novel ether core lipid with H-shaped C_{80}-isoprenoid hydrocarbon chain from the hyperthermophilic methanogen *Methanothermus fervidus*. Biochimica et Biophysica Acta 1390, 339-345.

Moyer, C.L., Tiedje, J.M., Dobbs, F.C., and Karl, D.M., 1998. Diversity of deep-sea hydrothermal vent archaea from Loihi Seamount, Hawaii. Deep-Sea Research 45, 303–317.

Olofsson, G., 1975. Thermodynamic quantities for the dissociation of the ammonium ion and for the ionization of aqueous ammonia over a wide temperature range. Journal of Chemical Thermodynamics 7, 507–514.

Pearson, A., Zhang, Z., Ingalls, A.E., Romanek, C.S., Wiegel, J., Freeman, K.H., Smittenberg, R.H., and Zhang, C.L., 2004. Nonmarine crenarchaeol in Nevada Hot Springs. Applied and Environmental Microbiology 70, 5229-5237.

Peterse, F., Kim, J.-H., Schouten, S., Klitgaard Kristensen, D., Koç, N., Sinninghe Damsté, J.S., 2009, Constraints on the application of the

MBT/CBT paleothermometer in high latitude environments (Svalbard, Norway). Organic Geochemistry 40, 692-699.
Pitcher,A., Hopmans, E.C., Mosier, A.C., Park, S.-J., Rhee, S.-K., Francis, C.A., Schouten, S., Sinninghe Damsté, J.S., 2011. Core and intact polar glycerol dibiphytanyl glycerol tetraether lipids of ammonia-oxidizing archaea enriched from marine and estuarine sediments. Applied and Environmental Microbiology 77, 3468-3477.
Rossel, P.E., Lipp, J.S., Fredricks, H.F., Arnds, J., Boetius, A., Elvert, M., Hinrichs, K.-U., 2008. Intact polar lipids of anaerobic methanotrophic archaea and associated bacteria. Organic Geochemistry 39, 992-999.
Russell, M.J., Hall, A.J., Martin, W., 2010. Serpentinization as a source of energy at the origin of life. Geobiology 8, 355-371.
Schouten, S., Hopmans, E.C., Pancost, R.D., and Sinninghe Damsté, J.S., 2000. Widespread occurrence of structurally diverse tetraether membrane lipids: Evidence for the ubiquitous presence of low-temperature relatives of hyperthermophiles. Proceedings of the National Academy of Sciences of the United States of America 97, 14421-14426.
Schouten, S., Hopmans, E.C., Schefuß, E., Sinninghe Damsté, J.S., 2002. Distributional variations in marine crenarchaeotal membrane lipids: a new tool for reconstructing ancient sea water temperatures? Earth and Planetary Science Letters 204, 265–274.
Schouten, S., van der Meer, M.T.J., Hopmans, E.C., Rijpstra, W.I.C., Reysenbach, A., Ward, D.M., and Sinninghe Damsté, J.S., 2007. Archaeal and bacterial glycerol dialkyl glycerol tetraether lipids in Hot Springs of Yellowstone National Park. Environmental Microbiology 73, 6181-6191.
Schouten, S., Hopmans, E.C., Baas, M., Boumann, H., Standfest, S., Konneke, M., Stahl, D.A., and Sinninghe Damsté, J.S., 2008a. Intact membrane lipids of "*Candidatus* Nitrosopumilus maritimus," a cultivated representative of the cosmopolitan mesophilic Group I Crenarchaeota. Applied and Environmental Microbiology 74, 2433-2440.
Schouten, S., Baas, M., Hopmans, E.C., Sinninghe Damsté, J.S., 2008b. An unusual isoprenoid tetraether lipid in marine and lacustrine sediments. Organic Geochemistry 39, 1033-1038.
Schrenk, M.O., Kelley, D.S., Bolton, S., and Baross, J.A., 2004. Low archaeal diversity linked to subseafloor geochemical processes at the Lost City Hydrothermal Field, Mid-Atlantic Ridge. Environmental Microbiology 10, 1086-1095.
Sinninghe Damsté, J.S., Schouten, S., Hopmans, E.C., van Duin, A.C.T., and Geenevasen, J.A.J., 2002. Crenarchaeol: the characteristic core glycerol dibiphytanyl glycerol tetraether membrane lipid of cosmopolitan pelagic Crenarchaeota. Journal of Lipid Research 43, 1641-1651.
Sinninghe Damsté, J.S., Ossebaar, J., Abbas, B., Schouten, Verschuren, D., 2009. Fluxes and distribution of tetraether lipids in an equatorial African lake: constraints on the application of the TEX_{86} palaeothermometer and

branched tetraether lipids in lacustrine settings. Geochimica et Cosmochimica Acta 73, 4232-4249.
Sinninghe Damsté, J.S., Rijpstra, W.I.C., Hopmans, E.C., Weijers, J.W.H., Foesel, B.U., Overmann, J., and Dedysh, S., 2011. 13,16-Dimethyl Octacosanedioic Acid (iso-Diabolic Acid), a Common Membrane-Spanning Lipid of Acidobacteria Subdivisions 1 and 3. Applied and Environmental Microbiology 77, 4147-4154.
Spang, A., Hatzenpichler, R., Brochier-Armanet, C., Rattei, T., Tischler, P., Spieck, E., Streit, W., Stahl, D.A., Wagner, M., and Schleper, C., 2010. Distinct gene set in two different lineages of ammonia-oxidizing archaea supports the phylum Thaumarchaeota. Trends in Microbiology 18, 331-340.
Stetter, K.O., Thomm, M., Winter, J., Wildgruber G., Huber, H., Zillig, W., Janecovic, D., Konig, H., Palm, P., and Wunderl, S., 1981. *Methanothermus-fervidus,* an extremely thermophilic methanogen. Mikrobiologie 2, 166-178.
Stewart, F.J., Ulloa, O., and DeLong, E.F., 2011. Microbial metatranscriptomics in a permanent marine oxygen minimum zone. Environmental microbiology 14, 23-40.
Sugai, A., Masuchi, Y., Uda, I., Itoh, T., and Itoh, Y.H., 2000. Core lipids of hyperthermophilic Archaeon *Pyrococcus horikoshii OT3.* Journal of Japan Oil Chemists' Society 49, 695-700.
Sugai, A., Uda, I., Itoh, Y., Itoh, Y.H., and Itoh, T., 2004. The core lipid composition of the 17 strains of hyperthermophilic archaea, Thermococcales. Journal of Oleo Science 53, 41-44.
Takai, K., Oida, H., Suzuki, Y., Hirayama, H., Nakagawa, S., Nunoura, T., Inagaki, F., Nealson, K., and Horikoshi, K., 2004. Spatial distribution of Marine Crenarchaeota Group I in the vicinity of deep-sea hydrothermal systems. Applied and Environmental Microbiology 70, 2404-2413.
Tiercelin, J., Thouin, C., Kalala, T., and Mondeguer, A., 1989. Discovery of sublacustrine hydrothermal activity and associated massive sulfides and hydrocarbons in the north Tanganyika trough, East African Rift. Geology 17, 1053-1056.
Tierney, J.E., and Russell, J.M., 2009. Distributions of branched GDGTs in a tropical lake system: Implications for lacustrine application of the MBT/CBT paleoproxy. Organic Geochemistry 40, 1032-1036.
Uda, I., Sugai, A., Itoh, Y.H. and Itoh, T., 2001. Variation in molecular species of polar lipids from *Thermoplasma acidophilum* depends on growth temperature. Lipids 36, 103-105.
Weijers, J.W.H., 2006, Schouten, S., Hopmans, E.C., Geenevasen, J.A.J., David, O.R.P., Coleman, J.M., Pancost, R.D., and Sinninghe Damsté, J.S., 2006. Membrane lipids of mesophilic anaerobic bacteria thriving in peats have typical archaeal traits. Environmental Microbiology 8, 648-657.
Weijers, J.W.H., Schouten, S., van den Donker, J.C., Hopmans, E.C., and

Sinninghe Damsté, J.S., 2007. Environmental controls on bacterial tetraether membrane lipid distribution in soils. Geochimica et Cosmochimica Acta 75, 3179-3190.

Weijers, J.W.H., Panoto, E., van Bleijswjk, J., Schouten, S., Rijpstra, W.I.C., Balk, M., Stams, A.J.M., and Sinninghe Damsté, J.S., 2009. Constraints on the biological source of the orphan branched tetraether membrane lipids. Geomicrobiology Journal 26, 402-414.

Yang, H., Ding, W., Zhang, C., Wu, X., Ma, X., He, G., Huang, J., Xie. S., 2011. Occurrence of tetraether lipids in stalagmites: Implications for sources and GDGT-based proxies. Organic Geochemistry 42, 108-115.

Zhang, C.L., Wang, J.X., Wei, Y., Zhu, C., Huang, L., Dong, H., 2012. Production of branced tetraether lipids in the Lower Pearl River and Estuary effects of extraction methods and impact on bGDGT proxies. Frontiers in Microbiology 2, 274.

Fig. 1. Structures of tetraether lipids detected in Lost City carbonates (1-9; 11) and discussed in text (10), archaeol (8), and equations used in proxy calculations. The position of the bond linking biphytane moieties in H-GDGT-0 (7) is unknown, as are the positions of methylation on the alkyl chains of brGDGTs.

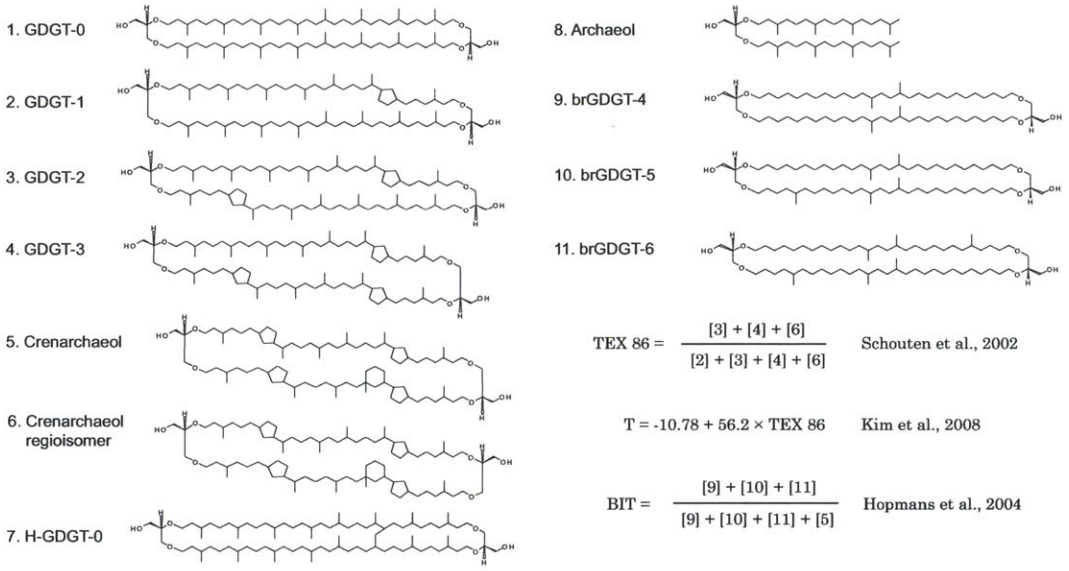

$$TEX\ 86 = \frac{[3] + [4] + [6]}{[2] + [3] + [4] + [6]}$$ Schouten et al., 2002

$$T = -10.78 + 56.2 \times TEX\ 86$$ Kim et al., 2008

$$BIT = \frac{[9] + [10] + [11]}{[9] + [10] + [11] + [5]}$$ Hopmans et al., 2004

Fig. 2. Location of the Lost City Hydrothermal Field.

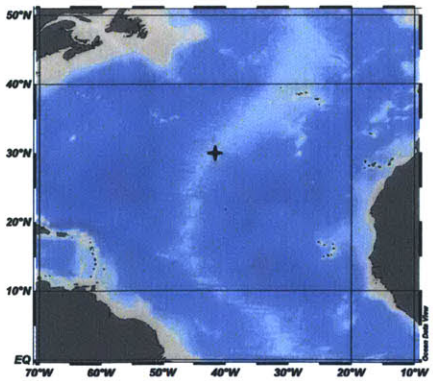

Fig. 3. Archaeol and tetraether lipid concentrations in active (red) and inactive (white) vent samples. No information about vent activity is available for sample 3867-1113 (gray).

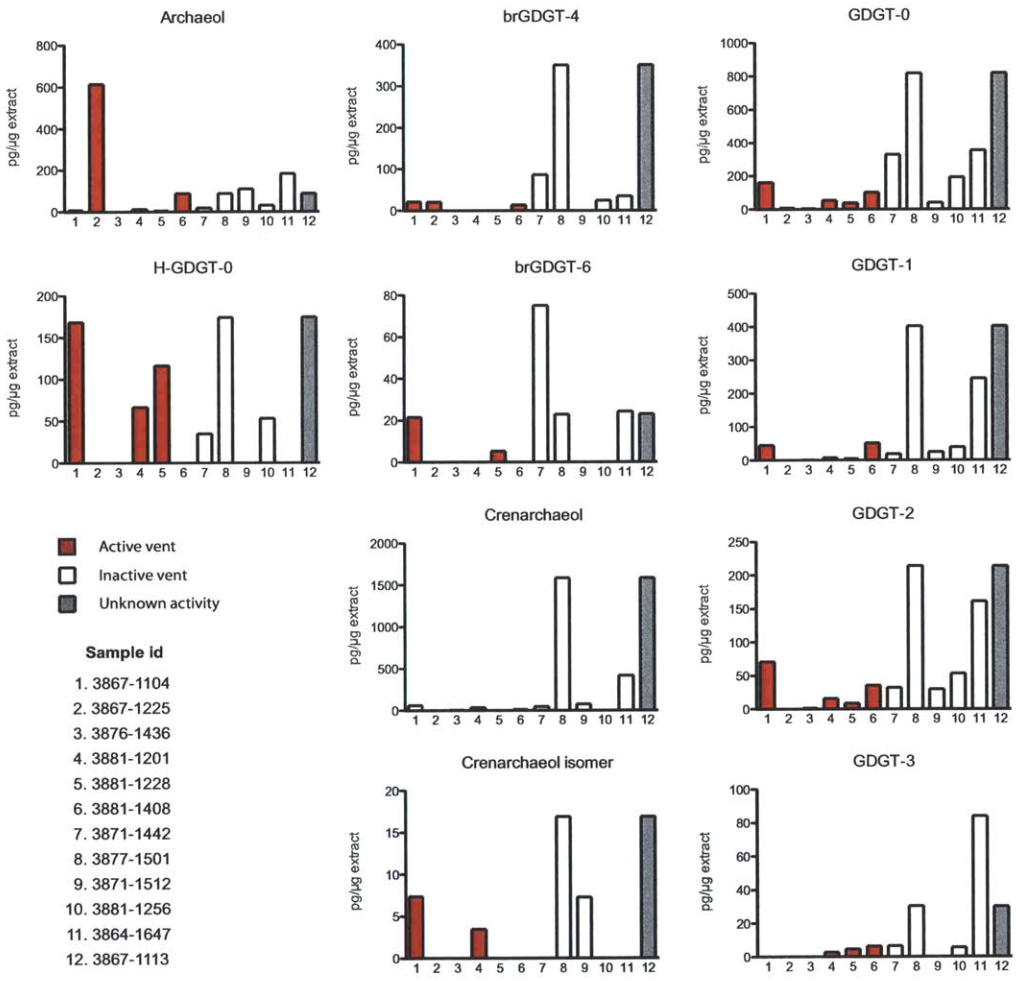

Fig. 4. Composite ion chromatograms of active vent sample 3867-1104 and inactive vent sample 3871-1442, with mass traces shown for sample 3871-1442. Peak numbers correspond to compounds numbered in Fig. 1: **1,** GDGT-0; **2**, GDGT-1; **3**, GDGT-2; **4**, GDGT-3; **5**, crenarchaeol; **7**, H-GDGT-0; **9**, brGDGT-4; **11**, brGDGT-6. Asterisks mark peaks of putative H-GDGT-1 and H-GDGT-2.

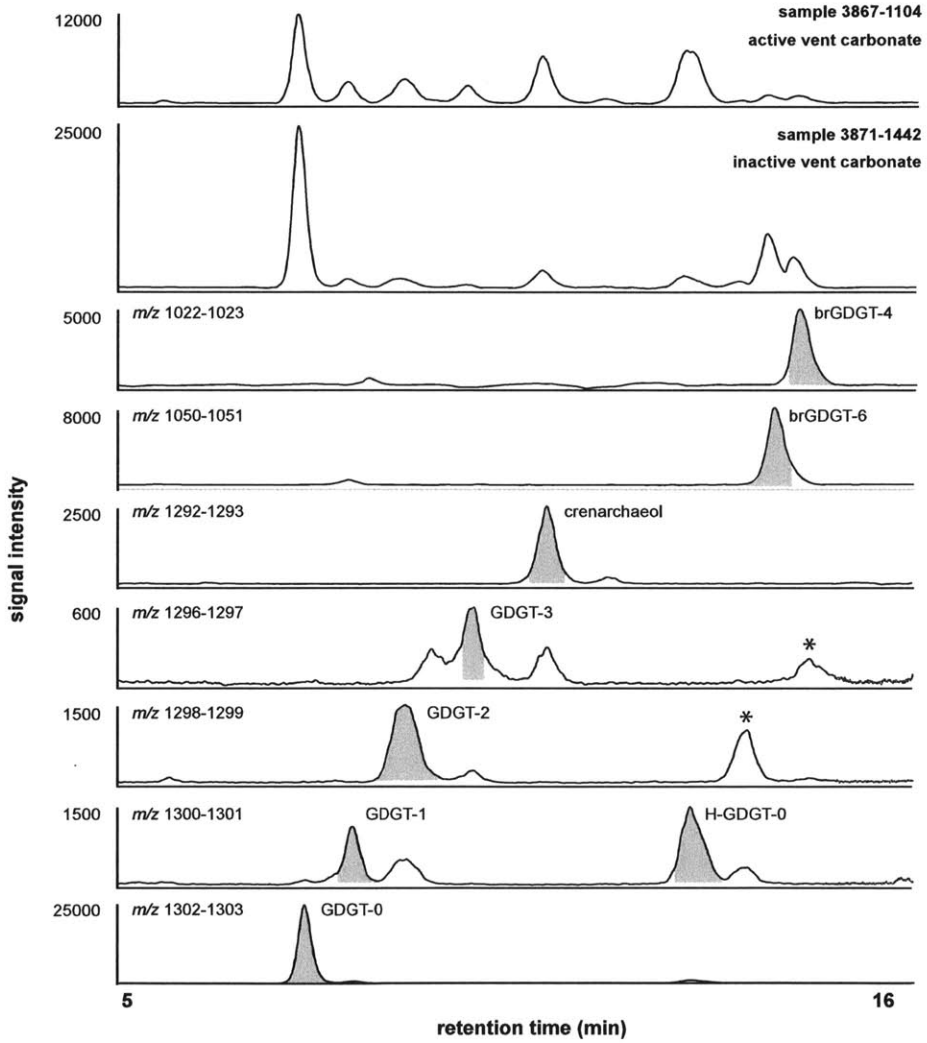

Table 1. H-GDGT-0 as a percent of total GDGTs measured, TEX_{86} temperature and BIT index calculations for Lost City carbonates. Vent type "A" denotes active and "I" inactive vents; no information about vent type is available for 3867-1113.

Sample	Vent type	H% total GDGTs	TEX_{86} T (C)	BIT
3867-1104	A	30	25.0	0.41
3867-1225	A	0	-	1.00
3876-1436	A	0	20.9	0.00
3881-1201	A	37	31.3	0.00
3881-1228	A	66	31.1	1.00
3881-1408	A	0	14.4	0.66
3871-1442	I	6	27.1	0.79
3877-1501	I	5	11.3	0.19
3871-1512	I	0	22.9	0.00
3881-1256	I	15	23.1	1.00
3864-1647	I	0	17.4	0.12
3867-1113	n/a	17	22.3	0.27

Appendix 1

Biomarkers: Informative molecules for studies in geobiology*

---

* Reprinted with permission from Fundamentals of Geobiology

15
BIOMARKERS: INFORMATIVE MOLECULES FOR STUDIES IN GEOBIOLOGY

Roger E. Summons and Sara A. Lincoln

Massachusetts Institute of Technology, Department of Earth and Planetary Sciences, 77 Massachusetts Ave., Cambridge MA 02139-4307, USA

Where have all life's molecules gone?
Recycled to carbon dioxide every one!
Ah! But look – a hardy few remain
As biomarkers imprisoned in the fossil domain
Geoffrey Eglinton (2004)

15.1 Introduction

Biomarker molecules are natural products that have distinctive structural and/or isotopic attributes. These attributes convey information about the origins of the molecule with various degrees of specificity. For environmental and geological studies the most effective biomarkers have a limited number of well-defined sources, are recalcitrant, are readily measured in environmental samples and can be tracked through diagenesis, that is, the chemical changes that ensue after death. Accordingly, biomarkers can be proxies for different biogeochemical processes taking place in modern environments as well as chemical fossils that afford a paleobiological record of the past activities of living communities (Brocks and Summons, 2003; Gaines *et al.*, 2009). This chapter briefly describes the chemistry and biological origins of some commonly encountered biomarkers, illustrated with examples of their use in environmental geomicrobiology and in paleoreconstruction.

15.2 Origins of biomarkers

In geobiology and astrobiology, the most commonly studied molecular biomarkers are lipids. These include pigments as well as cell wall and interior membrane constituents essential to the integrity and physiology of cells. Other biochemicals, such as carbohydrates, proteins and nucleic acids, are accessible food sources for bacteria and fungi and generally do not survive for long after the death of a cell. In contrast, lipids have recalcitrant, hydrophobic hydrocarbon moieties that are much more difficult to degrade, especially in the absence of oxygen. Thus, even fatty acids that were linked to glycerol by hydrolysable ester linkages have some preservation and diagnostic potential. Polycyclic or highly branched structures, such as are found in polyisoprenoid lipids, are even more resistant to biodegradation and have the greatest preservation potential. In this respect, cyclic triterpenoids, such as steroids (Fig. 15.1) and hopanoids (Fig. 15.2), are well established as excellent biomarkers for Eukarya and Bacteria, respectively (Brassell *et al.*, 1983). Further, their hydrocarbon cores can be preserved in sediments and petroleum for hundreds of millions to billions of years (Dutkiewicz *et al.*, 1998, 2006; Brocks *et al.*, 2003a; Eigenbrode *et al.*, 2008; George *et al.*, 2008; Grosjean *et al.*, 2009; Waldbauer *et al.*, 2009). Hydrocarbon biomarkers can be diagnostic, with varying degrees of confidence, for the physiological activities of organisms, paleoenvironmental conditions and the thermal history of sediments. Biomarkers have long been used in exploration for fossil fuels (Peters *et al.*, 2005).

15.3 Diagenesis

Biomarkers undergo transformations once an organism dies and its cellular contents are released into the

Fundamentals of Geobiology, First Edition. Edited by Andrew H. Knoll, Donald E. Canfield and Kurt O. Konhauser.

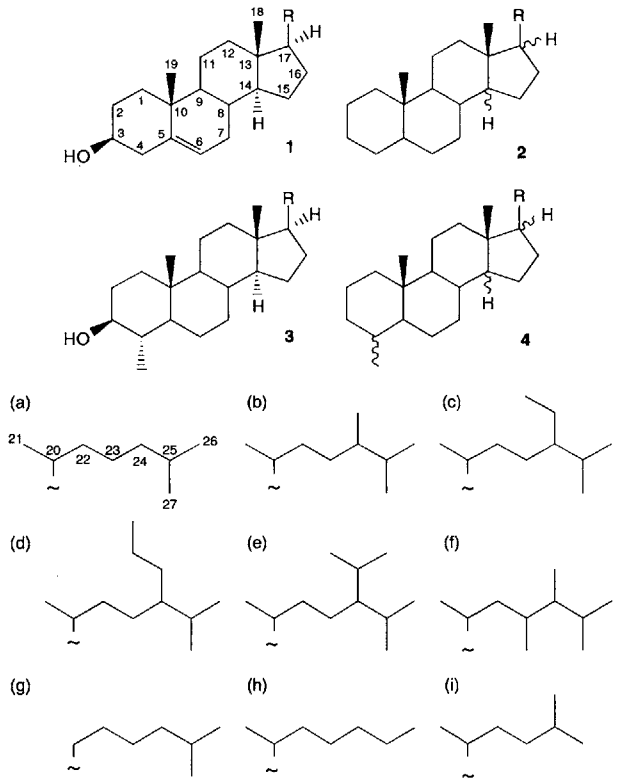

Figure 15.1 Generic structures of a Δ5-sterol (**1**) and a 4-methyl stanol (**3**) along with a selection of side-chains (**a–i**) that commonly are attached to C17. These steroids, including dinostanol (**3f**), sitosterol (**1c**) and cholesterol (**1a**), are typical of those found in the membranes of protists, plants and animals. The 4-methylsterane dinosterane (**4f**), stigmastane (sitostane) (**2c**) and cholestane (**2a**) are formed from their precursor sterols during burial and diagenesis and are representative of the diversity of eukaryotic molecular fossils found in sediments and petroleum.

environment. These alteration processes are termed diagenesis. Only the most recalcitrant structures survive. In the case of intact polar lipids (IPLs) the stable entities are the hydrocarbon cores, that is, the alkyl chains that are bound to glycerol by ester or ether bonds. Preservation of carbon compounds is strongly aided by the exclusion of electron acceptors such as oxygen and sulfate (Canfield, 1989) and a tight association with minerals (Hedges and Keil, 1995), and is enhanced by the presence of sulfide which is a reducing agent and can contribute to the removal of unstable features such as double bonds (Adam *et al.*, 2000; Hebting *et al.*, 2006; Kohnen *et al.*, 1989). Complex terpenoid lipids such as sterols, bacteriohopanepolyols (BHPs) and carotenoids can be reduced to their hydrocarbon skeletons without compromising the basic structural features that confer diagnostic utility. One important and potentially very useful aspect of diagenesis is the propensity of some lipids to undergo predictable stereochemical modifications as well as structural ones. These changes tend to be progressive and a sample in the earliest stage of diagenesis can already have a dizzying array of compounds derived from a single original precursor (Fig. 15.3). Biomarker stereochemistry can be used to assess the maturity of the sample and to investigate the possibility of contamination by younger organic matter.

15.4 Isotopic compositions

Accurate elucidation of the chemical structures of lipids from cultured organisms provided the original basis for assignments of the biological sources of chemical fossils (Eglinton, 1970). However, given the conservative aspects of lipid biochemistry, and the paucity of lipids that are exclusive to a single organism, such assignments are often ambiguous. Early on it was also realized that metabolites inherit C, H, N and O isotopic compositions that are set when the organism acquires its carbon and the precursor molecule is biosynthesized (Abelson and Hoering, 1961). Thus, isotopic data is another means of refining the assignments of biomarkers to their sources provided that we have sufficient knowledge to reliably interpret isotopic variations (Hayes, 2001, 2004).

The first-order controls on the isotopic compositions of an entire organism lie in how it acquires its carbon,

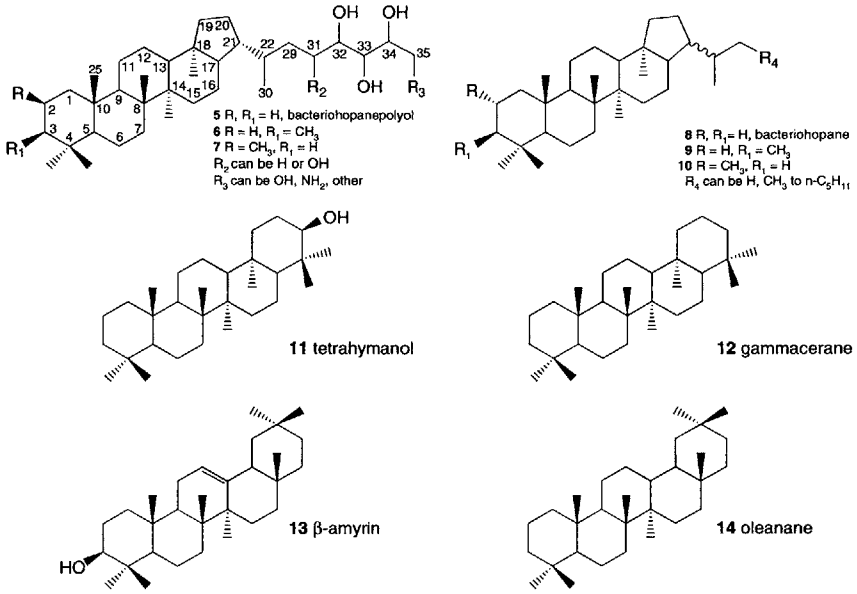

Figure 15.2 Structural diversity in bacteriohopanepolyols (BHP; **5–7**) and the derived hopanoid hydrocarbons (**8–10**) that are found in sediments and petroleum. 3β-Methylbacteriohopanepolyols (**6**) and 2β-methylbacteriohopanepolyols (**7**), and the derived hydrocarbons (**9** and **10**) have been have been proposed as biomarkers for methanotrophic bacteria and cyanobacteria respectively. Tetrahymanol (**11**) and β-amyrin (**13**) are represented in the fossil record by the hydrocarbons gammacerane (**12**) and oleanane (**14**) which are considered to be good biomarkers for bacteriovorous ciliates and flowering plants, respectively.

hydrogen, nitrogen and other elements, as well as the isotopic compositions of the substrates for these elements. In the case of carbon, this is determined by physiology, namely whether the organism is autotrophic or heterotrophic and, in the case of the former, the assimilation pathway (House *et al.*, 2003). Once assimilated, carbon is further fractionated during respiration and biosynthesis. The isotopic fractionations that take place as carbon flows through biosynthetic pathways are of particular interest (Hayes, 2001) and are discussed further below. Other variables known to affect the C-isotopic composition of biomass and individual components include the size of an organism, the rate of growth, the stage of the growth cycle and how the carbon is compartmentalized.

The burgeoning technical capability to conduct isotope analysis on individual compounds (i.e. compound-specific isotope analysis, CSIA) on trace amounts of lipid has greatly enhanced the accuracy of lipids as proxy for both the organisms that produced them and/or their physiologies (Bradley *et al.*, 2009; Ohkouchi *et al.*, 2008; Zhang *et al.*, 2009). Isotopic data also increase the depth of historical information that can be derived from fossil molecules and builds confidence in our interpretations of this record (Hayes, 2004). C-isotopic compositions of molecules are likely highly conserved over long periods of geological time because, without destroying a molecule, there are no known processes that allow exchange of its carbon atoms. Hydrogen isotopic compositions are also set during biosynthesis (Schimmelmann *et al.*, 1999; Sessions *et al.*, 1999) and, in the case of bacteria, reflect the physiology of NADPH production in central metabolism (Zhang *et al.*, 2009). However, δD values are also prone to progressive corruption through exchange reactions over long timescales; some H-atoms are more easily exchanged than others (Sessions *et al.*, 2004). The N-isotopic compositions of chlorophyll-derived biomarkers (Chikaraishi *et al.*, 2005, 2008 Ohkouchi *et al.*, 2006) provide important data on nitrogen sources for biosynthesis and can serve as a proxy for reconstructing ancient nitrogen cycling. Compound-specific oxygen isotopic measurements on lipids are more difficult because few lipids have high O/C ratios; for this reason, the O-isotopic composition of lipids has not been exploited to any extent in contrast to measurements on oxygen-rich molecules such as cellulose (Sternberg *et al.*, 1984). Most recently, a continuous flow technique utilizing inductively coupled plasma mass spectrometry (ICPMS) has been developed to measure the $\delta^{34}S$ values of individual compounds (Amrani *et al.*, 2009) thereby completing the array of light, bioactive

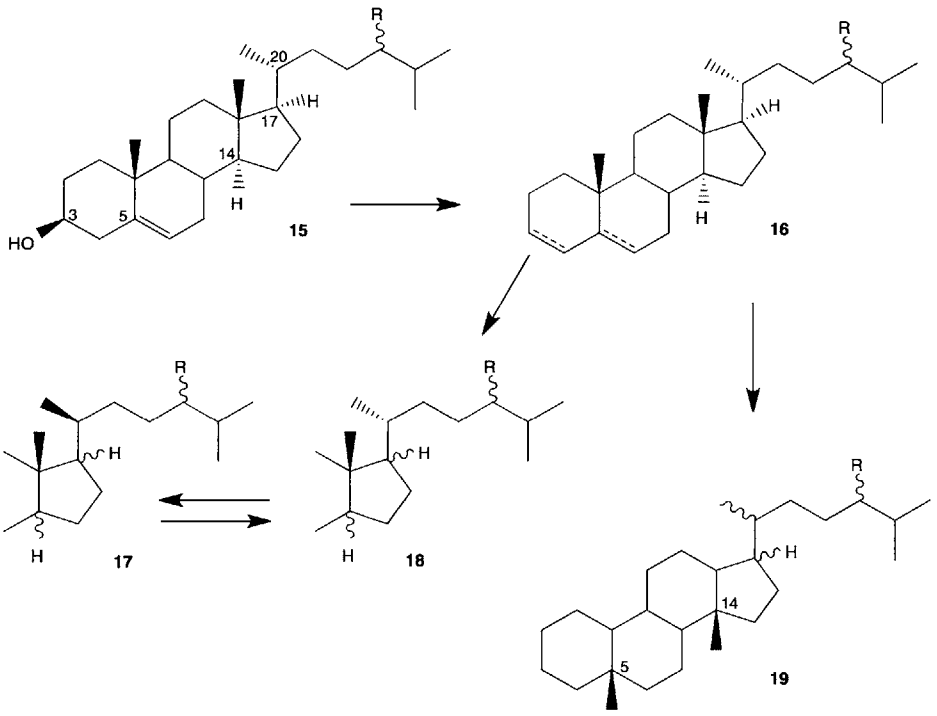

Figure 15.3 Some of the steps in the complex diagenetic pathway from sterols to steranes (Mackenzie *et al.*, 1982) and illustrating the major stereochemical changes. Sterenes and diasterenes (**16**) are initially formed from sterols and steryl esters by dehydration or elimination reactions and these are then reduced to the sterane isomers **17** and **18**. Alternatively, they may undergo a backbone rearrangement and reduction to form diasteranes (rearranged steranes; **19**).

elements amenable to isotopic analysis. Clearly, simultaneous measurement of C-, H-, O-, N- and S-isotopic compositions of an individual biomarker compound is challenging but would provide the ultimate characterization (Hinrichs *et al.*, 2001).

15.5 Stereochemical considerations

The vast majority of biomarkers exhibit some kind of stereospecificity. In some ways this is analogous to the homochirality that is characteristic of amino acids with the important difference being that biomarkers generally have multiple asymmetric centres. The common sterol cholesterol (Fig. 15.1, 1a) has eight. The plant sterol sitosterol (Fig. 15.1, 1c) has nine as does the dinoflagellate-specific dinosterol. Bacteriohopanepolyols (BHPs) are even more complex with bacteriohopanetetrol (BHtetrol) having at least eight in the C_{30} pentacyclic ring system and four in the side chain. This could result in a bewildering collection of potential stereoisomers except for the fact that biosynthesis generally produces one isomer exclusively (Figs 15.1–15.4). This fact immediately leads to a method for distinguishing the biomarkers of extant and recent organisms from those in the geologic past because the latter are invariably mixtures, often quite complex, of stereoisomers.

The post mortem stereochemical changes that biomarkers undergo encode valuable information about diagenetic conditions and thermal histories. Acyclic isoprenoids readily isomerize very early in their burial so that the fossil forms comprise mixtures of diastereoisomers (aka diastereomers) (Patience *et al.*, 1978). Steroids may form pairs of diastereoisomers at former sites of unsaturation (double bonds). Some hydrogen atoms at ring junctions are prone to isomerize while the whole steroid backbone may also rearrange especially if acidic clays are abundant in the enclosing sediment (Mackenzie *et al.*, 1982; van Kaam-Peters *et al.*, 1998). Diagenesis in carbonate sediments proceeds differently and such re-arrangements are often suppressed (Rullkötter *et al.*, 1984). As mentioned above, the changes are progressive so that in geological samples, which have experienced long periods of burial, all

biomarkers will come to comprise mixtures dominated by the most thermodynamically stable stereoisomers. This is illustrated for steroids (structures **1–4**) and triterpenoids (**5–14** and **15–19**) in Figs 15.1–15.3.

15.6 Lipid biosynthetic pathways

The hydrocarbon skeletons of lipids fall into two broad categories. First there are the acetogenic lipids which are those with straight chains (normal) or simple branching patterns (e.g. iso-, anteiso-, etc.). As the name implies, acetogenic lipids are constructed from acetate units originally donated from acetyl coenzyme-A (De Niro and Epstein, 1977; Hayes, 1993). Additional carbons can be acquired from other short-chain fatty acid precursors and from methyl groups donated by *S*-adenosyl methionine (SAM). The second major class of lipids comprises the polyisoprenoids. These are constructed from a five-carbon precursor, dimethylallyl diphosphate (DMAPP; **20**) or isopentyl diphosphate (IPP; **21**) leading to a diverse array of structures determined by number of 'isoprene' building blocks and the manner in which they are assembled (Fig. 14.4). For example, geranyldiphosphate (GPP; **22**) is formed when two C5 units are connected head to tail; phytol (**23**) is derived from four C5 units linked head to tail. A notable feature of acetogenic and polyisoprenoid lipids, and a point of contrast to other biopolymers such as nucleic acids and proteins, is that only a few specific classes of lipids contain hydrolysable linkages.

The acetyl building block of acetogenic lipids can also have multiple origins with consequences for the isotopic composition of its products. In photosynthetic organisms and heterotrophs acetate is formed primarily through the decarboxylation of pyruvate, itself a product of the synthesis or degradation of carbohydrates. In one of the first observations of intermolecular 'isotopic order,' DeNiro and Epstein (1977) made site-specific measurements of the isotopic compositions of each carbon atom in pyruvate and acetate in cultures of the bacterium *Escherichia coli*. They determined that a major fractionation accompanies the decarboxylation of pyruvate leading to a depletion of the carboxyl carbon atom depleted of approximately 15‰ relative to the methyl carbon atom. Overall, the acetate produced by *E. coli*, and the lipids that were formed from it, were depleted by 7–8‰ relative to glucose and the pyruvate precursors. Upon further investigation, and working with both yeast and *E. coli*, Monson and Hayes confirmed that individual fatty acids were depleted in ^{13}C by 7‰ relative to glucose carbon source and that the carbon atoms along the chain comprised two isotopically-distinct groups (Monson and Hayes, 1980, 1982). Odd-numbered carbon atoms, derived from the carboxyl carbon of acetate, were depleted by around 6‰ relative to the glucose while the even-numbered carbons were enriched by about 0.5‰. Research conducted since these seminal observations has further verified the phenomenon of intramolecular isotopic order and confirmed that acetogenic lipids are almost invariably depleted relative to total biomass and other biochemicals (Hayes, 2001; Schouten *et al.*, 2008c). However, additional factors can affect the isotopic composition of acetyl-CoA in organisms grown under different conditions and in environmental samples with consequences for correctly interpreting the results from analyses of geologic samples (Heuer *et al.*, 2006).

Polyisoprenoid lipids are constructed from C5 (isoprene) building blocks. The IPP and DMAPP precursors can be made from acetyl-CoA following the mevalonic acid (MVA) pathway. The elucidation of the MVA pathway was based on studies of yeast, and other easily manipulated organisms and tissues, and was long assumed to be the exclusive route (Bloch, 1992). However, in studying the biosynthesis of hopanoid triterpenoids in bacteria, Rohmer and colleagues (Rohmer, 2003) discovered evidence for a second pathway. They observed anomalous labeling patterns when [1-^{13}C] and [2-^{13}C] acetate were fed to hopanoid-producing bacteria such as *Rhodopseudomonas palustris* (Flesch and Rohmer, 1988). Further experiments with ^{13}C isotopomers of glucose (Rohmer *et al.*, 1993) enabled the unraveling of the mevalonate-independent methylerythritol phosphate (MEP) pathway (Rohmer, 2003), also known as the DOXP pathway. In this pathway, IPP and DMAPP are the products of condensation of a C_2 subunit formed by pyruvate decarboxylation and a C_3 moiety in the form of a triose phosphate. Methylerythritol 4-phosphate is the first committed intermediate, hence the naming of the pathway as MEP. MVA is the pathway common to Archaea and non-plastid bearing Eukarya. Bacteria can have either MEP or MVA while plastid-bearing Eukarya can have either or both (Hayes, 2001). However, MEP is widely present in the chloroplasts of plants (Eisenreich *et al.*, 1998) and their green algal cousins presumably reflecting inheritance from the cyanobacterial ancestor (Lichtenthaler *et al.*, 1997). A consequence of having two pathways for isoprenoid biosynthesis is that complexities abound in the interpretation of isotopic data for isoprenoids. At the same time, the MEP versus MVA dichotomy can be informative and useful in interpretations of the natural variability in the isotopic compositions of polyisoprenoids (Schouten *et al.*, 2008c).

15.7 Classification of lipids

Biological lipids are diverse cellular chemicals that are largely soluble in organic solvents and insoluble in water. Some of the important compound classes are discussed below.

15.7.1 Hydrocarbons

Hydrocarbons are a diverse compound class. They encompass some of the simplest and least specific biomarker compounds such as *n*-alkanes as well as complex isoprenoid hydrocarbons of the botryococcene type which, so far, appear to be exclusive to a single species of chlorophyte alga, *Botryococcus braunii*. Interestingly, methane, the simplest hydrocarbon of all, can be a biomarker in certain circumstances because its biosynthesis is exclusive to the methanogenic Archaea. However, caution is warranted because methane can have other origins, for example, the thermal cracking of complex organic matter. Isotopic and other data are crucial for understanding the origins of methane (Schoell, 1988).

Important biogenic hydrocarbons include the *n*-alkanes found in the leaf wax of plants (Eglinton, 1970), short-chain normal (*n*-) and branched alkanes produced by cyanobacteria (Han and Calvin, 1969; Jahnke *et al.*, 2004) and some algae, long-chain branched alkanes found in the waxy cuticles of insects and an array of distinctive isoprenoid hydrocarbons produced by algae of various types.

Hydrocarbons are also prominent components of petroleum and sedimentary bitumen (Peters *et al.*, 2005). Here, they are the fossilized remains of former functionalized lipids. Hydrocarbons are the main chemical form in which biomarkers are preserved in the geologic record and can be extracted from sediments with organic solvents (yielding bitumen), or released from macromolecular sedimentary organic matter (kerogen) by heating in a vacuum, in an inert gas such as helium or in reactive fluids such as water or hydrogen (Lewan *et al.*, 1979, 1985; Love *et al.*, 1995).

15.7.2 Fatty acids, alcohols and ketones

These are essentially hydrocarbons bearing one or more oxygen-containing functional groups. Fatty acids are most commonly found as the acyl chains in the IPLs of Bacteria and Eukarya. Their carbon numbers and sites of branching and/or unsaturation confer diagnostic utility (Guckert *et al.*, 1985). Besides the steroids and terpenoids discussed below, biomarker alcohols include components of plant leaf wax (Eglinton and Hamilton, 1967) and the esterifying moieties of chlorophyll. Phytol (**23**) is one of the most prominent alcohol biomarkers found in nature. It originates mainly from the side chain of chlorophylls a and b common to plants, algae and cyanobacteria. The hydrocarbons phytane and pristane, both of which can be derived from phytol, are amongst the most ubiquitous and abundant fossil biomarkers (Volkman and Maxwell, 1984).

The best studied ketones are the long-chain alkenones produced by haptophyte algae (Volkman *et al.*, 1980). The patterns of unsaturation in the C_{37} alkenones, presently known to be derived from haptophyte algae of the class Prymnesiophyceae, specifically *Emiliania huxleyi*, *Gephyrocapsa oceanica*, and members of the genera *Isochrysis* and *Chrysotila* (Rontani *et al.*, 2004), have been shown to vary systematically with the temperature of the waters in which they grew (Prahl and Wakeham, 1987; Sikes and Volkman, 1993). The C_{37} alkenones, therefore, encode a record of sea surface temperature (Brassell *et al.*, 1986) and this has resulted in the development, testing and widespread application of the U^{k}_{37}' sea surface temperature proxy (Rosell-Melé *et al.*, 1995; Sikes *et al.*, 1997).

15.7.3 Chlorophylls and carotenoids

The landmark 1936 paper by Alfred Treibs (Treibs, 1936) reporting discovery of fossilized organic nitrogen compounds laid foundations for the entire field of biomarker research. Tetrapyrroles preserved in rocks were so complex that they could only have been sourced from a few biological precursors, either hemes or chlorophylls. Consideration of their structures, natural abundances and distributions all pointed to an origin from the photosynthetic pigments such as the chlorophyll *a* (Chl *a*) that is ubiquitous in plants and algae. Although among the least stable of lipids, chlorophylls and bacteriochlorophylls (Bchls) can undergo a sequence of diagenetic transformations to ultimately form vanadyl and nickel porphyrins. Their structures, in combination with specific C- and N-isotopic compositions, can sometimes be exceptionally diagnostic (Boreham *et al.*, 1990; Chikaraishi *et al.*, 2005; Ohkouchi *et al.*, 2008). Even after oxidation leads to fragmentation of the tetrapyrrole ring-system some of the resulting products, maleimides (1*H*-pyrrole-2,5-diones), can be preserved. In most instances, these have simple methyl and ethyl substitution at positions 3 and 4, thereby rendering their precursor indistinct. However, maleimides having Me *n*-propyl and Me *i*-butyl substitutions are highly specific since these are only observed in Bchl *c*, *d* and *e*, common to the filamentous bacteria (Chloroflexaceae) the green sulfur bacteria (Chlorobiaceae) and the recently described Yellowstone isolate *Chloracidobacterium thermophilum* (Bryant *et al.*, 2007). In an elegant application of C-isotopic measurements, Grice and colleagues (Grice *et al.*, 1996) were able to measure the C-isotopic compositions of Me *n*-propyl and Me *i*-butyl maleimides in the Permian Kupferschiefer to show that, in part, they can derived from the bacteriochlorophylls of the green sulfur bacteria.

15.7.4 Steroids and triterpenoids

Steroids (tetracyclic triterpenoids; Fig. 15.1) and pentacyclic triterpenoids (Fig. 15.2) are of great interest in geobiology because they are demonstrably the most recalcitrant classes of biomarkers and also because they are related in having a common biosynthetic precursor, the ubiquitous C_{30} acyclic hydrocarbon squalene (**24**). The enzymes responsible for cyclization of squalene are also hypothesized to have a shared evolution (Ourisson

et al., 1979, 1987; Rohmer *et al.*, 1979). This has become known as the sterol–triterpenoid biosynthetic bifurcation (Nes, 1974). The bacterial enzyme (squalene–hopene cyclase: SHC) and the eukaryotic enzyme (oxidosqualene cyclase or OSC) have sequence similarities that betray a shared origin but this alone does not allow one to unambiguously identify which is the more primitive (Fischer and Pearson, 2007). However, a connection to the oxygenation of Earth's surface seems clear. Oxygen is required for biosynthesis of sterols but not hopanoids. In sterol biosynthesis (Fig. 15.4), both the conversion of squalene to oxidosqualene via the enzyme squalene monooxygenase (SQMO) and the downstream removal of the angular methyl groups at C4 and C14 of the protosterols, lanosterol (**27**) in the case of fungi and metazoa or cycloartenol (**28**) in plants, en-route to the functional

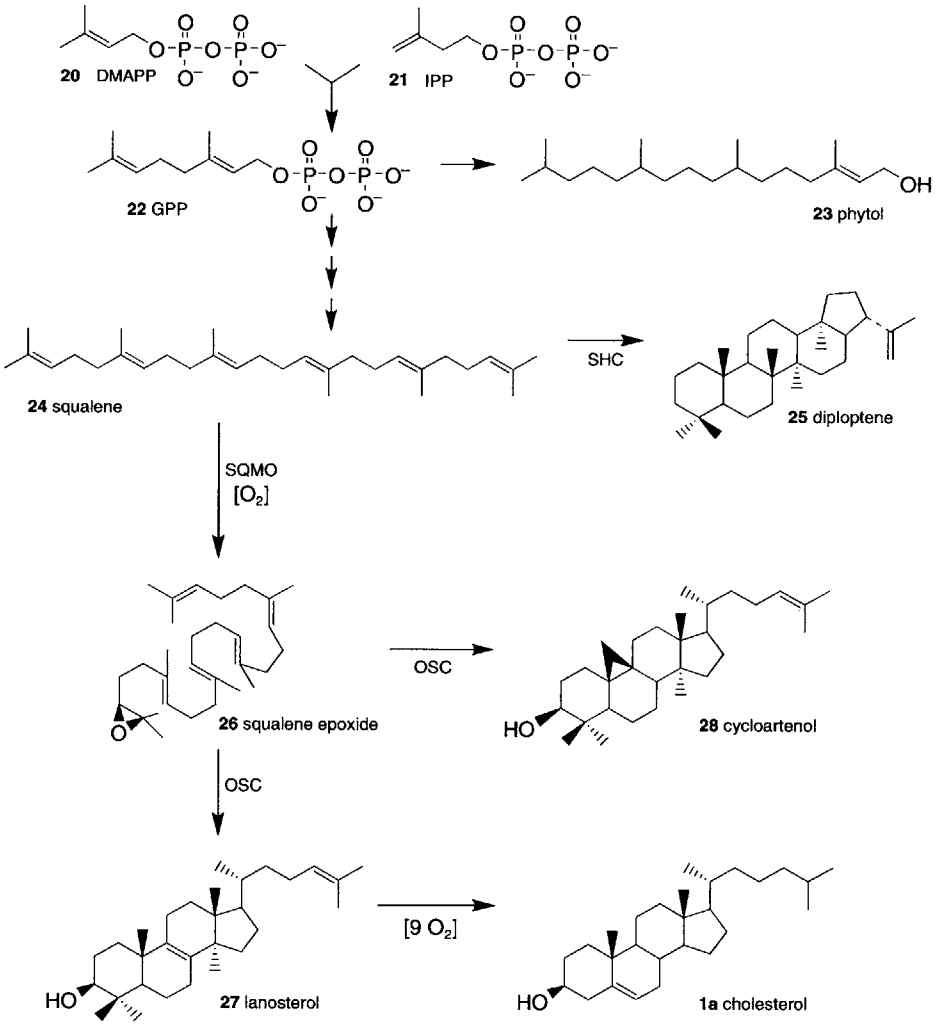

Figure 15.4 Key steps in the biosynthetic pathway to diterpenoids and triterpenoids such as phytol (**23**) and squalene (**24**) respectively. Squalene is the biosynthetic precursor of hopanoids such as diplopterol and diploptene (**25**) which are formed without involvement of molecular oxygen. One molecule of oxygen is required for the transformation of squalene to squalene epoxide (aka oxidosqualene; **26**) which is, in turn, the precursor of the either one of two protosterols lanosterol (**27**) or cycloartenol (**28**). An additional nine molecules of oxygen is required to complete the steroid biosynthetic pathway to cholesterol (**1a**). Oxidosqualene is also the precursor of β-amyrin (**13**) in the flowering plants. In contrast, oxygen is not required to form tetrahymanol (**11**); the oxygen in this sterol surrogate is derived from water.

steroids including cholesterol (**1a**), ergosterol and sitosterol (**1c**) require oxygen. In all, up to eleven moles of oxygen are necessary for the biosynthesis of a mole of cholesterol (Summons *et al.*, 2006). Bloch and colleagues hypothesized that significant functional improvement in sterols accompanied the evolution of the pathway from lanosterol to cholesterol (Bloch, 1979, 1987) while others have noted that sterol structure profoundly influences curvature and lipid phase separation in artificial membranes (Bacia *et al.*, 2005). More recent research on biochemical networks is consistent with this and identifies other areas where an increasing availability of molecular oxygen over geological time has resulted in elaboration of new pathways (Raymond and Segrè, 2006).

Other intriguing aspects of the evolutionary histories of SHCs and OSCs are encoded into the overall amino acid sequences, and especially the degree to which the active sites of these protein families are conserved. For example, alignment of the sequences of genes encoding for OSCs reveals a very high degree of conservation with the active site residues being absolutely conserved across the known eukaryotic diversity (Summons *et al.*, 2006), and the same is true for SHCs as applies to bacterial diversity (excluding the enigmatic Planctomycetes) (Fischer and Pearson, 2007).

15.7.5 *Intact polar lipids*

For environmental studies, intact polar lipids (IPLs) carry the most taxonomic information as they include both the core lipid (Figs 15.5 and 15.6), with its preservable carbon skeleton, along with potentially diagnostic polar head groups (Fig. 15.7). Recent advances in technical capabilities and instrumentation for liquid chromatography (LC) and mass spectrometry (MS) with soft ionization such as electrospray ionization and atmospheric pressure chemical ionization (APCI) have enabled routine analysis of IPLs including BHPs (Rutters *et al.*, 2002; Sturt *et al.*, 2004; Talbot *et al.*, 2003, 2007). This has stimulated development of a growing database for the taxonomic distributions of eukaryotic (McDonald *et al.*, 2007), bacterial (Van Mooy *et al.*, 2006) and archaeal IPLs (Hopmans *et al.*, 2000; Jahn *et al.*, 2004). LC-MS technology development has also increased the range of lipids that can be routinely studied and the precision with which they can be measured while considerably reducing the workload. In fact, the revelation of the diverse range of structures that exist within the membrane-spanning archaeal and bacterial glycerol dialkyl glycerol tetraethers (GDGTs) was only possible with the advent of LC-MS technologies (Hopmans *et al.*, 2000). IPL analyses are particularly powerful when combined with genomic information (e.g, ribosomal DNA clone libraries and metagenomes) that inform us about the taxonomic diversity of microbial communities. IPL analyses are also potentially quantitative thereby giving information on the absolute abundances of microbes in a sample (Lipp *et al.*, 2008).

15.7.6 *Biomarkers for physiology or phylogeny?*

Inspection of the phylogenetic distributions of lipid classes confirms that, for organisms known to date, there are significant correspondences between taxonomic positions of organisms and the predominant types of lipids expressed (Sturt *et al.*, 2004). This is especially the case for terpenoids and the hydrocarbon cores and head groups of IPL, at least at the domain and phylum levels (Brocks and Pearson, 2005). Isoprenoid ether lipids are, as far as we know, unique to the Archaea. Similarly, and as far as is known, the core GDGT crenarchaeol is unique to the Crenarchaeota. Because there are only a few known exceptions, such as Myxobacteria, desmethylsterols are robust biomarkers for the Eukarya. Similarly, C35 hopanoids (bacteriohopanepolyols) are robust biomarkers for Bacteria. There are a few notable cases where the structures of lipids are so distinctive that they can be used to identify organisms at the order, family, genus or even species level, for example ladderane lipids in the Planctomycetales (Rattray *et al.*, 2008), the botryococcene-related lipids in *Botryococcus braunii* (Metzger and Largeau, 2005) and the long-chain ketones of the prymnesiophytes (Volkman *et al.*, 1995).

On the other hand, a preoccupation with relationships between structure of biomarkers and phylogeny draws attention away from a potentially more profound aspect of biomarker chemistry: the relationship between lipid structure and physiology. Lipids always serve some physiological function. Nowhere is this more evident that in the process of anaerobic oxidation of ammonia (anammox) and the ladderane lipids of the Planctomycetales. Organisms living via anammox catabolism have anammoxosomes that contains the critical hydrazine/hydroxylamine oxidoreductase enzyme. The anammoxosome has to be impermeable to hydrazine and oxygen and this is presumed to be accomplished with the aid of membranes constructed from phospholipids known as ladderane lipids. The ladderane hydrocarbon cores, with their distinctive linearly concatenated cyclobutane moieties, are connected to the glycerol moiety via both ester and ether bonds. Protection from O_2 and provision of the essential nitrite electron acceptor is afforded through syntrophy with aerobic ammonia oxidizers. As far as is known, there is a direct relationship between the physiology of anammox and ladderane lipids (Jetten *et al.*, 2003; Sinninghe Damsté *et al.*, 2005). The recent paleorecord of ladderanes has recently been exploited as a tool for studying variations in the intensity of the oxygen minimum zone in the Arabian Sea over the past 1000 years (Jaeschke *et al.*, 2009). It is therefore somewhat ironic that such a direct connection cannot be explored in deep time because, despite the

robustness of anammoxosome membranes in living cells, the lipids themselves are thermally unstable on geological timescales (Jaeschke *et al.*, 2008).

Rather than asking questions like 'What organisms makes what lipids?' biomarker researchers are turning their attention to learning more about the physiological role of a specific compound, its cellular localization, the environmental conditions that require or allow its production and the phylogenetic distribution of its biosynthetic pathway(s) (Doughty *et al.*, 2009, 2011; Sessions *et al.*, 2009; Welander *et al.*, 2009, 2010).

15.8 Lipids diagnostic of Archaea

Three characteristics distinguish archaeal membrane lipids from those of bacteria: (1) hydrophobic cores are composed of isoprenoidal hydrocarbon rather than fatty acyl chains; (2) cores are linked to glycerol moieties by

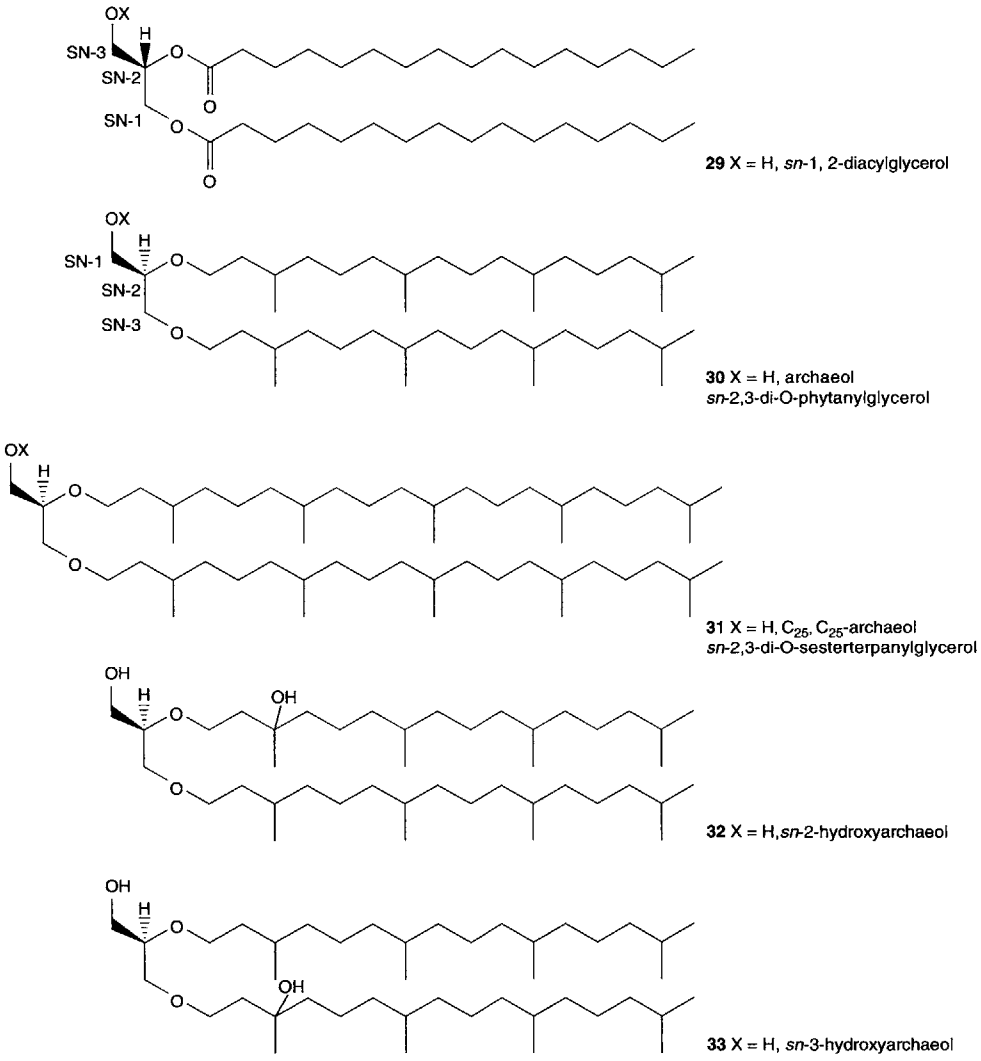

Figure 15.5 Comparison of the stereochemistry of bacterial glycerol diester lipids (e.g. **29**) with the dialkyl ether lipids of Archaea typified by the di-*O*-phytanyl glycerol archaeol (**30**). DGDs show structural variation including replacement of the C_{20} phytanyl chains by C_{25} (**31**) and hydroxylation to form *sn*-2 hydroxyarchaeol (**32**) and *sn*-3 hydroxyarchaeol (**33**).

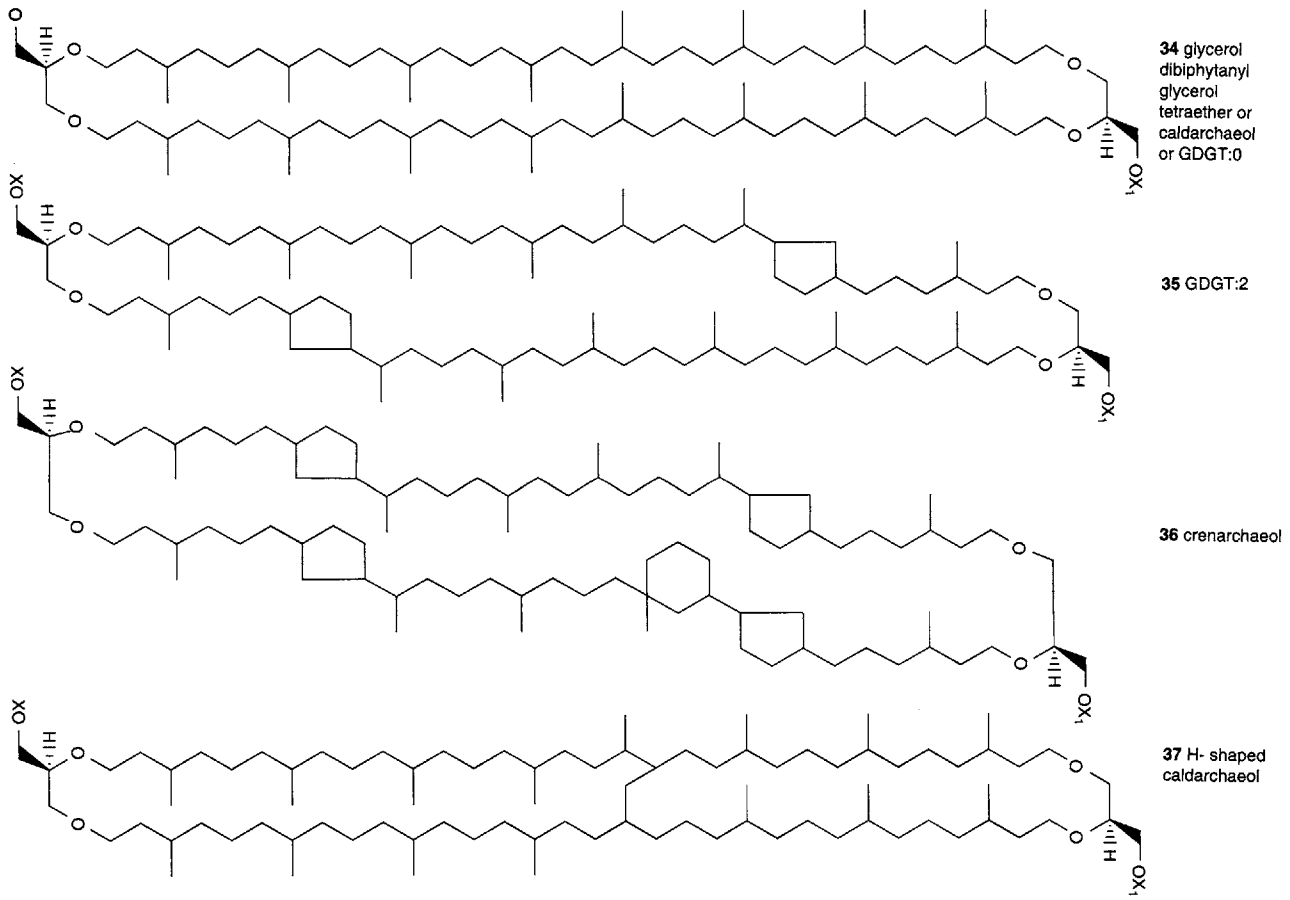

Figure 15.6 Structural variation in the glycerol dialkyl glycerol tetraethers (GDGTs) of Archaea. Caldarchaeols (**34–37**) can have multiple pentacyclic rings as illustrated by a GDGT-2 (**35**). Many of the polycyclic GDGTs are found in both the Euryarchaeota and the Crenarchaeota. However, crenarchaol (**36**) is thought to be confined to the Crenarchaeota while the 'H-shaped' caldarchaeol (**37**) has been found in thermophilic Euryarchaeota. X and X1 denote polar head groups which, in the case of the Archaea, are typically phosphate, phosphoglycosyl or glycosyl groups (Fig. 15.7 **i**, **q** or **p**).

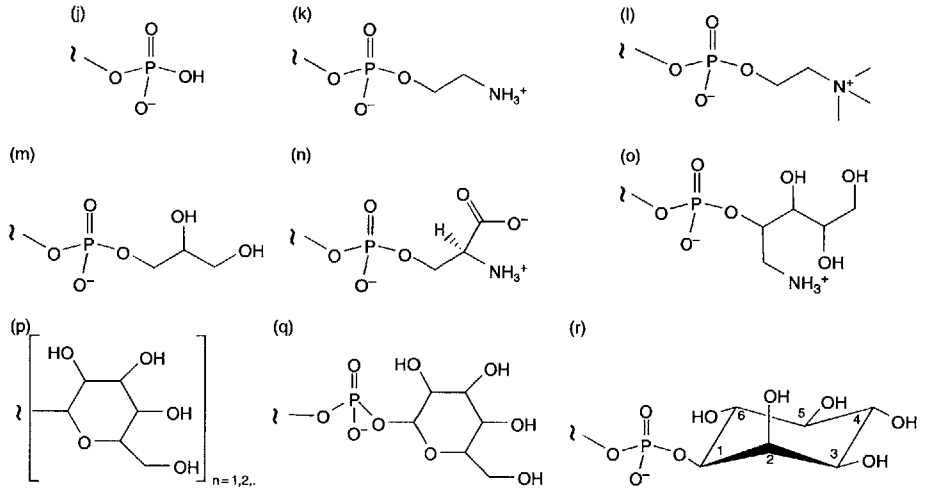

Figure 15.7 A selection of polar head groups that occur in the intact polar lipids of Archaea, Bacteria and Eukarya.

ether rather than ester bonds; and (3) glycerol stereochemistry is 2,3-*sn*-glycerol stereochemistry instead of the bacterial 1,2-*sn*-glycerol (Figs 15.5 and 15.6). However, it is important to recognize that ether lipids are not exclusive to Archaea and have been isolated from bacteria including Aquificales (Jahnke *et al.*, 2001), Mycoplasma (Wagner *et al.*, 2000) and Thermotogales (Sinninghe Damsté *et al.*, 2007). Some Archaea are also known to synthesize fatty acids (Gattinger *et al.*, 2002), but 2,3-*sn*-glycerol stereochemistry is an exclusive trait of Archaea (Peretó *et al.*, 2004) and the synthesis of lipids with both ether bonds and isoprenoid cores also appears confined to this domain (Koga and Morii, 2005).

15.8.1 Intact polar lipids of Archaea

Systematic investigations of the specific patterns of the cores and polar headgroups in archaeal lipids are relatively recent (Koga and Morii, 2005; Nishihara and Koga, 1995; Sturt *et al.*, 2004), and many gaps exist in our knowledge of them. It is not yet clear to what extent head group composition follows taxonomic lines. Complicating this picture is the apparent ability of single clades to synthesize GDGTs with a variety of headgroups. For example, the crenarchaeaon *Nitrosopumilus maritimus* (Schouten *et al.*, 2008b) synthesizes GDGTs with hexose, dihexose and phosphohexose head groups. Until a broader selection of cultures has been analysed it will be difficult to determine whether biosynthetic overlap between physiological groups is extensive; accordingly, the biomarker potential of archaeal IPLS cannot be fully realized at this time. However, isotopic analysis of IPLs is likely to provide additional information about archaeal metabolism in natural populations and will enable more extensive tracer experiments.

15.8.2 Core lipids

Broadly speaking, archaeal membrane core lipids can be divided into two classes: C43 diphytanyl glycerol diethers (DGDs; Fig. 15.5) and C_{86} membrane spanning glycerol dibiphytanyl glycerol tetraethers (GDGTs; Fig. 15.6), also called caldarchaeols. GDGTs have varying degrees of cyclization, containing 0–6 cyclopentane rings and 0–1 cyclohexane rings. One GDGT, crenarchaeol (**36**), has been given a common, non-IUPAC name; it contains one hexacyclic and four pentacyclic rings. The observation that temperature is one control on the degree of cyclization of caldarchaeol GDGTs (Gliozzi *et al.*, 1983) led to the development of the TEX-86 paleotemperature proxy based on their distribution in marine sediments (Schouten *et al.*, 2002). Crenarchaeol may alternatively be a biomarker specifically for ammonia-oxidizing Crenarchaeota (de la Torre *et al.*, 2008) or more generally for Group I Crenarchaeota, including heterotrophic species (Biddle *et al.*, 2006).

An unusual GDGT in which the biphytanyl moieties are covalently linked was first detected in the hyperthermophilic methanogen *Methanothermus fervidus* (Morii *et al.*, 1998). This 'H-shaped' core (**37**) has since been found in several euryarchaeal hydrothermal vent isolates and was recently detected in both marine and lacustrine sediments (Schouten *et al.*, 2008a), where its sources are, as yet, unknown.

DGDs, like GDGTs, show structural diversity (Fig. 15.5). Variations on the structure of archaeol (**30**) exist. Replacement of one or both of the C_{20} chains by C_{25} is common (e.g, **31**) while hydroxylation and unsaturation of the isoprenoid moieties is also seen (**32** and **33**). Macrocyclic archaeol, a diether containing 0–2 internal cyclopentane rings, has been identified in *Methanococcus janaschii* and in mud volcano carbonates (Comita and Gagosian, 1983; Stadnitskaia *et al.*, 2005).

15.8.3 *Taxonomic distribution of archaeal core lipids*

In Archaea certain lipid structural motifs appear to be conserved along phylogenetic lines. Within the cultured Euryarchaeota, halophiles synthesize DGDs such as archaeol (often as an unsaturated archaeol analogue, and sometimes substituting one or two C_{25} chains for C_{20}; **31**) (Kates, 1978). Archaeol (**30**) itself is broadly distributed, occurring in trace amounts in cultured Crenarchaeota and co-occurring with GDGTs in some methanogens. It has been suggested that DGDs may be intermediates in the biosynthesis of GDGTs, but the biosynthetic pathways leading to tetraethers are unresolved. Functionalized archaeols, such as *sn*-2 hydroxyarchaeol (**32**) and *sn*-3 hydroxyarchaeol (**33**) together with a dihydroxyarchaeol are prevalent in methanogenic and methanotrophic archaea (Sprott *et al.*, 1990; Nishihara and Koga, 1995; Bradley *et al.*, 2009). Pentamethylicosane (PMI) is also known from cultivated methanogens and methanotrophic microbial mats (Tornabene *et al.*, 1979; Schouten *et al.*, 1997; Thiel *et al.*, 1999). These particular lipids appear to be exclusively synthesized by Euryarchaeota.

Less phylogenetic specificity is apparent among the GDGTs. Some methanogens synthesize caldarchaeol GDGTs containing 1–3 cyclopentane rings (Gattinger *et al.*, 2002) and thermoacidophiles synthesize GDGTs with as many as 3 cyclopentane rings (Macalady *et al.*, 2004). Cultured Crenarchaeota, e.g. *Sulfolobus solfataricus*, previously known as *Caldariella acidophila*; (Gliozzi *et al.*, 1983) synthesize GDGTs with 0–6 cyclopentane rings, with up to four rings per biphytane moiety. Crenarchaeol, containing four cyclopentane and one cyclohexane ring, is ubiquitous in marine sediments and thought to be biosynthesized by marine Crenarchaeota. However, it has also been detected in soils and terrestrial hydrothermal environments (Pearson *et al.*, 2004) and in a cultured thermophile (de la Torre *et al.*, 2008).

15.8.4 *Preservation potential, geologic record*

Archaeal lipids, like all biomolecules, become defunctionalized during diagenesis. However, under favourable conditions archaeal core lipids can be preserved in the geologic record for hundreds of millions of years. Kuypers *et al.* (2001) found archaeal lipids to be a significant component of organic matter preserved in mid-Cretaceous shales deposited during an oceanic anoxic event. Caldarchaeol, GDGT:1, GDGT:2 and crenarchaeol were detected intact in these samples, and remain the oldest intact GDGTs known to date.

GDGT-derived isoprenoid hydrocarbons provide a means to trace the geologic history of Archaea in older sediments. The ether bonds of GDGTs and DGDs were broken when subjected to extreme temperatures in hydrous pyrolysis experiments simulating diagenesis (Rowland, 1990), yielding the more resistant hydrocarbons biphytane, phytane, and shorter-chained isoprenoids. Biphytane is specific to GDGT-synthesizing archaea and is therefore a useful biomarker. Biphytane and other archaeal biomarkers crocetane, pentamethylicosane and phytane occur in Late Pennsylvanian seep limestones, extending the record of the process of anaerobic oxidation of methane to 300 million years ago, an antiquity nearly double previous estimates based on macrofossil, isotopic and biomarker evidence (Birgel *et al.*, 2008).

15.9 Lipids diagnostic of Bacteria

The lipids of Bacteria have many features in common with those of Eukarya. Most bacterial membranes comprise alkyl chains linked to the *sn*-1 and *sn*-2 carbons of glycerol through ester bonds (Fig. 15.5; **29**). The polar head groups are also similar with phospholipids, glycolipids and phosphoglycolipids being common. Important differences occur in the length and functionalization of the acyl chains with 2-, 3- and 10-methyl branching, hydroxylation, distinctive unsaturation, cyclopropyl groups and ω-cyclohexyl groups common. In addition to lipids with hydrolysable acyl linkages, some bacteria biosynthesize glycerol ether lipids. These can be glycerol diethers, glycerols with one ether-linked alkyl and one acyl chain and membrane-spanning non-isoprenoidal GDGTs.

Lipids that appear to be diagnostic for bacterial taxa include the ladderanes specific to Planctomycetales (Sinninghe Damsté *et al.*, 2005), bacteriochlorophylls and the aromatic carotenoids that, although found in cyanobacteria (Graham *et al.*, 2008; Maresca *et al.*, 2008) and actinobacteria, are widely considered characteristic of the green and purple sulfur bacteria (Brocks and Summons, 2003; Brocks *et al.*, 2005). The stable hydrocarbon cores of the aromatic carotenoids have been found in rocks as old as 1.64 Ga (Brocks *et al.*, 2005). They occur widely in Phanerozoic sediments and are especially prevalent during oceanic anoxic events, attesting to the presence of anoxic and euxinic water columns, the conditions in which their modern counterparts thrive today (Schouten *et al.*, 2001; Smittenberg *et al.*, 2004; Wakeham *et al.*, 2007).

Box 15.1 Example study: Marine archaea

Biomarkers have proven to be useful tools for probing the physiology of the marine archaea, abundant but poorly understood players in marine microbial communities.

Since the discovery that members of the domain Archaea are widespread in the oceans (DeLong, 1992; Fuhrman *et al.*, 1992; DeLong *et al.*, 1998), numerous studies have confirmed their abundance and ubiquity. Once thought to be obligate extremophiles requiring high temperatures, acidic environments, or hypersaline conditions, archaea are now known to be cosmopolitan. Cultivation-independent genomic surveys have revealed that representatives of the Archaea are common in non-hydrothermal terrestrial environments and inhabit all marine environments, spanning the euphotic zone (Frigaard *et al.*, 2006), the mesopelagic (Karner *et al.*, 2001; Massana *et al.*, 1997), and the benthos (Biddle *et al.*, 2006; Lipp *et al.*, 2008) while their range extends from tropical to polar waters. Extrapolating from data obtained through fluorescence *in situ* hybridization at the North Pacific Subtropical Gyre and coastal sites, Karner *et al.* (2001) estimated that archaea comprise nearly a quarter of planktonic marine microbes. Of that number, the majority appear to be Marine Group I Crenarchaeota. Three marine euryarchaeal groups (II–IV) have been identified, but the Marine Group II Euryarchaeota are typically the most abundant of these (DeLong, 2006). Together the Marine Groups I and II account for the bulk of extractable archaeal rRNA in the ocean.

Although their importance to marine biogeochemistry is inevitable if only because of their sheer numbers, little is known about the carbon and energy metabolism of marine archaea. Few representatives exist in culture, so direct study is difficult. Studies of the isolates *Nitrosopumilus maritimus* and *N. yellowstonii* have shown that both marine and terrestrial Crenarchaeota are capable of oxidizing ammonium to nitrite (de la Torre *et al.*, 2008; Konneke *et al.*, 2005), while the presence of the light-driven proton pumping pigment proteorhodopsin in many photic zone Euryarchaeota points to a light-dependent lifestyle. Despite clues such as these, fundamental questions about marine archaea remain unanswered; importantly, the balance of autotrophy and heterotrophy is unknown. The stable carbon isotopic composition of GDGTs found in marine sediment did not provide conclusive evidence for either; their $\delta^{13}C$ value of −20 to −23‰ could indicate consumption of an isotopically heavy carbon source potentially derived from algae, or autotrophic uptake of bicarbonate that is generally enriched relative to CO_2 (Schouten *et al.*, 2008b). Benthic GDGTs also contain levels of radiocarbon that point in favour of autotrophic dominance (Pearson *et al.*, 2001), but which remain ambiguous due to potential confounding effects of the mixing of pre-aged material (Shah *et al.*, 2008).

Incubation studies have found evidence for both autotrophy and heterotrophy. Uptake of tritium-labelled amino acids has been documented in Archaea through a hybridized microautoradiography-FISH approach (Ouverney and Fuhrman, 2000; Teira *et al.*, 2006) while the uptake of isotopically labelled bicarbonate in mesocosms has also been seen (Herndl *et al.*, 2005; Wuchter *et al.*, 2003).

To investigate the importance of chemoautotrophy among marine archaea in the mesopelagic, Ingalls *et al.* (2006) conducted an *in situ* study in the North Pacific Gyre using natural radiocarbon as a tracer. Measuring the carbon isotopic composition of dissolved inorganic carbon (DIC) and that of individual GDGTs in >30,000, they found that surface Archaea incorporate modern carbon into GDGTs, but it was not possible to determine heterotrophy/autotrophy because the ^{14}C content of organic matter and DIC are similar in surface waters. At depth, however, the ^{14}C content becomes more informative. In the 670 m sample GDGTs contained more ^{14}C than expected for a purely autotrophic community. Using an isotopic mass balance model with end members of DIC (151‰) and surface-derived organic carbon (71‰), Ingalls *et al.* (2006) determined the mesopelagic archaeal community was ~80% autotrophic. Whether this figure represents different archaeal groups with different metabolisms or a mixotrophic community remains uncertain. In any case, the predominance of autotrophy suggests that the impact of marine Archaea on marine carbon and nitrogen cycling is significant.

The most ubiquitous of lipids diagnostic for bacteria, in both modern and ancient environments are, however, the hopanoids. These are C_{30}–C_{35} pentacyclic triterpenoids and, because of similarities in their structures, physical dimensions and biosynthetic origins, they have been hypothesized to fulfill a comparable function to the sterols that are obligatory membrane components of Eukarya (Ourisson *et al.*, 1987). However, it is important to stress that the role of hopanoids as direct sterol surrogates is hypothetical as there have been few successful studies that unambiguously link hopanoids to a specific physiological function. Furthermore, while all eukaryotes require sterols (or a sterol-like molecule such as tetrahymanol; **11**) for correct membrane function, hopanoids are not universally required by bacteria. Even within particular bacterial phyla, for example, the cyanobacteria, one

Box 15.2 Example Study: Bacterial and archaeal lipids of the Lost City hydrothermal system

Actively venting carbonate chimneys at the Lost City hydrothermal field (Kelley *et al.*, 2001, 2005) contain significant abundances of organic carbon (~0.6%) that include intact polar lipids diagnostic for a metabolically viable microbial community. Ribosomal DNA analyses show that the living microbial community includes Methanosarcinales and various groups of bacteria (Brazelton *et al.*, 2006). The $\delta^{13}C$ values of the total organic carbon in these chimneys can be as high as −2.8‰ VPDB and they contain high abundances of isoprenoidal and non-isoprenoidal ether lipids. These lipids also display extraordinary ^{13}C enrichments (Bradley *et al.*, 2009). Isoprenoidal ether lipid biomarkers with structures typical of methanogenic and methanotrophic Archaea, including *sn*-2 and *sn*-3 hydroxyarchaeols (**31** and **32**), have $\delta^{13}C$ values that range from −2.9 to +6.7‰ VPDB. In the same samples, non-isoprenoidal ether lipids, with structures similar to those produced by sulfate reducing bacteria in culture have $\delta^{13}C$ values between −11.8‰ and +3.6‰.

Assemblages of hydroxyarchaeols and nonisoprenoidal glycerol ether lipids have been reported in natural environments where methane is being oxidized anaerobically (Hinrichs *et al.*, 1999, 2000; Pancost *et al.*, 2000; Blumenberg *et al.*, 2004) and a feature of these lipids is their characteristic depletion in ^{13}C. Yet these same lipids in the Lost City carbonate towers are manifestly enriched in ^{13}C.

Biogeochemical cycles at Lost City environment are a reflection of the chemical environment created when ultramafic rocks interact with sea water in a process known as serpentinization. This leads to very high hydrogen concentrations in the vent fluids. Values of $[H_2]$ in excess of 14 mmol kg^{-1} have been measured in some cases. These high hydrogen concentrations make it thermodynamically feasible for an unusual co-existence of methanogenesis and sulfate reduction, while, at the same time, making it unfavourable for anaerobic methane oxidation. Further, the lipids specific to methane-cycling Archaea are enriched in ^{13}C relative to the methane in vent fluids, thereby making methane an unlikely carbon source. These observations lead one to surmise that the Methanosarcinales inhabiting the Lost City towers are methanogens and not methane-oxidizing methanotrophs (Bradley *et al.*, 2009). Moreover, microorganisms living in the chemical environment of Lost City, unlike the sulfate-requiring organisms of AOM consortia, are operating totally independently of surface photosynthesis and its by-products of oxygen, nitrate and sulfate. As such, they are a useful model for a biosphere that existed on Earth prior to the advent of oxygenic photosynthesis (Martin *et al.*, 2008; Martin and Russell, 2007).

finds closely related species with and without the capacity to make hopanoids. In a recent study of the purple non-sulfur bacterium *Rhodopseudomonas palustris* strain TIE-1, an absence of hopanoids induced by deletion of the *shc* gene encoding for SHC, the enzyme responsible for cyclization of squalene to the C_{30} hopanoids diploptene and diplopterol, results in a mutant that no longer produced any polycyclic triterpenoids (Welander *et al.*, 2009). Although this mutant is able to grow both heterotrophically and phototrophically, it also has a severe growth defect in that it incurs significant membrane damage when cells are grown at high or low pH. It is not yet known if compromising pH homeostasis is a direct or indirect effect of the inability to produce hopanoids (Welander *et al.*, 2009). Beyond this, the location of hopanoids in some specific kinds of bacterial membranes suggests a physiological connection to membrane behaviour (Doughty *et al.*, 2009). In the case of the nitrogen-fixing bacterium *Frankia*, the concentration of hopanoids in the vesicles housing the nitrogenase suggests an oxygen-protection function, at least in this organism (Berry *et al.*, 1993).

The biosynthesis of hopanoids is widely considered to have an evolutionary connection to the biosynthesis of sterols and the oxygen-carrying triterpenoids of plants. Amino acid sequences suggest that bacterial SHCs and the eukaryotic OSCs are homologous (Fischer and Pearson, 2007) despite their different substrates. Further, the domains that correspond to active sites required for cyclization are highly conserved. Phylogenetic trees constructed for the hopanoid and steroid cyclases suggest that they diverged from a common ancestor although, at the present time, there is no way to distinguish which appeared first (Fischer and Pearson, 2007). Studies of *sqhC* gene sequences drawn from environmental metagenomes now provides an important new window from which we might observe which bacteria produce hopanoids and where they are produced. A recent comparison of SHC amino acid sequences for cultured bacteria with the sequences for *sqhC* fragments in publicly available metagenomic libraries revealed the presence of many novel *sqhC* sequences putatively encoding for cyclase proteins, suggesting that the full diversity of hopanoid-producers remains to be discovered. The same data also suggested that hopanoid biosynthesis may be relatively uncommon, with <10% of the bacteria detected in these environmental metagenomes capable of producing hopanoids (Pearson *et al.*, 2007).

The precursors of sedimentary hopanoids are the BHPs, which have a primary carbon skeleton composed of 35 carbon atoms. BHPs are constructed from one of the C_{30} precursors, diplopterol or diploptene, linked to a moiety derived from a C_5 sugar, likely ribose. Adenosylhopane is a possible intermediate (Neunlist *et al.*, 1988). In fact, correlation of the known stereochemistry of adenosylhopane with a derivative of bacteriohopanetetrol from *Methylobacterium organophilum* enabled the determination of the configuration of all asymmetric centres of the bacteriohopanetetrol side-chain as 22R, 32R, 33R and 34S. While tetrasubstituted BHPs such as bacteriohopanetetrol are probably the most ubiquitous hopanoids in the organisms that have been studied (Rohmer *et al.*, 1984; Talbot *et al.*, 2008), the advent of LC-MS methods has revealed considerable structural diversity in the BHP side-chains (Talbot *et al.*, 2007, 2008). When viewed together with modifications to the basic ring system, where one finds unsaturation and additional methyl groups at either C2 or C3 (Rohmer *et al.*, 1984; Zundel and Rohmer, 1985a, b, c), there is tremendous richness in the chemistry of BHPs.

Although the vast majority of known hopanoid-producing bacteria are aerobes, oxygen is not required for any step in the biosynthesis of these triterpenoids (Rohmer *et al.*, 1984). Anaerobic hopanoid producers are now known through studies of cultured organisms' analyses of their genomes for biosynthetic capability (Sinninghe Damsté *et al.*, 2004a; Fischer *et al.*, 2005; Blumenberg *et al.*, 2006; Rashby *et al.*, 2007). Hopanoids bearing an extra methyl substituent on the A-ring are of particular interest in respect to O_2 in the environment. The 2β-methylbacteriohopanepolyols (2-MeBHPs; **7**) have been proposed as biomarkers for the cyanobacteria (Summons *et al.*, 1999) which are, in the main, oxygen-producing photoautotrophs. The 3β-methylbacteriohopanepolyols (3-MeBHPs; **6**) have been found in cultured acetic acid bacteria (*Acetobacter* sp.) and the methanotrophic bacteria (Type 1 methanotrophs; Zundel and Rohmer, 1985b) both of which are aerobes. Isotopic analyses allow one to distinguish between these possibilities in natural environmental samples and in chemical fossils because, when their isotopic compositions have been measured, 3-methylhopanoids (**9**) invariably have light $\delta^{13}C$ values consistent with an origin from the microaerophilic methanotrophs (Blumenberg *et al.*, 2007; Collister *et al.*, 1992).

2-Methylhopanoids have been found in the Rhizobiales order of α-Proteobacteria (specifically families Methylobacteriaceae and Rhizobiaceae) and in the Cyanobacteria where they are widely distributed across the taxonomy. A study of genomic data suggests that an *Acidobacterium* sp. is also able to make 2-methylhopanoids (Welander *et al.*, 2010). Within the Rhizobiales, the 2-methylhopanoids to be identified first were the 2β-methyldiplopterols and 2β-methyldiploptenes (Vilcheze *et al.*, 1994; Zundel and Rohmer, 1985c). These compounds, together with the extended side-chain version, 2β-methylbacteriohopanetetrol (**7**) were subsequently identified in a strain, TIE-1, of *Rhodopseudomonas palustris*, a member of the Rhizobiaceae (Rashby *et al.*, 2007). *R. palustris*, a metabolically versatile purple non-sulfur bacterium, is also distinctive in that, in addition to hopanoids, it also produces triterpenoids of the gammacerane type, including methylated analogs, (Bravo *et al.*, 2001). *R. palustris* can grow as an anoxygenic photoautotroph, a photoheterotroph and as an aerobic heterotroph. Based on its ability to produce 2-methylhopanoids under all these conditions, it is now clear that 2-MeBHPs are not directly required for oxygen-producing photosynthesis and are not exclusive to cyanobacteria. On the other hand, the presence of 2-MeBHPs in marine cyanobacterial mat samples (Allen *et al.*, 2010), and the distributions of 2-methylhopanoid hydrocarbons in sediments and petroleum, and especially their high abundances in marine carbonate rocks and sediments deposited during oceanic anoxic events suggests that cyanobacteria are the predominant source of these compounds in the marine sedimentary record (Farrimond *et al.*, 2004; Kuypers *et al.*, 2004; Knoll *et al.*, 2007; Talbot *et al.*, 2008; Cao *et al.*, 2009).

15.10 Lipids of Eukarya

Biosynthesis of sterols, with very few exceptions, is a characteristic of eukaryotic organisms (Rohmer *et al.*, 1979). Although sterols (or surrogates such as tetrahymanol) are required by all eukaryotes, animal, plant and fungal membranes have distinct complements of sterols that strongly suggest a connection between their structures and physiological roles (Volkman, 2005). Usually the sterols vary in their patterns of unsaturation and side-chain alkylation (Fig. 15.1; 1a–i). A variety of different sterol esters and steryl glycosides are found in plants and yeast. All eukaryotic organisms require sterols, or a sterol surrogate, for survival.

15.11 Preservable cores

Steroidal hydrocarbons (**2a–i**), most commonly those with 27, 28 and 29 carbon atoms are ubiquitous in sediments and oils. Less abundant are the C_{26} and C_{30} steranes which have more restricted distributions. Of these, C_{26} steranes with three distinct motifs are common (Moldowan *et al.*, 1991). Isomers of 21-norsterane (**2g**) are common in rocks of all ages but are particularly abundant in bitumens from hypersaline depositional environments (Bao and Li, 2001; Grosjean *et al.*, 2009). 27-Norsteranes (**2h**) are also ubiquitous and, along with the 21-norsteranes, likely reflect specific but unknown biological inputs (Moldowan *et al.*, 1991; Peters *et al.*, 2005). 24-Norsteranes

(**2i**) are the least common but also the most biologically diagnostic since culture studies have demonstrated that one of their sources are diatoms (Rampen *et al.*, 2007) consistent with their increased abundances in Cenozoic rocks and oils relative to older samples (Holba *et al.*, 1998a, b). Dinosteranes (**4f**) are known to be robust biomarkers for dinoflagellates (Moldowan and Talyzina, 1998; Summons *et al.*, 1987) while 24-*n*-propyl cholestanes (**2d**) are derived from the sterols of marine pelagophyte algae and useful for recognizing petroleums of marine origin (Moldowan, 1984). The isomeric 24-*i*-propylcholestanes (**2e**) are the only fossil steroids so far known to be derived from animals. Their sterol precursors (e.g, **1e**) are characteristic of sponges while the steranes are notably abundant in Terminal Neoproterozoic and Cambrian sediments and oils from (McCaffrey *et al.*, 1994; Love *et al.*, 2009).

15.11.1 Forms of bias in biomarker records

It is important to pay close attention to the numerous forms of bias when using biomarker records for paleoreconstruction. A prime example stems from operational considerations that lead to the heavy focus on the tractable and volatile saturated and aromatic hydrocarbon fractions of the solvent extractable component (bitumen) of sedimentary organic matter. It is rare to see as much attention paid to the dominant and demonstrably *in situ* insoluble component (i.e. the kerogen). Even microscopic analyses of kerogen can reveal much about the sources, heterogeneity and maturity of preserved organic matter.

To be detectable through molecular, isotopic or even microscopic analyses, source organisms have to be prolific and comprise a significant fraction of the environmental biomass, and/or their biomarkers of interest must be highly resistant to degradation. This leads to a preponderance of preserved organic matter derived from the dominant photoautotrophic components of an ecosystem such as plants, algae and cyanobacteria as well as robust records of the more stable isoprenoid lipids relative to more vulnerable acetogenic lipids. There are very few examples of known biomarkers representative of organisms at the top of trophic structures (e.g, most animals) as is the case for microbes that occupy highly specialized environmental niches (e.g, many symbionts). Ballasting, and rapid transport and burial in anoxic sediments, is an important pathway to organic matter preservation. Organics entrained in rapidly settling fecal pellets or adhering to biogenic minerals and clays (Hedges and Hare, 1987; Hedges and Keil, 1995) will be preserved in preference to organics dissolved in water.

The environment in which organic matter is formed has to be conducive to preservation. Organic matter produced, transported and sedimented subaerially is less well represented in the record compared to organics formed and sedimented subaqueously. Formation and transport through oxygen-rich waters is very destructive with roughly 95–99% of neoformed organic matter in the ocean being recycled through aerobic respiration. Bioturbated sedimentary environments, which are irrigated with waters containing oxygen, also tend to be poor sites for preservation. Respiration with nitrate and sulfate acting as electron acceptors consumes much of the organic matter remaining after sediments become anoxic. In contrast, sulfidic (euxinic) conditions, which can be associated with stratified water bodies and evaporitic environments, lead to exceptional preservation because the sulfide is toxic to most grazers. Sulfide is also a chemical reductant that assists in removing unstable functional groups and replaces them with C-S crosslinkages (Adam *et al.*, 2000; Kohnen *et al.*, 1989). Incorporation of sulfide is one of the most important diagenetic pathways through which organic matter is preserved but it introduces another source of bias by way of the preservation of especially susceptible entities. An understanding of the issues surrounding selective preservation is critical to accurate paleoenvironmental reconstructions.

The sedimentary rock record is, itself, biased. Sediments deposited on the passive margins of continents and in intracratonic basins are well represented in the record. Sediments deposited in the middle of ocean basins tend to be subducted and destroyed as are those continental settings that are uplifted and more readily eroded. Accordingly, the biota inhabiting passive continental margins, marine and continental evaporitic environments large rift lakes, deltas and estuarine systems are well-represented in the biomarker record.

15.11.2 Biomarkers in ancient sediments

Abundantly preserved organic matter is, in itself, a biomarker. There are no known examples of high TOC sediments where the organics are demonstrably abiogenic. The isotopic composition of biogenic organic matter overlaps with that of organic matter formed by abiotic processes (McCollom and Seewald, 2006, 2007). Although we know of abiogenic catalytic processes that can naturally form small hydrocarbons (Sherwood Lollar *et al.*, 2006; McCollom and Seewald, 2007; Proskurowski *et al.*, 2008), evidence for significant geological accumulations of carbonaceous matter formed by abiotic processes is lacking. Because of their potential as archives of early life, analysis and interpretations of molecular fossils from ancient sediments has been a prime focus of organic geochemists. This is especially so in the microbial world where the vast majority of the protagonists lack any preservable and recognizable

entities apart from their lipids. The prime enemies that conspire to prevent our having a representative sedimentary record of past microbial life are uplift and weathering, thermal metamorphism and damage from ionizing radiation. This leads to a rock record that is heavily skewed toward more recent geological periods and events. The Quaternary, Cenozoic and Mesozoic eras are all well documented in respect to the molecular fossil records of microbes and environments. Paleozoic sediments are also well represented, as are the major transitions in Earth's history including the Neoproterozoic–Cambrian interval that saw the rise of complex, multicellular life and the major mass extinction events of the Phanerozoic Eon.

The Proterozoic Eon, during which Earth's ocean, atmosphere and surface environments became oxygenated, is recorded on a few stable cratons with sedimentary rock sequences that contain abundant and well-preserved organic matter that has proved to be amenable to molecular and isotopic analysis. However, this record is temporally and/or geographically discontinuous and there are large gaps when momentous occurrences, including the 2.5–2.2 Ga 'Great Oxidation Event' and the 'Snowball Earth' intervals, have not been adequately evaluated using the tools of molecular organic geochemistry.

The Archean Eon is recorded in just a handful of sedimentary rock sequences that are amenable to molecular investigation. All the known ones, on the Pilbara, Kaapvaal and North American cratons have been heated well beyond the 'oil window', that is, they have time/temperature histories where hydrocarbon generation would have been complete. Only small contents of extractable hydrocarbons remain and their study is at the very edge of feasibility. Consequently, investigations of these rocks have attracted controversy because of the potential for contamination by younger hydrocarbons that have migrated through the rocks or which have been introduced inadvertently during sampling, handling storage and laboratory analysis (Grosjean and Logan, 2007; Sherman *et al.*, 2007; Brocks *et al.*, 2008). The rocks of the Hamersley Basin overlying the Pilbara Craton have received most attention and yielded suites of diagnostic, microbially derived hydrocarbons that were initially assessed as 'probably syngenetic' (Brocks *et al.*, 1999, 2003a, b). Interpretations of isotopic data by Rasmussen and colleagues (Rasmussen *et al.*, 2008) have been proposed to falsify the findings of Brocks *et al.*, 1999–2003 and others (Summons *et al.*, 1999). Unfortunately, the stratigraphic sampling intervals of the rocks analysed by Rasmussen *et al.* (2008) were not reported. Furthermore, conventional approaches to biomarker analysis in ancient rocks destroy them in the process so it is not possible to reproduce the exactly the same experiments on exactly the same samples. Therefore, we must turn to different cores and/or rock units and improve techniques and methodological approaches in order to test and retest this most challenging and contentious aspect of the biogeochemical record.

Different approaches to testing the provenance of the steroids and triterpenoids detected in Archean and Paleoproterozoic rocks have appeared recently. In one that circumvents the potential contamination problems inherent in studies of shale-hosted hydrocarbons Dutkiewicz, George and coworkers have extracted and analysed biomarkers from Palaeoproterozoic oil-bearing fluid inclusions (Dutkiewicz *et al.*, 2006; George *et al.*, 2008). They studied ca. 2.45 Ga fluvial sediments of the Matinenda Fm., Elliot Lake, Canada and, although the origin of oil is not completely constrained, the timing of its emplacement is. Most likely its source was the conformably overlying deltaic McKim Fm. Hydrocarbons trapped in quartz and feldspar crystals during early metamorphism of the host rock, probably before 2.2 Ga, have been entombed in a closed system, and protected from thermal cracking, evaporative loss and contamination ever since. The methodology is founded on identification and isolation of the inclusion-bearing crystals, fastidious cleaning protocols and achievement of system blank levels near to zero (George *et al.*, 1997).

In further studies of the Hamersley Basin sedimentary sequence that had earlier been investigated by Brocks, Eigenbrode employed statistical methods to investigate relationships between different classes of biomarkers extracted from 15 Neoarchean sediments and bulk geochemical properties of the host rocks (Eigenbrode, 2007). Of particular note were the observation of significant correlations between dolomite abundance and the 2-methylhopane index ($100 \times [\mathbf{10}/(\mathbf{10}+\mathbf{8})]$ %), a proxy for cyanobacteria, on one case and the $\delta^{13}C$ of kerogen and the 3-methylhopane index ($100 \times [\mathbf{9}/(\mathbf{9}+\mathbf{8})]$ %), a proxy for methane oxidizing bacteria, on the other. The relative abundances of 2α-methylhopanes in both shale and carbonate from shallow-water sediments showed a strong correlation to carbonate abundance as would be expected if these compounds were largely derived from organisms, such as cyanobacteria, that inhabit shallow water lagoonal environments where carbonate tends to be a predominant lithology (Eigenbrode, 2007; Eigenbrode *et al.*, 2008). Analyses of Phanerozoic petroleum yields a similar result; 2α-methylhopanes tend to be relatively more abundant in oils sourced from carbonates and marls deposited in low latitude paleoenvironments (Knoll *et al.*, 2007). In the same Hamersley Basin rocks, the relative abundances of 3β-methylhopanes were strongly anticorrelated to the $\delta^{13}C$ of coeval kerogen; more 3β-methylhopane was found in rocks having insoluble organic matter with higher $\delta^{13}C$ values (Eigenbrode *et al.*, 2008). This result, although unexpected, might be explained if the kerogens most enriched

in ^{13}C are derived from organic matter formed in the shallow water settings and, assuming that oxygenic photosynthesis was extant, this would also have been where oxygen was produced and available as an electron acceptor. In the modern world, at least, 3β-methylhopanoids are known to be biosynthesized by microaerophilic bacteria. Observations such as these will need to be further tested in other late Archean terrains as well as in the younger rock record to determine if they are reproducible.

In a third approach, the spatial and stratigraphic distributions of hydrocarbons were measured in two cores drilled 24 km apart on the Campbellrand Platform of the Neoarchean Kapvaal Craton, South Africa. Sediments of diverse lithologies, including iron formations, stromatolitic carbonates and shallow to deepwater shales were recovered under clean drilling, sampling, handling protocols (Knoll and Beukes, 2009; Sherman *et al.*, 2007). This was one of the prime goals of the Agouron Griqualand Drilling Project where over 2500 m of thermally mature, yet well-preserved Transvaal Supergroup sediments, dating from ca. 2.67 to 2.46 Ga were fully cored. The same stratigraphic sequence, representing different water depths, was intersected in the two wells and the various units could be correlated lithologically and from the presence of multiple impact spherule beds (Simonson *et al.*, 2009). Biomarker patterns from the correlated intervals showed similarities and differences which provide support for their syngenetic nature. Notably, these sediments were devoid of hydrocarbons known to be of anthropogenic origin (Brocks *et al.*, 2008) and there was a sharp discontinuity in molecular maturity parameters across the ~2 Gyr unconformity between the Neoarchean units and the overlying Permian Dwyka Formation. The suite of molecular fossils identified in these Neoarchean bitumens included hopanes attributable to bacteria, potentially including cyanobacteria and methanotrophic proteobacteria, and steranes of eukaryotic origin. The results, should they be reproducible in other, similarly ancient rocks, speak to the existence of cellular life comprising the three domains and, at that time, the existence of oxygenic photosynthesis and the anabolic use of O_2 (Waldbauer *et al.*, 2009).

15.11.3 Biomarkers in petroleum and bitumen

Petroleum is ubiquitous in the geological record of the Phanerozoic and there are traces of oil in rocks that are much older (Dutkiewicz *et al.*, 1998., 2006; Jackson *et al.*, 1986). Its status as a fossil fuel derives from the fact that petroleum constituents are the molecular remains of past organic life. Many of the molecules that occur abundantly in petroleum (acyclic isoprenoids, steroids and triterpenoids) are so structurally complex that they could not have been formed through non-biological processes. There are no robust data to support alternative theories (Gold, 1992) that specify a primordial nature for subsurface hydrocarbons.

The patterns of hydrocarbons in petroleum hold a detailed account of the history of photosynthetic organisms in the oceans, lakes and rivers of the past (Knoll *et al.*, 2007). However, it is a biased history since oil-prone sedimentary rocks reflect the preferential preservation of coastal margin and intracratonic basin environments. Sediments deposited at low paleolatitude are more disposed to preserve organic matter. Petroleum is also unevenly distributed through geological time with certain periods being biologically, climatically and tectonically favourable for the deposition of petroleum source rocks (Klemme and Ulmishek, 1991). Logically, it is also comprised of the remains of the most quantitatively significant organisms in sedimentary environments, being cyanobacteria and algae in the ocean and in lakes and vascular plants on land and coastal marine settings. Seemingly contrary to this, if one is interested in long-term evolutionary trends, analyses of petroleum samples avoids many of the biases inherent on looking at small pieces of rock from core or outcrop. Petroleum accumulates as fluids that are expelled over millions of years from large volumes of deeply buried sediment that were themselves deposited across aerially extensive basins and over multi-million year timescales (Tissot and Welte, 1978). Therefore a reservoir rock contains hydrocarbon that is spatially and temporally integrated. Volumetrically large samples of petroleum, provided that they have been carefully collected and curated, should also be less prone to contamination.

From analyses of petroleum samples one can discern secular successions in the ocean plankton (Grantham and Wakefield, 1988; Schwark and Empt, 2006). For example, the Triassic radiation and rise to prominence of dinoflagellates can be observed in the increasing quantitative importance of dinosteroids in bitumens and oils (Summons *et al.*, 1987, 1992; Moldowan and Talyzina, 1998). The Cenozoic rise of some diatom taxa is evident in the abundances of HBI and 24-norcholestanes (2i) in oils (Holba *et al.*, 1998a, b; Sinninghe Damsté *et al.*, 2004b). Aromatic hydrocarbons that are derived from land-plant debris have made an indelible imprint on the isotopic compositions of petroleum hydrocarbons (Sofer, 1984; Murray *et al.*, 1998). An evolving biochemistry of vascular plants, together with the Cenozoic rise of angiosperms and their paleogeographic distributions is also preserved in the patterns of petroleum hydrocarbons (Moldowan *et al.*, 1994). Lastly, the hydrocarbons found in bitumen and petroleum attest to the antiquity of specific taxa such as the green and purple sulfur bacteria (Brocks *et al.*, 2005) as well as the biosynthetic pathways they employed to build their lipids (Ourisson and Albrecht, 1992; Ourisson *et al.*, 1979).

Box 15.3 Example study: Mass extinctions

Biomarkers offer considerable promise for elucidating biogeochemical processes associated with mass extinction events. This is because much of the knowledge about these events stems from the study of the rich and diverse record of macroscopic and microscopic fossils; the entire Phanerozoic timescale is fundamentally underpinned by descriptions of profound changes in abundance and diversity of body organisms. In contrast, the record of molecular and isotopic fossils speaks to the successions of organisms that do not leave morphologically recognizable remains, the redox structure of water columns and, possibly, to atmospheric perturbations.

William Holser (Holser, 1977) was one of the first to link the overt disruption of ocean chemistry to biological mass extinction. Subsequent research has provided many examples of shifts in the isotopic compositions of carbon, oxygen and sulfur in marine sediments (Holser *et al.*, 1989) and their links to extinction-radiation of marine plankton, animals and plants. The term 'Strangelove Ocean' has been used to dramatize rapid trends near to the Proterozoic-Phanerozoic transition (Hsu *et al.*, 1985; Kump, 1991) that were interpreted as signifying a great reduction in biological activity. Various geological, paleoceanographic and biological processes have been explored in an effort to test the linkages between these chemical phenomena and the mass extinction and ensuing recovery in biodiversity. At the present time, there is no real consensus on the precise causal links between the chemical 'events' and biotic extinction and re-radiation. However, there is consensus about the existence of C-cycle isotopic anomalies associated with the Permian–Triassic Boundary (PTB) (Magaritz *et al.*, 1988, 1992; Cao *et al.*, 2002; Payne *et al.*, 2004), Cretaceous-Paleogene (K-P) (Arthur *et al.*, 1987; Zachos *et al.*, 1989; D'Hondt *et al.*, 1998; Arens and Jahren, 2000) and Paleocene-Eocene Thermal Maximum (PETM) (Kennett and Stott, 1991; Dickens, 2003; Zachos *et al.*, 2005) events.

One tool that has been applied only relatively recently is the study of secular trends in biomarker lipids. Time series of changes in biomarkers and their carbon isotopic compositions opens a window onto plankton successions and geomicrobiological processes which appear to be driving the C- and S-isotopic excursions that characterize many mass extinction events, and especially the PTB (Sephton *et al.*, 2002, 2005; Xie *et al.*, 2005; Grice *et al.*, 2006; Hays *et al.*, 2007; Wang, 2007; Wang and Visscher, 2007).

Precise correlations of geochronologic, biostratigraphic and chemostratigraphic data for the PTB have become available relatively recently and particularly relate to the Global Stratotype, Section and Point (GSSP) at Meishan, China. Biomarker data collected from sediment samples through a core recently drilled through the Meishan GSSP shows there was a protracted and global euxinic ocean prior to and throughout the Permian to Triassic transition. Of particular note are the trends in the abundances of biomarkers derived from the green sulfur bacteria (Chlorobiaceae) throughout sediments deposited throughout the last few million years of the Permian and into the Early Triassic implying shallow water euxinic conditions were pervasive and protracted (Cao *et al.*, 2009). Independent modelling shows that toxic hydrogen sulfide would have been upwelling from the deep ocean onto continental shelves and entering the atmosphere (Kump *et al.*, 2005; Riccardi *et al.*, 2006; Meyer *et al.*, 2008). Together, these results suggest sulfide toxicity may have contributed to the biological extinction in the marine realm as well as on land. Well-documented sections of PTB Event distributed across the Tethys, Panthalassic and Boreal oceans all show molecular evidence for euxinic conditions in the upper water column (Grice *et al.*, 2005; Hays *et al.*, 2006, 2007; Cao *et al.*, 2009). Isotopic and biomarker data from the Meishan section suggest there was a long-term disruption to the N-cycle and C-cycles. The relative abundances of hopanoids and steroids suggest that bacteria, and not algae, may have been the dominant primary producers in planktonic communities for significant periods of time presaging and following the extinction in the vicinity of Meishan (Cao *et al.*, 2009). Biomarker data, therefore, may record the existence of a 'bacterial ocean' at the end of the Permian Period with strong ocean redox stratification.

15.12 Outlook

Established biomarkers can be exploited to gain insight into nearly any question in geobiology. Increased exploration of unusual environments, as well as those as comparatively 'mundane' as the soil in our cities or the waters at our shores, gives us the opportunity to make progress toward understanding the transformations of matter and energy that occur there and to connect them to processes of the past. The geologic record is also largely unexplored, containing numerous paleoenvironmental transitions that have yet to be investigated using biomarkers. It is also important to expand the temporal breadth of our studies from the known perturbations and transitions to sediments deposited during the more stable times between in order to better position such extraordinary events in a larger geological context.

Box 15.4 Example study: Neoproterozoic radiation of sponges

Very few biomarkers qualify as proxies for animal life. One exception is a class of sedimentary steranes, the 24-isopropylcholestanes (McCaffrey *et al.*, 1994). Using sensitive GC-MS methodologies, these can be distinguished from the 24-*n*-propylcholestanes (**2d**) that are ubiquitous in, and diagnostic for, marine oils and marine petroleum source rocks through geological time (Moldowan, 1984). The 24-*n*-propylcholestanes are derived from 24-*n*-propyl sterols (**1d**) that are characteristic of marine pelagophyte algae. On the other hand, 24-isopropylcholestanes originate from sterols with 24-isopropyl substituents that are biosynthesized *de novo* (Silva *et al.*, 1991) by some demosponges (Bergquist *et al.*, 1991). Notably, the isopropylcholestanes were absent from a choanoflagellate, a member of the unicellular sister group of animals, that was investigated for its sterol content (Kodner *et al.*, 2008). Nor have isopropyl sterols been found in the calcisponges or hexactinellids (Love *et al.*, 2009).

A ratio of 24-isopropylcholestanes/24-*n*-propylcholestanes (*i/n*; **2e/2d**) ≥1 was first observed as an anomalous feature Neoproterozoic to Early Cambrian oils and bitumens from Oman, Australia, Siberia, the Urals and India (McCaffrey *et al.*, 1994) where it was attributed to the rise of sponges and/or their extinct reef-forming cousins, the Archaeocyathids. An *i/n* ratio ≤0.4, and usually much lower, is normal for oils sourced from rocks younger than Cambrian. Further, in an exhaustive study of bitumens and oils of the Huqf Supergroup, South Oman Salt Basin, an *i/n* ratio >0.4 was observed throughout the entire stratigraphy including in sediments laid down between the Sturtian (ca. 713 Ma) and Marinoan (ca. 635 Ma) 'Snowball Earth' glacial events (Love *et al.*, 2009) was. The appearance of these anomalously high levels of isopropylcholestanes during the Cryogenian period is consistent with divergence age estimates for Demospongiae based on molecular clocks calibrated to the first appearances of Paleozoic fauna (Peterson and Butterfield, 2005; Peterson *et al.*, 2007).

The demosponge steranes identified in Oman are a quantitatively significant component of the steroids in all samples analysed and may document the first significant accumulation of animal biomass in the sedimentary record. As molecular fossils, they predate the oldest Ediacaran megascopic animals of ca. 575 Ma (Narbonne and Gehling, 2003). They are also older than the first trace fossils of ca. 555 Ma (Droser *et al.*, 2002) and the likely animal embryos of c. 632 Ma (Xiao *et al.*, 1998; Yin *et al.*, 2007). If these observations are correct, dissolved oxygen concentrations (Fike *et al.*, 2006; Canfield *et al.*, 2007) of the shallow waters of the Cryogenian period were sufficient to support metazoan life 100 Ma, or more, in advance of the rapid diversification of the extant animal phyla during the Cambrian Explosion (Knoll and Carroll, 1999; Marshall, 2006).

Perhaps a greater challenge and opportunity in biomarker research lies in developing our understanding of the genetics responsible for biomarker biosynthesis. Even the genes responsible for key steps in biomarker synthesis in many cultured and genetically sequenced organisms remain unknown; moreover, the environment is replete with microbes of which we have far less knowledge. Once we know the genes responsible for a biomarker, we can then query environmental nucleic acid databases to understand whether the organisms we think contain the biomarker are present in the environments in which we find it. Thus, by exploring the biological underpinnings of biomarkers we can make them more robust tools in geobiology.

Physiology is another area in which geobiologists are poised to make great strides using tools of molecular biology. Perturbations on very different scales, from altering genes to experimenting with conditions in environmental mesocosms, have the potential to reveal the function of specific biomarker molecules. Ultimately, by understanding the function of a biomarker in an organism we can better interpret the presence of that biomarker in both the modern world and in deep time.

Acknowledgements

We are grateful for support from the NASA Astrobiology and Exobiology Programs, the NSF Biocomplexity, EAR and Chemical Oceanography Programs and the Agouron Institute. Jochen Brocks and Ann Pearson provided reviews which significantly improved the original manuscript.

References

Abelson PH, Hoering TC (1961) Carbon isotopic fractionation in formation of amino acids by photosynthetic organisms. *Proceedings of the National Academy of Sciences of the USA* **47**(5), 623–632.

Adam P, Schneckenburger P, Schaeffer P, Albrecht P (2000) Clues to early diagenetic sulfurization processes from mild chemical cleavage of labile sulfur-rich geomacromolecules. *Geochimica et Cosmochimica Acta* **64**(20), 3485–3503.

Allen MA, Burns BP, Neilan BA, Jahnke LL, Summons RE (2010) Lipid biomarkers in Hamelin Pool microbial mats and stromatolites. *Organic Geochemistry* **41**(11), 1207–1218.

Amrani A, Sessions AL, Adkins JF (2009) Compound-specific δ34S analysis of volatile organics by coupled GC/multicollector-ICPMS. *Analytical Chemistry* **81**(21), 9027–9034.

Arens NC, Jahren AH (2000) Carbon isotope excursion in atmospheric CO_2 at the Cretaceous-Tertiary boundary: evidence from terrestrial sediments. *PALAIOS* **15**(4), 314–322.

Arthur MA, Zachos JC, Jones DS (1987) Primary productivity and the Cretaceous/Tertiary boundary event in the oceans. *Cretaceous Research* **8**(1), 43–54.

Bacia K, Schwille P, Kurzchalia T (2005) Sterol structure determines the separation of phases and the curvature of the liquid-ordered phase in model membranes. *Proceedings of the National Academy of Sciences of the USA* **102**(9), 3272–3277.

Bao J, Li M (2001) Unprecedented occurrence of novel C26–C28 21-norcholestanes and related triaromatic series in evaporitic lacustrine sediments. *Organic Geochemistry* **32**(8), 1031–1036.

Bergquist PR, Karuso P, Cambie RC, Smith DJ (1991) Sterol composition and classification of the Porifera. *Biochemical Systematics and Ecology* **19**(1), 17–24.

Berry AM, Harriott OT, Moreau RA, Osman SF, Benson DR, Jones AD (1993) Hopanoid lipids compose the Frankia vesicle envelope, presumptive barrier of oxygen diffusion to nitrogenase. *Proceedings of the National Academy of Sciences of the USA* **90**(13), 6091–6094.

Biddle J, Lipp JS, Lever MA, *et al.* (2006) Heterotrophic Archaea dominate sedimentary subsurface ecosystems off Peru. *Proceedings of the National Academy of Sciences of the USA* **103**, 3846–3851.

Birgel D, Himmler T, Freiwald A, Peckmann J (2008) A new constraint on the antiquity of anaerobic oxidation of methane: Late Pennsylvanian seep limestones from southern Namibia. *Geology* **36**(7), 543–546.

Bloch K (1979) Speculations on the evolution of sterol structure and function. *CRC Critical Reviews of Biochemistry* **7**(1), 1–5.

Bloch K (1987) Summing up. *Annual Review of Biochemistry* **56**(1), 1–18.

Bloch K (1992) Sterol molecule: structure, biosynthesis, and function. *Steroids* **57**(8), 378–83.

Blumenberg M, Seifert R, Reitner J, Pape T, Michaelis W (2004) Membrane lipid patterns typify distinct anaerobic methanotrophic consortia. *Proceedings of the National Academy of Sciences of the USA* **101**(30), 11111–11116.

Blumenberg M, Krüger M, Talbot HM, *et al.* (2006) Biosynthesis of hopanoids by sulfate-reducing bacteria (genus *Desulfovibrio*). *Environmental Microbiology* **8**, 1220–1227.

Blumenberg M, Seifert R, Michaelis W (2007) Aerobic methanotrophy in the oxic-anoxic transition zone of the Black Sea water column. *Organic Geochemistry* **38**(1), 84–91.

Boreham CJ, Fookes CJR, Popp BN, Hayes JM (1990) Origin of petroporphyrins. 2. Evidence from stable carbon isotopes. *Energy & Fuels* **4**(6), 658–661.

Bradley A, Hayes J, Summons R (2009) Extraordinary ^{13}C enrichment of diether lipids at the Lost City Hydrothermal Field indicates a carbon-limited ecosystem. *Geochimica et Cosmochimica Acta* **73**(1), 102–118.

Brassell SC, Eglinton G, Maxwell JR (1983) The geochemistry of terpenoids and steroids. *Biochemical Society Transactions* **11**, 575–586.

Brassell SC, Eglinton G, Marlowe IT, Pflaumann U, Sarnthein M (1986) Molecular stratigraphy: a new tool for climatic assessment. *Nature* **320**(6058), 129.

Bravo JM, Perzl M, Hartner T, Kannenberg EL, Rohmer M (2001) Novel methylated triterpenoids of the gammacerane series from the nitrogen-fixing bacterium *Bradyrhizobium japonicum* USDA 110. *European Journal of Biochemistry* **268**(5), 1323–1331.

Brazelton WJ, Schrenk MO, Kelley DS, Baross JA (2006) Methane- and sulfur-metabolizing microbial communities dominate the lost city hydrothermal field ecosystem. *Applied and Environmental Microbiology* **72**(9), 6257–6270.

Brocks JJ, Pearson A (2005) Building the biomarker tree of life. *Reviews in Mineralogy and Geochemistry* **59**(1), 233–258.

Brocks JJ, Summons RE (2003) Sedimentary hydrocarbons, biomarkers for early life. In: *Treatise in Geochemistry*, Vol. Ch. 8.03 (eds Holland HD, Turekian K), pp. 65–115.

Brocks JJ, Logan GA, Buick R, Summons RE (1999) Archean molecular fossils and the early rise of eukaryotes. *Science* **285**(5430), 1033–1036.

Brocks JJ, Buick R, Logan GA, Summons RE (2003a) Composition and syngeneity of molecular fossils from the 2.78 to 2.45 billion-year-old Mount Bruce Supergroup, Pilbara Craton, Western Australia. *Geochimica et Cosmochimica Acta* **67**(22), 4289–4319.

Brocks JJ, Buick R, Summons RE, Logan GA (2003b) A reconstruction of Archean biological diversity based on molecular fossils from the 2.78 to 2.45 billion-year-old Mount Bruce Supergroup, Hamersley Basin, Western Australia. *Geochimica et Cosmochimica Acta* **67**(22), 4321.

Brocks JJ, Love GD, Summons RE, Knoll AH, Logan GA, Bowden SA (2005) Biomarker evidence for green and purple sulphur bacteria in a stratified Palaeoproterozoic sea. *Nature* **437**(7060), 866.

Brocks JJ, Grosjean E, Logan GA (2008) Assessing biomarker syngeneity using branched alkanes with quaternary carbon (BAQCs) and other plastic contaminants. *Geochimica et Cosmochimica Acta* **72**(3), 871–888.

Bryant DA, Costas AMG, Maresca JA, *et al.* (2007) Candidatus *Chloracidobacterium thermophilum*: an aerobic phototrophic Acidobacterium. *Science* **317**(5837), 523–526.

Canfield DE (1989) Sulfate reduction and oxic respiration in marine sediments: implications for organic carbon preservation in euxinic environments. *Deep Sea Research Part A. Oceanographic Research Papers* **36**(1), 121–138.

Canfield DE, Poulton SW, Narbonne GM (2007) Late-Neoproterozoic deep-ocean oxygenation and the rise of animal life. *Science* **315**(5808), 92–95.

Cao C, Wang W, Jin YG (2002) Carbon isotope excursions across the Permian-Triassic boundary in the Meishan section, Zhejiang Province, China. *Chinese Science Bulletin* **47**, 1125–1129.

Cao C, Love GD, Hays LE, Wang W, Shen S, Summons RE (2009) Biogeochemical evidence for a Euxinic Ocean and ecological disturbance presaging the end-Permian mass extinction event. *Earth and Planetary Science Letters* **288**, 188–201.

Chikaraishi Y, Matsumoto K, Ogawa NO, Suga H, Kitazato H, Ohkouchi N (2005) Hydrogen, carbon and nitrogen isotopic fractionations during chlorophyll biosynthesis in C3 higher plants. *Phytochemistry* **66**(8), 911–920.

Chikaraishi Y, Kashiyama Y, Ogawa NO, *et al.* (2008) A compound-specific isotope method for measuring the stable nitrogen isotopic composition of tetrapyrroles. *Organic Geochemistry* **39**(5), 510–520.

Collister JW, Summons RE, Lichtfouse E, Hayes JM. (1992) An isotopic biogeochemical study of the Green River oil shale. *Organic Geochemistry* **19**(1–3), 265.

Comita P. B. and Gagosian R. B. (1983) Membrane lipid from deep-sea hydrothermal vent methanogen: a new macrocyclic glycerol diether. *Science* **222**(4630), 1329–1331.

D'Hondt S, Donaghay P, Zachos JC, Luttenberg D, Lindinger M (1998) Organic carbon fluxes and ecological recovery from the Cretaceous-Tertiary mass extinction. *Science* **282**(5387), 276–279.

de la Torre JR, Walker CB, Ingalls AE, Könneke M, Stahl DA (2008) Cultivation of a thermophilic ammonia oxidizing archaeon synthesizing crenarchaeol. *Environmental Microbiology* **10**, 810–818.

De Niro MJ, Epstein S (1977) Mechanism of carbon isotope fractionation associated with lipid synthesis. *Science* **197**, 261–263.

DeLong EF (1992) Archaea in coastal marine environments. *Proceedings of the National Academy of Sciences of the USA* **89**(12), 5685–5689.

DeLong EF (2006) Archaeal mysteries of the deep revealed. *Proceedings of the National Academy of Sciences of the USA* **103**(17), 6417–6418.

DeLong EF, King LL, Massana R, *et al.* (1998) Dibiphytanyl ether lipids in nonthermophilic Crenarchaeotes. *Applied and Environmental Microbiology* **64**(3), 1133–1138.

Dickens GR (2003) Rethinking the global carbon cycle with a large, dynamic and microbially mediated gas hydrate capacitor. *Earth and Planetary Science Letters* **213**(3–4), 169–183.

Doughty DM, Hunter RC, Summons RE, Newman DK (2009) 2-Methylhopanoids are maximally produced in akinetes of *Nostoc punctiforme*: geobiological implications. *Geobiology* **7**(5), 524–532.

Doughty DM, Coleman ML, Hunter RC, Sessions AL, Summons RE, Newman D K (2011) Hopanoid lipids impact cell division by *Rhodopseudomonas palustris* at elevated growth temperatures. *Proceedings of the National Academy of Sciences of the USA* **108** (45), E1045–E1051.

Droser ML, Jensen S, Gehling JG (2002) Trace fossils and substrates of the terminal Proterozoic-Cambrian transition: Implications for the record of early bilaterians and sediment mixing. *Proceedings of the National Academy of Sciences of the USA* **99**(20), 12572–12576.

Dutkiewicz A, Rasmussen B, Buick R (1998) Oil preserved in fluid inclusions in Archaean sandstones. *Nature* **395**(6705), 885–888.

Dutkiewicz A, Volk H, George SC, Ridley J, Buick R (2006) Biomarkers from Huronian oil-bearing fluid inclusions: An uncontaminated record of life before the Great Oxidation Event. *Geology* **34**(6), 437–440.

Eglinton G (1970) *Chemical Fossils.* WH Freeman, New York.

Eglinton G, Hamilton RJ (1967) Leaf epicuticular waxes. *Science* **156**(3780), 1322–1335.

Eigenbrode JL (2007) Fossil lipids for life-detection: a case study from the early Earth record. *Space Science Reviews* **135**(1–4), 161–185.

Eigenbrode J, Summons RE, Freeman KH (2008) Methylhopanes in Archean sediments. *Earth and Planetary Science Letters* **273**, 323–331.

Eisenreich W, Schwarz M, Cartayrade A, Arigoni D, Zenk MH, Bacher A (1998) The deoxyxylulose phosphate pathway of terpenoid biosynthesis in plants and microorganisms. *Chemistry & Biology* **5**(9), R221–R233.

Farrimond P, Talbot HM, Watson DF, Schulz LK, Wilhelms A (2004) Methylhopanoids: molecular indicators of ancient bacteria and a petroleum correlation tool. *Geochimica et Cosmochimica Acta* **68**(19), 3873–3882.

Fike DA, Grotzinger JP, Pratt LM, Summons RE (2006) Oxidation of the Ediacaran Ocean. *Nature* **444**(7120), 744–747.

Fischer WW, Pearson A (2007) Hypotheses for the origin and early evolution of triterpenoid cyclases. *Geobiology* **5**(1), 19–34.

Fischer WW, Summons RE, Pearson A (2005) Targeted genomic detection of biosynthetic pathways: anaerobic production of hopanoid biomarkers by a common sedimentary microbe. *Geobiology* **3**(1), 33–40.

Flesch G, Rohmer M (1988) Prokaryotic hopanoids: the biosynthesis of the bacteriohopane skeleton. Formation of isoprenic units from two distinct acetate pools and a novel type of carbon/carbon linkage between a triterpene and D-ribose. *European Journal of Biochemistry* **175**(2), 405–411.

Frigaard N, Martinez A, Mincer TJ, DeLong EF (2006) Proteorhodopsin lateral gene transfer between marine planktonic Bacteria and Archaea. *Nature* **439**, 847–850.

Fuhrman JA, McCallum K, Davis AA (1992) Novel major archeabacterial group from marine plankton. *Nature* **356**, 148–149.

Gaines SM, Eglinton G, Rullkötter J (2009) *Echoes of Life: What Fossil Molecules Reveal about Earth History.* Oxford University Press, Oxford.

Gattinger A, Schloter M, Munch JC (2002) Phospholipid etherlipid and phospholipid fatty acid fingerprints in selected euryarchaeotal monocultures for taxonomic profiling. *FEMS Microbiology Letters* **213**(1), 133–139.

George SC, Krieger FW, Eadington PJ, *et al.* (1997) Geochemical comparison of oil-bearing fluid inclusions and produced oil from the Toro sandstone, Papua New Guinea. *Organic Geochemistry* **26**(3–4), 155.

George SC, Volk H, Dutkiewicz A, Ridley J, Buick R (2008) Preservation of hydrocarbons and biomarkers in oil trapped inside fluid inclusions for >2 billion years. *Geochimica et Cosmochimica Acta* **72**(3), 844–870.

Gliozzi A, Rolandi R, De Rosa M, Gambacorta A (1983) Monolayer black membranes from bipolar lipids of archaebacteria and their temperature-induced structural changes. *Journal of Membrane Biology* **75**(1), 45–56.

Gold T (1992) The deep, hot biosphere. *Proceedings of the National Academy of Sciences of the USA* **89**(13), 6045–6049.

Graham JE, Lecomte JTJ, Bryant DA (2008) Synechoxanthin, an aromatic C40 xanthophyll that is a major carotenoid in the

cyanobacterium *Synechococcus* sp. PCC 7002. *Journal of Natural Products* **71**(9), 1647–1650.

Grantham PJ, Wakefield LL (1988) Variations in the sterane carbon number distributions of marine source rock derived crude oils through geological time. *Organic Geochemistry* **12**, 61–73.

Grice K, Gibbison R, Atkinson JE, Schwark L, Eckardt CB, Maxwell JR (1996) Maleimides (1H-pyrrole-2,5-diones) as molecular indicators of anoxygenic photosynthesis in ancient water columns. *Geochimica et Cosmochimica Acta* **60**(20), 3913–3924.

Grice K, Cao C, Love GD, *et al.* (2005) Photic zone euxinia during the Permian-Triassic superanoxic event. *Science* **307**(5710), 706–709.

Grice K, Fenton S, Bottcher ME, Twitchett RJ, Summons RE, Grosjean E (2006) The biogeochemical cycling of sulfur, carbon and nitrogen across the Permian-Triassic (P-Tr) Hovea-3 borehole (Western Australia) and Schuchert Dal Section (Eastern Greenland). *Geochimica et Cosmochimica Acta* **70**(18, Supplement 1), A218.

Grosjean E, Logan GA (2007) Incorporation of organic contaminants into geochemical samples and an assessment of potential sources: examples from Geoscience Australia marine survey S282. *Organic Geochemistry* **38**, 853–869.

Grosjean E, Love GD, Stalvies C, Fike DA, Summons RE (2009) Origin of petroleum in the Neoproterozoic-Cambrian South Oman Salt Basin. *Organic Geochemistry* **40**(1), 87–110.

Guckert JB, Antworth CP, Nichols PD, White DC (1985) Phospholipid, ester-linked fatty acid profiles as reproducible assays for changes in prokaryotic community structure of estuarine sediments. *FEMS Microbiology Letters* **31**(3), 147–158.

Han J, Calvin M (1969) Hydrocarbon distribution of algae and bacteria and microbial activoty in sediments. *Proceedings of the National Academy of Sciences of the USA* **64**(2), 436–443.

Hayes JM (1993) Factors controlling 13C contents of sedimentary organic compounds: Principles and evidence. *Marine Geology* **113**(1–2), 111–125.

Hayes JM (2001) Fractionation of carbon and hydrogen isotopes in biosynthetic processes. *Reviews in Mineralogy & Geochemistry* **43**, 225–277.

Hayes JM (2004) Isotopic order, biogeochemical processes, and earth history: Goldschmidt lecture, Davos, Switzerland, August 2002. *Geochimica et Cosmochimica Acta* **68**(8), 1691–1700.

Hays LE, Love GD, Foster CB, Grice K, Summons RE (2006) Lipid biomarker records across the Permian–Triassic boundary from Kap Stosch, Greenland. *Eos Transactions AGU, 87(52), Fall Meeting Suppl., Abstract PP41B–1203.*

Hays LE, Beatty T, Henderson CM, Love GD, Summons RE (2007) Evidence for photic zone euxinia through the end-Permian mass extinction in the Panthalassic Ocean (Peace River Basin, Western Canada). *Palaeoworld* **16**(1–3), 39–50.

Hebting Y, Schaeffer P, Behrens A, *et al.* (2006) Biomarker evidence for a major preservation pathway of sedimentary organic carbon. *Science* **312**(5780), 1627–1631.

Hedges JI, Hare PE (1987) Amino acid adsorption by clay minerals in distilled water. *Geochimica et Cosmochimica Acta* **51**, 255–259.

Hedges JI, Keil RG (1995) Sedimentary organic matter preservation: an assessment and speculative synthesis. *Marine Chemistry* **49**(2–3), 81–115.

Herndl GJ, Reinthaler T, Teira E, *et al.* (2005) Contribution of Archaea to total prokaryotic production in the deep Atlantic Ocean. *Applied and Environmental Microbiology* **71**, 1715–1726.

Heuer V, Elvert M, Tille S, *et al.* (2006) Online $\delta^{13}C$ analysis of volatile fatty acids in sediment/porewater systems by liquid chromatography–isotope ratio mass spectrometry. *Limnology and Oceanography: Methods* **4**, 346–357.

Hinrichs K-U, Hayes JM, Sylva SP, Brewer PG, DeLong EF (1999) Methane-consuming archaebacteria in marine sediments. *Nature* **398**, 802–805.

Hinrichs K-U, Summons RE, Orphan V, Sylva SP, Hayes JM (2000) Molecular and isotopic analysis of anaerobic methane-oxidizing communities in marine sediments. *Organic Geochemistry* **31**, 1685–1701.

Hinrichs K-U, Eglinton G, Engel MH, Summons RE (2001) Exploiting the multivariate isotopic nature of organic compounds. *Geochemistry Geophysics Geosystems* **1**, Paper number 2001GC000142.

Holba AG, Dzou LIP, Masterson WD, *et al.* (1998a) Application of 24-norcholestanes for constraining source age of petroleum. *Organic Geochemistry* **29**(5–7), 1269–1283.

Holba AG, Tegelaar EW, Huizinga BJ, *et al.* (1998b) 24-norcholestanes as age-sensitive molecular fossils. *Geology* **26**(9), 783–786.

Holser WT (1977) Catastrophic chemical events in the history of the ocean. *Nature* **267**(5610), 403–408.

Holser WT, Schonlaub H-P, Attrep M, *et al.* (1989) A unique geochemical record at the Permian/Triassic boundary. *Nature* **337**(6202), 39–44.

Hopmans EC, Schouten S, Pancost RD, *et al.* (2000) Analysis of intact tetraether lipids in archaeal cell material and sediments by high performance liquid chromatography/atmospheric pressure chemical ionization mass spectrometry. *Rapid Communications in Mass Spectrometry* **14**(7), 585–589.

House CH, Schopf JW, Stetter KO (2003) Carbon isotopic fractionation by Archaeans and other thermophilic prokaryotes. *Organic Geochemistry* **34**, 345–356.

Hsu KJ, Oberhansli H, Gao JY, Shu S, Haihong C, Krahenbuhl U (1985) Strangelove ocean before the Cambrian explosion. *Nature* **316**, 809–811.

Ingalls AE, Shah SR, Hansman RL, *et al.* (2006) Quantifying archaeal community autotrophy in the mesopelagic ocean using natural radiocarbon. *Proceedings of the National Academy of Sciences of the USA* **103**, 6442–6447.

Jackson MJ, Powell TG, Summons RE, Sweet IP (1986) Hydrocarbon shows and petroleum source rocks in sediments as old as 1.7×10^9 years. *Nature* **322**(6081), 727–729.

Jaeschke A, Lewan MD, Hopmans EC, Schouten S, Damsté JSS (2008) Thermal stability of ladderane lipids as determined by hydrous pyrolysis. *Organic Geochemistry* **39**(12), 1735–1741.

Jaeschke A, Rooks C, Trimmer M, Nicholls JC, Hopmans EC, Schouten S, Sinninghe Damsté JS (2009) 'Comparison of ladderane phospholipid and core lipids as indicators for anaerobic ammonium oxidation (anammox) in marine sediments. *Geochimica et Cosmochimica Acta* **73**, 2077–2088.

Jahn U, Summons R, Sturt H, Grosjean E, Huber H (2004) Composition of the lipids of *Nanoarchaeum equitans* and their origin from its host *Ignicoccus* sp. strain KIN4/I. *Archives of Microbiology* **182**(5), 404.

Jahnke LL, Eder W, Huber R, *et al.* (2001) Signature lipids and stable carbon isotope analyses of Octopus Spring hyperthermophilic communities compared with those of Aquificales representatives. *Applied Environmental Microbiology* **67**(11), 5179–5189.

Jahnke LL, Embaye T, Hope J, *et al.* (2004) Lipid biomarker and carbon isotopic signatures for stromatolite-forming, microbial mat communities and *Phormidium* cultures from Yellowstone National Park. *Geobiology* **2**(1), 31–47.

Jetten MSM, Sliekers O, Kuypers M, *et al.* (2003) Anaerobic ammonium oxidation by marine and freshwater planctomycete-like bacteria. *Applied Microbiology and Biotechnology* **63**(2), 107–114.

Karner MB, Delong EF, Karl DM (2001) Archaeal dominance in the mesopelagic zone of the Pacific Ocean. *Nature* **409**, 507–510.

Kates M (1978) The phytanyl ether-linked polar lipids and isoprenoid neutral lipids of extremely halophilic bacteria. *Progress in Chemistry: Fats and Other Lipids* **15**(4), 301–342.

Kelley DS, Karson JA, Blackman DK, *et al.* (2001) An off-axis hydrothermal vent field near the Mid-Atlantic Ridge at 30 degrees N. *Nature* **412**(6843), 145–149.

Kelley DS, Karson JA, Fruh-Green GL, *et al.* (2005) A serpentinite-hosted ecosystem: the Lost City hydrothermal field. *Science* **307**(5714), 1428–1434.

Kennett JP, Stott LD (1991) Abrupt deep-sea warming, palaeoceanographic changes and benthic extinctions at the end of the Palaeocene. *Nature* **353**, 225–229.

Klemme HD, Ulmishek GF (1991) Effective petroleum source rocks of the world: stratigraphic distribution and controlling depositional factors. *AAPG Bulletin* **75**, 1809–1851.

Knoll AH, Beukes NJ (2009) Introduction: Initial investigations of a Neoarchean shelf margin-basin transition (Transvaal Supergroup, South Africa). *Precambrian Research* **169**(1–4), 1–14.

Knoll AH, Carroll SB (1999) Early animal evolution: emerging views from comparative biology and geology. *Science* **284**(5423), 2129–2137.

Knoll AH, Summons RE, Waldbauer JR, Zumberge J (2007) The geological succession of primary producers in the oceans. In: *The Evolution of Primary Producers in the Sea* (eds Falkwoski P, Knoll AH). Elsevier, Amsterdam, pp. 133–163.

Kodner RB, Summons RE, Pearson A, King N, Knoll AH (2008) Sterols in a unicellular relative of the metazoans. *Proceedings of the National Academy of Sciences of the USA* **105**(29), 9897–9902.

Koga Y, Morii H (2005) Recent advances in structural research on ether lipids from Archaea including comparative and physiological aspects. *Bioscience, Biotechnology, and Biochemistry* **69**(11), 2019–2034.

Kohnen MEL, Damste JSS, ten Haven HL, de Leeuw JW (1989) Early incorporation of polysulphides in sedimentary organic matter. *Nature* **341**(6243), 640.

Konneke M, Bernhard AE, de la Torre JR, Walker CB, Waterbury JB, Stahl DA (2005) Isolation of an autotrophic ammonia-oxidizing marine archaeaon. *Nature* **437**, 543–546.

Kump L (1991) Interpreting carbon-isotope excursions: Strangeloveoceans. *Geology* **19**, 299–302.

Kump LR, Pavlov A, Arthur MA (2005) Massive release of hydrogen sulfide to the surface ocean and atmosphere during intervals of oceanic anoxia. *Geology* **33**, 397–400.

Kuypers MMM, Blokker P, Erbacher J, *et al.* (2001) Massive expansion of marine Archaea during a mid-Cretaceous oceanic anoxic event. *Science* **293**(5527), 92–95.

Kuypers MMM, van Breugel Y, Schouten S, Erba E, Damsté JSS (2004) N_2-fixing cyanobacteria supplied nutrient N for Cretaceous oceanic anoxic events. *Geology* **32**(10), 853–856.

Lewan MD, Winters JC, McDonald JH (1979) Generation of oil-like pyrolyzates from organic-rich shales. *Science* **203**(4383), 897–899.

Lewan MD, Spiro B, Illich H, *et al.* (1985) Evaluation of petroleum generation by hydrous pyrolysis experimentation [and discussion]. *Philosophical Transactions of the Royal Society of London. Series A, Mathematical and Physical Sciences* **315**(1531), 123.

Lichtenthaler HK, Schwender J, Disch A, Rohmer M (1997) Biosynthesis of isoprenoids in higher plant chloroplasts proceeds via a mevalonate-independent pathway. *FEBS Letters* **400**(3), 271–274.

Lipp J, Morono Y, Inagaki F, Hinrichs K (2008) Significant contribution of Archaea to extant biomass in marine subsurface sediments. *Nature* **454**(7207), 991–994.

Love GD, Snape CE, Carr AD, Houghton RC (1995) Release of covalently-bound alkane biomarkers in high yields from kerogen via catalytic hydropyrolysis. *Organic Geochemistry* **23**(10), 981–986.

Love GD, Grosjean E, Stalvies C, *et al.* (2009) Fossil steroids record the appearance of Demospongiae during the Cryogenian period. *Nature* **457**(7230), 718–721.

Macalady JL, Vestling MM, Baumler D, Boekelheide N, Kaspar CW, Banfield JF (2004) Tetraether-linked membrane monolayers in *Ferroplasma* spp: a key to survival in acid. *Extremophiles* **8**(5), 411–419.

Mackenzie AS, Brassell SC, Eglinton G, Maxwell JR (1982) Chemical fossils: the geological fate of steroids. *Science* **217**(4559), 491–504.

Magaritz M, Bar R, Baud A, Holser WT (1988) The carbon-isotope shift at the Permian/Triassic boundary in the southern Alps is gradual. *Nature* **331**, 337–339.

Magaritz M, Krishnamurthy RV, Holser WT (1992) Parallel trends in organic and inorganic carbon isotopes across the Permian/Triassic boundary. *American Journal of Science* **292**(10), 727–739.

Maresca J, Graham J, Bryant D (2008) The biochemical basis for structural diversity in the carotenoids of chlorophototrophic bacteria. *Photosynthesis Research* **97**(2), 121–140.

Marshall CR (2006) Explaining the Cambrian explosion of animals. *Annual Review of Earth and Planetary Sciences* **34**(1), 355–384.

Martin W, Russell MJ (2007) On the origin of biochemistry at an alkaline hydrothermal vent. *Philosophical Transactions of the Royal Society B: Biological Sciences* **362**(1486), 1887–1926.

Martin W, Baross J, Kelley D, Russell MJ (2008) Hydrothermal vents and the origin of life. *Nature Reviews Microbiology* **6**(11), 805.

Massana R, Murray AE, Preston CM, DeLong EF (1997) Vertical distribution and phylogenetic characterization of marine planktonic Archaea in the Santa Barbara Channel. *Applied and Environmental Microbiology* **63**, 50–56.

McCaffrey MA, Michael Moldowan J, Lipton PA, *et al.* (1994) Paleoenvironmental implications of novel C30 steranes in Precambrian to Cenozoic Age petroleum and bitumen. *Geochimica et Cosmochimica Acta* **58**(1), 529.

McCollom TM, Seewald JS (2006) Carbon isotope composition of organic compounds produced by abiotic synthesis under hydrothermal conditions. *Earth and Planetary Science Letters* **243**(1–2), 74–84.

McCollom TM, Seewald JS (2007) Abiotic synthesis of organic compounds in deep-sea hydrothermal environments. *Chemical Reviews (Washington, DC, United States)* **107**(2), 382–401.

McDonald JG, Thompson B, McCrum EC, Russell DW (2007) Extraction and analysis of sterols in biological matrices by high-performance liquid chromatography electrospray ionization mass spectrometry. *Methods in Enzymology* **432**, 143–168.

Metzger P, Largeau C (2005) *Botryococcus braunii*: a rich source for hydrocarbons and related ether lipids. *Applied Microbiology and Biotechnology* **66**(5), 486–496.

Meyer KM, Kump LR, Ridgwell A (2008) Biogeochemical controls on photic-zone euxinia during the end-Permian mass extinction. *Geology* **36**(9), 747–750.

Moldowan JM (1984) C30-steranes, novel markers for marine petroleums and sedimentary rocks. *Geochimica et Cosmochimica Acta* **48**(12), 2767–2768.

Moldowan JM, Talyzina NM (1998) Biogeochemical evidence for dinoflagellate ancestors in the early Cambrian. *Science* **281**(5380), 1168–1170.

Moldowan JM, Lee CY, Watt DS, Jeganathan A, Slougui N-E, Gallegos EJ (1991) Analysis and occurrence of C26-steranes in petroleum and source rocks. *Geochimica et Cosmochimica Acta* **55**(4), 1065–1081.

Moldowan JM, Dahl J, Huizinga BJ, *et al.* (1994) The molecular fossil record of oleanane and its relation to angiosperms. *Science* **265**(5173), 768–771.

Monson KD, Hayes JM (1980) Biosynthetic control of the natural abundance of carbon 13 at specific positions within fatty acids in *Escherichia coli*. Evidence regarding the coupling of fatty acid and phospholipid synthesis. *Journal of Biological Chemistry* **255**(23), 11435–11441.

Monson KD, Hayes JM (1982) Carbon isotopic fractionation in the biosynthesis of bacterial fatty acids. Ozonolysis of unsaturated fatty acids as a means of determining the intramolecular distribution of carbon isotopes. *Geochimica et Cosmochimica Acta* **46**(2), 139–149.

Morii H, Eguchi T, Nishihara M, Kakinuma K, König H, Koga Y (1998) A novel ether core lipid with H-shaped C80-isoprenoid hydrocarbon chain from the hyperthermophilic methanogen *Methanothermus fervidus*. *Biochimica et Biophysica Acta (BBA) – Lipids and Lipid Metabolism* **1390**(3), 339–345.

Murray AP, Edwards D, Hope JM, *et al.* (1998) Carbon isotope biogeochemistry of plant resins and derived hydrocarbons. *Organic Geochemistry* **29**(5–7), 1199–1214.

Narbonne GM, Gehling JG (2003) Life after snowball: the oldest complex Ediacaran fossils. *Geology* **31**(1), 27–30.

Nes W (1974) Role of sterols in membranes. *Lipids* **9**(8), 596–612.

Neunlist S, Bisseret P, Rohmer M (1988) The hopanoids of the purple non-sulfur bacteria *Rhodopseudomonas palustris* and *Rhodopseudomonas acidophila* and the absolute configuration of bacteriohopanetetrol. *European Journal of Biochemistry* **171**(1–2), 245–252.

Nishihara M, Koga Y (1995) Two new phospholipids, hydroxyarchaetidylglycerol and hydroxyarchaetidylethanolamine, from the Archaea *Methanosarcina barkeri*. *Biochimica et Biophysica Acta (BBA) – Lipids and Lipid Metabolism* **1254**(2), 155–160.

Ohkouchi N, Kahiyama Y, Chikaraishi Y, Ogawa NO, Tada R, Kitazato H (2006) Nitrogen isotopic composition of chlorophylls and porphyrins in geological samples as tools for reconstructing paleoenvironment. *Geochimica et Cosmochimica Acta* **70**(18, Supplement 1), A452.

Ohkouchi N, Nakajima Y, Ogawa NO, *et al.* (2008) Carbon isotopic composition of the tetrapyrrole nucleus in chloropigments from a saline meromictic lake: a mechanistic view for interpreting the isotopic signature of alkyl porphyrins in geological samples. *Organic Geochemistry* **39**(5), 521–531.

Ourisson G, Albrecht P (1992) Geohopanoids: the most abundant natural products on Earth? *Accounts of Chemical Research* **25**, 298–402.

Ourisson G, Albrecht P, Rohmer M (1979) The hopanoids. palaeochemistry and biochemistry of a group of natural products. *Pure and Applied Chemistry* **51**(4), 709–729.

Ourisson G, Rohmer M, Poralla K (1987) Prokaryotic hopanoids and other polyterpenoid sterol surrogates. *Annual Review of Microbiology* **41**, 301–333.

Ouverney CC, Fuhrman JA (2000) Marine planktonic archaea take up amino acids. *Applied and Environmental Microbiology* **66**, 1429–143x.

Pancost RD, Sinninghe Damsté JS, de Lint S, van der Maarel MJEC, Gottschal JC, Party MSS (2000) Biomarker evidence for widespread anaerobic methane oxidation in Mediterranean sediments by a consortium of methanogenic Archaea and Bacteria. *Applied and Environmental Microbiology* **66**(3), 1126–1132.

Patience RL, Rowland SJ, Maxwell JR (1978) The effect of maturation on the configuration of pristane in sediments and petroleum. *Geochimica et Cosmochimica Acta* **42**(12), 1871–1875.

Payne JL, Lehrmann DJ, Wei J, Orchard MJ, Schrag DP, Knoll AH (2004) Large perturbations of the carbon cycle during recovery from the end-Permian extinction. *Science* **305**(5683), 506–509.

Pearson A, McNichol AP, Benitez-Nelson BC, Hayes JM, Eglinton TI (2001) Origins of lipid biomarkers in Santa Monica Basin surface sediment: a case study using compound-specific [Delta]14C analysis. *Geochimica et Cosmochimica Acta* **65**(18), 3123–3137.

Pearson A, Huang Z, Ingalls AE, *et al.* (2004) Nonmarine crenarchaeol in Nevada hot springs. *Applied and Environmental Microbiology* **70**(9), 5229–5237.

Pearson A, Page SRF, Jorgenson TL, Fischer WW, Higgins MB (2007) Novel hopanoid cyclases from the environment. *Environmental Microbiology* **9**(9), 2175–2188.

Peretó J, López-García P, Moreira D (2004) Ancestral lipid biosynthesis and early membrane evolution. *Trends in Biochemical Sciences* **29**(9), 469–477.

Peters KE, Walters CC, Moldowan JM (2005) *The Biomarker Guide*, 2nd edn. Cambridge University Press, Cambridge.

Peterson KJ, Butterfield NJ (2005) Origin of the Eumetazoa: testing ecological predictions of molecular clocks against the Proterozoic fossil record. *Proceedings of the National Academy of Sciences of the USA* **102**(27), 9547–9552.

Peterson KJ, Summons RE, Donoghue PCJ (2007) Molecular palaeobiology. *Palaeontology* **50**(4), 775–809.

Prahl FG, Wakeham SG (1987) Calibration of unsaturation patterns in long-chain ketone compositions for palaeotemperature assessment. *Nature* **330**(6146), 367–369.

Proskurowski G, Lilley MD, Seewald JS, *et al.* (2008) Abiogenic hydrocarbon production at Lost City hydrothermal field. *Science* **319**(5863), 604–607.

Rampen SW, Schouten S, Abbas B, *et al.* (2007) On the origin of 24-norcholestanes and their use as age-diagnostic biomarkers. *Geology* **35**(5), 419–422.

Rashby SE, Sessions AL, Summons RE, Newman DK (2007) Biosynthesis of 2-methylbacteriohopanepolyols by an anoxygenic phototroph. *Proceedings of the National Academy of Sciences of the USA* **104**(38), 15099–15104.

Rasmussen B, Fletcher IR, Brocks JJ, Kilburn MR (2008) Reassessing the first appearance of eukaryotes and cyanobacteria. *Nature* **455**, 1101–1104.

Rattray J, van de Vossenberg J, Hopmans E, *et al.* (2008) Ladderane lipid distribution in four genera of anammox bacteria. *Archives of Microbiology* **190**(1), 51.

Raymond J, Segrè D (2006) The effect of oxygen on biochemical networks and the evolution of complex life. *Science* **311**(5768), 1764–1767.

Riccardi AL, Arthur MA, Kump LR (2006) Sulfur isotopic evidence for chemocline upward excursions during the end-Permian mass extinction. *Geochimica et Cosmochimica Acta* **70**, 5740–5752.

Rohmer M (2003) Mevalonate-independent methylerythritol phosphate pathway for isoprenoid biosynthesis. Elucidation and distribution. *Pure and Applied Chemistry* **75**(2–3), 375–387.

Rohmer M, Bouvier P, Ourisson G (1979) Molecular evolution of biomembranes – structual equivalents and phylogenetic precursors of sterols. *Proceedings of the National Academy of Sciences of the USA* **76**(2), 847–851.

Rohmer M, Bouvier-Nave P, Ourisson G (1984) Distribution of hopanoid triterpanes in prokaryotes. *Journal of General Microbiology* **130**, 1137–1150.

Rohmer M, Knani M, Simonin P, Sutter B, Sahm H (1993) Isoprenoid biosynthesis in bacteria: a novel pathway for the early steps leading to isopentenyl diphosphate. *Biochemical Journal* **295**, 517–524.

Rontani J-F, Beker B, Volkman JK (2004) Long-chain alkenones and related compounds in the benthic haptophyte *Chrysotila lamellosa* Anand HAP 17. *Phytochemistry* **65**, 117–126.

Rosell-Melé A, Eglinton G, Pflaumann U, Sarnthein M (1995) Atlantic core-top calibration of the U37K index as a sea-surface palaeotemperature indicator. *Geochimica et Cosmochimica Acta* **59**(15), 3099–3107.

Rowland SJ (1990). Production of acyclic isoprenoid hydrocarbons by laboratory maturation of methanogenic bacteria. *Organic Geochemistry* **15**, 9–16.

Rullkötter J, Aizenshtat Z, Spiro B (1984) Biological markers in bitumens and pyrolyzates of Upper Cretaceous bituminous chalks from the Ghareb Formation (Israel). *Geochimica et Cosmochimica Acta* **48**(1), 151–157.

Rutters H, Sass H, Cypionka H, Rullkotter J (2002) Phospholipid analysis as a tool to study complex microbial communities in marine sediments. *Journal of Microbiological Methods* **48**(2–3), 149.

Schimmelmann A, Lewan MD, Wintsch RP (1999) D/H isotope ratios of kerogen, bitumen, oil, and water in hydrous pyrolysis of source rocks containing kerogen types I, II, IIS, and III. *Geochimica et Cosmochimica Acta* **63**(22), 3751–3766.

Schoell M (1988) Multiple origins of methane in the Earth. *Chemical Geology* **71**(1–3), 1–10.

Schouten S, Van Der Maarel MJEC, Huber R, Damsté JSS (1997) 2,6,10,15,19-Pentamethylicosenes in *Methanolobus bombayensis*, a marine methanogenic archaeon, and in *Methanosarcina mazei*. *Organic Geochemistry* **26**(5–6), 409–414.

Schouten S, Rijpstra WIC, Kok M, *et al.* (2001) Molecular organic tracers of biogeochemical processes in a saline meromictic lake (Ace Lake). *Geochimica et Cosmochimica Acta* **65**(10), 1629.

Schouten S, Hopmans EC, Schefuß E, Sinninghe Damsté JS (2002) Distributional variations in marine crenarchaeotal membrane lipids: a new organic proxy for reconstructing ancient sea water temperatures? *Earth and Planetary Science Letters* **204**, 265–274.

Schouten S, Baas M, Hopmans EC, Sinninghe Damsté JS (2008a) An unusual isoprenoid tetraether lipid in marine and lacustrine sediments. *Organic Geochemistry* **39**(8), 1033–1038.

Schouten S, Hopmans EC, Baas M, *et al.* (2008b) Intact membrane lipids of 'candidatus *Nitrosopumilus maritimus*,' a cultivated representative of the cosmopolitan mesophilic Group I Crenarchaeota. *Applied and Environmental Microbiology* **74**(8), 2433–2440.

Schouten S, Özdirekcan S, van der Meer MTJ, *et al.* (2008c) Evidence for substantial intramolecular heterogeneity in the stable carbon isotopic composition of phytol in photoautotrophic organisms. *Organic Geochemistry* **39**(1), 135–146.

Schwark L, Empt P (2006) Sterane biomarkers as indicators of palaeozoic algal evolution and extinction events. *Palaeogeography, Palaeoclimatology, Palaeoecology* **240**(1–2), 225–236.

Sephton MA, Looy CV, Veefkind RJ, Brinkhuis H, De Leeuw JW, Visscher H (2002) Synchronous record of $\delta^{13}C$ shifts in the oceans and atmosphere at the end of the Permian. *Geological Society of America Special Paper* **356**, 455–462.

Sephton MA, Looy CV, Brinkhuis H, Wignall PB, de Leeuw JW, Visscher H (2005) Catastrophic soil erosion during the end-Permian biotic crisis. *Geology* **33**(12), 941–944.

Sessions AL, Burgoyne TW, Schimmelmann A, Hayes JM (1999) Fractionation of hydrogen isotopes in lipid biosynthesis. *Organic Geochemistry* **30**(9), 1193–1200.

Sessions AL, Sylva SP, Summons RE, Hayes JM (2004) Isotopic exchange of carbon-bound hydrogen over geologic timescales. *Geochimica et Cosmochimica Acta* **68**(7), 1545–1559.

Sessions AL, Doughty DM, Welander PV, Summons RE, Newman DK (2009) The continuing puzzle of the Great Oxidation Event. *Current Biology* **19**(14), R567–R574.

Shah SR, Mollenhauer G, Ohkouchi N, Eglinton TI, Pearson A (2008) Origins of archaeal tetraether lipids in sediments: insights from radiocarbon analysis. *Geochimica et Cosmochimica Acta* **72**(18), 4577–4594.

Sherman L S, Walbauer JR, Summons RE (2007) Methods for biomarker analyses of high maturity Precambrian rocks. *Organic Geochemistry* **38**, 1987–2000.

Sherwood Lollar B, Lacrampe-Couloume G, Slater GF, *et al.* (2006) Unravelling abiogenic and biogenic sources of methane in the Earth's deep subsurface. *Chemical Geology* **226**(3–4), 328–339.

Sikes EL, Volkman JK (1993) Calibration of alkenone unsaturation ratios (Uk'37) for paleotemperature estimation in cold polar waters. *Geochimica et Cosmochimica Acta* **57**(8), 1883–1889.

Sikes EL, Volkman JK, Robertson LG, Pichon J-J (1997) Alkenones and alkenes in surface waters and sediments of the Southern Ocean: Implications for paleotemperature estimation in polar regions. *Geochimica et Cosmochimica Acta* **61**(7), 1495–1505.

Silva CJ, Wunsche L, Djerassi C (1991) Biosynthetic studies of marine lipid 35. The demonstration of de novo sterol biosynthesis in sponges using radiolabeled isoprenoid precursors. *Comparative Biochemistry and Physiology Part B: Biochemistry and Molecular Biology* **99**(4), 763.

Simonson BM, Sumner DY, Beukes NJ, Johnson S, Gutzmer J (2009) Correlating multiple Neoarchean-Paleoproterozoic impact spherule layers between South Africa and Western Australia. *Precambrian Research* **169**(1–4), 100–111.

Sinninghe Damsté JS, Muyser G, Abbas B, *et al.* (2004a) The rise of the rhizosolenid diatoms. *Science* **304**(5670), 584–587.

Sinninghe Damsté JS, Rijpstra WIC, Schouten S, Fuerst JA, Jetten MSM, Strous M (2004b) The occurrence of hopanoids in planctomycetes: implications for the sedimentary biomarker record. *Organic Geochemistry* **35**(5), 561–566.

Sinninghe Damsté JS, Rijpstra WIC, Geenevasen JAJ, Strous M, Jetten MSM (2005) Structural identification of ladderane and other membrane lipids of planctomycetes capable of anaerobic ammonium oxidation (anammox). *FEBS Journal* **272**(16), 4270–4283.

Sinninghe Damsté JS, Rijpstra W, Hopmans E, Schouten S, Balk M, Stams A (2007) Structural characterization of diabolic acid-based tetraester, tetraether and mixed ether/ester, membrane-spanning lipids of bacteria from the order Thermotogales. *Archives of Microbiology* **188**(6), 629.

Smittenberg RH, Pancost RD, Hopmans EC, Paetzel M, Sinninghe Damsté JS (2004) A 400-year record of environmental change in an euxinic fjord as revealed by the sedimentary biomarker record. *Palaeogeography, Palaeoclimatology, Palaeoecology* **202**(3–4), 331–351.

Sofer Z (1984) Stable carbon isotope compositions of crude oils: application to source depositional environments and petroleum alteration. *AAPG Bulletin* **68**, 31–49.

Sprott GD, Ekiel I, Dicaire C (1990) Novel, acid-labile, hydroxydiether lipid cores in methanogenic bacteria. *Journal of Biological Chemistry* **265**(23), 13735–13740.

Stadnitskaia A, Muyser G, Abbas B, *et al.* (2005) Biomarker and 16S rDNA evidence for anaerobic oxidation of methane and related carbonate precipitation in deep-sea mud volcanoes of the Sorokin Trough, Black Sea. *Marine Geology* **217**(1–2), 67–96.

Sternberg LO, Deniro MJ, Johnson HB (1984) Isotope ratios of cellulose from plants having different photosynthetic pathways. *Plant Physiology***74**(3), 557–561.

Sturt HF, Summons RE, Smith K, Elvert M, Hinrichs K-U (2004) Intact polar membrane lipids in prokaryotes and sediments deciphered by high-performance liquid chromatography/electrospray ionization multistage mass spectrometry – new biomarkers for biogeochemistry and microbial ecology. *Rapid Communications in Mass Spectrometry* **18**, 617–628.

Summons RE, Volkman JK, Boreham CJ (1987) Dinosterane and other steroidal hydrocarbons of dinoflagellate origin in sediments and petroleum. *Geochimica et Cosmochimica Acta* **51**(11), 3075.

Summons RE, Thomas J, Maxwell JR, Boreham CJ (1992) Secular and environmental constraints on the occurrence of dinosterane in sediments. *Geochimica et Cosmochimica Acta* **56**(6), 2437.

Summons RE, Jahnke LL, Hope JM, Logan GA (1999) 2-Methylhopanoids as biomarkers for cyanobacterial oxygenic photosynthesis. *Nature* **400**(6744), 554–557.

Summons RE, Bradley AS, Jahnke LL, Waldbauer JR (2006) Steroids, triterpenoids and molecular oxygen. *Philosophical Transactions of the Royal Society B–Biological Sciences* **361**(1470), 951–968.

Talbot HM, Squier AH, Keely BJ, Farrimond P (2003) Atmospheric pressure chemical ionisation reversed-phase liquid chromatography/ion trap mass spectrometry of intact bacteriohopanepolyols. *Rapid Communications in Mass Spectrometry* **17**(7), 728–737.

Talbot HM, Rohmer M, Farrimond P (2007) Rapid structural elucidation of composite bacterial hopanoids by atmospheric pressure chemical ionisation liquid chromatography/ion trap mass spectrometry. *Rapid Communications in Mass Spectrometry* **21**(6), 880–892.

Talbot HM, Summons RE, Jahnke LL, Cockell CS, Rohmer M, Farrimond P (2008) Cyanobacterial bacteriohopanepolyol signatures from cultures and natural environmental settings. *Organic Geochemistry* **39**(2), 232–263.

Teira E, van Aken H, Veth C, Herndl GJ (2006) Archaeal uptake of enantiomeric amino acids in the meso- and bathypelagic waters of the North Atlantic. *Limnology and Oceanography* **51**, 60–69.

Thiel V, Peckmann J, Seifert R, Wehrung P, Reitner J, Michaelis W (1999) Highly isotopically depleted isoprenoids: molecular markers for ancient methane venting. *Geochimica et Cosmochimica Acta* **63**(23/24), 2959–3966.

Tissot BP, Welte DH (1978) *Petroleum Formation and Occurrence: A New Approach to Oil and Gas Exploration*. Springer-Verlag, Berlin.

Tornabene TG, Langworthy TA, Holzer G, Oro J (1979) Squalenes, phytanes and other isoprenoids as major neutral lipids of methanogenic and thermoacidophilic 'Archaebacteria'. *Journal of Molecular Evolution* **13**(1), 73–83.

Treibs A (1936) Chlorophyll- und Häminderivate in organischen Mineralstoffen. *Angewandte Chemie* **49**(38), 682–686.

van Kaam-Peters HME, Köster J, van der Gaast SJ, Dekker M, de Leeuw JW, Sinninghe Damsté JS (1998) The effect of clay minerals on diasterane/sterane ratios. *Geochimica et Cosmochimica Acta* **62**(17), 2923.

Van Mooy BAS, Rocap G, Fredricks HF, Evans CT, Devol AH (2006) Sulfolipids dramatically decrease phosphorus demand by picocyanobacteria in oligotrophic marine

environments. *Proceedings of the National Academy of Sciences of the USA* **103**(23), 8607–8612.

Vilcheze C, Llopiz P, Neunlist S, Poralla K, Rohmer M (1994) Prokaryotic triterpenoids: new hopanoids from the nitrogen-fixing bacteria *Azotobacter vinelandii*, *Beijerinckia indica* and *Beijerinckia mobilis*. *Microbiology* **140**(10), 2749–2753.

Volkman JK (2005) Sterols and other triterpenoids: source specificity and evolution of biosynthetic pathways. *Organic Geochemistry* **36**(2), 139–159.

Volkman JK, Maxwell JR (1984) Acyclic isoprenoids as biological markers. In: *Biological Markers in the Sedimentary Record* (ed. Johns RB). Elsevier, Amsterdam, pp. 1–42.

Volkman JK, Eglinton G, Corner EDS, Sargent JR (1980) Novel unsaturated straight-chain C37–C39 methyl and ethyl ketones in marine sediments and a coccolithophore *Emiliania huxleyi*. *Physics and Chemistry of the Earth* **12**, 219–227.

Volkman JK, Barrerr SM, Blackburn SI, Sikes EL (1995) Alkenones in *Gephyrocapsa oceanica*: implications for studies of paleoclimate. *Geochimica et Cosmochimica Acta* **59**(3), 513–520.

Wagner F, Rottem S, Held H-D, Uhlig S, Zähringer U (2000) Ether lipids in the cell membrane of *Mycoplasma fermentans*. *European Journal of Biochemistry* **267**(20), 6276–6286.

Wakeham SG, Amann R, Freeman KH, *et al.* (2007) Microbial ecology of the stratified water column of the Black Sea as revealed by a comprehensive biomarker study. *Organic Geochemistry* **38**, 2070–2097.

Waldbauer JR, Sherman LS, Sumner DY, Summons RE (2009) Late Archean molecular fossils from the Transvaal Supergroup record the antiquity of microbial diversity and aerobiosis. *Precambrian Research* **169**, 28–47.

Wang C (2007) Anomalous hopane distributions at the Permian-Triassic boundary, Meishan, China – evidence for the end-Permian marine ecosystem collapse. *Organic Geochemistry* **38**(1), 52–66.

Wang C, Visscher H (2007) Abundance anomalies of aromatic biomarkers in the Permian-Triassic boundary section at Meishan, China – evidence of end-Permian terrestrial ecosystem collapse. *Palaeogeography, Palaeoclimatology, Palaeoecology* **252**(1–2), 291–303.

Welander PV, Hunter RC, Zhang L, Sessions AL, Summons RE, Newman DK (2009) Hopanoids play a role in membrane integrity and pH homeostasis in *Rhodopseudomonas palustris* TIE-1. *Journal of Bacteriology* **191**(19), 6145–6156.

Welander PV, Coleman M, Sessions AL, Summons RE, Newman DK (2010) Identification of a methylase required for 2-methylhopanoid production and implications for the interpretation of sedimentary hopanes. *Proceedings of the National Academy of Sciences of the USA* **107**, 8537–8542.

Wuchter CS, Schouten S, Boschker HTS, Sinninghe Damsté JS (2003) Bicarbonate uptake by marine Crenarchaeota. *FEMS Microbiology Letters* **219**, 203–207.

Xiao S, Zhang Y, Knoll AH (1998) Three-dimensional preservation of algae and animal embryos in a Neoproterozoic phosphorite. *Nature* **391**(6667), 553–558.

Xie S, Pancost RD, Yin H, Wang H, Evershed RP (2005) Two episodes of microbial change coupled with Permo/Triassic faunal mass extinction. *Nature* **434**, 494–497.

Yin L, Zhu M, Knoll AH, Yuan X, Zhang J, Hu J (2007) Doushantuo embryos preserved inside diapause egg cysts. *Nature* **446**(7136), 661–663.

Zachos JC, Arthur MA, Dean WE (1989) Geochemical evidence for suppression of pelagic marine productivity at the Cretaceous/Tertiary boundary. *Nature* **337**(6202), 61–64.

Zachos JC, Rohl U, Schellenberg SA, *et al.* (2005) Rapid acidification of the ocean during the Paleocene-Eocene thermal maximum. *Science* **308**(5728), 1611–1615.

Zhang X, Gillespie AL, Sessions AL (2009) Large D/H variations in bacterial lipids reflect central metabolic pathways. *Proceedings of the National Academy of Sciences of the USA* **106**(31), 12580–12586.

Zundel M, Rohmer M (1985a) Hopanoids of the methylotrophic bacteria *Methylococcus capsulatus* and *Methylomonas* sp. as possible precursors of C_{29} and C_{30} hopanoid chemical fossils. *FEMS Microbiology Letters* **28**, 61–64.

Zundel M, Rohmer M (1985b) Prokaryotic triterpenoids. *European Journal of Biochemistry* **150**(1), 23–27.

Zundel M, Rohmer M(1985c) Prokaryotic triterpenoids. 3. The biosynthesis of 2 beta-methylhopanoids and 3 beta-methylhopanoids of *Methylobacterium organophilum* and *Acetobacter pasteurianus* ssp. *pasteurianus*. *European Journal of Biochemistry* 150(1), 35–39.

Appendix 2

A culture-based calibration of benthic foraminiferal paleotemperature proxies: $\partial^{18}O$ and Mg/Ca results*

Abstract

Benthic foraminifera were cultured for five months at four temperatures (4, 7, 14 and 21 °C) to establish the temperature dependence of foraminiferal calcite $\delta^{18}O$ and Mg/Ca. Two Bulimina species (B. aculeata and B. marginata) were most successful in terms of calcification, adding chambers at all four temperatures and reproducing at 7 and 14 °C. Foraminiferal $\delta^{18}O$ values displayed ontogenetic variations, with lower values in younger individuals.The $\delta^{18}O$ values of adult specimens decreased with increasing temperature in all but the 4 °C treatment, exhibiting a relationship consistent with previous $\delta^{18}O$ paleotemperature calibration studies. Foraminiferal Mg/Ca values, determined by laser ablation inductively coupled plasma mass spectrometry, were broadly consistent with previous Mg/Ca calibration studies, but extremely high values in the 4°C treatment and higher than predicted values at two of the other three temperatures make it challenging to interpret these results.

---

* Published as: Filipsson, H.I., Bernhard, J.M., Lincoln, S.A., and McCorkle, D.C. 2010. A culture-based calibration of benthic foraminiferal paleotemperature proxies: $\partial^{18}O$ and Mg/Ca results. Biogeosciences 7, 1335-1347.

Biogeosciences, 7, 1335–1347, 2010
www.biogeosciences.net/7/1335/2010/
doi:10.5194/bg-7-1335-2010

Biogeosciences

A culture-based calibration of benthic foraminiferal paleotemperature proxies: $\delta^{18}O$ and Mg/Ca results

H. L. Filipsson[1], J. M. Bernhard[2], S. A. Lincoln[3], and D. C. McCorkle[2]

[1]GeoBiosphere Science Centre, Dept. of Geology, Quaternary Sciences, Lund University, Sölvegatan 12, 22362 Lund, Sweden
[2]Geology and Geophysics Department, Woods Hole Oceanographic Institution, Woods Hole, MA 02543, USA
[3]Dept. of Earth, Atmospheric and Planetary Sciences, Massachusetts Institute of Technology, Cambridge, MA 02139, USA

Received: 16 December 2009 – Published in Biogeosciences Discuss.: 18 January 2010
Revised: 15 April 2010 – Accepted: 20 April 2010 – Published: 29 April 2010

Abstract. Benthic foraminifera were cultured for five months at four temperatures (4, 7, 14 and 21 °C) to establish the temperature dependence of foraminiferal calcite $\delta^{18}O$ and Mg/Ca. Two *Bulimina* species (*B. aculeata* and *B. marginata*) were most successful in terms of calcification, adding chambers at all four temperatures and reproducing at 7 and 14 °C. Foraminiferal $\delta^{18}O$ values displayed ontogenetic variations, with lower values in younger individuals. The $\delta^{18}O$ values of adult specimens decreased with increasing temperature in all but the 4 °C treatment, exhibiting a relationship consistent with previous $\delta^{18}O$ paleotemperature calibration studies. Foraminiferal Mg/Ca values, determined by laser ablation inductively coupled plasma mass spectrometry, were broadly consistent with previous Mg/Ca calibration studies, but extremely high values in the 4 °C treatment and higher than predicted values at two of the other three temperatures make it challenging to interpret these results.

1 Introduction

Quantitative paleoceanographic reconstructions are an essential component of efforts to understand the oceans' role in climate, to document natural climate variability on a range of time scales, and to predict the impact of future climate change. The isotopic and elemental compositions of the calcium carbonate tests (shells) of fossil foraminifera are widely used to estimate ocean chemistry and temperature at the time of calcification (e.g., Shackleton et al., 1984; Rosenthal et al., 1997; Lear et al., 2000). Most foraminiferal paleochemical and paleotemperature reconstructions rely on modern-ocean empirical calibrations, which are based on core-top sediments, but the inherent environmental variability in the ocean, and the co-variation of many important environmental, ecological, and physiological factors in the ocean can complicate interpretation of these empirical calibrations. An alternative way to investigate the controls on foraminiferal geochemical proxies is to grow the foraminifers in the laboratory under known environmental conditions.

Culturing studies using planktonic foraminifera provide well-known examples of this approach (e.g., Erez and Luz, 1982; Bijma et al., 1990; Nürnberg et al., 1996; Lea and Spero, 1992; Spero et al., 1997; Bemis et al., 1998; Bijma et al., 1999). Culturing studies also have been used to investigate the stable oxygen and carbon isotopic composition (Chandler et al., 1996; Wilson-Finelli et al., 1998; McCorkle et al., 2008; Barras et al., 2010) and trace metal content (Russell et al., 1994; Toyofuku et al., 2000; Toyofuku and Kitazato, 2005; Havach et al., 2001; Segev and Erez, 2006; Hintz et al., 2006a, b) of benthic foraminifera. Here, we used a single seawater reservoir to culture benthic foraminifera at four different temperatures. Because microhabitat effects were minimized and the water chemistry kept constant across the range of temperatures, our culture experiment addresses key uncertainties in the existing, field-based calibrations of benthic foraminiferal $\delta^{18}O$ and Mg/Ca.

Correspondence to: H. L. Filipsson
(Helena.filipsson@geol.lu.se)

Published by Copernicus Publications on behalf of the European Geosciences Union.

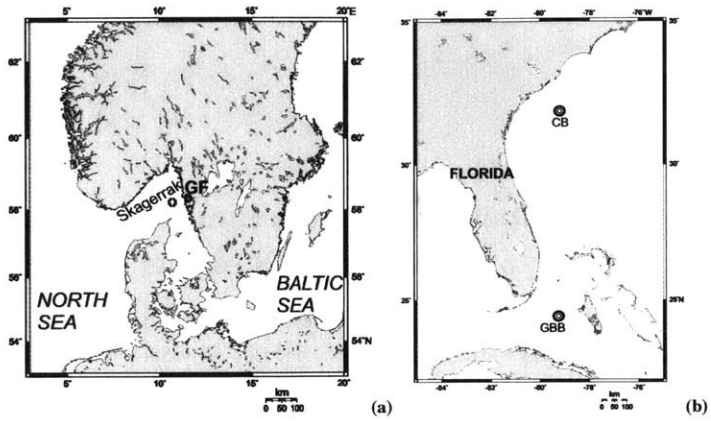

Fig. 1. Figure 1a Map showing sampling locations, indicated with crosses, in the NE Skagerrak and Gullmar Fjord (GF). Figure 1b. Sampling locations indicated with circles at Charleston Bump (CB) and Great Bahama Bank (GBB). Map from www.aquarius.ifm-geomar.de

Table 1. Sampling details from the sites in the North Atlantic.

Site	Date	Water depth (m)	Water T (°C)	Corer	Screen size (μm)
Gullmar Fjord	8/2006	118	6	Gemini	63
Charleston Bump	5/2006	~220	9	Soutar boxcorer	90, 125, 500
Skagerrak	8/2006	330	6.7	Gemini	63
Adjacent to Great Bahama Bank	5/2006	466–814	8–10	Soutar boxcorer	90, 125, 500

2 Methods

2.1 Collection and maintenance

Living foraminifera were obtained by coring the seafloor at various locations and transporting surface sediments (top ~2 cm) to the laboratory at Woods Hole Oceanographic Institution (WHOI), USA. Samples were collected from the northeastern Skagerrak (330 m), Gullmar Fjord, Sweden (118 m), the Charleston Bump off South Carolina, USA (~220 m), and at three sites near the Great Bahama Bank (466–814 m) (Fig. 1, Table 1). Bottom water was collected at each site using a CTD-Niskin rosette, maintained at near bottom-water temperatures, and used for sieving to remove fine material and concentrate the benthic foraminifera. Immediately after sieving, the samples were transferred to a plastic container and stored at 5–7 °C until the samples were transported in coolers to WHOI after the cruise.

In our shore-based 7 °C environmental room, the sample containers were plumbed into a recirculating seawater system, designed to maintain stock cultures of benthic foraminifera (Chandler and Green, 1996). The foraminifera were fed weekly with a mixture of *Dunaliella tertiolecta* and *Isochrysis galbana* (Hintz et al., 2004). Subsamples were taken from the stock cultures and sieved, using chilled artificial sea water, over a 63-μm screen. Specimens showing signs of activity, by containing algae or having colored cytoplasm, were picked from the >63-μm fraction and incubated at 7 °C in Petri dishes with artificial sea water and calcein (10 mg/l) solution for two to four weeks, following Bernhard et al. (2004). The samples were fed every week and the calcein solution was changed every 3–4 days.

Just before initiation of the experiment, specimens were examined using epifluorescence microscopy at 480-nm excitation and 520-nm emission, and fluorescent specimens, which had precipitated calcite during the calcein incubation, were picked using a fine brush or pipette. All examination, sorting, and picking were carried out on ice. Fluorescent specimens were transferred to cell tissue culture cups (8-ml volume; 8-μm nominal pore diameter) and placed in acrylic culture chambers (Hintz et al., 2004). Each culture cup contained a 2–3 mm thick layer of HPLC-grade silt-sized silica to provide a substrate for the foraminifera.

Most culture chambers were inoculated with a mix of species, with all inoculates in any given culture chamber from the same sampling site. The exceptions were three

"monoculture" chambers that contained a mix of *Bulimina aculeata* and*B. marginata* from Charleston Bump and adjacent to the Great Bahama Bank (see below). Skagerrak species included *Bolivina skagerrakensis, Bolivinellina pseudopunctata, Bulimina marginata, Cassidulina laevigata, Globobulimina turgida, Hyalinea balthica, Melonis barleeanum, Pullenia bulloides, Quinqueloculina seminulum, Stainforthia fusiformis,* and *Uvigerina* spp.; Gullmar Fjord species included *Bolivina skagerrakensis, Bolivinellina pseudopunctata, Bulimina marginata, C. laevigata, Elphidium excavatum, G. turgida, H. balthica, Nonionella turgida, Nonionellina labradorica, Pyrgo williamsoni, Q. seminulum,* and *S. fusiformis*; Charleston Bump species included *Bulimina aculeata, Bulimina marginata, Bulimina mexicana, Cibicidoides* spp. *Lenticulina* sp., *Melonis barleeanum,* and *Uvigerina* spp.; Bahamas species included *Bulimina aculeata, Bulimina marginata, Bulimina mexicana, C. laevigata, Cibicides lobatulus, Cibicidoides* spp., Globobulimina sp., Lenticulina sp., *Melonis barleeanum,* and *Uvigerina* spp. As noted, three culture chambers contained "monocultures" of the *Bulimina aculeata/B. marginata* complex. These two species were not separated, as juveniles of these two species were indistinguishable, and even the adult populations exhibited a spectrum of morphologies – some specimens appeared as typical *B. marginata* or *B. aculeata* while others exhibited traits of both species. Thus, we refer to our results on these species from the Charleston Bump and Great Bahama Bank to be from the *Bulimina aculeata/B. marginata* species complex.

The experiment was initiated on 19 December 2006, and was terminated between 15 and 23 May 2007. Five culture chambers were placed in each of three refrigerators (4, 7, 14 °C) and, in addition, two were placed at room temperature (~21 °C). Temperatures were monitored using Onset Tidbit T loggers. The culture chambers were individually plumbed, each with two outlets and two inlets at the top and at the bottom, to avoid geochemical gradients in the culture chambers, following Hintz et al. (2004). All culture chambers were connected to one single reservoir (200 L) of filtered surface seawater from the Gulf Stream, which was diluted with 8.4 L of MilliQ water to achieve a salinity of 35; this dilution also lowered the alkalinity from 2390 μeq/kg to 2258 μeq/kg. The water from the large reservoir was pumped to a header tank and both tanks were continuously bubbled with air from the building air intake. The air was first bubbled through a carboy of distilled water to increase its relative humidity. From the header tank, the water flowed to culture chambers by gravity; flow rates averaged 4 ml/min. The residence time of water in culture chambers was approximately 2 min.

Every 10 days, flow was stopped and a mixture of *D. tertiolecta* and *I. galbana* was introduced into each culture chamber to allow the foraminifera to feed. After an hour, the flow was reinstated after the algae settled to the silica surface. After experiment termination, the material from each culture chamber was rinsed over a 63-μm sieve and sorted into juveniles (63–200 μm), young adults (200–300 μm) and adults (> 300 μm). Non-fluorescent calcite, which formed during the experiment as new chambers or offspring, was identified using epifluorescence microscopy as noted above.

Sampling for salinity, alkalinity, dissolved inorganic carbon (DIC), and $\delta^{18}O_w$ from the reservoir tank occurred approximately every third week. Salinity samples were measured by the WHOI Hydrographic Analysis Facility using an Autosal salinometer. The alkalinity and DIC data were analyzed by closed-vessel titration of large-volume (~100 ml) samples using an automated titration system (Bradshaw et al., 1981; Brewer et al., 1986), and the alkalinity and DIC concentrations were determined using a nonlinear curve fitting approach (Department of Energy, 1994), and standardized using certified reference materials obtained from Dr. A. Dickson (Scripps Institution of Oceanography). The standard deviation of replicate analyses of culture water was 0.4 μeq/kg for alkalinity and 1.3 μmol/kg for DIC (n=6 pairs). The carbonate ion concentration [CO_3^{2-}] and the pH (total scale, "pH(t)") were calculated from the alkalinity and DIC data using the "CO2SYS" program (Lewis and Wallace, 1998), with the carbonate dissociation constants of Roy et al. (1993), the calcite solubility of Mucci (1983), and the assumption that the boron/salinity ratio of the culture system water was equal to the seawater value.

The $\delta^{18}O$ of water was analyzed in the laboratory of Dr. D. Schrag (Harvard Univ.) using a VG Optima mass spectrometer with a VG Isoprep 18 automated shaker/equilibrator (Schrag et al., 2002). The standard deviation of replicate $\delta^{18}O$ analyses was 0.04‰ ($n = 6$); $\delta^{18}O_w$ values are reported relative to Standard Mean Ocean Water (SMOW).

2.2 Stable oxygen isotopes of foraminiferal calcite

The stable oxygen isotopic composition of foraminiferal calcite was determined using a Kiel III Carbonate Device connected to a Finnigan MAT 253 mass spectrometer. The instrument was calibrated via NBS-19 and NBS-18 standards, with a long-term precision of replicate NBS-19 and in-house standards of <0.08‰ (Lynch-Stieglitz et al., 2009). Procedures and precision for this instrument can be found at: http://www.whoi.edu/paleo/mass-spec/. Depending on available calcite mass, samples consisted of pooled individuals ranging from 3 to 80 individuals or portions of individuals (see below). Foraminiferal stable isotopic data is expressed relative to VPDB. The paleotemperature equation

$$(T = 16.5 - 4.80 \cdot (\delta^{18}O_{c,VPDB} - (\delta^{18}O_{w,SMOW} - 0.27))$$

was used to calculate $\delta^{18}O$ equilibrium values ($\delta^{18}O_{eq}$), the $\delta^{18}O$ values of calcite ($\delta^{18}O_{c,VPDB}$) in equilibrium with water ($\delta^{18}O_{w,SMOW}$) at the given temperature (Bemis et al., 1998).

2.3 Microdissection using laser ablation

In cases where an inoculate specimen added chambers during the experiment, the pre-existing (fluorescent) calcite was removed from the non-fluorescent calcite formed during the experiment using laser ablation microdissection (Hintz et al., 2006b). A conservative approach was used when microdissecting. We preferred to lose some of the newly added calcite rather than risk inclusion of pre-existing calcite in the subsequent analyses.

2.4 Mg/Ca analysis

Benthic foraminifera from deep-sea sediments are typically cleaned before solution ICP-MS Mg/Ca analysis, and several protocols (e.g., Martin and Lea, 2002) have been designed to remove clay and adhering contaminants that may be high in Mg relative to foraminiferal calcite, as well as high-Mg phases of calcite known to occur in some planktonic foraminifera (e.g., Brown and Elderfield, 1996; Dekens et al., 2002). The specimens in this study were not cleaned because the cultured foraminifera were lightly calcified and fragile, and rigorous chemical cleaning would likely have precluded analysis at 4 °C and reduced the number of analyses possible at 7, 14 and 21 °C. This approach seemed justified because the culture substrate (HPLC-grade silica) was clean, minimizing the risk of contamination.

Specimens chosen for Mg/Ca analysis were affixed to trimmed, gridded micropaleontology slides with gum tragacanth, and individually photographed under both reflected light and epifluorescence microscopy before analysis. Several mm-sized crystals of the OKA carbonatite standard (Bice et al., 2005) were also affixed to each slide. Mg/Ca analyses were made using the Thermo Element HR-ICP-MS equipped with a New Wave UP213 laser ablation sampling device. Raster patterns were defined in the NewWave software, using each specimen's micrographs to guide selection of a suitable sampling region. Raster paths were typically spaced 30 μm from one another but on several specimens with few experimentally precipitated chambers the paths were condensed to 20 μm spacing. Scan speed was 5 μm/s, repetition rate 10 Hz, scan depth 0 μm, spot size 40 μm and laser power 50%. Ablated material was removed from the chamber by helium carrier gas (0.42–0.5 L/minute) which was combined with argon (0.8 L/min) to form the final sample gas. Mass spectrometer settings closely followed those outlined in Hathorne et al. (2003). Isotope masses monitored were ^{25}Mg, ^{43}Ca, ^{48}Ca, ^{86}Sr, and ^{88}Sr, with each analysis consisting of 70 to 90 cycles through these five masses.

Blanks (run without laser input) and the OKA carbonatite standard were analyzed after every 3–6 samples, and ^{25}Mg and ^{43}Ca curves were constructed for blanks and standards analyzed over the course of each day's analyses. These blank values were subtracted from both samples and standards, and the sample ^{25}Mg/^{43}Ca ratio was normalized to an OKA Mg/Ca of 4.55 mmol/mol, as determined by (Bice et al., 2005). In some cases, Mg and Ca intensities varied significantly over the course of an analysis. When Mg and Ca intensities peaked simultaneously this was interpreted as the result of rapid introduction of calcite to the mass spectrometer, perhaps when a larger-than-typical amount of calcite was ablated. Other, less regular fluctuations in signal intensity, including the anticorrelation of Mg and Ca, may reflect instrument tuning problems, though we cannot rule out the possibility of extremely heterogeneous material. Only those analyses in which the individual peak intensities remained stable over a minimum of 25 contiguous cycles were considered acceptable; analyses not meeting this criterion were rejected. Mg/Ca error for each data point was determined using a standard error propagation formula (Weiss, 2004). Analyses of the OKA carbonatite standard provide one estimate of the reproducibility of LA-ICP-MS Mg/Ca measurements: the relative standard deviation for 12 OKA measurements made over two months was 1.7%. However, no direct test of the reproducibility of LA-ICP-MS Mg/Ca measurements of foraminiferal calcite was possible because specimens are likely to exhibit intratest and intertest heterogeneity (Pena et al., 2008).

3 Results

3.1 Water chemistry

The cytoplasm of all specimens born in culture was green at the end of the experiment, indicating active feeding at that time. We assume that most calcification by these specimens, and by the adults as well, occurred in the final months of the experiment, and focus on water chemistry between February and May 2007. The salinity increased from 35.0 to ~35.8 during the entire experiment (Fig. 2a), and $\delta^{18}O_w$ increased from 0.7‰ to 0.95‰ (Fig. 2b). The average $\delta^{18}O_w$ value between February and May was 0.9‰ (range 0.1‰) and the average temperatures for the same period were 3.8 °C (range ~1 °C), 7.0 °C (range 0.5–1 °C), 14.1 °C (range 0.5–1 °C), 21.0 °C (range 1–2 °C) (Fig. 2c), abbreviated to 4, 17, 14, and 21 °C. The coldest and warmest treatments showed the most temperature variation. Temperature did not systematically increase or decrease over the experiment, although long-term trends were noted in the 21 °C treatment, which was not thermostatted.

Alkalinity increased by 0.7% during the course of the experiment, from 2258 μeq kg^{-1} to 2273 μeq kg^{-1} (Fig. 3a, Table 2). This increase is smaller than would be predicted from the observed salinity increase, suggesting a modest consumption of alkalinity, either due to the release of metabolites, or to leaching of trace acidity from the system components (tubing, culture chambers, etc.) during the experiment. Dissolved inorganic carbon (DIC) showed a similar increase through most of the experiment, but decreased in

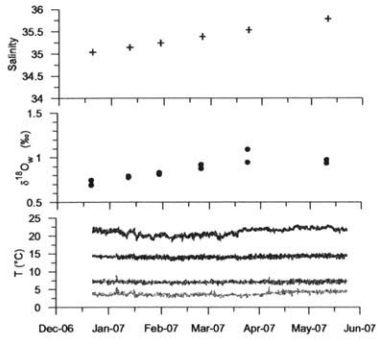

Fig. 2. Salinity, $\delta^{18}O_w$, and temperature measured during the experiment. Two water samples from the reservoir tank were taken for salinity and δ^{18}Ow at each sampling occasion, temperature was measured continuously with data loggers.

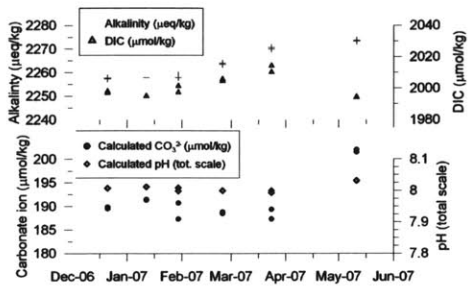

Fig. 3. Water chemistry data during the course of the experiment. Alkalinity and DIC were analyzed from water samples from the reservoir tank, and used to calculate $[CO_3^{2-}]$ and pH(t).

Table 2. Water chemistry measured during the course of the experiment together with calculated values of pH(total scale), CO_3^{2-} and Ω. The average measured salinity, alkalinity, and DIC of the 200L reservoir (35.35 (SD 0.26); 2264.0 µeq/kg (SD 6.6), and 2001.0 µmol/kg (SD 6.8)) were used for calculations at all four temperatures, the standard deviations are presented within parenthesis, shorten to SD.

Temperature (°C)	Calc. pH (total scale)	Calc. $[CO_3^{2-}]$ (µmol/kg)	Ω
3.8	8.304	182.5	4.30
7.0	8.248	182.7	4.35
14.1	8.129	187.5	4.46
21.0	8.018	191.5	4.57

April and May 2007 (Fig. 3a). Because alkalinity and DIC covaried, the carbonate ion concentration $[CO_3^{2-}]$ remained relatively constant at values between 188 and 191 µmol/kg, increasing to 202 µmol/kg in the final sample (Fig. 3b). The pH(t) showed a similar trend, ranging between 8.00 and 8.03 (Fig. 3b).

3.2 Calcification at different temperatures

Bulimina aculeata and *B. marginata* were the most successful taxa in the experiment, in terms of calcification, so we focus on these two species. In addition, *Cassidulina laevigata* also reproduced at 7 °C. The reproductive yield of *C. laevigata* was sparse, and the mass produced was insufficient for proxy analyses. Specimens of *Hyalinea balthica* and *Melonis barleeanum*, originally from the Skagerrak, also added a few new chambers at all temperatures except at 21 °C. The specimens originating from the Gullmar Fjord grew little and did not reproduce at any of the temperatures; we omit further discussion of the fjord material. A few specimens of *Rosalina* sp. occurred in all culture chambers except those at room temperature, despite not being observed in the initial inoculate.

At the lowest temperature (4 °C), several specimens of *B. aculeata/B. marginata* added one to three chambers to their tests, but little growth occurred in the remaining 4 °C specimens, and no reproduction took place at 4 °C (Table 3). At 7 °C, *B. marginata* from the Skagerrak reproduced abundantly, yielding approximately 90 new specimens, which had reached the 63 to 200 µm size fraction (the smallest fraction collected) by the end of the experiment (Table 3). Considerable growth of *B. aculeata/B. marginata* occurred in the three remaining 7 °C culture chambers, enabling microdissection of new (experimental) calcite from many specimens (Table 3). Reproduction also occurred at 14 °C, producing hundreds of offspring that had reached the 63–200 µm size fraction by the end of the experiment (Table 3). Some specimens of the *B. aculeata/B. marginata* complex also reproduced at 14 °C, and a large proportion of those offspring grew to the >300 µm size fraction (Table 3). It is likely that more than one reproduction event occurred at this temperature because there were specimens ranging from juveniles to adult that were all born in culture (Table 3). Dozens of inoculate specimens displayed substantial new growth, adding at least three chambers and increasing in test volume by up to a factor of 5. In the two culture chambers at room temperature (21 °C), reproduction did not occur; those specimens that grew added just one or two new chambers (Table 3).

Table 3. Number of inoculated specimens from the different source regions together with the results from the culturing experiment, organized according to temperature and size classes. "Monoculture" refers to monocultures of *Bulimina aculeata/marginata*, originating from the Charleston Bump and near the Great Bahama Bank. Juveniles, young adults, and adults were born in culture; "new growth" is material precipitated during the experiment.

Culture chamber	Geographical source area	T (°C) (experimental)	No. of inoculated *B. aculeata/ B. marginata*	Juveniles (63–200 μm)	Young adults (200–300 μm)	Adults (>300 μm)	New growth (no. micro-dissected specimens)
13	Skagerrak	3.8	19	–	–	–	6
14	Gullmar Fjord	3.8	12	–	–	–	–
15	C. Bump	3.8	50	–	–	–	2
16	Monoculture	3.8	~60	–	–	–	6
17	Bahamas	3.8	64	–	–	–	–
7	Skagerrak	7.0	20	70	17	5	6
8	Gullmar Fjord	7.0	12	–	–	–	–
9	C. Bump	7.0	50	–	–	–	19
10	Monoculture	7.0	~60	–	–	–	24
11	Bahamas	7.0	62	–	–	–	48
1	Skagerrak	14.1	20	~100	38	9	–
2	Gullmar Fjord	14.1	10	–	–	–	–
3	C. Bump	14.1	50	8	16	24	23
4	Monoculture	14.1	~60	2	11	42	11
5	Bahamas	14.1	62	–	–	–	47
19	Skagerrak	21.0	0	–	–	–	–
20	Monoculture	21.0	30	–	–	–	9

3.3 Stable oxygen isotopes

The amount and type of test material available for *B. aculeata/B. marginata* stable isotope analyses (microdissected new growth vs. offspring born in culture) varied between the different temperatures (Table 4). In general, larger specimens (>300 μm) at 7 °C were closer to $\delta^{18}O_{eq}$ than smaller specimens (Fig. 4a). At 14 °C the oxygen isotope data from all size classes were similar, and slightly higher than the predicted $\delta^{18}O_{eq}$, except for the 14 °C juveniles which had lower $\delta^{18}O$ values (Fig. 4b). For comparison with the cultured specimens, stable isotopic analyses were also performed on pre-existing calcite from samples originating from the Skagerrak, Charleston Bump, and Great Bahamas Bank (Table 4); the $\delta^{18}O$ values from the pre-existing calcite varied depending on source region where the largest scatter came from the monocultures of *B. aculeata/marginata* complex.

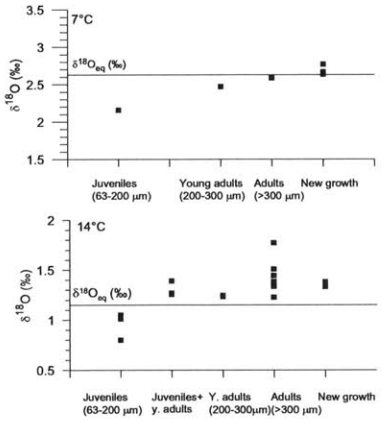

Fig. 4. The uppermost panel **(a)** shows $\delta^{18}O$ values at 7 °C and the lower panel **(b)** for 14 °C for the different size classes, together with the equilibrium calcite line for each temperature.

3.4 Mg/Ca ratios

Mg/Ca analyses were performed on microdissected, new growth from all four temperatures, and on young adults and adult specimens born in culture from the 14 °C treatment. The foraminiferal Mg/Ca values ranged from 3.4 to 22.7 mmol/mol (Table 5, Fig. 5). No significant difference in Mg/Ca was observed between specimens from different culture chambers maintained at a single temperature (e.g., culture chambers 3 and 10 at 7 °C; culture chambers 15 and 16 at 4 °C), and the Mg/Ca of specimens born in culture at 14 °C did not differ significantly from that of chambers added during the course of the experiment at this temperature (Fig. 5).

4 Discussion

4.1 Growth and reproduction with respect to temperature

Bulimina aculeata and *B. marginata* occur widely, ranging latitudinally as well as by water depth, occurring from deltas to the deep sea (Murray, 2006). In the South Atlantic

Table 4. Stable oxygen isotopic data for the cultured foraminifera presented for each temperature and size class, together with isotope data for pre-existing calcite. The standard deviations refer the analytical precision of the mass spectrometer. "Monoculture" refers to monocultures of *Bulimina aculeata/marginata*, originating from the Charleston Bump and near the Great Bahama Bank. N refers to number of specimens or microdissected parts of specimens analyzed. * = small samples with lower analytical precision.

Culture chamber	Source area	T (°C)	Material	$\delta^{18}O$ mean (‰)	$\delta^{18}O$ SD (‰)	N
13+15+16	Skagerrak+C. Bump+Monoculture	3.8	New Growth	1.27	0.06	13
7	Skagerrak	7.0	Juveniles	2.16	0.03	74
7	Skagerrak	7.0	Young adults	2.47	0.04	15
7	Skagerrak	7.0	Adults	2.59	0.03	5
9	C. Bump	7.0	New growth	2.67	0.04	6
10	Monoculture	7.0	New growth	2.63	0.02	10
11	Bahamas	7.0	New Growth	2.77	0.03	10
1	Skagerrak	14.1	Juveniles	0.80	0.04	80
1	Skagerrak	14.1	Juveniles	1.01	0.04	42
1	Skagerrak	14.1	Young adults	1.25	0.02	20
1	Skagerrak	14.1	Young adults	1.23	0.01	24
1	Skagerrak	14.1	Adults	1.23	0.04	5
1	Skagerrak	14.1	Adults	1.77	0.05	4
3	C. Bump	14.1	Juv.+ young adults	1.27	0.03	13
3	C. Bump	14.1	Juv.+ young adults	1.26	0.03	14
3	C. Bump	14.1	Adults	1.34	0.03	5
3	C. Bump	14.1	Adults	1.44	0.04	5
4	Monoculture	14.1	Juv.+ young adults	1.39	0.04	13
4	Monoculture	14.1	Adults	1.35	0.02	8
4	Monoculture	14.1	Adults	1.38	0.02	8
4	Monoculture	14.1	Adults	1.51	0.04	8
5	Bahamas	14.1	New growth	1.33	0.02	6
5	Bahamas	14.1	New growth	1.38	0.05	6
20	Monoculture	21.0	New growth	−0.20*	0.17	
3	C. Bump	NA	Pre-existing	−0.79	0.04	8
4	Monoculture	NA	Pre-existing	0.14	0.05	8
5	Bahamas	NA	Pre-existing	−0.64	0.02	20
9	C. Bump	NA	Pre-existing	−0.11	0.05	10
10	Monoculture	NA	Pre-existing	0.13	0.04	13
11	Bahamas	NA	Pre-existing	0.16	0.02	16
13	Skagerrak	NA	Pre-existing	2.69	0.05	5
15	C. Bump	NA	Pre-existing	−1.55*	0.05	3
20	Monoculture	NA	Pre-existing	−0.76	0.09	9

Ocean, *B. aculeata* is present at sites with temperatures as low as 0.5 °C (Mackensen et al., 1993) demonstrating that this species can grow and reproduce below 4 °C. Here, however, the cultured specimens grew at 4 °C, but they did not reproduce. The cultured specimens may not have been adapted to this lowest temperature; the temperatures at the coring sites ranged from ~7 °C (Skagerrak) to ~8–10 °C on the Charleston Bump and the Great Bahama Bank (Bernhard et al., 2006, SMHI database SHARK). At the lowest culture temperature, growth is likely to be slow, so a longer experiment may have been required to produce similar mass as at higher experimental temperatures. The specimens from the Charleston Bump and the Bahamas grew at 7 °C, but only the *Bulimina marginata* specimens from the Skagerrak reproduced at this temperature. This temperature is similar to the average temperature at the sampling site in NE Skagerrak, and is slightly warmer than the reported lower temperature limit for *B. marginata* (Husum and Hald, 2004). The highest yield reproduction events took place at 14 °C, and were observed in specimens from all collection sites. This temperature is considerably higher than the temperature at any of the sampling sites. However, we note that both species (*B. aculeata* and *B. marginata*) have been reported from areas with relatively high temperatures; *B. marginata* for instance from the South Brazilian Shelf (13–20 °C) (Eichler et al., 2008) and the Red Sea (Edelman-Furstenberg et al.,

Table 5. Mg/Ca data for the calcite precipitated during the experiment presented for each temperature and analyzed material (new growth; young adults and adults) together with specimen length and length to LA raster.

Culture chamber	T (°C)	Material	Total length of specimen (μm)	Length to analyzed calcite (μm)	Mg/Ca (mmol/mol) uncertainty (%)	Mg/Ca
15	3.8	New growth	238	145	10.91	21
15	3.8	New growth	374	274	18.43	7
16	3.8	New growth	188	152	22.70	23
10	7.0	New growth	553	249	5.92	5
10	7.0	New growth	478	297	4.83	7
10	7.0	New growth	432	307	4.22	7
9	7.0	New growth	630	400	4.50	7
9	7.0	New growth	425	354	3.92	7
10	7.0	New growth	483	314	2.97	7
10	7.0	New growth	414	284	3.97	7
9	7.0	New growth	395	321	6.35	9
9	7.0	New growth	527	390	6.13	7
9	7.0	New growth	505	341	6.04	7
9	7.0	New growth	505	343	6.15	7
9	7.0	New growth	434	345	9.78	7
9	7.0	New growth	472	343	6.19	9
9	7.0	New growth	528	379	3.35	5
3	14.1	Young adult	240	134	5.18	8
3	14.1	Young adult	265	111	6.22	8
3	14.1	Adult	331	220	6.97	8
3	14.1	Adult	398	275	7.46	8
3	14.1	Adult	352	289	6.69	8
3	14.1	New growth	551	363	4.55	8
3	14.1	New growth	529	405	10.17	8
3	14.1	New growth	450	302	10.07	8
3	14.1	New growth	465	324	3.92	8
3	14.1	New growth	465	305	6.15	8
20	21.0	New growth	401	304	9.48	5
20	21.0	New growth	376	255	8.25	6
20	21.0	New growth	410	330	7.89	6

2001), and *B. aculeata* from the Ebro Delta (14–19 °C) (Murray, 2006; Cartes et al., 2007).

We do not know whether successful reproduction in culture implies that the slightly warmer temperature was more favorable for the foraminifera, or whether reproduction was a stress response to the elevated temperature. The absence of reproduction at higher (21 °C) and lower (4 °C) temperatures suggests that temperature stress does not consistently promote reproduction. These results – elevated reproduction at intermediate temperatures – are consistent with the observations of Barras et al. (2009).

4.2 Ontogenetic trends in isotopic values

A substantial fraction of the observed oxygen isotopic variability is related to test size, suggesting age-related (ontogenetic) effects on test chemistry (Fig. 4). Several studies have suggested that younger (smaller) individuals precipitate $CaCO_3$ with lower $\delta^{18}O$ values than older (larger) specimens (e.g., Dunbar and Wefer, 1984; Schmiedl et al., 2004; McCorkle et al., 2008), though this pattern does not always exist (e.g., Wefer and Berger, 1991; Corliss et al., 2002). A size-linked (ontogenetic) trend is seen in the 7 °C $\delta^{18}O$ data, with the most pronounced depletions in the smallest specimens (Fig. 4a). This pattern is less clear in the 14 °C data, where all groups >200 μm show similar $\delta^{18}O$ values (Fig, 4b). Ontogenetic isotopic depletions were most pronounced in the smallest size fractions analyzed by McCorkle et al. (2008), who suggested that adult specimens approach an asymptotic isotopic composition. Indeed, our data suggest a tendency for older (larger) specimens to approach isotopic equilibrium.

4.3 Oxygen isotopic composition as a function of temperature

Variability in foraminiferal $\delta^{18}O_c$, including the impact of ontogenetic effects, can be assessed by considering the offsets ($\Delta\delta^{18}O$ values) between the observed foraminiferal

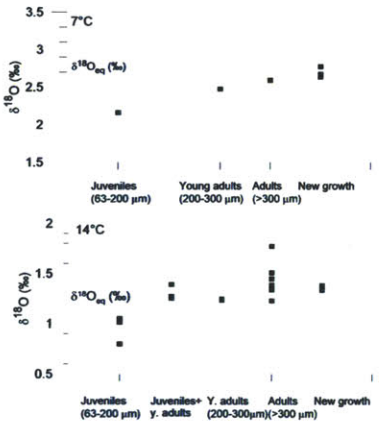

Fig. 5. Mg/Ca (mmol/mol) over the experimental temperature gradient, presented by sample type (new growth and size classes). For 7 and 14 °C, data is presented in two columns to allow visualization of result from different samples types, see legend for details.

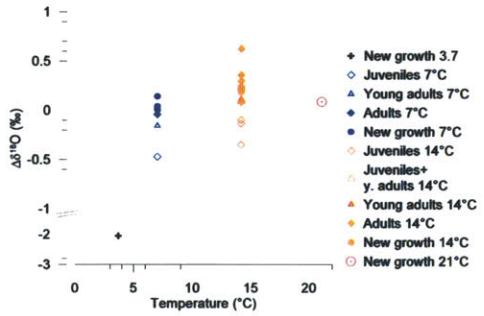

Fig. 6. The difference between $\delta^{18}O_c$ and the $\delta^{18}O_{(eq)}$ vs experimental temperature. $\delta^{18}O_{(eq))}$ is indicated with a dotted line and calculated using the Bemis et al. (1998) paleotemperature equation, together with a $\delta^{18}O_w$ of 0.92 (average between FeB. and May). All calcite was precipitated during the experiment; the symbols refer to the different material, see legend for details.

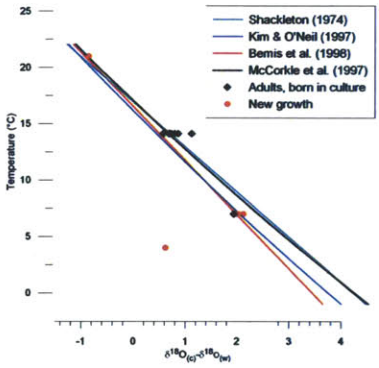

Fig. 7. Temperature vs. $\delta^{18}O_c - \delta^{18}O_w$, together with the paleotemperature equations from Shackleton (1974), Kim and O'Neil (1997), McCorkle et al. (1997), and Bemis et al. (1998). The symbols represent calcite precipitated during the experiment.

$\delta^{18}O_c$ and the predicted foraminiferal $\delta^{18}O_{eq}$ for each experimental temperature (Fig. 6). These $\Delta\delta^{18}O$ values were calculated using the paleotemperature equation from Bemis et al. (1998). Where there are sufficient data (7 °C and 14 °C), similar $\delta^{18}O_c$ values (Table 4) and $\Delta\delta^{18}O$ values (Figure 6) are seen in both new growth and born-in-culture specimens. The range in $\Delta\delta^{18}O$ for new growth and adult specimens at the three warmest temperatures (roughly 0.6) was only slightly larger than the range of $\Delta\delta^{18}O$ values previously observed in single-temperature culturing experiments, which ranged between 0.2 and 0.5‰ (McCorkle et al., 2008). The observed $\Delta\delta^{18}O$ range is also similar to that reported for field samples of *B. aculeata,* (McCorkle et al., 1997; Mackensen et al., 2000).

The foraminiferal $\delta^{18}O_c$ values decreased with increasing temperature from 7 °C to 21 °C (Fig. 7). However, the single, unreplicated value at 4 °C (0.62‰) is roughly 2‰ lower than we would expect from the paleotemperature equation estimates discussed below, and instead is similar to the $\delta^{18}O_c - \delta^{18}O_w$ values of the 14 °C specimens (Fig. 7). This 4 °C isotopic analysis used microdissected, new growth calcite from multiple specimens, raising the possibility that the sample inadvertently included some pre-existing calcite, precipitated at a higher temperature in the field. We do not think that this occurred, but while we have no reason simply to reject the data point at 4 °C, we will not use it in the following assessment of the temperature dependence of *Bulimina* $\delta^{18}O$.

The $\delta^{18}O_c - \delta^{18}O_w$ values provide a culture-based assessment of published oxygen isotope paleotemperature equations (Fig. 7) (Shackleton, 1974; Kim and O'Neil, 1997; McCorkle et al., 1997; Bemis et al., 1998). Although the 14 °C culture data are most consistent with the "warmer" paleotemperature equations (Shackleton, 1974; McCorkle et al., 1997), the best overall agreement, over the 21 °C to 7 °C temperature range, is with the paleotemperature equation of Bemis et al. (1998) (Fig. 7).

A previous culture study reported small depletions from predicted equilibrium calcite $\delta^{18}O$ values (McCorkle et al., 2008) and proposed that these isotopic offsets could reflect the elevated carbonate ion concentration of the culture system, relative to typical bottom-water values, following the

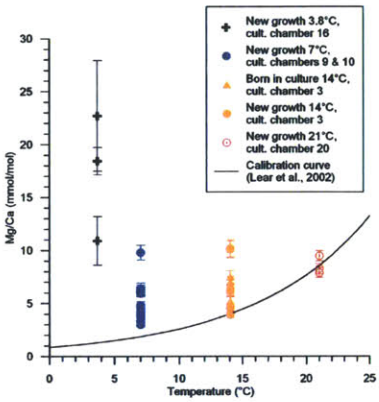

Fig. 8. Mg/Ca vs Temperature including *Cibicidoides* core top calibration of Lear et al. (2002), Mg/Ca= $0.867 \pm 0.49 \exp(0.109+0.007 \cdot BWT)$, where BWT is bottom water temperature).

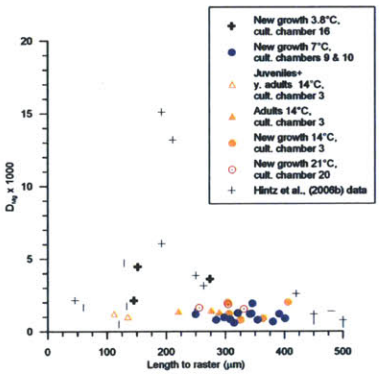

Fig. 9. Mg distribution coefficients plotted versus length from the proloculus to LA raster, presented together with the data from Hintz et al. (2006a) study of ontogenetic effects on Mg/Ca of *B. aculeata*. D_{Mg} for the cultured foraminifera from the present study was calculated assuming a sea water Mg/Ca ratio of 5.109.

results of Spero and co-workers (Lea and Spero, 1992; Spero et al., 1997; Bijma et al., 1999). However, the Bemis et al. (1998) paleotemperature expression, which provides the best match to the multiple temperature results of this study, would have been in better agreement with the $\delta^{18}O$ data of McCorkle et al. (2008), obviating the need to invoke a carbonate ion effect. The higher-than-predicted $\delta^{18}O$ values in the 14 °C cultures cannot be explained by elevated carbonate ion concentrations, which are expected to cause depleted isotopic values (and which were, in any case, present at all four temperatures). At present, we have no proposed mechanism for the 14 °C offset.

4.4 Mg/Ca ratios with respect to temperature

The foraminiferal Mg/Ca values from the 21 °C treatment vary by roughly ± 10% about a mean of 8.5 mmol/mol, but the Mg/Ca values from the other three temperatures show much more scatter, varying by factors of 2 to 3. In addition to this variability, the absolute values of the foraminiferal Mg/Ca ratios in the 4, 7, and 14 °C treatments are much higher than the values predicted by studies of core-top field specimens. To illustrate this offset, we plot our culture data with the benthic foraminiferal (*Cibicidoides*) Mg/Ca temperature calibration curve of Lear et al. (2002) (Fig. 8). The Mg/Ca values from the 21 °C cultures span the Lear et al. calibration curve, but the remainder of our Mg/Ca data are substantially higher than predicted by the Lear et al. (2002) relationship, and other published calibrations (Martin et al., 2002; Healey et al., 2008). Anand and Elderfield (2005) and Sadekov et al. (2005, 2008) observed high intra-test variability in the Mg/Ca of planktonic foraminifera, and inferred that factors other than calcification temperature can influence test Mg/Ca. However, while deep-water Mg/Ca paleothermometry continues to be a topic of active study and debate, none of the field-based data sets report low-temperature values approaching those we observed (Lear et al., 2002; Martin et al., 2002; Marchitto et al., 2007; Healey et al., 2008).

We do not believe that the high Mg/Ca values reflect species-dependent variation in Mg incorporation. We know of two sets of Mg/Ca analyses of field collected *Bulimina*, including ~4.5 °C deep-sea data from Lear et al. (2002), and shallow water data (~7 °C) from the Skagerrak and Gullmar Fjord (Groeneveld and Filipsson, personal communication). These *Bulimina* field data agree well with the Lear et al. (2002) *Cibicidoides* calibration curve, and include no values higher than ~2.5 mmol/mol.

Dissard et al. (2010) reported no difference between the Mg/Ca values of the shallow-water benthic foraminifera *Ammonia tepida* cultured at 10 °C and at 20 °C. However, strongly elevated *Bulimina* Mg/Ca values were observed in a previous culturing study (Hintz et al., 2006b). Single-individual whole-specimen Mg/Ca values, cultured at 7 °C and measured by solution ICP-MS, reached values equal to the highest LA-ICP-MS values observed in this study, and included several specimens with Mg/Ca values above 5 mmol/mol. In Hintz et al. (2006b), elemental analyses of laser microdissected chambers revealed that chambers located between ~150–225 µm from the test apex – similar in size to our study's 4 °C foraminifera – had the highest Mg contents (Fig. 9). Ontogenetic effects, and their underlying variations in calcification mechanisms, may explain the elevated Mg/Ca values in our study. However until these trends have been observed again over a temperature range,

and cleaning and analytical artifacts including the possible effect of the Mg content in the algal chlorophyll have been further tested and ruled out, we are unwilling to take these first multiple temperature culture-based Mg/Ca data at face value.

5 Conclusions

We cultured benthic foraminifera at 4, 7, 14, and 21 °C, and observed reproduction and copious calcification of *Bulimina aculeata/marginata* at temperatures close to or slightly higher than in situ temperatures (7 and 14 °C treatments), with no reproduction and less calcification at either substantially lower (4 °C) or higher (21 °C) temperatures. The absence of reproduction at higher and lower temperatures suggests that temperature stress does not consistently promote reproduction; instead there appears to be a temperature window where environmental conditions are most beneficial for these species' reproduction and growth.

Observed ontogenetic variations in foraminiferal stable oxygen isotope values are consistent with patterns observed in culturing studies by McCorkle et al. (2008) and Barras et al. (2010). Further, the observed $\delta^{18}O$ data are more consistent with the paleotemperature equation proposed by Bemis et al. (1998) than with those proposed by e.g., Shackleton (1974), and McCorkle et al. (1997). In contrast, the high observed foraminiferal Mg/Ca values in this study are not consistent with published benthic foraminiferal Mg/Ca: temperature relationships. This discrepancy may reflect ontogenetic variations in foraminiferal elemental compositions, but at present we cannot rule out sample cleaning or analytical explanations for these high values.

Acknowledgements. We thank the captains, crews, and scientific parties of the RV *Arne Tiselius* and RV *Oceanus* during our collection cruises, D. R. Ostermann, M. Jeglsinki, and M. Parmenter for technical assistance, and D. Schrag for performing water $\delta^{18}O$ analyses. We also thank the two reviewers, Lennart de Nooijer and Gerhard Schmiedl for helpful and constructive comments. Funding was provided by US NSF OCE-0647899 to DCM and JMB, and by the Swedish Research Council (grant no 621-2005-4265), the Lamm Foundation, and the Engkvist Foundation to HLF. A Fulbright fellowship to HLF together with traveling grants from Göteborg University, the Crafoord Foundation, and the Royal Physiographic Society in Lund enabled HLF's Postdoc stay and subsequent visits to WHOI.

Edited by: J. Bijma

References

Anand, P. and Elderfield, H.: Variability of Mg/Ca and Sr/Ca between and within the planktonic foraminifers *Globigerina bulloides* and *Globorotalia truncatulinoides*, Geochem. Geophy. Geosy., 6, Q11D15, doi:10.1029/2004GC000811, 2005.

Barras, C., Geslin, E., Duplessy, J. C., and Jorissen, F. J.: Reproduction and growth of the deep-sea benthic foraminifera *Bulimina marginata* under different laboratory conditions, J. Foraminifer. Res., 39, 155–165, 2009.

Barras, C., Duplessy, J.-C., Geslin, E., Michel, E., and Jorissen, F. J.: Calibration of $\delta^{18}O$ of cultured benthic foraminiferal calcite as a function of temperature, Biogeosciences, 7, 1349–1356, 2010, http://www.biogeosciences.net/7/1349/2010/.

Bemis, B. E., Spero, H. J., Bijma, J., and Lea, D. W.: Reevaluation of the oxygen isotopic composition of planktonic foraminifera: Experimental results and revised paleotemperature equations, Paleoceanography, 13, 150–160, 1998.

Bernhard, J. M., Blanks, J. K., Hintz, C. J., and Chandler, G. T.: Use of the fluorescent calcite marker calcein to label foraminiferal tests, J. Foraminifer. Res., 34, 96–101, 2004.

Bernhard, J. M., Ostermann, D. R., Williams, D. S., and Blanks, J. K.: Comparison of two methods to identify live benthic foraminifera: A test between rose bengal and celltracker green with implications for stable isotope paleoreconstructions, Paleoceanography, 21, doi:10.1029/2006PA001290, 2006.

Bice, K. L., Layne, G. D., and Dahl, K.: Application of secondary ion mass spectrometry to the determination of Mg/Ca in rare, delicate, or altered planktonic foraminifera: Examples from the Holocene, Paleogene, and Cretaceous, Geochem. Geophy. Geosy., 6, Q12p07, doi:10.1029/2005gc000974, 2005.

Bijma, J., Faber, W. W., and Hemleben, C.: Temperature and salinity limits for growth and survival of some planktonic foraminifers in laboratory cultures., J. Foraminifer. Res., 20, 95–116, 1990.

Bijma, J., Spero, H. J., and Lea, D.: Reassessing foraminiferal stable isotope geochemistry: Impact of the oceanic carbonate system (experimental results), in: Use of proxies in paleoceanography: Examples from the South Atlantic, edited by: Fischer, G., and Wefer, G., Springer Verlag, Berlin Heidelberg, 489–512, 1999.

Bradshaw, A. L., Brewer, P. G., Shafer, D. K., and Williams, R. T.: Measurements of total carbon-dioxide and alkalinity by potentiometric titration in the geosecs program, Earth Planet. Sc. Lett., 55, 99–115, 1981.

Brewer, P. G., Bradshaw, A. L., and Williams, R. T.: Measurements of total carbon dioxide and alkalinty in the North Atlantic ocean in 1981, in: The global carbon cycle: Analysis of the natural cycle and implications of anthropogenic alterations for the next centruy edited by: Reichle, D., Springer-Verlag, Berlin, 358–381, 1986.

Brown, S. J. and Elderfield, H.: Variations in Mg/Ca and Sr/Ca ratios of planktonic foraminifera caused by postdepositional dissolution: Evidence of shallow Mg-dependent dissolution, Paleoceanography, 11, 543–551, 1996.

Cartes, J. E., Papiol, V., Palanques, A., Guillén, J., and Demestre, M.: Dynamics of suprabenthos off the Ebro Delta (Catalan Sea: Western Mediterranean): Spatial and temporal patterns and relationships with environmental factors, Estuar. Coast. Shelf S., 75, 501–515, 2007.

Chandler, G. T. and Green, A. S.: A 14-day harpacticoid copepod reproduction bioassay for laboratory and field contaminated muddy sediments, in: New techniques in aquatic toxicology, edited by: Ostrander, G., Lewis Publ. Inc., 23–39, 1996.

Chandler, G. T., Williams, D. F., Spero, H. J., and Gao, X. D.: Sediment microhabitat effects on carbon stable isotopic signatures of microcosm-cultured benthic foraminifera, Limnol. Oceanogr., 41, 680–688, 1996.

Corliss, B. H., McCorkle, D. C., and Higdon, D. M.: A time series study of the carbon isotopic composition of deep- sea benthic foraminifera, Paleoceanography, 17, Art. no. 1036, 2002.

Dekens, P. S., Lea, D. W., Pak, D. K., and Spero, H. J.: Core top calibration of Mg/Ca in tropical foraminifera: Refining paleotemperature estimation, Geochem. Geophy. Geosy., 3, doi:102210.1029/2001gc000200, 2002.

Department of Energy: Handbook of methods for the analysis of various parameters of the carbon dioxide system in seawater; version 2, in: Ornl/cdiac-74, edited by: Dickson, A. G. and Goyet, C., 1994.

Dissard, D., Nehrke, G., Reichart, G. J., and Bijma, J.: Impact of seawater pCO_2 on calcification and Mg/Ca and Sr/Ca ratios in benthic foraminifera calcite: results from culturing experiments with Ammonia tepida, Biogeosciences, 7, 81–93, 2010, http://www.biogeosciences.net/7/81/2010/.

Dunbar, R. B. and Wefer, G.: Stable isotope fractionation in benthic foraminifera from the Peruvian continental margin, Mar. Geol., 59, 215–225, 1984.

Edelman-Furstenberg, Y., Scherbacher, M., Hemleben, C., and Almogi-Labin, A.: Deep-sea benthic foraminifera from the central Red Sea, J. Foraminifer. Res., 31, 48–59, 2001.

Eichler, P. P. B., Sen Gupta, B. K., Eichler, B. B., Braga, E. S., and Campos, E. J.: Benthic foraminiferal assemblages of the south Brazil: Relationship to water masses and nutrient distributions, Cont. Shelf Res., 28, 1674–1686, 2008.

Erez, J. and Luz, B.: Temperature control of oxygen-isotope fractionation of cultured planktonic foraminifera, Nature, 297, 220–222, 1982.

Hathorne, E. C., Alard, O., James, R. H., and Rogers, N. W.: Determination of intratest variability of trace elements in foraminifera by laser ablation inductively coupled plasma-mass spectrometry, Geochem. Geophy. Geosy., 4, doi:840810.1029/2003gc000539, 2003.

Havach, S. M., Chandler, G. T., Wilson-Finelli, A., and Shaw, T. J.: Experimental determination of trace element partition coefficients in cultured benthic foraminifera, Geochim. Cosmochim. Ac., 65, 1277–1283, 2001.

Healey, S. L., Thunell, R. C., and Corliss, B. H.: The Mg/Ca-temperature relationship of benthic foraminiferal calcite: New core-top calibrations in the < 4 degrees c temperature range, Earth Planet. Sc. Lett., 272, 523–530, doi:10.1016/j.epsl.2008.05.023, 2008.

Hintz, C. J., Chandler, G. T., Bernhard, J. M., McCorkle, D. C., Havach, S. M., Blanks, J. K., and Shaw, T. J.: A physicochemically constrained seawater culturing system for production of benthic foraminifera, Limnol. Oceanogr.-Meth., 2, 160–170, 2004.

Hintz, C. J., Shaw, T. J., Chandler, G. T., Bernhard, J. M., McCorkle, D. C., and Blanks, J. K.: Trace/minor element : Calcium ratios in cultured benthic foraminifera. Part I: Inter-species and inter-individual variability, Geochim. Cosmochim. Ac., 70, 1952–1963, 2006a.

Hintz, C. J., Shaw, T. J., Bernhard, J. M., Chandler, G. T., McCorkle, D. C., and Blanks, J. K.: Trace/minor element: Calcium ratios in cultured benthic foraminifera. Part II: Ontogenetic variation, Geochim. Cosmochim. Ac., 70, 1964–1976, 2006b.

Husum, K. and Hald, M.: Modern foraminiferal distribution in the subarctic Malangen Fjord and adjoining shelf, northern norway, J. Foraminifer. Res., 34, 34–48, 2004.

Kim, S. T. and O'Neil, J. R.: Equilibrium and nonequilibrium oxygen isotope effects in synthetic carbonates, Geochim. Cosmochim. Ac., 61, 3461–3475, 1997.

Lea, D. W. and Spero, H. J.: Experimental determination of barium uptake in shells of the planktonic foraminifera *Orbulina universa* at 22 °C., Geochim. Cosmochim. Ac., 56, 2673–2680, 1992.

Lear, C. H., Elderfield, H. and Wilson, P. A.: Cenozoic deep-sea temperatures and global ice volumes from Mg/Ca in benthic foraminiferal calcite, Science, 287(5451), 269–272, 2000.

Lear, C. H., Rosenthal, Y., and Slowey, N.: Benthic foraminiferal Mg/Ca-paleothermometry: A revised core-top calibration, Geochim. Cosmochim. Ac., 66, 3375–3387, 2002.

Lewis, E. and Wallace, D. W. R.: Program developed for CO_2 system calculations. Ornl/cdiac-105 in, edited by: Carbon Dioxide Information Analysis Center, O. R. N. L., U.S. Department of Energy, Oak Ridge, Tennessee, 1998.

Lynch-Stieglitz, J., Curry, W. B. and Lund, D. C.: Florida Straits density structure and transport over the last 8000 years, Paleoceanography, 24(9), PA3209, doi:10.1029/2008PA001717, 2009.

Mackensen, A., Futterer, D. K., Grobe, H., and Schmiedl, G.: Benthic foraminiferal assemblages from the eastern South Atlantic polar front region between 35-degrees and 57-degrees distribution, ecology and fossilization potential, Mar. Micropaleontol., 22, 33–69, 1993.

Mackensen, A., Schumacher, S., Radke, J., and Schmidt, D. N.: Microhabitat preferences and stable carbon isotopes of endobenthic foraminifera: Clue to quantitative reconstruction of oceanic new production?, Mar. Micropaleontol., 40, 233–258, 2000.

Marchitto, T. M., Bryan, S. P., Curry, W. B., and McCorkle, D. C.: Mg/Ca temperature calibration for the benthic foraminifer *Cibicidoides pachyderma*, Paleoceanography, 22, PA1203, doi:10.1029/2006PA001287, 2007.

Martin, P. A. and Lea, D. W.: A simple evaluation of cleaning procedures on fossil benthic foraminiferal Mg/Ca, Geochem. Geophy. Geosy., 3, 8401 doi:10.1029/2001gc000280, 2002.

Martin, P. A., Lea, D. W., Rosenthal, Y., Shackleton, N. J., Sarnthein, M., and Papenfuss, T.: Quaternary deep sea temperature histories derived from benthic foraminiferal Mg/Ca, Earth Planet. Sc. Lett., 198, 193–209, 2002.

McCorkle, D. C., Corliss, B. H., and Farnham, C. A.: Vertical distributions and stable isotopic compositions of live (stained) benthic foraminifera from the north Carolina and California continental margins, Deep-Sea Res. Pt. I, 44, 983–1024, 1997.

McCorkle, D. C., Bernhard, J. M., Hintz, C. J., Blanks, J. K., Chandler, G. T., and Shaw, T. J.: The carbon and oxygen stable isotopic composition of cultured benthic foraminifera, in: Biogeochemical controls on palaeoceanographic environmental proxies, edited by: Austin, W. E. N. and James, R. H., Geological Society, London, Special Publications, 135–154, 2008.

Mucci, A.: The solubility of calcite and aragonite in seawater at var-

ious salinities, temperatures, and one atmosphere total pressure, Am. J. Sci., 283, 780–799, 1983.

Murray, J. W.: Ecology and applications of benthic foraminifera, Cambridge University Press, Cambridge, 426 pp., 2006.

Nürnberg, D., Bijma, J., and Hemleben, C.: Assessing the reliability of magnesium in foraminiferal calcite as a proxy for water mass temperatures, Geochim. Cosmochim. Ac., 60, 803–814, 1996.

Pena, L. D., Cacho, I., Calvo, E., Pelejero, C., Eggins, S., and Sadekov, A.: Characterization of contaminant phases in foraminifera carbonates by electron microprobe mapping, Geochem. Geophy. Geosy. 9(12), Q07012 doi:10.1029/2008gc002018, 2008.

Rosenthal, Y., Boyle, E. A. and Slowey, N.: Temperature control on the incorporation of magnesium, strontium, fluorine, and cadmium into benthic foraminiferal shells from Little Bahama Bank: Prospects for thermocline paleoceanography, Geochim. Cosmochim. Ac., 61(17), 3633–3643, 1997.

Roy, R. N., Roy, L. N., Vogel, K. M., Portermoore, C., Pearson, T., Good, C. E., Millero, F. J., and Campbell, D. M.: The dissociation-constants of carbonic-acid in seawater at salinities 5 to 45 and temperatures 0 °C to 45 °C, Mar. Chem., 44, 249–267, 1993.

Russell, A. D., Emerson, S., Nelson, B. K., Erez, J., and Lea, D. W.: Uranium in foraminiferal calcite as a recorder of seawater uranium concentrations, Geochim. Cosmochim. Ac., 58, 671–681, 1994.

Sadekov, A., Eggins, S. M., and De Deckker, P.: Characterization of Mg/Ca distributions in planktonic foraminifera species by electron microprobe mapping, Geochem. Geophy. Geosy., 6, Q12P06, doi:10.1029/2005GC000973, 2005.

Sadekov, A., Eggins, S. M., De Deckker, P., and Kroon, D.: Uncertainties in seawater thermometry deriving from intratest and intertest Mg/Ca variability in *Globigerinoides ruber*, Paleoceanography, 23, PA1215, doi:10.1029/2007PA001452, 2008.

Schmiedl, G., Pfeilsticker, M., Hemleben, C., and Mackensen, A.: Environmental and biological effects on the stable isotope composition of recent deep-sea benthic foraminifera from the western Mediterranean Sea, Mar. Micropaleontol., 51, 129–152, 2004.

Schrag, D. P., Adkins, J. F., McIntyre, K., Alexander, J. L., Hodell, D. A., Charles, C. D., and McManus, J. F.: The oxygen isotopic composition of seawater during the last glacial maximum, Quaternary Sci. Rev., 21, 331–342, 2002.

Segev, E. and Erez, J.: Effect of Mg/Ca ratio in seawater on shell composition in shallow benthic foraminifera, Geochem. Geophy. Geosy., 7, Q02P09, doi:10.1029/2005GC000969, 2006.

Shackleton, N. J.: Attainment of isotopic equilibrium between ocean water and the benthonic foraminifera genus *Uvigerina*; isotopic changes in the ocean during the last glacial., in: Colloq. CNRS, edited by: Labeyrie, L., 203–209, 1974.

Shackleton, N. J, Backman, J., Zimmerman, H., Kent, D. V., Hall, M. A., Robers, D. G., Schnitker, D. and Baldauf, J.: Oxygen isotope calibration of the onset of ice-rafting and history of glaciation in the North Atlantic region, Nature, 307, 620–623, 1984

SMHI hydrographic data base SHARK http://www.smhi.se/klimatdata/oceanografi/marin-fysik-kemi-och-biologi/oceanografiskt-datacenter-1.3798, last access: 2009.

Spero, H. J., Bijma, J., Lea, D. W., and Bemis, B. E.: Effect of seawater carbonate concentration on foraminiferal carbon and oxygen isotopes, Nature, 390, 497–500, 1997.

Toyofuku, T., Kitazato, H., Kawahata, H., Tsuchiya, M., and Nohara, M.: Evaluation of Mg/Ca thermometry in foraminifera: Comparison of experimental results and measurements in nature, Paleoceanography, 15, 456–464, 2000.

Toyofuku, T. and Kitazato, H.: Micromapping of Mg/Ca values in cultured specimens of the high-magnesium benthic foraminifera, Geochem. Geophy. Geosy., 6, Q11P05, doi:10.1029/2005GC000961, 2005.

Wefer, G. and Berger, W. H.: Isotope paleontology: Growth and composition of extant calcareous species, Mar. Geol., 100, 207–248, 1991.

Weiss, N. A.: Introductory statistics, Addison-Wesley, New York, 2004.

Wilson-Finelli, A., Chandler, G. T., and Spero, H. J.: Stable isotope behavior in paleoceanographically important benthic foraminifera: Results from microcosm culture experiments, J. Foraminifer. Res., 28, 312–320, 1998.